

INFORMATION TO USERS

This manuscript has been reproduced from the microfilm master. UMI films the text directly from the original or copy submitted. Thus, some thesis and dissertation copies are in typewriter face, while others may be from any type of computer printer.

The quality of this reproduction is dependent upon the quality of the copy submitted. Broken or indistinct print, colored or poor quality illustrations and photographs, print bleedthrough, substandard margins, and improper alignment can adversely affect reproduction.

In the unlikely event that the author did not send UMI a complete manuscript and there are missing pages, these will be noted. Also, if unauthorized copyright material had to be removed, a note will indicate the deletion.

Oversize materials (e.g., maps, drawings, charts) are reproduced by sectioning the original, beginning at the upper left-hand corner and continuing from left to right in equal sections with small overlaps. Each original is also photographed in one exposure and is included in reduced form at the back of the book.

Photographs included in the original manuscript have been reproduced xerographically in this copy. Higher quality 6" x 9" black and white photographic prints are available for any photographs or illustrations appearing in this copy for an additional charge. Contact UMI directly to order.

UMI

A Bell & Howell Information Company
300 North Zeeb Road, Ann Arbor MI 48106-1346 USA
313/761-4700 800/521-0600

CHEMISTRY OF SOME CATION-LIKE SILYL ZIRCONOCENE COMPLEXES

by

Vladimir K. Dioumaev

Department of Chemistry

McGill University,

Montreal

A thesis submitted to the Faculty of Graduate Studies and Research in partial fulfillment of
the requirements for the degree of Doctor of Philosophy.



National Library
of Canada

Acquisitions and
Bibliographic Services

395 Wellington Street
Ottawa ON K1A 0N4
Canada

Bibliothèque nationale
du Canada

Acquisitions et
services bibliographiques

395, rue Wellington
Ottawa ON K1A 0N4
Canada

Your file Votre référence

Our file Notre référence

The author has granted a non-exclusive licence allowing the National Library of Canada to reproduce, loan, distribute or sell copies of this thesis in microform, paper or electronic formats.

The author retains ownership of the copyright in this thesis. Neither the thesis nor substantial extracts from it may be printed or otherwise reproduced without the author's permission.

L'auteur a accordé une licence non exclusive permettant à la Bibliothèque nationale du Canada de reproduire, prêter, distribuer ou vendre des copies de cette thèse sous la forme de microfiche/film, de reproduction sur papier ou sur format électronique.

L'auteur conserve la propriété du droit d'auteur qui protège cette thèse. Ni la thèse ni des extraits substantiels de celle-ci ne doivent être imprimés ou autrement reproduits sans son autorisation.

0-612-29921-X

Canada

ABSTRACT

The aim of this study was to explore applied and mechanistic aspects of the silane dehydropolymerization reaction catalyzed by cationic early transition metallocene compounds. This problem was dealt with by a combination of spectroscopic techniques, kinetic studies, and trapping of reaction intermediates. The results of this integrated approach allow the proposal of a new redox mechanism for the dehydropolymerization reaction which explains and predicts the reactivity and selectivity of cationic early transition metal catalysts. The understanding of the structure-reactivity relationship allows improvement of the outcome of the dehydropolymerization reaction, e.g. improvement of the molecular weight of the resulting polymers via design of new and more efficient catalysts.

The novel zirconocene complexes $[\text{Cp}'_2\text{Zr}(\mu\text{-H})(\text{SiHR})]_2^{2+}[\text{BR}'_n(\text{C}_6\text{F}_5)_{4-n}]_2^{2-}$ ($\text{Cp}' = \text{Cp}, \text{MeCp}, \text{Me}_5\text{Cp}$; $\text{R} = \text{Ph}$ or PhCH_2 ; $\text{R}' = \text{Bu}$ or H) were isolated from silane dehydropolymerization reaction mixtures catalyzed by $\text{Cp}'_2\text{ZrCl}_2/2\text{BuLi}/\text{B}(\text{C}_6\text{F}_5)_3$ or by $[\text{Cp}'_2\text{Zr}(\mu\text{-H})\text{H}]_2/2\text{B}(\text{C}_6\text{F}_5)_3$ combination catalysts. A total structure analysis of these compounds, performed by multinuclear, multidimensional NMR spectroscopy, shows that each zirconocene fragment bears a positive charge, which is delocalized between the metal center and the hydrosilane ligand. Reactions and intermediates leading to zirconocene complexes $[\text{Cp}'_2\text{Zr}(\mu\text{-H})(\text{SiHR})]_2^{2+}[\text{BR}'_n(\text{C}_6\text{F}_5)_{4-n}]_2^{2-}$ ($\text{Cp}' = \text{Cp}, \text{MeCp}, \text{Me}_5\text{Cp}$; $\text{R} = \text{Ph}$ or PhCH_2 ; $\text{R}' = \text{Bu}$ or H .) were investigated *in situ*, by NMR and EPR studies, and by trapping unstable intermediates with PMe_3 . Two novel Zr(III) complexes, $[\text{Cp}_2\text{Zr}^{\text{III}}]^+[\text{BBu}_n(\text{C}_6\text{F}_5)_{4-n}]^-$ and $[\text{Cp}_2\text{Zr}^{\text{III}}(\text{PMe}_3)_2]^+[\text{BBu}_n(\text{C}_6\text{F}_5)_{4-n}]^-$ were identified by EPR spectroscopy. The unstable, diamagnetic compound $[\text{Cp}_2\text{Zr}^{\text{IV}}\text{Bu}]^+[\text{BBu}_n(\text{C}_6\text{F}_5)_{4-n}]^-$ was identified by ^1H - ^1H COSY and ^1H - ^{13}C HMQC experiments at -20°C . Redistribution of the borate butyl and pentafluorophenyl ligands was found to occur by a direct boron to boron migration and not by a metal assisted mechanism. The latter was ruled out by an

independent synthesis of expected reaction intermediates for both reaction pathways ($[\text{Ph}_3\text{C}][\text{BBu}(\text{C}_6\text{F}_5)_3]$, $[\text{Cp}_2\text{Zr}(\text{C}_6\text{F}_5)]^+[\text{BBu}_n(\text{C}_6\text{F}_5)_{4-n}]^-$, $[\text{Cp}_2\text{Zr}(\text{C}_6\text{F}_5)(\mu_3\text{-HB}(\text{C}_6\text{F}_5)_3)]_2$) and an investigation of their model redistribution reactions by NMR spectroscopy.

A key step in the synthesis of the active dehydrocoupling catalyst is the thermal decomposition of Cp_2ZrBu_2 , which at room temperature affords paramagnetic Cp_2ZrR ($\text{R}=\text{Bu}$, crotyl and H) and other minor paramagnetic compounds. The pathway and the trends of this reductive decomposition were investigated in detail by EPR and multinuclear, multidimensional NMR spectroscopy. A number of intermediates were characterized. Reactions leading to the above compounds are rationalized from mechanistic and thermochemical points of view. Although it has not been possible to identify all of the decomposition products, the very fact that the $\text{Cp}_2\text{ZrCl}_2/2\text{BuLi}$ reagent contains substantial amounts of Zr(III) explains the origin of the unusual reactivity of the $\text{Cp}_2\text{ZrCl}_2/2\text{BuLi}$ reagent in dehydropolymerization of silanes and sheds new light on the reaction mechanism.

A kinetic study of the photochemical reaction of $[\text{Cp}_2\text{Zr}(\text{SiHPh})(\mu\text{-H})]_2^{2+}[\text{BBu}_n(\text{C}_6\text{F}_5)_{4-n}]_2^{2-}$ with benzylsilane was carried out with a combination of NMR and EPR spectroscopy. The role of the paramagnetic intermediate, $[\text{Cp}_2\text{Zr}^{\text{III}}]^+[\text{BBu}_n(\text{C}_6\text{F}_5)_{4-n}]^-$, was investigated. The rate law and qualitative observations support a new Zr(IV)/Zr(III) redox mechanism.

The use of "cation-like" metallocene combination catalysts ($\text{Cp}'_2\text{MCl}_2 - 2\text{BuLi} - \text{B}(\text{C}_6\text{F}_5)_3$; $\text{Cp}' = \eta^5\text{-cyclopentadienyl}$, or substituted $\eta^5\text{-cyclopentadienyl}$; $\text{M}=\text{Ti}$, Zr , Hf , U) for dehydropolymerization of silane significantly improves the polymer molecular weight. The influence of various factors (steric and electronic effects of the cyclopentadienyl ligands, the nature of the metal, temperature, solvent, concentration and structure of silane) on the buildup of polysilane chains are systematically analyzed in terms of the new redox mechanism.

RÉSUMÉ

L'objectif de cette étude est d'explorer les aspects mécanistiques et applicatifs des réactions de silanodéhydropolymérisation catalysées par les composés métallocènes cationiques de transition. Ce problème a été traité par la combinaison des techniques spectroscopiques, vitesses de réactions et en piégeant les dérivés intermédiaires de réactions. Les résultats de cette approche intégrale permet la proposition d'un nouveau mécanisme d'oxydo-réduction pour la déhydropolymérisation, qui explique et prédit la réactivité et la sélectivité des catalyseurs cationiques à métaux de transition du groupe 4. La compréhension de la relation qui existe entre la structure et la réactivité, nous permet l'amélioration des résultats de la réaction de déhydropolymérisation, c'est à dire, l'amélioration du poids moléculaire des polymers obtenus par l'étude de nouveaux catalyseurs efficaces.

Les nouveaux complexes du zirconocène $[\text{Cp}'_2\text{Zr}(\mu\text{-H})(\text{SiHR})]_2^{2+}[\text{BR}'_n(\text{C}_6\text{F}_5)_{4-n}]_2^{2-}$ ($\text{Cp}' = \text{Cp}, \text{MeCp}, \text{Me}_5\text{Cp}$; $\text{R} = \text{Ph}$ ou PhCH_2 ; $\text{R}' = \text{Bu}$ ou H) ont été isolés des mélanges réactionnels de silanodehydropolymérisation catalysées par $\text{Cp}'_2\text{ZrCl}_2/2\text{BuLi}/\text{B}(\text{C}_6\text{F}_5)_3$ ou par combinaison de catalyseurs $[\text{Cp}'_2\text{Zr}(\mu\text{-H})\text{H}]_2/2\text{B}(\text{C}_6\text{F}_5)_3$. L'analyse totale de la structure de ces composés performée par spectroscopie de RMN multinucléaire et multidimensionnelle montre que chaque fragment de zirconocène porte une charge positive qui est délocalisée entre le centre du métal et le ligand hydrosilane. Les réactions et intermédiaires principaux qui mènent au complexes du zirconocène $[\text{Cp}'_2\text{Zr}(\mu\text{-H})(\text{SiHR})]_2^{2+}[\text{BR}'_n(\text{C}_6\text{F}_5)_{4-n}]_2^{2-}$ ($\text{Cp}' = \text{Cp}, \text{MeCp}, \text{Me}_5\text{Cp}$; $\text{R} = \text{Ph}$ ou PhCH_2 ; $\text{R}' = \text{Bu}$ ou H .) ont été étudiés *in situ* par des études de RMN, de RPE et aussi en piégeant des intermédiaires instables par PMe_3 . Deux nouveaux complexes de $\text{Zr}(\text{III})$, $[\text{Cp}_2\text{Zr}^{\text{III}}]^+[\text{BBu}_n(\text{C}_6\text{F}_5)_{4-n}]^-$ et $[\text{Cp}_2\text{Zr}^{\text{III}}(\text{PMe}_3)_2]^+[\text{BBu}_n(\text{C}_6\text{F}_5)_{4-n}]^-$, ont été identifiés par spectroscopie RPE. Le composé diamagnétique instable

$[\text{Cp}_2\text{Zr}^{\text{IV}}\text{Bu}]^+[\text{BBu}_n(\text{C}_6\text{F}_5)_{4-n}]^-$ a été identifié par des expériences ^1H - ^1H COSY et ^1H - ^{13}C HMQC à -20°C . La redistribution du butyl de borate et des ligands de pentafluorophenyl est attribuée directement à la migration bore à bore et non à la migration catalysés par le métal. La dernière a été écartée après la synthèse indépendante d'intermédiaires réactionnels par les deux voies de synthèse ($[\text{Ph}_3\text{C}][\text{BBu}(\text{C}_6\text{F}_5)_3]$, $[\text{Cp}_2\text{Zr}(\text{C}_6\text{F}_5)]^+[\text{BBu}_n(\text{C}_6\text{F}_5)_{4-n}]^-$, $[\text{Cp}_2\text{Zr}(\text{C}_6\text{F}_5)(\mu_3\text{-HB}(\text{C}_6\text{F}_5)_3)]_2$) et par une investigation de leur modèles de redistribution de réactions par spectroscopie RMN.

Une étape clé dans la synthèse de catalyseur de déhydrocouplage est la décomposition thermique du Cp_2ZrBu_2 qui à température ambiante procure le complexe paramagnétique Cp_2ZrR ($\text{R}=\text{Bu}$, crotyl et la H) ainsi que d'autres composés paramagnétiques secondaires. La voie ainsi que la tendance de cette décomposition réductrice ont été étudiées en détail par spectroscopie RPE ainsi que par RMN multinucléaire et multidimensionnelle. Un nombre d'intermédiaires ont été ainsi caractérisés. Les principales réactions de plusieurs composés sont rationalisées à partir des points de vue mécanistiques et thermochimiques. Bien qu'il ne soit pas possible d'identifier tous les produits de décomposition, le fait que le $\text{Cp}_2\text{ZrCl}_2/2\text{BuLi}$ contienne une quantité substantielle de Zr(III), explique l'origine de l'inhabituelle réactivité du $\text{Cp}_2\text{ZrCl}_2/2\text{BuLi}$ dans la dépolymérisation des silanes et répand une nouvelle lumière sur le mécanisme de la réaction.

Une étude cinétique de la réaction photochimique de $[\text{Cp}_2\text{Zr}(\text{SiHPh})(\mu\text{-H})]_2^{2+}[\text{BBu}_n(\text{C}_6\text{F}_5)_{4-n}]_2^{2-}$ avec le benzylsilane a été effectuée avec une combinaison de spectroscopie RPE et RMN. Le rôle de l'intermédiaire paramagnétique, $[\text{Cp}_2\text{Zr}^{\text{III}}]^+[\text{BBu}_n(\text{C}_6\text{F}_5)_{4-n}]^-$, a été recherché. La loi de la vitesse et les observations quantitatives soutiennent l'hypothèse d'un nouveau mécanisme d'oxydo-réduction Zr(IV)/Zr(III).

L'utilisation de catalyseurs combinés de metallocènes cationiques "semblants" ($\text{Cp}'_2\text{MCl}_2 - 2\text{BuLi} - \text{B}(\text{C}_6\text{F}_5)_3$; $\text{Cp}' = \eta^5\text{-cyclopentadienyl}$, ou substitué $\eta^5\text{-}$

cyclopentadienyl; $M = \text{Ti, Zr, Hf, U}$) pour une déhydropolymérisation significative du silane, améliore considérablement le poids moléculaire du polymère. L'influence de divers facteurs (effets stériques et électroniques des ligands, la nature du métal, température, solvant, concentration et structure du silane) dans la construction des chaînes de polysilane est symétriquement analysée dans les conditions du nouveau mécanisme d'oxydo-réduction.

FOREWORD

In accordance with guideline 7 of the "Guidelines Concerning Thesis Preparation" (Faculty of Graduate Studies and Research), the following text is cited:

"The candidate has the option, subject to the approval of the Department, of including as part of this thesis the text or duplicated published text (see below), of an original paper, or papers. In this case the thesis must still conform to all other requirements explained in the Guidelines Concerning Thesis Preparation. Additional material (procedural and design data as well as descriptions of equipment) must be provided in sufficient detail (e.g. in appendices) to allow a clear and precise judgment to be made of the importance and originality of the research reported. The thesis should be more than a mere collection of manuscripts published or to be published. It must include a general abstract, a full introduction and literature review and a final overall conclusion. Connecting texts which provide logical bridges between different manuscripts are usually desirable in the interests of cohesion.

It is acceptable for these to include as chapters authentic copies of papers already published, provided these are duplicated clearly on regulation thesis stationery and bound as an integral part of the thesis. Photographs or other materials which do not duplicate well must be included in their original form. In such instances, connecting texts are mandatory and supplementary explanatory material is almost always necessary.

The inclusion of manuscripts co-authored by the candidate and others is acceptable but the candidate is required to make an explicit statement on who contributes to

such a work to what extent, and supervisors must attest to the accuracy of the claims, e.g., before the Oral Committee. Since the task of the Examiners is made more difficult in these cases, it is the candidate's interest to make the responsibilities of authors perfectly clear. Candidates following this option must inform the Department before it submits the thesis for review."

This dissertation is written in the form of five papers. Each paper comprises one chapter, with an introduction of this work in Chapter 1 and general conclusions in Chapter 7. Following normal procedure, all the papers have been or will be submitted shortly for publication in scientific journals. A list of papers is given below:

- Chapter 2: An Unusual 'Cation-like' Zirconocene Hydrosilyl Complex. Silylium Ligand or a Nonclassically Bonded Si-H?
Dioumaev, V. K.; Harrod, J. F.; *Organometallics*, **1996**, 15, 3859-3867.
- Chapter 3: Studies of the Formation and Decomposition Pathways for Some Cationic Zirconocenedihydrosilyl Complexes
Dioumaev, V. K.; Harrod, J. F.; submitted for publication to *Organometallics*.
- Chapter 4: The Nature of the Species Present in the Zirconocene Dichloride-Butyllithium Reaction Mixture
Dioumaev, V. K.; Harrod, J. F.; submitted for publication to *Organometallics*.
- Chapter 5: An Oxidative Addition - Reductive Elimination Mechanism for the Reaction of "Cation-Like" Zirconocene with Primary Silanes
Dioumaev, V. K.; Harrod, J. F.; manuscript in preparation

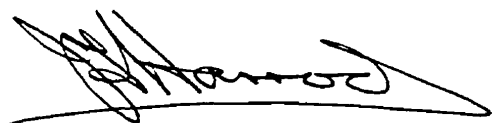
Chapter 6: A Systematic Analysis of the Structure-Reactivity Trends for some
“Cation-Like” Early Transition Metal Catalysts for Dehydropolymerization
of Silanes

Dioumaev, V. K.; Harrod, J. F.; *J. Organomet. Chem.*, **1996**, 521,
133-143.

All of the papers include the research director, Dr. John F. Harrod, as co-author. Other than the supervision, advice and direction of Dr. John F. Harrod all of the work presented in this dissertation was performed by the author.

I hereby give the copyright clearance for the inclusion of the following papers, of which I am co-author, in the dissertation of Vladimir K. Dioumaev.

1. An Unusual 'Cation-like' Zirconocene Hydrosilyl Complex. Silylium Ligand or a Nonclassically Bonded Si-H?
2. Studies of the Formation and Decomposition Pathways for Some Cationic Zirconocenehydridosilyl Complexes
3. The Nature of the Species Present in the Zirconocene Dichloride-Butyllithium Reaction Mixture
4. An Oxidative Addition - Reductive Elimination Mechanism for the Reaction of "Cation-Like" Zirconocene with Primary Silanes
5. A Systematic Analysis of the Structure-Reactivity Trends for some "Cation-Like" Early Transition Metal Catalysts for Dehydropolymerization of Silanes



Professor John F. Harrod
Department of Chemistry
McGill University

Date November 6, 1996

ACKNOWLEDGMENTS

The following persons deserve special mention for their contributions during the course of this work.

Professor John F. Harrod - for his endless encouragement, enthusiasm and advice. His considerable knowledge of chemistry is in particular much appreciated.

My friends and colleagues in the laboratory, namely, Dr. M. Scarlete, Dr. K. Rahimian, Dr. J. Ng, Dr. M.-L. Abasq, Dr. S. Xin, Dr. M. Spescha, Dr. D. Hall, Dr. H. Boily, Dr. D. Trojansek, Dr. H.-G. Woo, Dr. L. Tarazano, Dr. J. He, Dr. M. El-Khateeb, Dr. L. Hao, Dr. B. El-Mouatassim and R. Shu for their friendship, support and the enjoyable working environment.

Dr. K. Rahimian, Dr. H.-G. Woo, Dr. S. Xin and N. Skrynnikov for their helpful discussion and professional advice.

Special thanks to K. Rahimian for proof reading this thesis.

Dr. F. Sauriol - for the hands-on training in modern NMR spectroscopy and for her invaluable help in programming the customized pulse sequences and troubleshooting.

Dr. A.-M. Lebuis at the McGill X-ray Crystallography Laboratory - for endless and patient attempts to help me out with my crystals, which just don't crystallize well.

Ms. Renée Sharron - for her help in dealing with the red tape in my years at McGill.

All the members of the support staff in the Department of Chemistry and Mr. F. Kluck, in particular.

My family and friends for unconditional love and sympathy.

TABLE OF CONTENTS

ABSTRACT	II
RÉSUMÉ	IV
FOREWORD	VII
ACKNOWLEDGMENTS	XI
TABLE OF CONTENTS	XII
LIST OF FIGURES	XX
LIST OF CHARTS	XXVII
LIST OF SCHEMES	XXVII
LIST OF TABLES	XXIX
LIST OF ABBREVIATIONS	XXX
LIST OF COMPOUNDS	XXXIII

	Page
CHAPTER 1 Review of Literature	1
1.1 Statement of Purpose	1
1.2 Homogeneous Group 4 Metallocene Catalyzed Dehydrogenative Polymerization of Hydrosilanes	2
1.2.1 Summary of the Applied Aspects of the Dehydrogenative Polymerization of Hydrosilanes	3
1.2.1.1 Catalysts	3
1.2.1.2 Substrates	4
1.2.1.3 Solvent and Temperature Effects	4
1.2.2 Mechanistic Aspects	4
1.2.3 Towards More Active Catalysts	6
1.2.4 An Outline of the Thesis	7
1.3 Cationic Group 4 Metallocene Complexes	8
1.3.1 Basic Synthetic Routes to Cationic Group 4 Complexes	8

1.3.1.1	Synthesis of Cationic Group 4 Complexes via Ligand Abstraction by a Neutral Lewis Acid	8
1.3.1.2	Oxidative Cleavage of M-R Bonds of Group 4 Complexes	9
1.3.1.3	Brønsted or Ionic Lewis Acid Induced Cleavage of M-R Bonds	12
1.3.1.4	Other Routes	14
1.3.1.5	Modification of Ligands at the Cationic Metal Center	16
1.3.2	Structural Features of Cationic Group 4 Complexes	18
1.3.3	Conclusions	24
1.4	Quest for a Stable R_3Si^+ Ion in the Condensed Phase	26
1.4.1	Silylium Salts with Strongly Coordinating Counterions	27
1.4.1.1	Conductance Measurements	28
1.4.1.2	Molecular Weight Determinations	29
1.4.1.3	NMR Studies	29
1.4.2	Silylium Salts with Weakly Coordinating Counterions	33
1.4.3	Silylium and Related Ligands in Organometallic Complexes	38
1.4.4	Conclusions	40
	References	42

CHAPTER 2 An Unusual “Cation-like” Zirconocene Hydrosilyl Complex. Silylium Ligand or a Nonclassically Bonded Si-H?

	Abstract	58
2.1	Introduction	59
2.2	Results and Discussion	59
2.2.1	Total Structure Determination Strategy	59

2.2.2	²⁹ Si NMR Studies of Ion Pairs in Solution	76
2.2.3	Ion Exchange Reaction	78
2.3	Conclusions	78
2.4	Experimental Section	79
2.4.1	Materials and Methods	79
2.4.2	Physical and Analytical Measurements	80
2.4.3.1	[Cp ₂ Zr(μ-H)(SiHPh)] ₂ ²⁺ [BBu _n (C ₆ F ₅) _{4-n}] ₂ ²⁻ (29a), Low Temperature Synthesis	81
2.4.3.2	[Cp ₂ Zr(μ-H)(SiHPh)] ₂ ²⁺ [BBu _n (C ₆ F ₅) _{4-n}] ₂ ²⁻ (29a), Room Temperature Synthesis	82
2.4.3.3	[Cp ₂ Zr(μ-H)(SiHCH ₂ Ph)] ₂ ²⁺ [BBu _n (C ₆ F ₅) _{4-n}] ₂ ²⁻ (29b)	82
2.4.3.4	[Cp' Cp'' Zr(μ-H)(SiHPh)] ₂ ²⁺ [BBu _n (C ₆ F ₅) _{4-n}] ₂ ²⁻ (Cp' Cp'' = CpCp*, (MeCp) ₂) (29c , 29d)	82
2.4.3.5	[(MeCp) ₂ Zr(μ-H)(SiHPh)] ₂ ²⁺ [BH(C ₆ F ₅) ₃] ₂ ²⁻ (29e)	82
2.4.3.6	²⁹ Si NMR Studies of Ion Pairing in Solution	83
2.4.3.7	Reaction of 29a with CsF	84
	Acknowledgment	84
	References	85

CHAPTER 3	Studies of the Formation and Decomposition Pathways for Some Cationic Zirconocenehydridosilyl Complexes	90
	Abstract	90
3.1	Introduction	91
3.2	Results and discussion	92
3.2.1	Formation pathway for 29	92
3.2.1.1	Low temperature reaction	92

3.2.1.2	Room temperature reaction	94
3.2.2	Ligand Redistribution	98
3.2.3	Reactivity, Thermal and Photolytic Degradation of 29a	103
3.3	Conclusions	107
3.4	Experimental Section	107
3.4.1	Materials and Methods	107
3.4.2	Physical and Analytical Measurements	108
3.4.3.1	Low Temperature reaction of Cp_2ZrBu_2 with $\text{B}(\text{C}_6\text{F}_5)_3$	109
3.4.3.2	Quenching Cp_2ZrBu_2 - $\text{B}(\text{C}_6\text{F}_5)_3$ - PhSiH_3 mixture with PMe_3	110
3.4.3.3	Reaction of Cp_2ZrBu with $\text{B}(\text{C}_6\text{F}_5)_3$	111
3.4.3.4	Reaction of Cp_2ZrBu with $[\text{Ph}_3\text{C}]^+[\text{BBu}_n(\text{C}_6\text{F}_5)_{4-n}]^-$ (average $n=1$)	111
3.4.3.5	Thermal degradation of 30	111
3.4.3.6	Reaction of $[\text{Cp}_2\text{Zr}^{\text{III}}]^+[\text{BBu}_n(\text{C}_6\text{F}_5)_{4-n}]^-$ with PhSiH_3	112
3.4.3.7	$[\text{Cp}_2\text{Zr}^{\text{III}}(\text{PMe}_3)_2]^+[\text{BBu}_n(\text{C}_6\text{F}_5)_{4-n}]^-$ (36)	112
3.4.3.8	$[\text{Ph}_3\text{C}]^+[\text{BBu}_n(\text{C}_6\text{F}_5)_{4-n}]^-$, (average $n=1$)	112
3.4.3.9	$\text{Cp}_2\text{Zr}(\text{C}_6\text{F}_5)_2$	113
3.4.3.10	$[\text{Cp}_2\text{Zr}(\text{C}_6\text{F}_5)(\mu\text{-H})]_2$	114
3.4.3.11	Reaction of $[\text{Cp}_2\text{Zr}(\text{C}_6\text{F}_5)(\mu\text{-H})]_2$ with $\text{B}(\text{C}_6\text{F}_5)_3$ in C_6D_6	114
3.4.3.12	Reaction of $[\text{Cp}_2\text{Zr}(\text{C}_6\text{F}_5)(\mu\text{-H})]_2$ with $\text{B}(\text{C}_6\text{F}_5)_3$ in THF	115
3.4.3.13	Reaction of $[\text{Cp}_2\text{Zr}(\text{C}_6\text{F}_5)(\mu\text{-H})]_2$ with $[\text{Ph}_3\text{C}]^+[\text{BBu}_n(\text{C}_6\text{F}_5)_{4-n}]^-$	115
3.4.3.14	Reaction of 29a with $\text{PhCH}_2\text{SiH}_3$	116
3.4.3.15	Thermal Degradation of 29a	116
3.4.3.16	Photolytic Degradation of 29a	116
3.4.3.17	Photolytic Degradation of 29c	117

3.4.3.18	Reaction of 29a with PMe_3	117
3.4.3.18.1	Dark reaction	117
3.4.3.18.2	Photoreaction	118
	Acknowledgment	118
	References	119
CHAPTER 4	The Nature of the Species Present in the Zirconocene Dichloride-Butyllithium Reaction Mixture	
	Mixture	123
	Abstract	123
4.1	Introduction	124
4.2	Results	126
4.3	Discussion	143
4.3.1	A reaction scheme for decomposition of Cp_2ZrBu_2	143
4.3.2	Some thermochemical aspects of the proposed reaction steps	149
4.4	Conclusions	153
4.5	Experimental	155
4.5.1	Materials and Methods	155
4.5.2	Physical and Analytical Measurements	155
4.5.3.1	Preparation of a Cp_2ZrBu_2 NMR sample	156
4.5.3.2	Thermal Decomposition of Cp_2ZrBu_2	156
4.5.3.3	$\text{Cp}_2\text{ZrBu}(\text{PMe}_3)$	157
4.5.3.4	Preparation of $\text{MeCH}=\text{CHCH}_2\text{MgBr}$	157
4.5.3.5	Preparation of a $\text{Cp}_2\text{Zr}(\text{RCH}=\text{CHCH}_2)\text{H}$ ($\text{R}=\text{Me}, \text{H}$) NMR sample	158
4.5.3.6	Quenching with HCl or DCl	158

	Acknowledgment	159
	References	160
CHAPTER 5	A Photo-Redox Mechanism For The Reaction Of 'Cation-like' Zirconocene With Primary Silanes	165
	Abstract	165
5.1	Introduction	165
5.2	Results and Discussion	168
5.2.1	The Hydrosilane Exchange Reaction	168
5.2.2	Kinetic Study Using NMR Spectroscopy	172
5.2.3	Semiquantitative Kinetic Study Followed by EPR Spectroscopy	178
5.3	Conclusions	180
5.4	Experimental Section	181
5.4.1	Materials and Methods	181
5.4.2	Physical and Analytical Measurements	181
5.4.3.1	Reactions Followed by NMR	182
5.4.3.2	Reactions Followed by EPR	183
5.4.3.3	Rate Law	183
	Acknowledgment	184
	References	185
CHAPTER 6	A Systematic Analysis of the Structure- Reactivity Trends for some "Cation-Like" Early Transition Metal Catalysts for Dehydropolymerization of Silanes	189
	Abstract	189

6.1	Introduction	190
6.2	Results and discussion	191
6.2.1	Choice of the central metal	196
6.2.2	Catalyst preparation strategy	199
6.2.3	Solvent, temperature and concentration effects	201
6.2.4	Fine tuning of the steric and electronic effects of the cyclopentadienyl ligands	203
6.2.5	Dehydropolymerization of other monomers	205
6.2.6	Fractional precipitation of polysilanes	205
6.3	Conclusions	207
6.4	Experimental details	207
6.4.1	General methods	207
6.4.2.1	Silane polymerization experiments with $\text{Cp}'\text{Cp}''\text{MCl}_2/2\text{BuLi}/\text{B}(\text{C}_6\text{F}_5)_3$ ($\text{M} = \text{Ti}, \text{Zr}, \text{Hf}, \text{U}$) combination catalyst	209
6.4.2.2	Silane polymerization experiments with $\text{Cp}'\text{Cp}''\text{ZrCl}_2/2\text{BuLi}$ combination catalyst	210
6.4.2.3	Silane polymerization experiments with $\text{Cp}_2\text{ZrR}_2/m\text{B}(\text{C}_6\text{F}_5)_3$ or $\text{Cp}'\text{Cp}''\text{ZrR}_2/m[\text{Ph}_3\text{C}][\text{B}(\text{C}_6\text{F}_5)_4]$ ($\text{R}=\text{Me}$ or H and $m=1$ or 2) combination catalyst	210
6.4.2.4	Silane polymerization experiments with $\text{Cp}_2\text{ZrMe}_2/4\text{PhSiH}_3/\text{B}(\text{C}_6\text{F}_5)_3$ or $\text{Cp}_2\text{ZrMe}_2/4\text{PhSiH}_3/[\text{Ph}_3\text{C}][\text{B}(\text{C}_6\text{F}_5)_4]$ combination catalyst	211
6.4.2.5	Silane polymerization experiment with $(\text{MeCp})_2\text{ZrCl}_2/2\text{BuLi}/4\text{PhSiH}_3/\text{B}(\text{C}_6\text{F}_5)_3$ combination catalyst	211

6.4.2.6	Fractional separation of polyphenylsilane	211
6.4.2.7	Reaction of $B(C_6F_5)_3$ with $RSiH_3$ ($R=Ph, CH_2Ph$)	212
6.4.2.8	Reaction of $[Ph_3C][B(C_6F_5)_4]$ with $PhSiH_3$	212
6.4.2.9	Reaction of $B(C_6F_5)_3$ with polyphenylsilane	212
	Acknowledgment	213
	References	214
CHAPTER 7	Conclusions, Contributions to Original Knowledge, and Suggestions for Future Work	218
7.1	Conclusions and Contributions to Original Knowledge	218
7.2	Suggestions for Future Work	220
APPENDIX 1	Supplementary Material for Chapter 4	223

LIST OF FIGURES

Figure	Title	Page
Figure 1-1.	Proposed mesomer structures for $[\text{Et}_3\text{Si}(\text{toluene})]^+$.	37
Figure 1-2.	Proposed mesomer structures for $[\text{}^i\text{Pr}_3\text{Si}]^+[\text{Br}_6\text{CB}_{11}\text{H}_6]^-$.	37
Figure 1-3.	Proposed mesomer structures for 28 .	39
Figure 2-1.	^1H NMR spectrum of 29a in C_6D_6 .	60
Figure 2-2.	Proposed mesomer structures for 29a-e and their topological representation.	70
Figure 2-3.	Topological representation of all isomers of 29c , which agree with the results of the NOESY experiment. Cis stands for an arrangement of both Cp ligands on one side of the bisectorial plane; trans, on opposite sides.	72
Figure 2-4.	Fragment of an ^1H NOESY plot for 29c which shows that each of the bridging hydrides exhibits a cross-correlation to a different Cp ligand, which can be rationalized in terms of distorted Zr-H-Zr or inherently asymmetric Zr-Si-H-Zr bridges.	72
Figure 2-5.	Fragment of an ^1H NOESY plot for 29c which shows that the SiH and Ph groups have NOEs with different Cp ligands, confirming that they appear on different sides of the bisectorial plane (Figure 3, (<i>S,S</i>)- or (<i>R,R</i>)- <i>trans</i> - 29c structure).	73

Figure 2-6.	Variable temperature ^{19}F NMR spectra for compound 29c in C_7D_8 . The number of ^{19}F resonances is doubled when the sample is cooled to $-20\text{ }^\circ\text{C}$, due to the formation of a second liquid phase (29c - C_7D_8 clathrate). The clathrate phase solidifies upon further decrease of temperature ($-90\text{ }^\circ\text{C}$), and the ^{19}F spectrum simplifies accordingly.	74
Figure 2-7.	^{29}Si chemical shift (o) and the $^1J_{\text{SiH}}$ coupling constant (Δ) versus concentration plots for 29a . The sample does not exhibit any ion pairing effects in the studied range of concentrations.	77
Figure 3-1.	The EPR spectrum of the clathrate of $[\text{Cp}_2\text{Zr}]^+[\text{BBu}_n(\text{C}_6\text{F}_5)_{4-n}]^-$ in toluene.	95
Figure 3-2.	An EPR spectrum of the thermal decomposition products of 30 in toluene. The main peak is tentatively assigned to $[\text{Cp}_2\text{Zr}]^+[\text{BBu}_n(\text{C}_6\text{F}_5)_{4-n}]^-$.	96
Figure 3-3.	The EPR spectrum of $[\text{Cp}_2\text{Zr}(\text{PMe}_3)_2]^+[\text{BBu}_n(\text{C}_6\text{F}_5)_{4-n}]^-$ in C_6D_6 .	97
Figure 3-4.	An ^{19}F NMR spectrum of $[\text{Ph}_3\text{C}][\text{BBu}_n(\text{C}_6\text{F}_5)_{4-n}]$ in C_6D_6 . There is an extra set of ^{19}F NMR resonances, marked by an asterisk, in addition to the signals due to the $[\text{Ph}_3\text{C}][\text{BBu}_2(\text{C}_6\text{F}_5)_2]$ and $[\text{Ph}_3\text{C}][\text{B}(\text{C}_6\text{F}_5)_4]$, which is in slow dynamic exchange with the former. The extra set of ^{19}F NMR signals is not due to $[\text{Ph}_3\text{C}][\text{BBu}(\text{C}_6\text{F}_5)_3]$ and can be tentatively attributed to the postulated bridging diborate compound $[\text{Ph}_3\text{C}]_2[\text{B}_2\text{Bu}_4(\text{C}_6\text{F}_5)_4]$.	102
Figure 3-5.	The EPR spectrum of $[\text{CpCp}^*\text{Zr}]^{+*}[\text{BBu}_n(\text{C}_6\text{F}_5)_{4-n}]^-$ in toluene.	105

Figure 4-1.	An ^1H NMR spectrum of a mixture of 37 and 39a in toluene- d_8 at $+25^\circ\text{C}$. The Cp, C_aH_2 , C_cH and Me signals of 39a exhibit dynamic broadening while C_bH is sharp.	130
Figure 4-2.	Schematic representation of the π - σ - π dynamic processes in 39a .	131
Figure 4-3.	An ^1H - ^{13}C HMQC spectrum of a mixture of 38a , 39a and 40a in THF- d_8 at -40°C . Pairs of cross peaks having a common ^{13}C chemical shift belong to diastereotopic methylene groups.	133
Figure 4-4.	An ^1H NMR spectrum of a mixture of 38a , 39a and 40a in THF- d_8 at -20°C . The multiplicity of the C_aH_2 group in 38a and 40a is characteristic of a small cycle with two diastereotopic geminal protons having considerably different coupling constants, gauche and eclipsed, to the same vicinal neighbor.	134
Figure 4-5.	An ^1H - ^1H NOESY spectrum (negative contours) of a mixture of 38a and 39a in THF- d_8 at 0°C . Both C_aH_2 resonances of 39a are in dynamic exchange with each other and with every C_aH_2 signal of 38a . However, there is no exchange within C_aH_2 and C_cH_2 pairs of 38a .	136
Figure 4-6.	Schematic representation of a dynamic exchange between 38a and 39a .	137
Figure 4-7a.	Schematic representation of a fragment of the 3D structure of 45 as determined by NOESY.	139
Figure 4-7b.	Proposed structure for 45 .	139
Figures 4-8a and 4-8b.	Experimental and spin simulated ^1H NMR spectrum of 45 respectively.	140

Figure 4-9.	An EPR spectrum of a mixture of 31 and unidentified paramagnetic compounds in toluene. The main peak is an apparent triplet due to the hyperfine coupling to the butyl ligand.	141
Figure 4-10.	An EPR spectrum of a mixture of 47 and $\text{Cp}_2\text{Zr}(\text{CH}_2\text{CH}=\text{CHMe})$ in THF. The doublet peak is due to the hyperfine coupling to the hydride ligand.	143
Figure 4-11a and 4-11b.	Generic σ -bond metathesis transition states for β - and γ -H abstraction. 4-11a: two flat zirconacycles are lying in the same plane and have no conformational freedom. 4-11b: - still bicyclic, but one of the cycles does not have to be planar and can twist to meet the geometry requirements of the other one.	145
Figure 4-12.	The ^1H NMR spectrum of 37 in THF- d_8 at -40°C .	223
Figure 4-13.	An ^1H NMR spectrum of a mixture of 37 , 38a , 39a and 40a in THF- d_8 at -40°C .	224
Figure 4-14.	A fragment of the ^1H - ^1H COSY spectrum of 39a in THF- d_8 at -40°C , which shows the connectivity pattern. An asterisk denotes a cross peak of an unknown impurity.	225
Figure 4-15.	A fragment of an ^1H - ^1H COSY spectrum in THF- d_8 at 0°C , which shows a connectivity pattern for 37 , 38a and 40a . The tie-lines in the top left half are for 37 (bold) and 38a (narrow). The tie-lines in the bottom right half are for butane (bold) and 40a (narrow).	226
Figure 4-16.	A fragment of an ^1H - ^1H COSY spectrum in THF- d_8 at $+25^\circ\text{C}$, which shows a connectivity pattern for 41a .	227

Figure 4-17.	A fragment of an ^1H - ^1H COSY spectrum in THF- d_8 at +25°C, which shows a connectivity pattern for 45 .	228
Figure 4-18.	A fragment of an ^1H - ^1H TOCSY spectrum in THF- d_8 at -40°C, which shows a connectivity pattern for 38a and 39a .	229
Figure 4-19.	A fragment of an ^1H - ^1H TOCSY spectrum in THF- d_8 at +25°C, which shows a connectivity pattern for 40a and 45 .	230
Figure 4-20.	A fragment of an ^1H - ^1H TOCSY spectrum in THF- d_8 at -40°C, which shows a connectivity pattern for 41a .	231
Figure 4-21.	A more expanded version of the ^1H - ^{13}C HMQC spectrum shown in Figure 4-3, which shows all cross peaks for 39a in addition to 38a and 40a . (The labels for the latter two are given in Figure 4-3). The intensity of allylic resonances is low as the NMR experiment was specifically adjusted for a better sensitivity for aliphatic cross peaks. An asterisk denotes traces of relaxation noise arising from the solvent.	232
Figure 4-22.	A fragment of an ^1H - ^{13}C HMQC spectrum of a mixture of 41a and 45 in THF- d_8 at +25°C. Pairs of cross peaks having a common ^{13}C chemical shift belong to diastereotopic methylene groups. Cross peaks marked by an asterisk belong to a single ligand, which has not been identified.	233

- Figure 4-23. A fragment of an ^1H - ^1H NOESY spectrum in THF- d_8 at +25°C, which exhibits the connectivity of $\mu\text{-H-Zr}$ to Cp, and $\text{C}_\alpha\text{H}_2$ groups in **45**. An asterisk denotes traces of relaxation noise arising from butane. 234
- Figure 5-1. A kinetic plot for the reaction of **29a** with benzylsilane as a function of rate vs. concentration of **29a**, which shows a first-order behavior in **[29a]**. Initial $[\text{PhCH}_2\text{SiH}_3] = 0.37 \text{ M}$. The line $y = -10.2(0.3) + 0.99(0.04)x$ represents the least-squares fit to the data points (the quantities in parentheses are the 95% confidence limits; $R^2 = 0.987$). 173
- Figure 5-2a. Kinetic plot for the reaction of **29a** with benzylsilane as a function of concentration of **29a** vs. time, which shows a first-order behavior in **[29a]**. Initial $[\textbf{29a}] = 0.00095 \text{ M}$; $[\text{PhCH}_2\text{SiH}_3] = 0.37 \text{ M}$. The line $y = 0.02(0.02) - 3.81(0.07) \times 10^{-2}x$ represents the least-squares fit to the data points (the quantities in parentheses are the 95% confidence limits; $R^2 = 0.999$). 174
- Figure 5-2b. Kinetic plot for the reaction of **29a** with benzylsilane as a function of k_{observed} vs. initial concentration of **29a**, which shows an inverse dependence on $[\textbf{29a}]_0$. Initial $[\text{PhCH}_2\text{SiH}_3] = 0.37 \text{ M}$. The line $y = 0.000(0.001) + 3.5(0.2) \times 10^{-5}x$ represents the least-squares fit to the data points (the quantities in parentheses are the 95% confidence limits; $R^2 = 0.996$). 175

- Figure 5-3. Kinetic plot for the reaction of **29a** with benzylsilane as a function of initial rate vs. concentration of benzylsilane, which shows a zero-order behavior in $[\text{PhCH}_2\text{SiH}_3]$. Initial $[\text{PhCH}_2\text{SiH}_3] = 0.0039 \text{ M}$. The bars indicate an $\ln(5\%) = 1.6\%$ error. The line $y = -9.99(0.07) - 0.00(0.04)x$ represents the least-squares fit to the data points (the quantities in parentheses are the 95% confidence limits). 176
- Figure 5-4. Kinetic plot for the reaction of **29a** with benzylsilane as a function of rate vs. optical density of the filters, which shows a first-order behavior in light intensity. Initial $[\textbf{29a}] = 0.0057 \text{ M}$; $[\text{PhCH}_2\text{SiH}_3] = 0.14 \text{ M}$. The line $y = -4.49(0.02) - 0.89(0.05)x$ represents the least-squares fit to the data points (the quantities in parentheses are the 95% confidence limits; $R^2 = 0.997$). 177
- Figure 6-1. GPC traces for oligophenylsilane samples: a) obtained with $\text{Cp}_2\text{ZrCl}_2/2\text{BuLi}/\text{B}(\text{C}_6\text{F}_5)_3$ catalyst after 10 days, b) obtained with $\text{Cp}(\text{Me}_5\text{C}_5)\text{ZrCl}_2/2\text{BuLi}/\text{B}(\text{C}_6\text{F}_5)_3$ catalyst after 1 day, c) improved by fractional precipitation from toluene - petroleum ether. 206
- Figure 7-1 A schematic representation of the σ -bond metathesis transition states for the polymerization of phenylsilane 220

LIST OF CHARTS

Chart	Title	Page
Chart 1-1	Some low oxidation state titanocene complexes isolated from dehydropolymerization reaction	5

LIST OF SCHEMES

Scheme	Title	Page
Scheme 1-1	The Tilley σ -bond metathesis mechanism for silane dehydropolymerization ($R=Ar$ or Alk ; $R'=H$ or $(SiHR)_nH$)	5
Scheme 1-2	Modification of ligands at the cationic ZrH center	16
Scheme 1-3	Modification of ligands at the cationic ZrC center	17
Scheme 1-4	Low-lying empty orbitals of d^0 neutral and cationic group 4 metallocenes	19
Scheme 1-5	Possible equilibria between "naked" cationic species and their adducts with counterions, solvent molecules, or chelation of their own ligands	20
Scheme 3-1	Reactions and intermediates in the $Cp_2ZrCl_2/2BuLi/B(C_6F_5)_3/PhSiH_3$ system	93
Scheme 3-2	Conceivable ligand redistribution pathways for $[BPhF_nBu_{4-n}]^-$ anions	99
Scheme 3-3	An attempted pentafluorophenyl group transfer reaction from zirconium to boron nuclei	100

Scheme 3-4	The routes for the dark and photoreaction of 29a with PMe_3	106
Scheme 4-1	A proposed sequence of reactions occurring during decomposition of Cp_2ZrBu_2	146
Scheme 5-1	The Tilley σ -bond metathesis mechanism for reactions of silanes with early transition silylmetallocenes ($\text{R}=\text{Ar}$ or Alk ; $\text{R}'=\text{H}$ or $(\text{SiHR})_n\text{H}$)	166
Scheme 5-2	A proposed redox mechanism for reactions of silanes with 'cation-like' silylzirconocenes ($\text{R}=\text{Ar}$ or Alk ; $\text{R}'=\text{H}$ or $(\text{SiHR})_n\text{H}$)	170
Scheme 5-3	A schematic representation of the σ -bond metathesis transition states for the polymerizations of propylene and phenylsilane respectively. The metallocene catalysts are too sterically congested to accommodate two bulky ligands in the metallocene wedge, which casts serious doubts on the possibility of a transition state with two polysilane random coils in the coordination sphere of zirconium	172
Scheme 5-4	A complete kinetic description of the reaction of 29a with benzylsilane	176
Scheme 6-1	The Tilley σ -bond metathesis mechanism for silane dehydropolymerization ($\text{R}=\text{Ar}$ or Alk ; $\text{R}'=\text{H}$ or $(\text{SiHR})_n\text{H}$)	198
Scheme 6-2	A tentative one-electron oxidative addition-reductive elimination mechanism for silane dehydropolymerization ($\text{R}=\text{Ar}$ or Alk ; $\text{R}'=\text{H}$ or $(\text{SiHR})_n\text{H}$)	199

LIST OF TABLES

Table	Title	Page
Table 1-1.	Spectroscopic and structural parameters for silylium salts	35
Table 2-1.	^1H NMR data for 29a-e	61
Table 2-2.	^{13}C and ^{29}Si NMR data for 29a-e	63
Table 2-3.	^{19}F NMR chemical shifts for $[\text{BBu}_n(\text{C}_6\text{F}_5)_{4-n}]^-$ anion	64
Table 2-4.	^{13}C NMR chemical shifts for the C_6F_5 groups of the $[\text{BBu}_n(\text{C}_6\text{F}_5)_{4-n}]^-$ anion	65
Table 2-5.	Spacial relationship of the Cp, Cp*, $\mu\text{-H}$ and Si ligands in 29a , 29b and 29c	71
Table 4-1.	NMR Data	127
Table 4-2.	Bond Disruption Enthalpies (kcal/mol)	151
Table 6-1.	Some results for the polymerization of phenylsilane in toluene	192
Table 6-2.	Some results for the polymerization of phenylsilane in neat monomer	194
Table 6-3.	Some results for the fractional precipitation of polyphenylsilane	207

LIST OF ABBREVIATIONS

Å	Ångstrom ($1\text{Å} = 10^{-10}\text{ m}$)
BDE	bond disruption enthalpy
Bu	butyl
ⁿ Bu	<i>normal</i> -butyl
kcal	kilocalorie ($1\text{ kcal} = 4186.8\text{ J}$)
COSY	Correlation Spectroscopy
Cp	η^5 -cyclopentadienyl
Cp*	η^5 -pentamethylcyclopentadienyl
D	Dalton ($1 = 1\text{ atomic mass unit}$)
EBI	ethylene-1,2-bis(η^5 -1-indenyl)
EPR	electron paramagnetic resonance
Et	ethyl
FT-IR	Fourier-transform infrared spectroscopy
GPC	gel permeation chromatography
ⁿ Hx	<i>normal</i> -hexyl
HMBC	Heteronuclear Multiple Bond Correlation
HMQC	Heteronuclear Multiple Quantum Coherence
Ind	indenyl
IR	infrared
M _n	number average molecular weight (g/mol)
M _w	weight average molecular weight (g/mol)
Me	methyl
MS	mass spectrum
MW	molecular weight (g/mol)
na	not applicable

nd	not determined
NMR	nuclear magnetic resonance
NOESY	nuclear Overhauser effect spectroscopy
PDI	polydispersity index (= M_w/M_n)
Ph	phenyl
ppm	parts per million
<i>R</i>	a symbol used to describe the stereochemical configuration in <i>R,S</i> nomenclature
<i>rac</i>	racemic
<i>S</i>	a symbol used to describe the stereochemical configuration in <i>R,S</i> nomenclature
THF	tetrahydrofuran
THI	η^5 -4,5,6,7-tetrahydroindenyl
THT	tetrahydrothiophene
TMS	tetramethylsilane
TOCSY	total correlation spectroscopy
UV-vis	Ultraviolet and visible spectroscopy

Abbreviations used to describe NMR signals

AX q	second order AX quartet
br m	broad multiplet
br s	broad singlet
d	doublet
d m	doublet of multiplets
m	multiplet
s	singlet

t triplet

Abbreviations used to describe IR bands

m medium

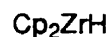
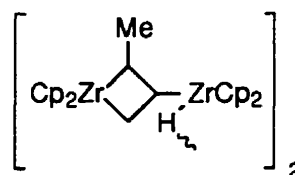
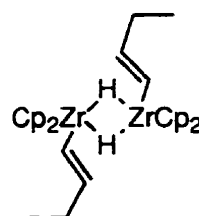
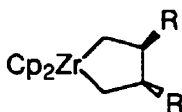
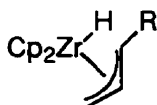
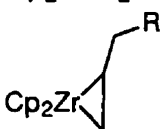
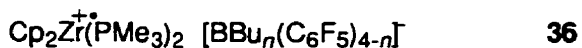
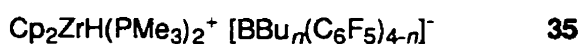
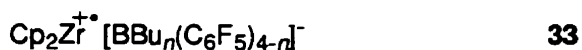
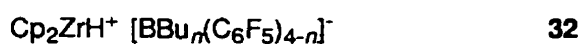
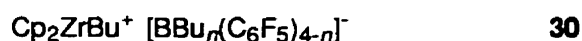
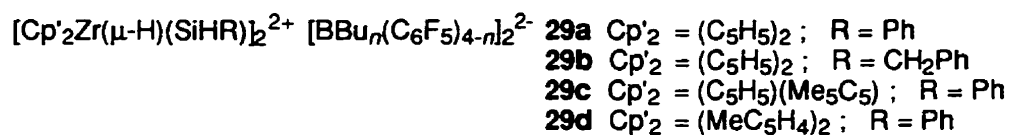
s strong

vs very strong

vw very weak

w weak

LIST OF COMPOUNDS



CHAPTER 1

Review of Literature

1.1 Statement of Purpose

The experimental material of this thesis encompasses a wide area of polymer, organometallic, and main group chemistry, including silicon-containing polymers, silylium ions in condensed phase, neutral and cationic early transition metallocene catalysts, and applied and mechanistic aspects of the silane dehydrocoupling reaction. In an attempt to keep the size of this manuscript within reasonable margins, detailed discussion of the literature has been limited to the following subjects:

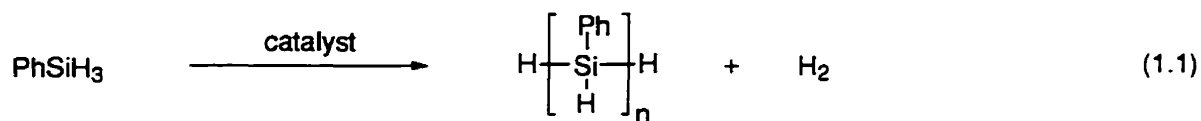
A brief introduction to the applied and mechanistic aspects of the silane dehydrocoupling reaction,

The basic synthetic pathways to, and main structural types of cationic Group 4 metallocene complexes,

The possibility of existence of silylium ions in condensed phase.

1.2 Homogeneous Group 4 Metallocene Catalyzed Dehydrogenative Polymerization of Hydrosilanes

Synthetic routes to polysilanes are of scientific and technological interest as these polymers have a great potential in the field of advanced materials for electronics and integrated optics.¹⁻⁶ Wurtz-like coupling of halosilanes with molten alkali metals is currently the most useful industrial method.³⁻⁶ An alternative, less hazardous synthetic strategy is the catalytic dehydropolymerization of silanes.



The first accounts of formation of Si-Si bonds via catalytic dehydrocoupling of hydrosilanes date back to the early 1970's using rhodium and platinum catalysts.^{7,8} Dimers and very short chain oligomers ($n = \text{up to } 6$) were formed along with significant amounts of disproportionation products. It was not until the mid 1980's that the first facile and quantitative dehydropolymerization was reported (eq 1.1).⁹ The reaction was catalyzed by dimethyltitanocene, and short oligosilanes (up to 18 Si atoms in the oligomer chain) were formed. Other sandwich and half-sandwich complexes of Ti, Zr, and Hf were also applied.¹⁰ Such transition metal catalysts offer some control over the stereochemistry of the polymeric products and the cyclic/linear chain selectivity,¹¹⁻¹⁴ as well as a greater tolerance towards functional groups, which can be incorporated into the polymer.¹⁵⁻¹⁷ The major drawback of this route is the low molecular weight of the resulting polymers,¹⁴ which affects the mechanical and optical properties. A considerable improvement in polysilane molecular weight has been achieved over the past decade by a combination of both: an extensive blind screening of various neutral early transition metallocenes,^{10,14} as well as studies of the reaction products, intermediates, and mechanisms.^{9,18-21} These

results have been extensively summarized elsewhere^{13,14,19,22-25} and will be mentioned only briefly in this review.

1.2.1 Summary of the Applied Aspects of the Dehydrogenative Polymerization of Hydrosilanes

1.2.1.1 Catalysts

The most suitable catalysts for silane polymerization are $\text{Cp}'_2\text{MR}_2$ (where Cp' = substituted Cp, R = alkyl, silyl or hydride, and M = Ti, Zr, Hf).^{14,19} The reaction is sensitive to steric effects and is readily tunable by modifying the Cp ligand. The best current catalysts utilize CpCp^* or similar ligand combinations.¹⁴ The structure of R, on the other hand, has little effect on the reaction, as this ligand is cleaved during the induction period and is not present in the actual catalytic species, *vide infra*. Other ligands (R = aryloxy²⁶ and dialkylamido²⁷) can be also used. In general, zirconium and hafnium catalysts have comparable catalytic properties and outperform titanium catalysts in terms of molecular weight of the polysilane products.^{14,28} Hafnium catalysts are also more thermally robust and are slightly less sensitive to the steric effects of the Cp ligands. Other metallocenes (Sc, Y, V, Nb, Ta, Cr, Mo, W, Th, U, and lanthanides) produce only low molecular weight products.^{10,29-32}

A new generation of cationic $[\text{Cp}'_2\text{MR}]^+[\text{X}]^-$ (M = Zr or Hf) catalysts, recently introduced by us^{33,34} and by Tilley and coworkers³⁵ have proved to be the best so far. They are not reviewed here and will be discussed at large in the following chapters of this thesis.

1.2.1.2 Substrates

High molecular weight polysilanes can be obtained from MeSiH_3 , but the polymer is crosslinked. PhSiH_3 furnishes linear, relatively air stable polymers. Other primary silanes (RSiH_3 , where $\text{R} = \text{PhCH}_2$, or alkyl) also undergo dehydropolymerization but the molecular weights decrease dramatically in the order $\text{Me} \gg \text{Ph} > \text{PhCH}_2 \geq \text{alkyl}$ ¹³.

The dehydrocoupling of secondary silanes is sluggish and does not go beyond formation of pentamers.³⁶⁻³⁸ Tertiary and quaternary silanes do not produce any Si-Si bonds.

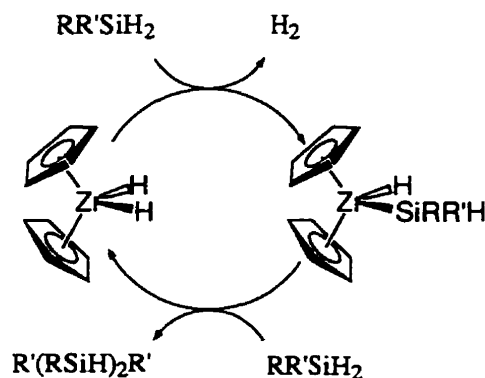
1.2.1.3 Solvent and Temperature Effects

The best results are obtained when the reaction is conducted without solvent, in neat monomer and at room temperature. An increase of temperature leads to an increase in the depolymerization reaction and lower molecular weight polysilanes.¹⁴ Addition of solvent (toluene or halocarbon) causes similar results.¹⁴

1.2.2 Mechanistic Aspects

The most widely accepted mechanism, formulated by Tilley and coworkers, consists of a two step σ -bond metathesis process with fixed oxidation state for the metal (Scheme 1-1).^{14,15,20,21,24} This mechanism is based on kinetic^{20,21,39} and structural⁴⁰⁻⁴² studies of zircono- and hafnocenes. Both steps in the sequence can be reversible, which explains the depolymerization reaction. Application of this σ -bond metathesis model led to a significant improvement in the reaction performance.¹⁴ Thus, the balance of polymerization and depolymerization reactions was discussed in conjunction with the steric and electronic effects of silane and cyclopentadienyl substituents on the transition states.¹⁴

The same mechanism was extended to lanthanide and scandium catalysts on the basis of kinetic experiments and nonlocal density functional calculations.^{29,43,44} It should be pointed out that the results of the calculations are not unequivocal since both steps of the sequence were calculated to be endothermic by 3 and 10 kJ mol⁻¹, respectively, and chain scission should prevail.



Scheme 1-1 The Tilley σ -bond metathesis mechanism for silane dehydropolymerization¹⁴
(R=Ar or Alk; R'=H or (SiHR)_nH)

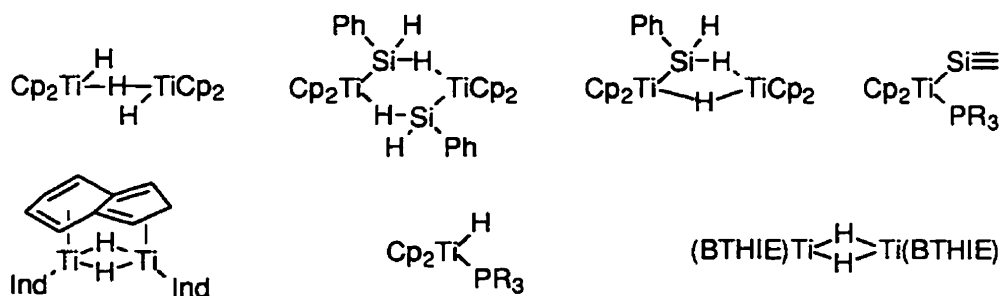


Chart 1-1 Some low oxidation state titanocene complexes isolated from dehydropolymerization reaction

Investigations of titanocene catalysts reported by Harrod *et al* suggests that the reaction mechanism may be more diverse. A number of mono- and dimetallic reduced Ti^{III} and mixed oxidation state Ti^{III/IV} and Ti^{II/III} compounds were isolated and structurally characterized (Chart 1-1).^{9,18,45-50} The relation of these compounds to the active catalytic

species has not been clearly established, but they are formed in high yields without significant decrease of the catalyst efficiency, and they interconvert with each other. This suggests that M^{III} species can be intermediates in the catalytic cycle. In the case of other group 4 metal catalyzed reactions of silanes, germanes, and stannanes, intense colors, indicative of the formation of lower oxidation state species, have also been observed although no investigation of their role has been reported to date.^{36,40,51,52} A number of reaction schemes have been proposed, including metal-silylene and silyl radical mechanisms.^{19,53,54} A silylene-based mechanism, studied kinetically and with the use of density functional theory, was concluded to be feasible.^{54,55} Formation of silylene, although endothermic by 40 kJ mol^{-1} , proceeds with a moderate kinetic barrier and is followed by an exothermic, -48 kJ mol^{-1} , silane insertion step.⁵⁵ A strong argument against the silylene mechanism is that it requires two available covalent bonds on the metal, whereas Tilley's studies clearly demonstrated catalytic activity with $\text{CpCp}'M(R)\text{Cl}$ ($M = \text{Zr, Hf}$ and $R = \text{H, SiR}_3$ or alkyl) complexes, which have only one reactive bond.^{20,21,24} The possibility of a propagation of the polysilicon chains by coupling of silyl radicals was mentioned briefly in conjunction with the metal-silylene mechanism and was not tested experimentally.⁵⁴

1.2.3 Towards More Active Catalysts

Although the mechanism of the dehydrocoupling reaction is still under discussion, the most widely accepted one is a constant oxidation state σ -bond metathesis^{14,20,21} with a transition state similar to that postulated for Ziegler-Natta olefin polymerization. Much of the progress in the field has been based on the results of experimental measurements and theoretical calculations performed for the Ziegler-Natta catalysts.

The highly active olefin polymerization catalysts are believed to be 14-electron cationic Cp_2MR^+ complexes of group 4 or actinide metals, or the neutral $\text{Cp}_2\text{M}'\text{R}$

isoelectronic compounds of group 3 or lanthanide metals.^{56,57} Their activity is attributed to the high degree of electronic and steric unsaturation, which should be an important factor for dehydrogenative silane polymerization as well.

The goal of this thesis is to investigate the possibility of applying such catalysts to dehydrocoupling of silanes, to optimize the reaction conditions, and to get some insight into the factors governing them.

1.2.4 An Outline of the Thesis

There are a number of strategies which have been used to synthesize cationic Ziegler-Natta catalysts, which can also be used in polymerization of silanes. These strategies will be reviewed further on in this chapter. The results of dehydropolymerization of silanes with such catalysts are discussed in Chapter 6. Investigation of the nature of the active catalyst and the possible catalytic intermediates, reported in Chapter 2-4, lead us to isolation of a novel cation-like metallocene with a silyl ligand, which bears significant positive charge on silicon. The literature precedents for the existence of such silicon cations (silylium ions) in condensed phase is reviewed in Chapter 1. A new mechanism for the reaction of cation-like zirconocenes with primary silanes, based on kinetic and spectroscopic study, is presented in Chapter 5. Finally, Chapter 7 contains conclusions, contribution to original knowledge, and suggestions for future work. The conclusions section parallels and, sometimes, repeats individual conclusions made in every chapter (paper), but the general conclusions are more consistent and put everything in perspective.

1.3 Cationic Group 4 Metallocene Complexes

Since Ziegler's discovery of polymerization of ethylene with the $\text{TiCl}_4\text{-AlClEt}_2$ catalyst in 1954, olefin polymerization has developed into a giant industry. A significant share of it is now dominated by metallocene-based catalysts, which are, or are believed to be, cationic species. Naturally, the amount of literature on this subject is enormous. Most of it deals with applied aspects and elaborate blind optimizations of the catalyst performance, and is not discussed herein. A number of recent reviews can be recommended instead.^{57,58} The discussion in this section will address only the basic synthetic pathways and main structural types of the cationic Group 4 complexes, with a special emphasis on applied aspects, such as catalytic activity and solubility. For a more detailed account of such compounds the following literature can be recommended.^{56,59-61} Surface-bound metal hydrocarbyls can be also viewed as cationic species,⁶² but little is known about their structure, and the present discussion will be limited to the individual molecular compounds.

1.3.1 Basic Synthetic Routes to Cationic Group 4 Complexes

1.3.1.1 Synthesis of Cationic Group 4 Complexes via Ligand Abstraction by a Neutral Lewis Acid

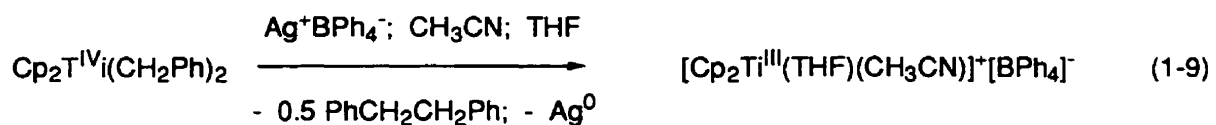
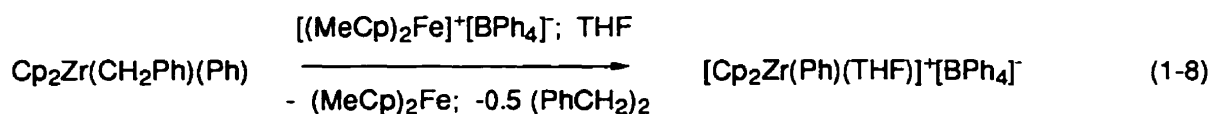
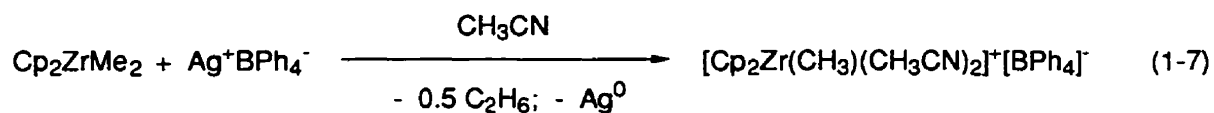
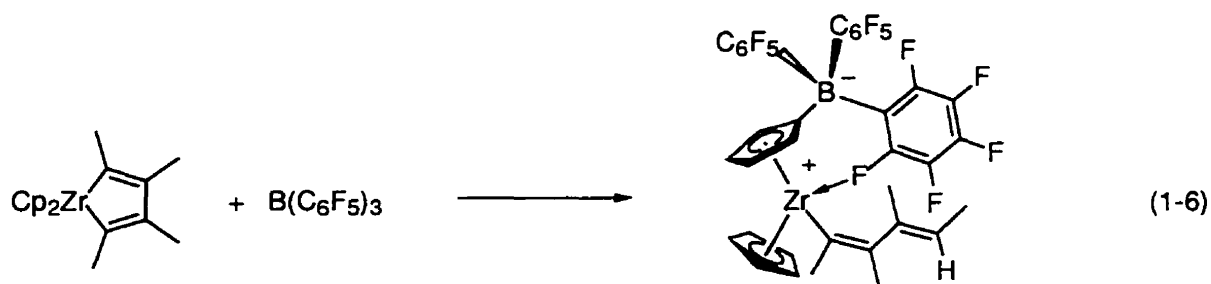
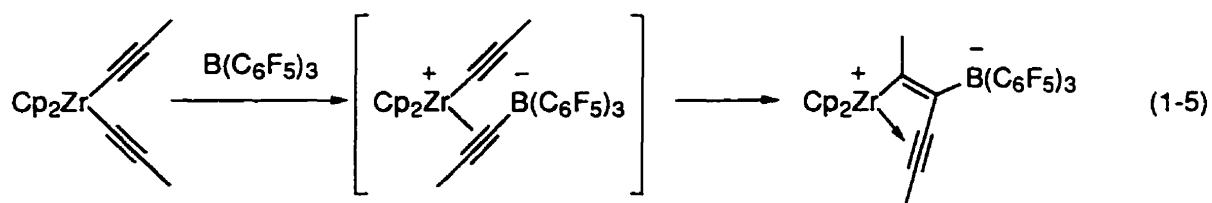
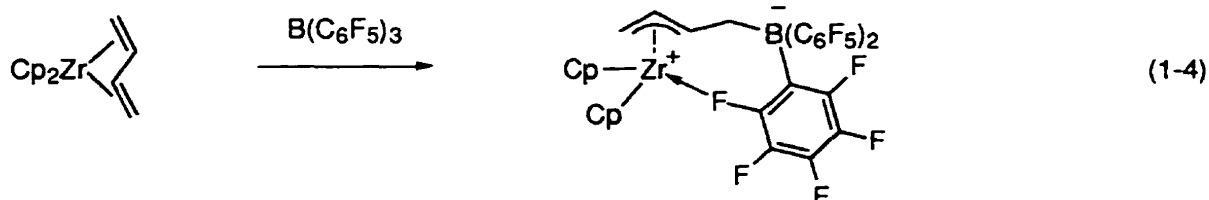
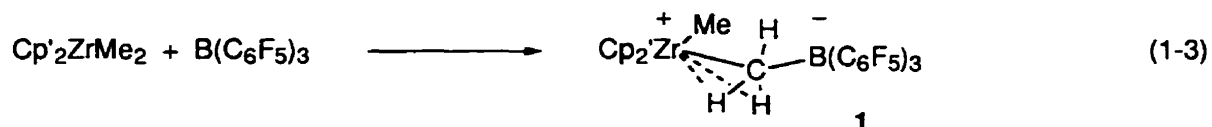
The oldest and the most widely used route to cationic group 4 compounds in industry is the reaction of an M-R bond with a strong, neutral Lewis acid, AlR'_3 (where $\text{R}' = \text{Alk, Cl}$) or methylaluminoxane (MAO) (eq 1-2). The first, well-characterized examples of cationic complexes were isolated from such Ziegler-Natta type systems. Kaminsky *et al.* reported $[\text{Cp}_2\text{ZrCH}_2\text{CH}(\text{AlEt}_2)_2]^+[\text{Cp}]^-$ in the reaction of Cp_4Zr and AlEt_3 ^{63,64} and Eisch *et al.* synthesized $[\text{Cp}_2\text{TiC}(\text{SiMe}_3)=\text{C}(\text{Me})(\text{Ph})]^+[\text{AlCl}_4]^-$ via a reaction of Cp_2TiCl_2 with $[\text{AlMeCl}_2]_2$ and $\text{Me}_3\text{SiC}\equiv\text{CPh}$.⁶⁵ However, most of the Al-containing systems give

complex mixtures of products, which prompted the development of new synthetic strategies and new weakly coordinating anions for model studies.⁶⁶ Marks and coworkers recently introduced an isoelectronic Lewis acid, $B(C_6F_5)_3$, which acts similarly to MAO, but furnishes individual molecular compounds (eqs 1-3 and 1-4).⁶⁷ Depending on the ligand environment of the metal, the product can be a zwitterion **1**^{67,68}, a tight ion pair **2**,⁶⁹ or completely ionic compound **3**.⁷⁰ All kinds of nonpolar solvents, including alkanes, can be used since the starting borane is neutral and extremely soluble. Half-sandwich and nonsandwich (alkyl- and alkoxide-) complexes, **4** and **5**, can be synthesized by the same route from suitable precursors.⁷¹⁻⁷⁴ Reactions are generally quantitative and instantaneous with no byproducts being formed (some reduction was reported for Cp^*TiMe_3 and $Cp^*Ti(CH_2Ph)_3$ complexes^{75,76}), which makes this route an excellent method for *in situ* generation of the base-free cationic catalysts. However, caution should be used when unsaturated σ -ligands are attached to the metal center. Abstraction of such ligands with borate often leads to zwitterionic compounds, which further undergo unexpected intramolecular rearrangements and C-C coupling reactions (eqs 1-5 and 1-6).⁷⁷⁻⁷⁹

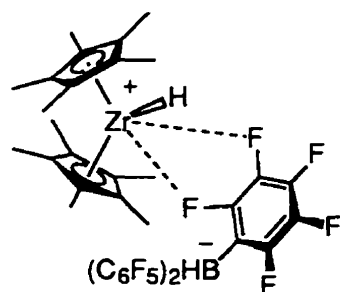
Other neutral Lewis acidic metal halides, e.g. $SbCl_6$, can be used instead of $B(C_6F_5)_3$, but they have little if any advantage over it. The products $[(CpTiCl_n(MeCN)_m)[SbCl_6]_{3-n}]$, where $n = 1-3$, $m = 3-5$ are crystalline, but NMR studies indicate tight coordination of the counterion in solution.⁸⁰

1.3.1.2 Oxidative Cleavage of M-R Bonds of Group 4 Complexes

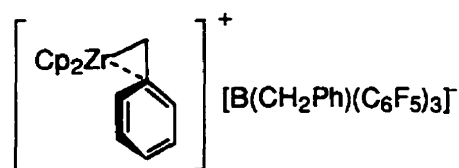
One-electron oxidizing agents such as Ag^+ and Cp'_2Fe^+ (where $Cp' = Cp$, or $MeCp$) can be used to cleave metal-carbon and metal-silicon⁸¹ bonds of symmetric Cp''_2MR_2 and asymmetric Cp''_2MRR' ($M = Zr$ and Hf , $Cp'' =$ substituted Cp 's and indenyls) metallocenes,⁸²⁻⁸⁷ $CpZrR_3$ half-sandwiches,^{86,88} and $Zr(CH_2Ph)_4$ tetraalkyl



complexes⁶⁰ (eqs 1-7 and 1-8). The reaction is believed to proceed via an outer-sphere one-electron transfer, followed by a loss of R^\bullet radical. Quantitative studies are in good agreement with the Marcus theory both for homogeneous (Cp'_2Fe^+), and heterogeneous (rotating Pt electrode) oxidation processes.⁸⁹ The ease of Zr-R bond cleavage by Cp'_2Fe^+ reagent is governed by a combination of the Zr-R bond strength and the stability of the formed radical R^\bullet : $Zr-CH_2Ph > Zr-CH_3 > Zr-Ph$.⁹⁰ Surprisingly, $Cp_2Zr(Me)Ph$ mainly undergoes an oxidative cleavage of the Zr-Ph bond instead of Zr-Me.⁹⁰



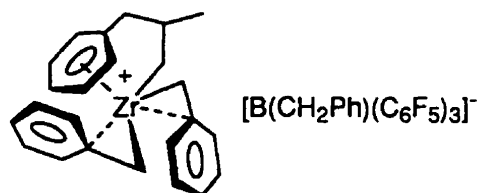
2



3



4



5

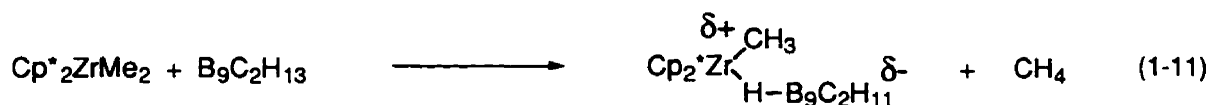
Cationic metallocene complexes are strong Lewis acids, and often tightly coordinate or react with their counterions (BF_4^- , PF_6^- , $SbCl_6^-$, ClO_4^- , $HC(SO_2CF_3)_2$, or $CF_3SO_3^-$).^{80,81,84,91-94} It is preferable to use weakly coordinative, inert anions such as BPh_4^- . The use of the unsubstituted ferrocenium salt is limited due to its poor thermal stability,⁶⁰ whereas Ag^+ oxidants can be used only in CH_3CN , which often inserts in the M-R of the resulting cationic metallocene.⁶⁰ Further, Ag^+ salts are light sensitive, which makes them even less convenient reagents. $[MeCp_2Fe]^+[BPh_4]^-$ proved to be the most

useful oxidizing agent as it is thermally stable and can be used in THF, CH₂Cl₂, and toluene.^{60,82}

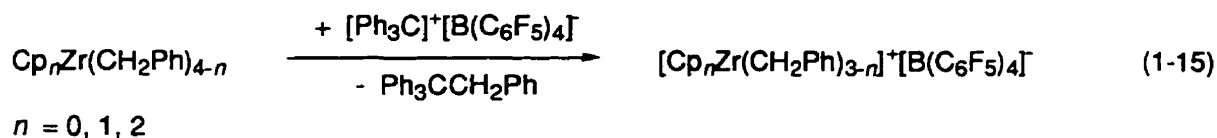
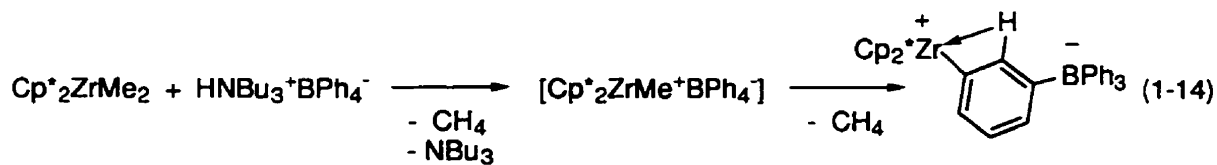
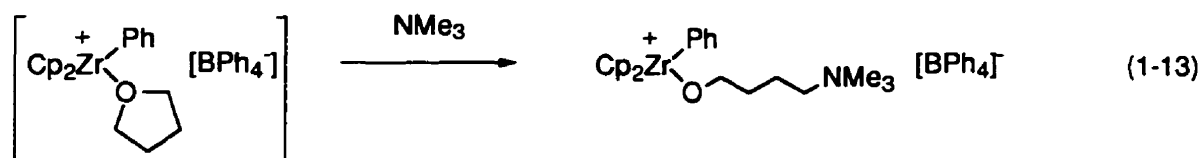
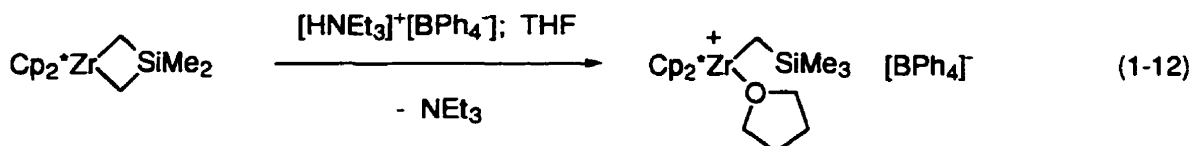
Oxidation of titanocenes generally does not lead to cationic complexes. For instance, reaction of Cp₂TiMe₂ with Ag[BPh₄] is sluggish,⁹¹ and oxidation of Cp₂Ti(CH₂Ph)₂ yields Ti(III) products instead (eq 1-9).^{60,95} In this case, one-electron oxidation induces net reductive elimination. However, electrochemical oxidation of Cp₂TiCl₂ proceeds smoothly in CH₂Cl₂ and CH₃CN to furnish Cp₂TiCl(solvent)⁺ products.⁹⁶

1.3.1.3 Brønsted or Ionic Lewis Acid Induced Cleavage of M-R Bonds

Cationic group 4 complexes can also be synthesized by reaction of Brønsted acids (carboranes with acidic protons⁹⁷, or [HNR₃]⁺[X]⁻, where X = BR₄ or metal dicarbollide^{98,99}) with Cp'₂MR₂ metallocenes,^{90,100-102} CpMR₃ half-sandwiches,^{103,104} MR₄ nonsandwich (alkyl- and alkoxide-) complexes,^{74,103} and LMR₂ porphyrin or aza-macrocycle complexes¹⁰⁵ (eqs 1-10 - 1-12). The order of reactivity with unhindered reagents is Zr-Ph > Zr-CH₃ > Zr-CH₂Ph,⁹⁰ which is opposite to the one observed for oxidative cleavage, and parallels the order for the acidolysis reactions of main group organometallics.¹⁰⁶ Bulkier ammonium salts (HNⁿBu₃⁺ or HNMe₂Ph⁺) and less coordinative anions (BPh₄⁻, B(C₆F₅)₄⁻, carboranes, or (dicarbollide)₂M, where M = Fe, Co) provide more general routes with less side reactions.^{60,107}



The Lewis acidity of such cationic complexes is so high, that they often attack their own ligands (Cp*,¹⁰⁸ Me¹⁰⁹) and solvents (haloalkanes and THF) (eq 1-13).⁹⁰ The base-free 14-electron species even react with such fairly inert anion as BPh₄⁻. For example, Turner obtained a zwitterionic compound Cp*₂Zr⁺(3-C₆H₄)BPh₃⁻ as a result of Zr⁺ electrophilic attack on the arylborate (eq 1-14).⁹⁷



The protolytic route often provides better yields than the oxidative path, especially for titanocene complexes, where cationic compounds can be obtained practically without any reduction to Ti(III).¹⁰² The major disadvantage of the protolytic reagents, [HNR₃]⁺[X]⁻, is the inevitable presence of the conjugate base, amine, which can coordinate to the metal center and reduce its electrophilicity and reactivity, *vide infra*. This problem is avoided by using Lewis acidic reagents, [Ph₃C][BR₄],¹¹⁰⁻¹¹² which do not generate any donor byproducts (eq 1-15). This route is one of the most general and convenient.

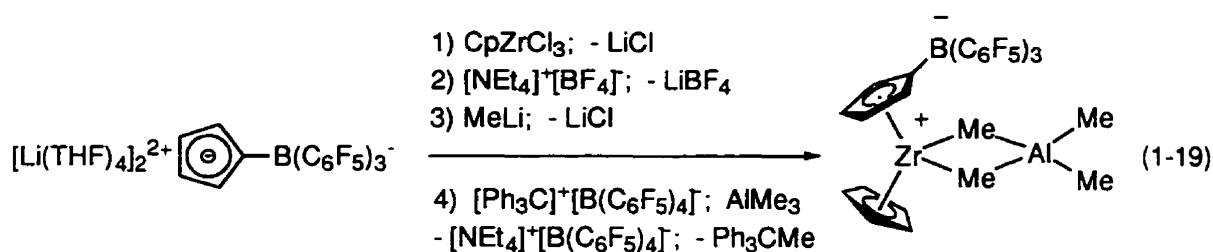
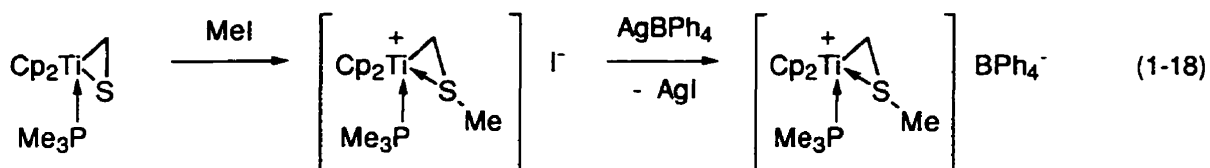
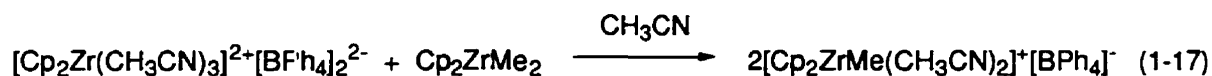
1.3.1.4 Other Routes

A neutral donor assisted salt metathesis reaction between $\text{Na}[\text{BPh}_4]$ and $\text{Cp}_2\text{Ti}(\text{R})\text{Cl}$ in the presence of phosphines, nitriles, or pyridine furnishes base-stabilized cationic metallocenes (eq 1-16).^{91,100} The yield strongly depends on the steric and donor properties of the neutral base, e.g. weakly basic THF and crowded phosphines like PPh_3 and $\text{Me}_2\text{PCH}_2\text{CH}_2\text{PMe}_2$ fail to react. Cationic Ti(III) compounds can be prepared via the same route from $[\text{Cp}_2\text{Ti}^{\text{III}}\text{Cl}]_2$ and $\text{Na}[\text{BPh}_4]$, or from Cp_2TiCl_2 , Zn dust and $\text{Na}[\text{BPh}_4]$.^{113,114} Other salts, such as $\text{Ag}[\text{BPh}_4]$ and $\text{Tl}[\text{BPh}_4]$, have proved to be inefficient, and neither of these reactions has been useful for the synthesis of mono cationic zirconium complexes.⁶⁰ However, dicationic titano- and zirconocene complexes can be synthesized from metal halides and $\text{Ag}[\text{BPh}_4]$, AgOTf , or AgAsF_6 .¹¹⁵⁻¹¹⁷ These compounds can further react with neutral metallocenes to yield monocationic products through comproportionation (eq 1-17).¹¹⁵ Other reagents, e.g. AgPF_6 and AgBF_4 , have a very limited usage since the resulting cationic metallocenes are unstable due to the side reactions with their anions.^{84,118} A number of salts (activity: $\text{AgClO}_4 \geq \text{AgOTf} > \text{AgSbF}_6 > \text{AgPF}_6 \gg \text{AgBF}_4$) have been used with $\text{Cp}_2\text{Zr}(\text{H})\text{Cl}$ for *in situ* generation of cationic catalysts, but no characterization of the resulting organometallic species has been done.¹¹⁹

Base-stabilized cationic metallocenes can be prepared via oxidation of neutral M(III) metallocenes (Cp^*_2TiMe ¹²⁰ or $[\text{Cp}_2\text{ZrCl}]_2$ ⁶⁰) by AgX ($\text{X} = \text{BPh}_4^-$, BF_4^- , or ClO_4^-) in donor solvents. The reagent $[\text{HNEt}_3]^+[\text{Fe}(\text{B}_9\text{C}_2\text{H}_{11})_2]^-$ can act as an acid and an oxidant at the same time. Thus one equivalent of it converts two equivalents of $\text{Cp}^*_2\text{ThMe}_2$ into $[\text{Cp}^*_2\text{ThMe}]_2^{2+}[\text{Fe}(\text{B}_9\text{C}_2\text{H}_{11})_2]^{2-}$.⁹⁹ The oxidation methods, however, have very few applications due to the limited number of easily accessible low valent starting compounds.

Grubbs *et. al.* synthesized a cationic titanocene complex from $\text{Cp}_2\text{Ti}(\eta^2\text{-SCH}_2)(\text{PMe}_3)$ and methyl iodide (eq 1-18).¹²¹ The anion, I^- , can be further

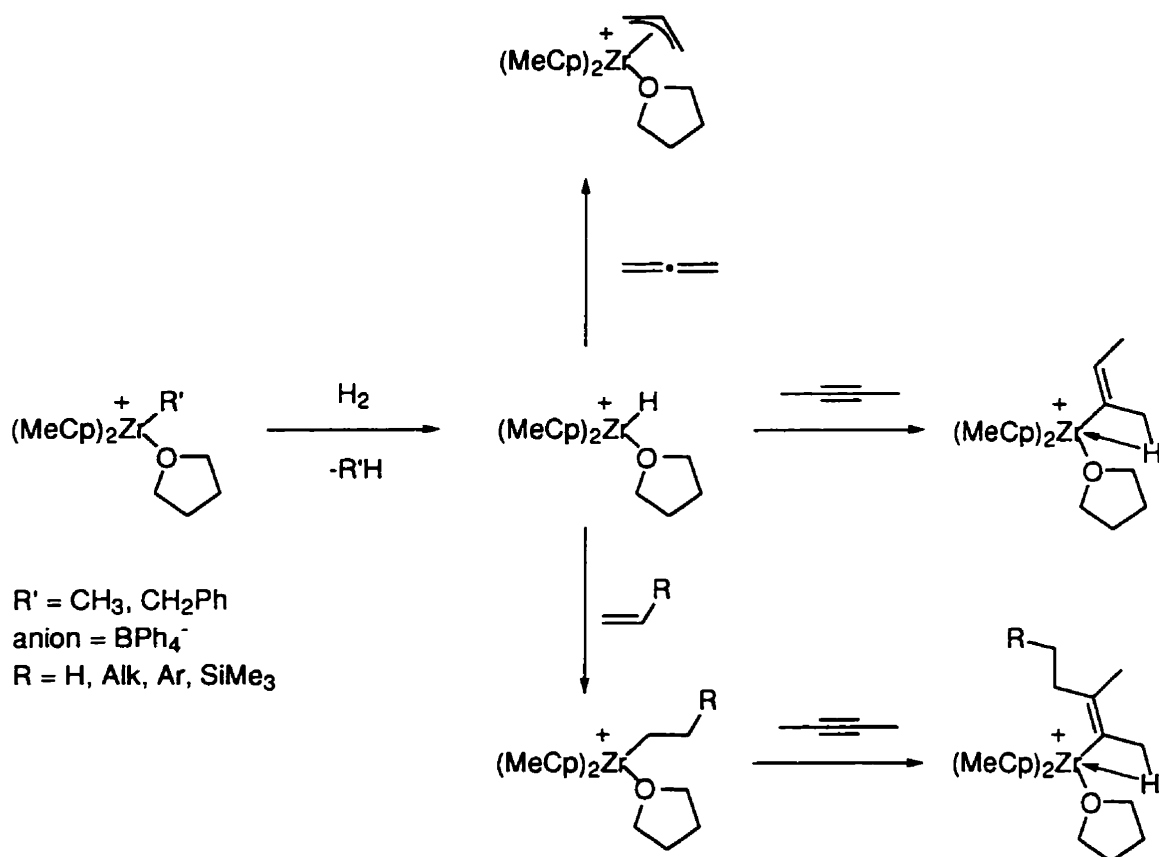
exchanged for the less coordinative BF_4^- or BPh_4^- via reaction with the appropriate silver salt.



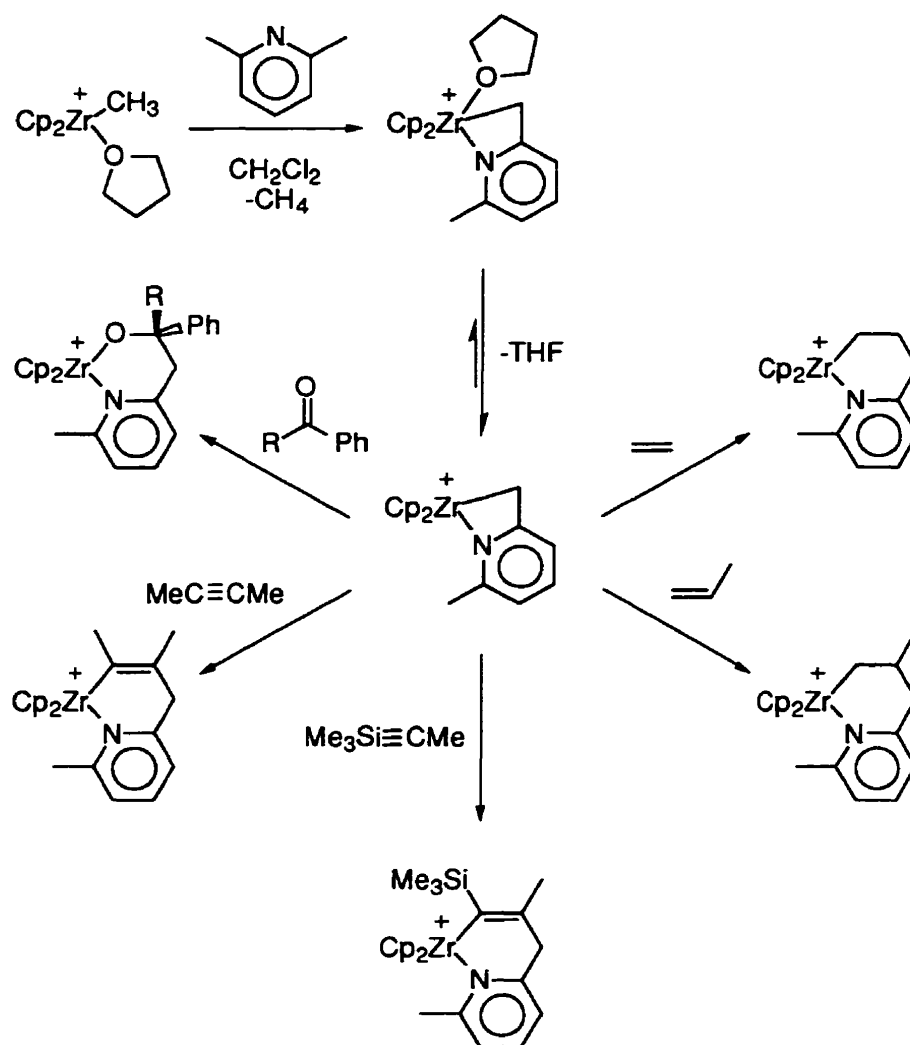
Zwitterionic complexes, in which borate anion is a substituent in the Cp ring, were prepared according to equation 1-19.¹²² Alternatively, a borate substituent can be attached to the Cp ring via $[(\text{C}_6\text{F}_5)_2\text{BH}]_2$ hydroboration of metallocenes with (alkenyl)cyclopentadienyl ligands.¹²³ Other polydentate ligands (e.g. alkenyl or butadienyl) can be also modified to accommodate a borate moiety (eq. 1-4).^{68,124} Such complexes are promising one component catalysts for olefin polymerization.^{122,123,125} They are very soluble in hydrocarbon solvents and exhibit high activity.

1.3.1.5 Modification of Ligands at the Cationic Metal Center

Cationic metal hydrides can be synthesized from cationic metal alkyls by hydrogenolysis (Scheme 1-2).^{87,126} The former in turn are useful precursors for the synthesis of higher alkyl-, alkenyl-, and allyl-cationic metallocenes (Scheme 1-2),^{60,127} which are not available by other routes as the parent bis-hydrocarbyl compounds are often unstable. Most of these cationic zirconocenes with linear alkyl chains are stable, but the ones which are branched at the α -carbon undergo β -H elimination below room temperature.⁶⁰



Scheme 1-2 Modification of ligands at the cationic ZrH center



Scheme 1-3 Modification of ligands at the cationic ZrC center

Cationic metal alkyls also react with alkenes and alkynes (including alkynylmetal complexes) via CH activation and single, or multiple insertion routes and furnish cationic alkenyl, allyl, and alkynyl metallocenes.^{105,128-136} CH activation can be significantly facilitated by chelating effects. Thus N-heterocycles react with $\text{Cp}_2\text{ZrMe}(\text{THF})^+\text{BPh}_4^-$ to yield azazirconacycles,¹³⁷ which can further insert alkenes, alkynes, CO, nitriles and ketones, (Scheme 1-3).¹³⁸⁻¹⁴³ Acyclic cationic metal alkyls similarly insert CO, nitriles

and isonitriles,^{91,100,124a,127,144-147} unless the reaction is inhibited by a multidentate (e.g. allyl) ligand.¹⁴⁸

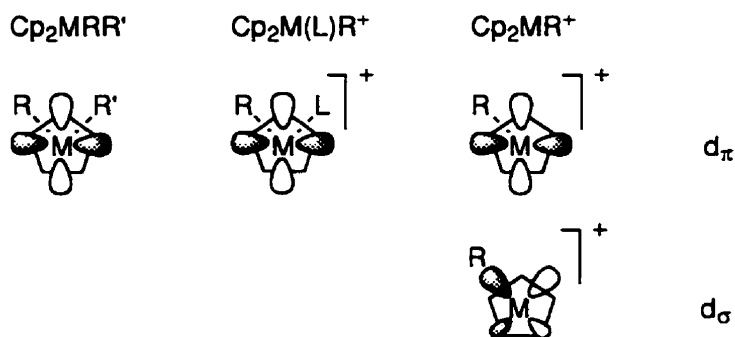
Cationic alkoxy- or thiolatometallocenes can be synthesized by alcoholysis of the metal-alkyl bond with bulky (e.g. ^tBuOH and ^tBuSH) reagents.^{149,150} Reactions with less hindered alcohols lead to intractable mixtures of unidentified products. Ring opening of THF also leads to cationic alkoxymetallocene products (eq 1-13).^{90, 151}

1.3.2 Structural Features of Cationic Group 4 Complexes

Neutral 16-electron group 4 metallocene complexes have one metal-centered LUMO localized in the equatorial plane of the sandwich (Scheme 1-4).¹⁵² The electronic structure of the base-stabilized cationic complexes, $\text{Cp}_2\text{M(L)}\text{R}^+\text{X}^-$, is similar, but the LUMO is stabilized by the metal charge, enhancing the Lewis acidity of the metal and making it more favorable for the incoming electron rich substrates. The base-free 14-electron species, $\text{Cp}_2\text{MR}^+\text{X}^-$, have two low-lying, empty orbitals, with the d_σ orbital (Scheme 1-4) being most suitable for the substrate coordination. Such metal centers are very electrophilic and in the absence of other substrates can tightly coordinate molecules of solvent, counterions, or chelate their own ligands (R or Cp). Needless to say, these interactions reduce the Lewis acidity of the metal and block coordination sites. Naturally, kinetic and thermodynamic aspects of such interactions are of great interest with respect to potential catalytic properties of the complexes. The following paragraph will briefly discuss the main examples of such compounds.

The geometry of the neutral group 4 metallocenes, $\text{Cp}'_2\text{MRR}'$, is pseudo tetrahedral, with the two Cp' ligands occupying one coordination site each, and the other two bonding (d_σ) orbitals, together with one nonbonding LUMO (d_π) orbital, lying in the bisectorial plane. In the cationic analogs, the second d_σ orbital is either used by a neutral donor ligand (pseudo tetrahedral geometry), or is not occupied (pyramidal geometry¹⁵³).

When the Cp' ligands are bulky, *e. g.* Cp*, the base-stabilized complexes have undistorted geometry, and no specific interactions with the counterion were found in the crystal structures.^{120,154} These compounds proved to be poor olefin polymerization catalysts, presumably for steric reasons. For ligands with an α -heteroatom, the inertness can also be due to a partial double bonding, which blocks the only coordination site available. Thus, a short M-OR distance, such as observed for $[\text{Cp}^*_2\text{Ti}(\text{OH})(\text{H}_2\text{O})][\text{BPh}_4]\cdot 2\text{THF}$ and $[\text{Cp}_2\text{Zr}(\text{O}^t\text{Bu})(\text{THF})][\text{BPh}_4]$ indicates substantial π -bonding.^{120,149} The out-of-bisectorial plane orientation of the THF ligand in $\text{Cp}_2\text{ZrMe}(\text{THF})^+[\text{BPh}_4]^-$, and THT (tetrahydrothiophene) in $\text{Cp}^*_2\text{ZrMe}(\text{THT})^+[\text{BPh}_4]^-$ also implies partial double bonding.^{85,155} Lack of any interactions with the counterion is thus usually indicative of a strong internal (steric or electronic) stabilization, which often results in poor reactivity.¹⁵⁵

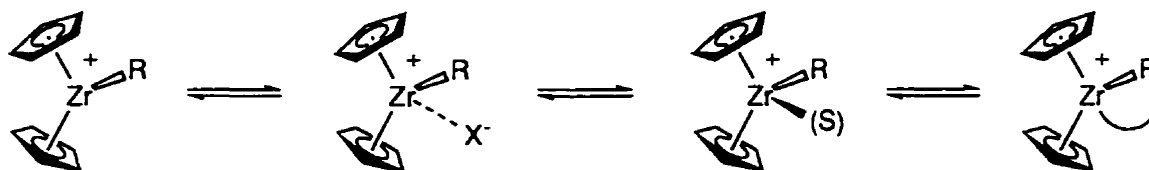


Scheme 1-4 Low-lying empty orbitals of d^0 neutral and cationic group 4 metallocenes

The unstabilized, or poorly stabilized compounds, on the other hand, inevitably develop cation-anion, cation-solvent, or cation-ligand interactions.¹⁵⁶ They can be viewed as the resting states of the active “naked” cationic catalyst, and the modalities of their equilibria (Scheme 1-5) are the key to the high performance catalysts.

Naturally, one of the most common interactions is the coordination of the counterion.¹⁵⁷ Thus tetraarylborates, BPh_4^- and $\text{B}(\text{C}_6\text{F}_5)_3(\text{CH}_2\text{Ph})^-$, can coordinate as an olefin, or an arene, (*e.g.* complexes **6**, **4** and **7**).^{71,73,103,158-160} Fluoro-substituted

tetraarylborates, $B(p\text{-C}_6\text{H}_4\text{F})_4^-$ and $B(\text{C}_6\text{F}_5)_4^-$, are less basic and less coordinative. Consequently, their complexes with zirconocenes are more potent polymerization catalysts than the $B\text{Ph}_4^-$ containing analogs. Nevertheless, there are several examples (2, 8 and 9) of close $M\cdots\text{F}$ contacts for such anions.^{69,161,162} In the case of $B(\text{C}_6\text{F}_5)_3\text{Me}$ borate, 1, the Me group forms a long and weak $\text{B-Me}\cdots\text{Zr}$ bridge in the solid state, and the complex is zwitterionic.^{67,70,163,164} However, it is believed to dissociate partially in solution. The ΔG for the ion pair dissociation in various $\text{Cp}'_2\text{ZrMe}^+\text{MeB}(\text{C}_6\text{F}_5)_3^-$ complexes was measured to be 14 to 20 kcal/mol, with the smaller values associated with the more polar (fluoro- and chlorocarbon) solvents.^{163,165-168} Marks *et al* have recently reported sterically hindered anions, $[\text{B}(\text{C}_6\text{F}_4\text{SiR}_3)_4]^-$, which are even less coordinative. Still, there is NMR evidence for the formation of tight ion pairs and anion coordination via fluorine contacts.¹⁶⁵

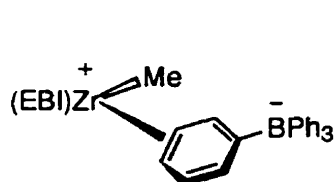


X^- = counterion; S = solvent

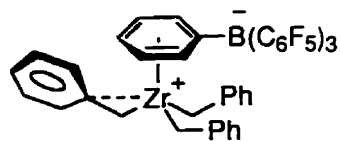
Scheme 1-5 Possible equilibria between “naked” cationic species and their adducts with counterions, solvent molecules, or chelation of their own ligands

Another class of weakly coordinating counterions is the cage carborane anion, which includes carboranyl and metal dicarbollide anions; e.g. $[\text{Cp}_2\text{ZrMe}]^+[\text{M}(\text{C}_2\text{B}_9\text{H}_{11})_2]^-$ ($\text{M} = \text{Fe}, \text{Co}, \text{or Ni}$) salts.¹⁶⁹ An equilibrium between tight- and solvent-separated ion pairs has been observed spectroscopically.¹⁶⁹ On the other hand, carboranyl anions have been shown to form single and multiple H-bridges with their counterions (10, 11),^{86,97,99} which for 11 results in low catalytic activity. As in the case of arylborates, the basicity of

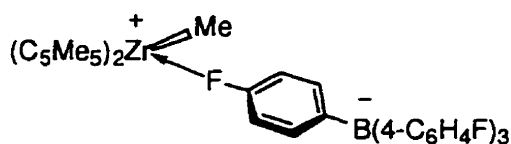
carboranyl anions can be reduced by electron withdrawing substituents (Cl, Br, or I).¹⁷⁰⁻¹⁷² Such anions, although they have so far not been used in group 4 cationic complexes, are very attractive for model studies, as they generally furnish high quality crystalline materials as opposed to perfluoroarylborate derivatives, which usually form oils.



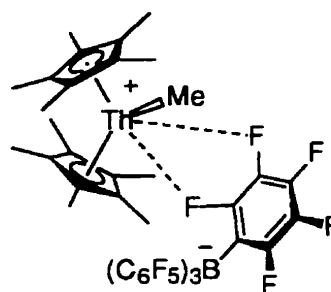
6



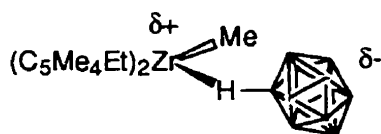
7



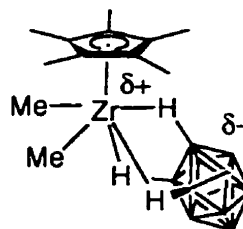
8



9



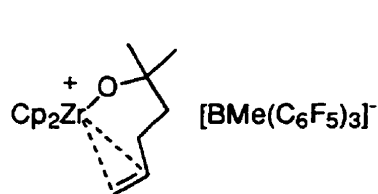
10



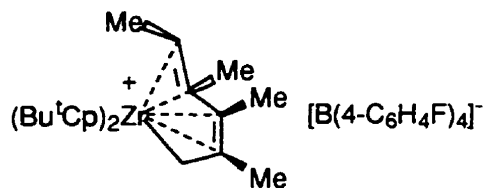
11

These weakly coordinative anions often lead to completely ionic compounds or ion pair equilibria,^{173,174} when a solvent (arene, THF, CH_3CN , or halocarbon) or any other component of the mixture (e.g. NR_3) can act as a neutral donor. Adducts of the type $[Cp_2ZrMe(L)_n]^+$ ($n = 1$ or 2) are formed.^{83,85} More basic donors (e.g. N^tBu_3) form

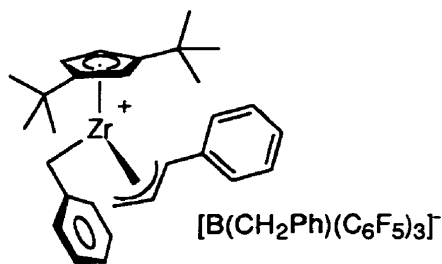
stronger adducts and shift the equilibrium towards donor stabilized free ions, but reduce the catalytic activity.^{107,175}



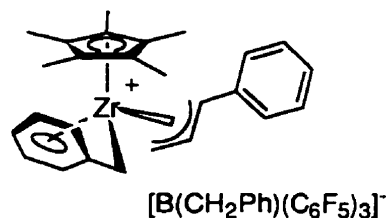
12



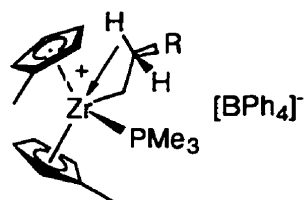
13



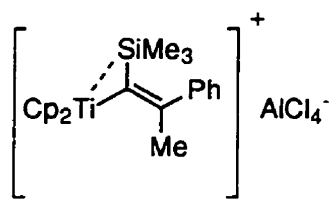
14



15



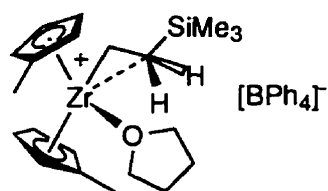
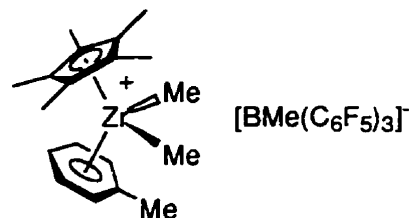
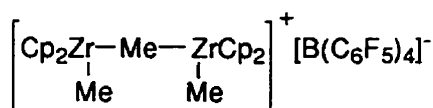
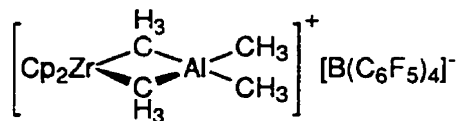
16



17

In contrast to hydride and methyl complexes, the longer chain hydrocarbyl ligands often stabilize their cationic central atoms internally by a π - (η^n -aryl,^{70,82,83,86,103,112,134,160,176-179} alkenyl,^{130,180,181} or alkynyl¹³⁰) or σ -electron (agostic CH,^{127,182,183} CSi^{65,161,184}, or SiCl¹⁸⁵) donation (e.g. **3**, **5**, **12-18**). When donation leads to conformational strain, it is not very strong and in most cases does not

poison the catalyst. On the contrary, it lends the necessary stabilization for the resting state preventing tight anion coordination, while yielding to an olefin substrate and providing excellent catalytic activity.¹¹² It is especially important for sterically unsaturated non-sandwich compounds, which otherwise form inert aryl complexes with the solvent, e.g. **19**.^{72,186} The conformationally nonstrained stabilizing interactions, such as in **5**, on the other hand, are at least as strong as the arene solvent complexes, and such compounds exhibit low catalytic activity.^{178,181} Thus solvent-free mono-Cp complexes are active for polymerization of styrene, propylene, and higher olefins, which cannot be polymerized with sandwich compounds, but the solvent-stabilized analogs are comparatively unreactive.^{186b}

**18****19****20****21**

Neutral metal alkyls, $\text{Cp}'_2\text{MR}_2$ and AlR'_3 , also can stabilize the cationic center (e.g. **20** and **21**)^{129,162,187,188} These adducts themselves do not have vacant coordination sites, but they are fairly unstable and easily liberate active catalytic species. It is believed that the large excess of MAO, used in the industrial Ziegler-Natta polymerization processes, is required mostly for this kind of stabilization.⁵⁹

1.3.3 Conclusions

The problem of choice of the strategy for the synthesis of cationic catalysts can be subdivided into the following:

- the anion: should be the least coordinating, and as inert as possible. Presently, the anions of choice are fluoroarylborates and halocarboranes.

- the solvent: should also be the least coordinating and as inert as possible (preferably an alkane), but should provide sufficient solubility for the reaction to occur. The choice of the solvent strongly depends on the choice of the reagent, *vide infra*.

- the cation generating reagent: should contain an anion of choice ($\text{Cl}_6\text{CB}_{11}\text{H}_6$ or $\text{B}(\text{Ar}^F)_4^-$) or its precursor ($\text{B}(\text{Ar}^F)_3$), and should not give any products capable of specific coordination (e.g. $[\text{Ph}_3\text{C}]^+$ is a more suitable cation than $[\text{HNR}_3]^+$). The best reagents are currently $\text{B}(\text{Ar}^F)_3$ and $[\text{Ph}_3\text{C}]^+[\text{X}]^-$. The former has an additional advantage: it is neutral and very soluble, which allows its use in virtually any solvent, including pentane and liquid ethylene, even at -197 K .¹⁷⁵

- the ancillary ligands: should provide sufficient steric and electronic protection, but should interfere as little as possible with the catalytic reactions of interest. This problem is the most difficult to address for a number of reasons. Firstly, there is an inherent contradiction between "sufficient protection" and "noninterference". Secondly, the delicate balance of steric and electronic effects strongly depends on the substrate and has to be determined individually for every reaction. Thirdly, the ligand environment (especially for the σ -ligands) can change in the course of reaction. The only obvious conclusion is, that the biscyclopentadienyl metallocenes have so far been the most versatile class of homogeneous ethylene polymerization catalysts. The half-sandwich- and tetraalkyl compounds are also promising reagents, but generally their stability and selectivity decrease with the decrease in the number of Cp ligands. Neither carbollide-, nor porphyrin-complexes have so far shown any interesting results. A slightly different, but very potent

class of catalysts are heterogeneous surface supported compounds. Unfortunately, these catalysts are less suitable for model studies and are not explored in the present thesis. There is however no doubt that supported catalysts have and will have very important industrial applications.

1.4 Quest for a Stable R_3Si^+ Ion in the Condensed Phase

Silicon is a close neighbor of carbon in the periodic table, and there is a certain similarity between them. It is thus tempting to assume that silylium cations play an essential role in reactions of organosilicon compounds, as carbenium cations do in organic transformations. According to the Pauling electronegativity scale, R_3Si^+ species should be formed even more easily than R_3C^+ . Indeed, the existence of silylium ions is well documented in the gas phase. However, the larger atomic radius makes trisubstituted silicon significantly more coordinatively unsaturated than its carbon analog. In the condensed phase this unsaturation is somewhat compensated for by coordination to a solvent molecule or a counterion, which is often followed by electrophilic attack of R_3Si^+ on such a coordinated neighbor. It is thus difficult to furnish conclusive evidence for the existence of silylium cations in solution. This problem has been intensively studied, but according to most reviewers, this is still one of the most controversial subjects in organosilicon chemistry, and the existence of stable R_3Si^+ is still questionable.¹⁸⁹⁻¹⁹³

Most of the early attempts to generate stable R_3Si^+ cations were unsuccessful, which is not surprising in view of the present knowledge on the behavior of silicon. Much work has been carried out to apply organic procedures of carbenium cation generation to silicon compounds. Conductance studies of Ar_3SiX compounds ($X = \text{halogen or OH}$) in solvents such as pyridine or liquid SO_2 proved that the Si-X bond is less susceptible to ionization than C-X in R_3CX compounds. "Super-acid" media, such as $FSO_3H-SbF_5-SO_2$, which were used for generation of numerous carbon cations, proved to be ineffective for silicon. Facile formation of silicon fluorides was observed instead. The strong affinity of Si for F also prohibited utilization of conventional "weakly coordinating" counterions such as BF_4^- and PF_6^- . It is now generally recognized, that no stable silylium species were generated in the above mentioned experiments. A thorough discussion of this history can be found elsewhere¹⁸⁹⁻¹⁹¹.

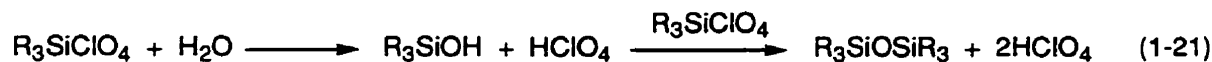
Various approaches were used to probe the existence of silylium ions. Reactions of halosilanes and silyl triflates with strongly Lewis acidic halides of boron, aluminum and antimony furnished polarized complexes instead of ionic compounds.¹⁹⁴⁻¹⁹⁷ Trapping experiments indicated participation of R_3Si^+ intermediates in various rearrangements.^{192,198,199} Kinetics of hydrogen abstraction reactions between R_3SiH and trityl carbenium cation were studied, and the results were interpreted in terms of a single electron transfer mechanism. Formation of silylium ion was considered to be the rate limiting step.²⁰⁰⁻²⁰⁴ A number of coordinatively saturated ($R_3L_2Si^+$ and $Cp^*_2SiH^+$) compounds have been synthesized and studied by X-ray crystallography,^{205,206} conductance measurements, molecular weight determination and various spectroscopic techniques.²⁰⁷⁻²¹³ Analytical characteristics and stability put these derivatives in a different class from R_3Si^+ compounds. One can regard them as trapped (donor stabilized) silylium intermediates, which are classified as siliconium ions.

All of these experiments lend some support to the concept of silylium ion as reaction intermediate. However, our primary interest in the following work is the existence of stable tricoordinated ionic compounds. A more detailed discussion of kinetic and trapping experiments is beyond the scope of this review.

1.4.1 Silylium Salts with Strongly Coordinating Counterions

In the 1980's, most attempts to generate R_3Si^+ cation were concentrated on silyl perchlorates. The earliest study of the ionic nature of these compounds dates back to 1957.²¹⁴ Chemical trapping experiments lead to the conclusion that $Ph_3SiOClO_3$ is a covalent compound, which was confirmed by subsequent NMR spectroscopy and conductance measurements.²¹⁵ The solid state structure unambiguously proved the covalent nature of this compound.²¹⁶ However, more recently Lambert and coworkers revised these studies and reported the presence of ion pairs in diluted solutions.²¹⁷⁻²²⁰

These studies are based on generation of silyl perchlorate by Corey's method²²¹ from R_3SiH and trityl perchlorate (eq 1-20, $R = Me, Ph, EtS, \text{ or } Pr^iS$). The nature of the bonding was probed by conductance measurements, molecular weight determination and multinuclear NMR spectroscopy. Although, at first glance, these three methods seem to contribute independent results, this is not the case. All suffer from the same major drawback - artifacts which can be due to hydrolysis instead of ionization. Indeed, the only solid conclusion which can be drawn from all these experiments, is that dilute solutions of R_3SiClO_4 contain ionic species. As shown in equation 1-21, hydrolysis can mimic this result and produce ionic compounds which are independent of the silylium cation. The reported precautions are insufficient to exclude the possibility of partial hydrolysis for such dilute samples, *vide infra*. The following is a critical review of these experiments according to the method used for the measurements.



1.4.1.1 Conductance Measurements

Perhaps the most misleading results of the nature of bonding in the silylperchlorates were generated by the conductance measurements. Numerous experiments have been carried out with various silyl (Me_3Si , Ph_3Si , $(Pr^iS)_3Si$ and $PhMe_2Si$) perchlorates and triflates in dichloromethane, sulfolane and acetonitrile. The high conductance of the studied solutions²¹⁷⁻²²⁰ is certainly a good indication of ionization. On the other hand, it tells nothing about the nature of such ionic species, as there are no means to follow the purity and preservation of the starting compound after numerous dilutions and electrochemical reactions. Judging from the experimental details, a routine syringe and rubber septa

technique was used for these measurements, and no special purification of the inert gas was done. Unfortunately, any single transfer operation with this level of precautions can introduce a considerable amount of contamination. For example, the degree of hydrolysis for trimethylsilyl perchlorate in "dry" dichloromethane and sulfolane was measured by proton NMR studies and found to be in the range of 10 to 50 %.²²⁰

1.4.1.2 Molecular Weight Determinations

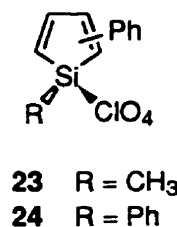
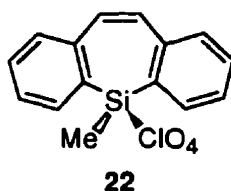
Molecular weight determinations were carried out for $R_3SiOClO_3$ ($R = Pr^iS$, Me or Ph) in sulfolane by the depression of melting point.^{217,218,220} The data fit a two particle model (ionic) with an error of 2-7 % ; one (covalent) and three (ionic dimer) particle models deviate by 50 and 20 %, respectively. There is a certain lack of consistency among these results and conductance measurements. Thus, Me_3SiOTf in sulfolane exhibited high conductance (ionic) yet the MW fits a one particle model (covalent) at the same time. It is also not clear why it should be a two particle model, since the other techniques indicated an equilibrium mixture of covalent and ionic species with less than 60 % dissociation.²²²

The concentration range of 0.02-0.05 M imposes the same problem of hydrolysis and reliability. The MW determination technique was based on the assumption of a pure compound in an ideal solution, whereas the actual system contained 1 equivalent of Ph_3CH and 1 equivalent of $R_3SiOClO_3$, which is in turn hydrolyzed to some extent. Besides, $R_3SiOClO_3$ and the hydrolysis products are dissociated to a certain degree, but well short of 100 %. It is thus not realistic to fit the system in a one or two particle formalism.

1.4.1.3 NMR Studies

Thorough NMR spectroscopic studies were performed with practically every magnetic nucleus of the silyl perchlorates. 1H and ^{13}C chemical shifts did not give any

conclusive evidence supporting the ionic model. The difference in ^{13}C chemical shifts between $\text{R}_3\text{SiOCIO}_3$ and the corresponding R_3SiH is in the order of 2-5 ppm,²¹⁷⁻²²⁰ which is in the reasonable range for a substituent effect. Dilution and solvent effects are even less pronounced: ± 0.1 ppm for ^1H and ^{13}C chemical shifts in the concentration range of 0.27-0.009 M²²⁰ and ± 0.15 ppm for the change in ^{13}C chemical shifts in going from CD_2Cl_2 to sulfolane. Although they have been interpreted in terms of ion-pair equilibria and charge delocalization, they could as well be attributed to normal solvent and dilution effects without any charged species involved. However, substituents do not participate much in charge delocalization and it is not surprising that the chemical shifts of these nuclei are not very sensitive to the presence or absence of positive charge on silicon. Similar trends have been observed for well defined carbenium ions.^{217,220}



The major difference between covalent and ionic models of silyl perchlorates is the share of positive charge on silicon, which makes ^{29}Si chemical shifts the only direct and sensitive method for probing the nature of bonding in solution. The ^{29}Si chemical shifts for naked Me_3Si^+ and Ph_3Si^+ were estimated to be 250 ± 25 and 125 ± 25 ppm, respectively, based on the correlation between analogous substituted silanes and methanes.²²³ Individual gauge for different localized orbitals (IGLO) calculations give an even more deshielded chemical shift for Me_3Si^+ , 355.7 ppm.¹⁹⁷ None of the silyl perchlorates exhibited chemical shifts close to the predicted values.^{197,217,219,220,224} $\text{Ph}_3\text{SiOCIO}_3$ gives a signal at 3 ppm^{217,219}, which is in very good agreement with the covalent structure identified by X-ray crystallography and solid state NMR spectroscopy

(1.4 ppm for ^{29}Si chemical shift).²¹⁶ Trimethylsilyl- and triisopropoxysilyl- perchlorates have chemical shifts of 47 and 18 ppm, respectively, as is expected for covalent compounds.^{220,224,225} No significant deshielding was observed for the ^{29}Si chemical shifts of **22-24** (23, 22.8, and 3.8 ppm, respectively).¹⁹⁷

$^{35}/^{37}\text{Cl}$ NMR spectroscopy was used as a symmetry probe for the counterion. Both magnetic isotopes of chlorine have large quadrupole moments. In so far as quadrupole relaxation is ineffective in a symmetrical tetrahedral environment, the linewidth for free ClO_4^- is significantly narrower than for asymmetrical covalent perchlorate. ^{35}Cl and ^{37}Cl NMR studies in sulfolane revealed a dramatic concentration dependence for $\text{Ph}_3\text{SiOClO}_3$ and $\text{Me}_3\text{SiOClO}_3$. The line width decreased from thousands to tens of Hz over a concentration range of 0.584-0.0047 M. The chemical shifts varied over a range of approximately 30 ppm shifting to lower field upon dilution.^{217,222} The degree of ionization was calculated to be about 50 % at approximately 0.03 M concentration and practically 100 % at about 0.005M. Lickiss pointed out that it is very strange for two sterically and electronically different compounds ($\text{Ph}_3\text{SiOClO}_3$ and $\text{Me}_3\text{SiOClO}_3$) to ionize to the same extent at the same concentration.¹⁸⁹ Another contradiction is between this ionization data and the ^{29}Si chemical shifts for $\text{Me}_3\text{SiOClO}_3$. According to Olah, the ^{29}Si chemical shift remained constant for neat trimethylsilyl perchlorate and for 0.584, 0.29 and 0.15 M solutions in sulfolane,²²⁵ but judging by ^{35}Cl and ^{37}Cl NMR studies these solutions are 20, 29 and 35 % ionized. Assuming a lower limit for the ^{29}Si chemical shift of Me_3Si^+ to be 225 ppm, the equilibrium mixture of ionic and covalent compounds should give average resonances at 82, 99 and 109 ppm, respectively.²²⁵ However, the chemical shift of 47 ppm was constant through the whole range of concentrations. Both Lickiss and Olah interpret these contradictions as a result of hydrolysis. The estimated level of residual water does not accurately account for the extent of "ionization" at all concentrations, but the experimental technique used leaves room for a larger uncertainty.

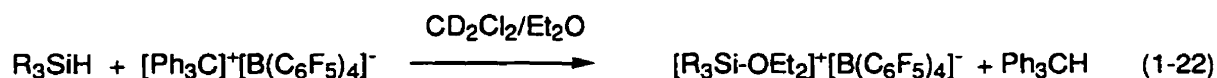
Solvent complexation was studied by conductimetric titration and ^{15}N NMR spectroscopy. Acetonitrile and sulfolane showed no evidence for complexation, whereas N-methylpyrrole and pyridine proved to form adducts.^{217,218,220,224} Based on more recent results and our present knowledge, it is hard to believe that highly electrophilic and coordinatively unsaturated R_3Si^+ does not expand its coordination sphere in the presence of a neutral donor ligand. A number of 4- and 5-coordinated siliconium cations stabilized by one or two nitrogen or oxygen containing ligands have been recently synthesized.^{207,209,211,212,226} Even weakly coordinative solvents such as toluene proved to form adducts of the type $\text{R}_3\text{Si}(\text{toluene})^+$, as shown by X-ray studies, *vide infra*.^{227,228} Lack of complexation with acetonitrile can thus be better explained by a covalent tetrasubstituted silyl perchlorate, which is less susceptible to solvent coordination, rather than by an ionic model.

Further support for covalent bonding between silicon and perchlorate came from solvolysis studies for $(\text{Me}_3\text{Si})_3\text{CSi}(\text{Me})_2\text{OCIO}_3$.²²⁹ If there is any silylium character in this compound, it is expected to be well ionized in good ionizing solvents such as MeOH and $\text{CF}_3\text{CH}_2\text{COH}$. An extremely rapid reaction between the ionized species and solvent would be expected. However, the half life in MeOH (1 M) is about 24 min and virtually no solvolysis occurs in $\text{CF}_3\text{CH}_2\text{COH}$ (0.052 M).

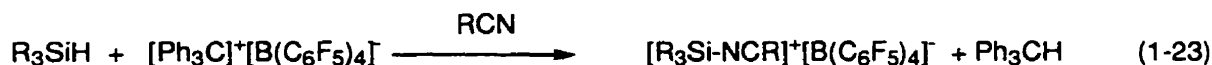
The extent of silylium character in solvated and solvent-free silyl halides and perchlorates has also been extensively studied by high level *ab initio* calculations, which invariably point to a lack of ionic nature in such species.²³⁰⁻²³² It is of interest, that the calculations predict large solvent shifts in the ^{29}Si resonances, even for covalent compounds. Silyl perchlorates in nucleophilic solvents form strong adducts with one or two solvent molecules (complexation energies can be as high as 100 kcal/mol). Such adducts can dissociate to form $\text{R}_3\text{Si}(\text{S})_n^+$ ions, but they have no silylium character, as the positive charge is largely transferred to the coordinated solvent molecules.

1.4.2 Silylium Salts with Weakly Coordinating Counterions

Design and development of highly active ionic catalysts has recently attracted much interest, as has the problem of weak interactions of counterions. Arylborates and carborane anions have been successfully introduced as weakly coordinating counterions for organometallic catalysts.⁶⁶ Following these reports, new attempts to generate stable silylium with these anions were undertaken.



$\text{R}_3 = \text{Me}_3, \text{Ph}_2\text{Me}, (2\text{-Thienyl})_2\text{Me}$



$\text{R}_3 = \text{}^t\text{Bu}_2\text{}^s\text{Bu}, \text{}^t\text{BuMe}_2, \text{Et}_3, \text{Ph}_2\text{Me}, \text{}^t\text{Bu}_2\text{H}, (\text{OCH}_2\text{CH}_2)_3\text{N}, (\text{EtO})_3$

Perhaps the first successful, although ill documented, step in this direction was done with tetraphenyl borate BPh_4^- .²²⁰ Unfortunately, the product was either not stable enough or not handled properly. A similar outcome resulted with tetrakis[bis(3,5-trifluoromethyl)phenyl]borate, $[\text{B}(3,5\text{-(CF}_3)_2\text{C}_6\text{H}_3)_4]^-$. The major decomposition pathway proved to be halogen abstraction (fluorine from anion or chlorine from CH_2Cl_2).^{226,233} Silylium salts were not isolated but in the presence of strong coordinating solvents, stable silyloxonium and silylnitrilium adducts were formed with cationic charge mainly localized on oxygen and nitrogen (eqs 1-22 and 1-23). The reactivity of short-lived intermediates formed in these transformations greatly contrasts with the behavior of the silyl perchlorates and is as high as one would expect from a true silylium.

Unfortunately, bonds like aromatic CH in tetraphenyl borate or aliphatic CF in $[\text{B}(3,5\text{-(CF}_3)_2\text{C}_6\text{H}_3)_4]^-$ react with silylium. One way to avoid this problem is to use tetrakis[pentafluorophenyl]borate $[\text{B}(\text{C}_6\text{F}_5)_4]^{-111}$ which has more robust aromatic CF bonds. Another class of inert weakly coordinating anions are halocarboranes.¹⁷² Trityl salts of both types of anions were recently used to generate silylium from hydrosilanes. The products were studied by single crystal X-ray diffraction and multinuclear NMR spectroscopy. Important structural and spectroscopic parameters of these compounds are listed in table 1-1.

In all cases described herein the silicon atom has three normal bonds to organic substituents and one significantly elongated bond to the solvent or counterion. The bond order of the latter is small and, sometimes, is closer to a weak interaction than a true chemical bond. The title compounds clearly have a high degree of cationic character. Thus, the structure of $[\text{Et}_3\text{Si}(\text{toluene})]^+[\text{B}(\text{C}_6\text{F}_5)_4]^-$ demonstrates that the $[\text{B}(\text{C}_6\text{F}_5)_4]^-$ anion has no significant interactions with silylium. In this respect, $[\text{B}(\text{C}_6\text{F}_5)_4]^-$ seems to be a less coordinating anion than halocarboranes which exhibit a highly elongated Si-X bond with one of the halogens. However, even in the case of $[\text{B}(\text{C}_6\text{F}_5)_4]^-$, silicon can not be considered as a pure planar three-coordinated silylium. The coordinative unsaturation is partially relieved by an interaction with a solvent molecule. Such bonding, in terms of Pauling's bond order, is weaker than bonding in the silylcarborates (table 1-1). On the other hand, the latter causes less distortion from planar geometry (table 1-1). ^{29}Si chemical shifts were also mooted in the argument for determining the current winner of the "silylium rush", and $[\text{}^i\text{Pr}_3\text{Si}]^+[\text{Cl}_6\text{CB}_{11}\text{H}_6]^-$ seems to outperform $[\text{}^i\text{Pr}_3\text{Si}]^+[\text{B}(\text{C}_6\text{F}_5)_4]^-$ by 7.4 ppm in the solid state. However, this is most likely an effect on the chemical shift of quadrupole chlorine nuclei in close vicinity to silylium in the former compound. The chemical shift tensor has a rather complicated relationship to structure, charge, orientation, counterion and solvent effects and is not a reliable gauge in a marginal case such as this, unless accompanied by adequate calculations. $[(\text{TMS})_3\text{Si}]^+[\text{B}(\text{C}_6\text{F}_5)_4]^-$ clearly demonstrates this

by having more than 200 ppm deshielding compared to the parent (TMS)₃SiH, while all other parameters indicate a normal bonding pattern.

Table 1-1. Spectroscopic and structural parameters for silylium salts

Compound	$\delta^{29}\text{Si}$, ($\Delta\delta^{29}\text{Si}$) ^a ppm, solvent	Si-L ^b , Å, (bond order) ^c , CSiC _{mean} , deg	ref
Solvent Separated Ion Pairs			
[Me ₃ Si(S)] ⁺ [B(C ₆ F ₅) ₄] ⁻	83.6, (101.1), C ₆ D ₆		234
[Et ₃ Si(S)] ⁺ [B(C ₆ F ₅) ₄] ⁻	92.3, (92.1), C ₆ D ₆	2.18, (0.28), 114.0	227,234
[ⁱ Pr ₃ Si(S)] ⁺ [B(C ₆ F ₅) ₄] ⁻	107.5, (95.5), C ₆ D ₆ 107.6, (95.5), none		234
[ⁱ Bu ₃ Si(S)] ⁺ [B(C ₆ F ₅) ₄] ⁻	99.5, C ₆ D ₆		234
[Me ⁱ Pr ₂ Si(S)] ⁺ [B(C ₆ F ₅) ₄] ⁻	96.9, (92.6), C ₆ D ₆		234
[Hx ₃ Si(S)] ⁺ [B(C ₆ F ₅) ₄] ⁻	90.3, (96.8), C ₆ D ₆		234
[MePh ₂ Si(S)] ⁺ [B(C ₆ F ₅) ₄] ⁻	73.6, C ₆ D ₆		234
[(TMS) ₃ Si(S)] ⁺ [B(C ₆ F ₅) ₄] ⁻	111.1, (228.5), C ₆ D ₆		234
[ⁱ Pr ₃ Si(S)] ⁺ [B(C ₆ F ₅) ₄] ⁻	94.0, (81.9), C ₇ D ₈		171
[ⁱ Pr ₃ Si(CD ₃ CN)] ⁺ [Br ₅ CB ₉ H ₅] ⁻	33.8, (21.7), CD ₃ CN	1.82, (0.71), 115.6	171
[^t Bu ₃ Si(OH ₂)] ⁺ [Br ₆ CB ₁₁ H ₆] ⁻	46.7, none	1.78, (0.79), 116.0	235
[Me ₃ Si(NC ₅ H ₅)] ⁺ [I] ⁻		1.86, (0.61), 113.5	236
Tight Ion Pairs			
[ⁱ Pr ₃ Si] ⁺ [Cl ₆ CB ₁₁ H ₆] ⁻	115.0, (102.9), none	2.32, (0.43), 117.3	237
[ⁱ Pr ₃ Si] ⁺ [Br ₆ CB ₁₁ H ₆] ⁻	109.8, (97.7), none 105.0, (92.9), C ₇ D ₈	2.48, (0.40), 117.0	170
[ⁱ Pr ₃ Si] ⁺ [I ₆ CB ₁₁ H ₆] ⁻	97, (84.9), none	2.66, (0.43), 115.6	237
[^t Bu ₂ MeSi] ⁺ [Br ₆ CB ₁₁ H ₆] ⁻	112.8, none	2.47, (0.42), 115.3	238
[^t Bu ₃ Si] ⁺ [Br ₆ CB ₁₁ H ₆] ⁻		2.47, (0.42), 116.2	238
[Et ₃ Si] ⁺ [Br ₆ CB ₁₁ H ₆] ⁻	111.8 and 106.2, ^d none	2.44, (0.46), 115.0 ^d 2.43, (0.48), 116.3 ^d	238
[ⁱ Pr ₃ Si] ⁺ [Br ₅ CB ₉ H ₅] ⁻	97.9, (85.8), C ₇ D ₈	2.46, (0.43), 115.8	171

$[\text{Ph}_3\text{Si}]^+[\text{OCIO}_3]^-$	3, (20), $\text{CD}_2\text{Cl}_2/\text{CD}_3\text{CN}$	1.74, (0.68), 113.5	²¹⁶
---	---	---------------------	----------------

^a $\Delta\delta = \delta(\text{R}_3\text{Si-L}) - \delta(\text{R}_3\text{SiH})$. ^bL - coordinated solvent (S) or counterion. ^cThe bond order was calculated by the equation derived by Pauling²³⁹ ^dThe structure contained two independent molecules.

Compounds listed in table 1-1 were claimed to be true or "closely approaching" silylium ions.^{170,171,227,228,237} The claim stirred a controversy and other research groups challenged those results on the basis of theoretical calculations and trapping experiments.²³⁹⁻²⁴³ The major discussion concentrated on the bonding pattern for the toluene molecule in $[\text{Et}_3\text{Si}(\text{toluene})]^+[\text{B}(\text{C}_6\text{F}_5)_4]^-$. Theoretical calculations favor carbocationic mesomer **25** over silylium **27** (Figure 1-1). Thus, the Wiberg bond index for the $[\text{SiH}_3(\text{benzene})]^+$ complex is 0.44, which indicates a relatively strong bond.^{240,241} A more careful comparison of the experimental results to the calculated ones reveals that the real $[\text{Et}_3\text{Si}(\text{toluene})]^+[\text{B}(\text{C}_6\text{F}_5)_4]^-$ in the solid state differs a bit from the gas phase calculated structure. The experimental bond distance between the *para*-C and Si is longer than the calculated value and the aromatic ring is less distorted, which favor mesomers with a weaker C-Si interaction (**26** or **27** over **25**). The Wiberg bond index should thus be smaller than 0.44 and closer to the Pauling bond order of 0.35²³⁹ or 0.28^{234,244} calculated for experimental structures. In addition, the calculated complexation energy for $[\text{Me}_3\text{Si}(\text{toluene})]^+$ is 23.0 kcal/mol, which is almost as low as those in typical van der Waals complexes (< 10 kcal/mol).²⁴² It is certainly true that an interaction with a bond order 0.28-0.35 can not be totally discarded. On the other hand, compounds like LiCl are often specifically solvated and have a similar bond order but are referred to as ionic structures. An X-ray crystal structure of $[\text{Et}_3\text{Si}(\text{toluene})]^+[\text{B}(\text{C}_6\text{F}_5)_4]^-$ is better described in terms of π -arene complex **26** with a positive charge primarily on silicon than σ -arenium **25**.^{170,234,244} The solid state ¹³C NMR spectrum does not indicate any significant charge

on toluene, which also supports mesomer **26**. The upper limit of dissociative exchange of toluene, estimated by dynamic NMR studies in solution (13 kcal/mol), is also consistent with this model.^{234,244}

Olah *et al* reproduced the synthesis of $[\text{Et}_3\text{Si}(\text{toluene})]^+[\text{B}(\text{C}_6\text{F}_5)_4]^-$, quenched the product with a hindered base, and obtained triethylsilyltoluene in 7 % yield.^{241a} This result, however, does not prove the nature of bonding between silicon and toluene in $[\text{Et}_3\text{Si}(\text{toluene})]^+[\text{B}(\text{C}_6\text{F}_5)_4]^-$, as both **25** and **26** are expected to give the same products from a basic workup, and no differentiation would be achieved.^{234,244}

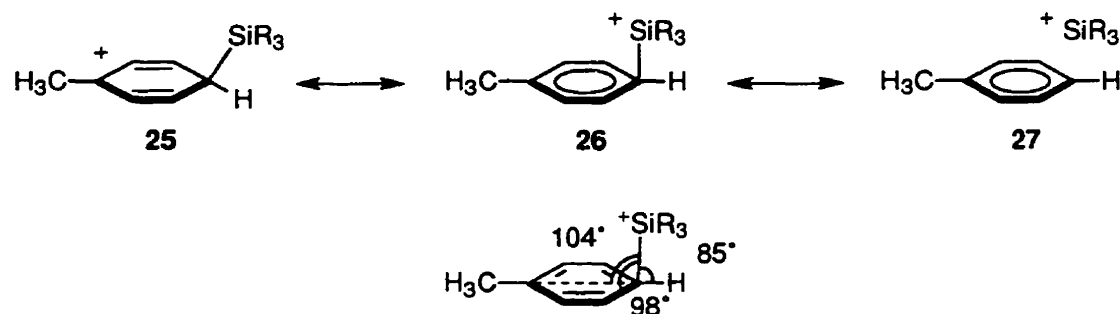


Figure 1-1. Proposed mesomer structures for $[\text{Et}_3\text{Si}(\text{toluene})]^+$.

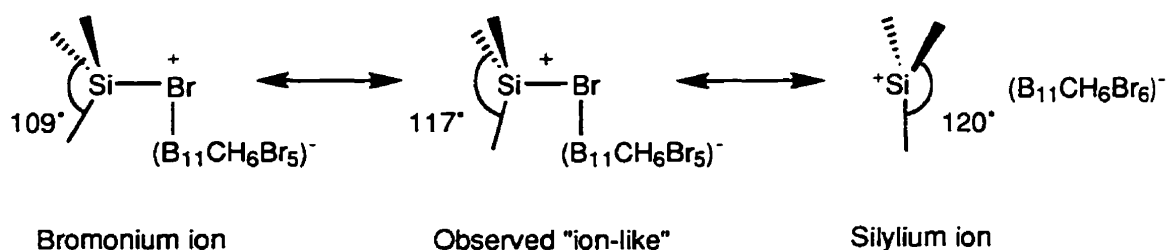
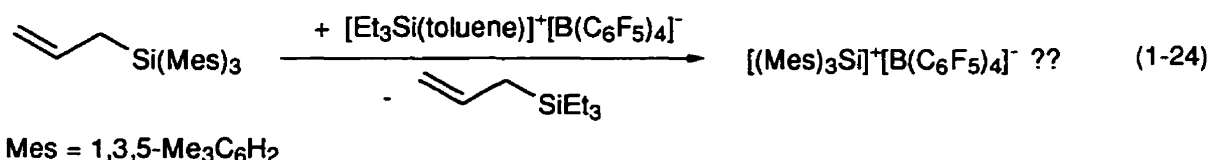


Figure 1-2. Proposed mesomer structures for $[\text{iPr}_3\text{Si}]^+[\text{Br}_6\text{CB}_{11}\text{H}_6]^-$.

The claim of silylium character of $[\text{iPr}_3\text{Si}]^+[\text{Br}_6\text{CB}_{11}\text{H}_6]^-$ and $[\text{iPr}_3\text{Si}]^+[\text{Br}_5\text{CB}_9\text{H}_5]^-$ salts was subjected to the same criticism. The tightly coordinated anion can be considered as the fourth substituent on silicon, and a substantial share of the positive charge might be localized on the bridging bromine. However, according to the

analysis of the structural features, these compounds lie on a continuum between a bromonium and a silylium ion (Figure 1-2), being closer to the latter, and the title of "closely approaching silylium ion" is thus perfectly valid.

Recently, Lambert *et. al.* utilized a new strategy for the synthesis of sterically hindered silylium compounds (eq 1-24).²⁴⁵ The product has an unprecedentedly high ²⁹Si NMR chemical shift of 225 ppm, which closely matches the estimations for a true Ar₃Si⁺. Unfortunately, attempts to crystallize it have so far been unsuccessful.



1.4.3 Silylium and Related Ligands in Organometallic Complexes

The problem with isolation of silylium ion is due in part to the lack of appropriate stabilizing substituents on silicon. Thus, C-C and C-H bonding orbitals, which play an important role in mesomeric and hyperconjugative stabilization of carbenium ions, are so different in energy and dimensions from silicon orbitals that they can at best provide a very poor stabilization.²³¹ Furthermore, carbon is more electronegative (2.55) than silicon (1.90) which causes inductive destabilization in hydrocarbyl-substituted silylium ions.²¹⁵ A better stabilizing substituent for silylium would be an element of the third or lower rows of the periodic table, which has orbitals of suitable energy and geometry. Highly electropositive character for such a substituent is also desirable. For example, extended Hückel calculations for [Co]- and [Mo]-SiR₂⁺ complexes predict silylium to be significantly stabilized by an interaction with the metal center.²⁴⁶ However, there are very few reports in which the existence of [M]-SiR₂⁺ has been postulated,²⁴⁷ and the only documented example is [(1,3,5-Me₃-C₆H₃)Ni(SiEt₂)₂]²⁺[AlCl₄]₂²⁻.²⁴⁸ Multinuclear NMR spectroscopy revealed a narrow ²⁷Al signal, characteristic of a symmetric AlCl₄⁻

environment and a deshielded ^{29}Si chemical shift at 111.0 ppm compared to 16.2 ppm in the starting $[(1,3,5\text{-Me}_3\text{-C}_6\text{H}_3)\text{Ni}(\text{SiCl}_3)_2]$, but no diffraction study was done. This report did not attract any criticism and no “chloronium versus silylium structure” discussions occurred. It is however reasonable to assume, that the titled compound bears a certain similarity to silylium perchlorates or halocarboranes, and silicon is at least partially coordinated to chlorine and is unlikely to be purely cationic. Besides, the electron-rich Ni can form double bonds with Si by donation of its nonbonding electron pairs, and the structure could be a hybrid of two mesomers, $[\text{M}^+=\text{Si}]$ and $[\text{M}-\text{Si}^+]$, more close to the former. Such base-stabilized²⁴⁹⁻²⁵⁴ and base-free²⁵⁵⁻²⁶¹ cationic silylene compounds, $[\text{M}^+=\text{Si}]$, are well known.

Recently, Berry *et. al.* isolated and structurally characterized a stable germyl cation bonded to tungsten, **28a**.^{262,263} The remarkable stability of this compound can be attributed to a strong hyperconjugation between an empty germyl- and a bonding W-H orbital. Such hyperconjugation also explains an unusual twisted geometry of the complex and a short Ge-W bond (2.487 versus 2.58-2.61 Å). As a result of these internal stabilizing interactions, the germyl cation is well separated from its counterion, even in the solid state. However, the “purity” of cationic character of germanium remains questionable, as another mesomeric structures with a positive charge on tungsten, **28b**, can be drawn (Figure 1-3).

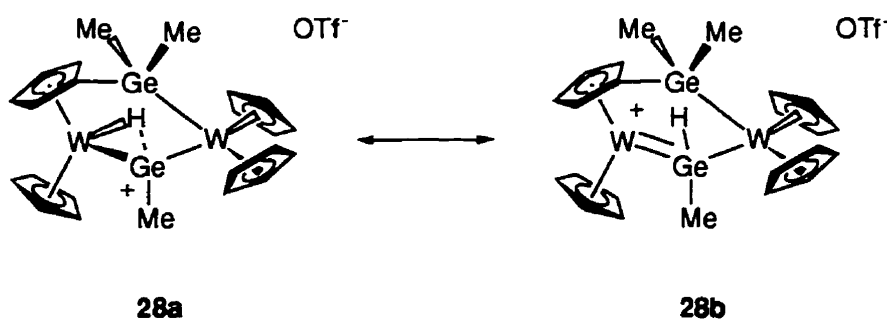


Figure 1-3. Proposed mesomer structures for **28**.

1.4.4 Conclusions

The controversy of the silylium quest arises from the definition of the goal itself. The idea of obtaining a literally naked charged particle in solution is rather absurd. Such a hypothetical ion will be inevitably surrounded by solvent and counterion molecules. The borderline between so called naked ions and ion pairs of various degree of association is arbitrary and deals with the distance between the positively charged center and any other atom in the close vicinity, which can be defined as truly nonbonding. The usual criterion is the sum of the van der Waals radii. However, species, which have no external stabilization within the van der Waals range, are stabilized internally. The borderline between an interaction and a bond for such internal stabilization is even more ambiguous, as a variety of partial delocalized single or multiple bonding patterns is possible.

Obviously, to achieve the highest degree of dissociation one must seek the least nucleophilic solvent and a counterion with the weakest coordinating ability. An ideal weakest coordinating ion should satisfy the following constraints: high kinetic and thermodynamic stability, low overall charge, large size and high charge delocalization.⁶⁶ Absence of basic sites (lone electron pairs) is also desirable, however certain halogenated carboranes proved to be among the least coordinating anions.^{170,171,237} The possibilities of designing new counterions seem to be endless, as is the quest for the ultimate naked silylium cation. However, it is worth keeping in mind that the goal itself is elusive, as naked particles do not exist in solution. From our point of view, charged silicon compounds with weakly coordinative anions recently characterized by Lambert and coworkers,^{227,228,234,244} and Reed and coworkers^{170,171,237} are best described as silylium ions. The charge distribution, oxidation states and bond polarities are formal descriptions which are anchored to the nearest extreme structure, e.g. in case of silylium compounds with weakly coordinative counterions, it is more appropriate to describe the bonding situation in terms of an ionic $[R_3Si]^+[X]^-$ rather than a covalent interaction.

"Cation-like" or "closely approaching the silylium ion" are also valid and are even more accurate names. But then, the terminology in organic chemistry should be revised accordingly, as a lot of carbenium ions are even less pure cations than these specially designed cases of silylium compounds.

Discussions of the ultimate purity of this or that quality are not new for chemistry. For instance, there is a long standing discussion of S_N2 versus SET mechanisms, which has very little chance to be won by one side or the other. Perhaps the most ridiculous one is a question of aromaticity. There are hard liners who argue that the only truly aromatic compound is benzene and even toluene deviates significantly enough and can not be considered absolutely aromatic. It is certainly true, that no matter how many experiments and calculations will be done, there is only one purest, least coordinated and 100 % cationic structural pattern. This uniquely successful candidate is a monoatomic, monocation in the gas phase under high vacuum conditions and the rest of the charged chemical particles are either stabilized by coordination or have some of the positive charge dissipated among the other atoms of the molecule, or by solvation, aggregation and other ambiguities.

What can we finally learn from all this? So far, there is no generally accepted criterion for the amount of electron density which still can be considered to be truly cationic. For instance, a discussion of whether a bond order of 0.28 is still a bond, or a +0.77 charge is still a cation can go on forever. (Most "ionic" inorganic compounds have even less positive charge than +0.77.) There is no well defined borderline here and any conclusion would be subjective. In my opinion, the answer to the old question "Do silylium ions exist in solution?" is yes, but they are more coordinatively saturated than their carbon analogs and, under equal conditions, tend to coordinate to solvent or counterion more strongly.

References

- (1) *Inorganic and Organometallic Polymers*; Zeldin, M.; Wynne, K. J.; Allcock, H. R., Ed.; American Chemical Society: Washington, DC, 1988.
- (2) Mark, J. E.; Allock, H. R.; West, R. C. In *Inorganic Polymers* Prentice Hall: Englewood Cliffs, 1992; pp 186-236.
- (3) *Silicon-Based Polymer Science: A Comprehensive Resource*; Ziegler, J. M.; Fearon, F. W. G., Ed.; American Chemical Society: Washington, DC, 1990.
- (4) West, R. *J. Organomet. Chem.* **1986**, *300*, 327-346.
- (5) Miller, R. D.; Michl, J. *Chem. Rev.* **1989**, *89*, 1359-1410.
- (6) Ziegler, J. M. *Mol. Cryst. Liq. Cryst.* **1990**, *190*, 265-282.
- (7) Yamamoto, K.; Okinoshima, H.; Kumada, M. *J. Organomet. Chem.* **1971**, *27*, C31-C32.
- (8) Ojima, I.; Inaba, S.-I.; Kogure, T.; Nagai, Y. *J. Organomet. Chem.* **1973**, *55*, C7-C8.
- (9) Aitken, C. T.; Harrod, J. F.; Samuel, E. *J. Am. Chem. Soc.* **1986**, *108*, 4059-4066.
- (10) Aitken, C.; Barry, J.-P.; Gauvin, F.; Harrod, J. F.; Malek, A.; Rousseau, D. *Organometallics* **1989**, *8*, 1732-1736.
- (11) Gauvin, F.; Harrod, J. F. *Can. J. Chem.* **1990**, *68*, 1638-1640.
- (12) Banovetz, J. P.; Stein, K. M.; Waymouth, R. M. *Organometallics* **1991**, *10*, 3430-3432.
- (13) Harrod, J. F. In *Inorganic and Organometallic Polymers with Special Properties*; R. M. Laine, Ed.; Kluwer Academic: Dordrecht, 1992; Vol. 206; pp 87-98.
- (14) Tilley, T. D. *Acc. Chem. Res.* **1993**, *26*, 22-29.
- (15) Tilley, T. D.; Woo, H.-G. *Polym. Prepr., Am. Chem. Soc. Div. Polym. Chem.* **1990**, *31*, 228-229.

- (16) Banovetz, J. P.; Suzuki, H.; Waymouth, R. M. *Organometallics* **1993**, *12*, 4700-4703.
- (17) Woo, H.-G.; Kim, S.-Y.; Han, M.-K.; Cho, E. J.; Jung, I. N. *Organometallics* **1995**, *14*, 2415-2421.
- (18) Samuel, E.; Harrod, J. F. *J. Am. Chem. Soc.* **1984**, *106*, 1859-1860.
- (19) Harrod, J. F. In *Inorganic and Organometallic Polymers*; M. Zeldin; K. J. Wynne and H. R. Allcock, Ed.; American Chemical Society: Washington DC, 1988; pp 89-100.
- (20) Woo, H.-G.; Tilley, T. D. *J. Am. Chem. Soc.* **1989**, *111*, 3757-3758.
- (21) Woo, H.-G.; Tilley, T. D. *J. Am. Chem. Soc.* **1989**, *111*, 8043-8044.
- (22) Harrod, J. F.; Mu, Y.; Samuel, E. *Polyhedron* **1991**, *10*, 1239-1245.
- (23) Gauvin, F. Ph.D. Thesis, McGill, 1992.
- (24) Tilley, T. D. *Comments Inorg. Chem.* **1990**, *10*, 37-51.
- (25) Yamashita, H.; Tanaka, M. *Bull. Chem. Soc. Jpn.* **1995**, *68*, 403-419.
- (26) Bourg, S.; Corriu, R. J. P.; Enders, M.; Moreau, J. J. E. *Organometallics* **1995**, *14*, 564-566.
- (27) Dioumaev, V. K.; Harrod, J. F. unpublished results.
- (28) Li, H.; Gauvin, F.; Harrod, J. F. *Organometallics* **1993**, *12*, 575-577.
- (29) Forsyth, C. M.; Nolan, S. P.; Marks, T. J. *Organometallics* **1991**, *10*, 2543-2545.
- (30) Tilley, T. D.; Radu, N. S.; Walzer, J. F.; H.-G., W. *Polym. Prepr., Am. Chem. Soc. Div. Polym. Chem.* **1992**, *33*, 1237-1238.
- (31) Sakakura, T.; Lautenschlager, H.-J.; Nakajima, M.; Tanaka, M. *Chem. Lett.* **1991**, 913-916.
- (32) Watson, P. L.; Tebbe, F. N. U.S. Patent No. 4,965,386, 1990.
- (33) Dioumaev, V. K.; Harrod, J. F. *Organometallics* **1994**, *13*, 1548-1550.
- (34) Dioumaev, V. K.; Harrod, J. F. *J. Organomet. Chem.* **1996**, *521*, 133-143.
- (35) Imori, T.; Tilley, T. D. *Polyhedron* **1994**, *13*, 2231.

- (36) Corey, J. Y.; Zhu, X.-H. *Organometallics* **1992**, *11*, 672-683.
- (37) Shaltout, R. M.; Corey, J. Y. *Tetrahedron* **1995**, *51*, 4309-4320.
- (38) Corey, J. Y.; Huhmann, J. L.; Zhu, X.-H. *Organometallics* **1993**, *12*, 1121-1130.
- (39) Woo, H.-G.; Heyn, R. H.; Tilley, T. D. *J. Am. Chem. Soc.* **1992**, *114*, 5698-5707.
- (40) Aitken, C.; Harrod, J. F.; Samuel, E. *Can. J. Chem.* **1986**, *64*, 1677-1679.
- (41) Takahashi, T.; Hasegawa, M.; Suzuki, N.; Saburi, M.; Rousset, C. J.; Fanwick, P. E.; Negishi, E.-i. *J. Am. Chem. Soc.* **1991**, *113*, 8564-8566.
- (42) Mu, Y.; Aitken, C.; Cote, B.; Harrod, J. F.; Samuel, E. *Can. J. Chem.* **1991**, *69*, 264-276.
- (43) Radu, N. S.; Tilley, T. D. *J. Am. Chem. Soc.* **1995**, *117*, 5863-5864.
- (44) Ziegler, T.; Folga, E. *J. Organomet. Chem.* **1994**, *478*, 57-65.
- (45) Samuel, E.; Mu, Y.; Harrod, J. F.; Dromzee, Y.; Jeannin, Y. *J. Am. Chem. Soc.* **1990**, *112*, 3435-3439.
- (46) Gauvin, F.; Britten, J.; Samuel, E.; Harrod, J. F. *J. Am. Chem. Soc.* **1992**, *114*, 1489-1491.
- (47) Harrod, J. F.; Mu, Y.; Samuel, E. *Can. J. Chem.* **1992**, *70*, 2980-2984.
- (48) Britten, J.; Mu, Y.; Harrod, J. F.; Polowin, J.; Baird, M. C.; Samuel, E. *Organometallics* **1993**, *12*, 2672-2676.
- (49) Woo, H. G.; Harrod, J. F.; Henique, J.; Samuel, E. *Organometallics* **1993**, *12*, 2883-2885.
- (50) Xin, S.; Harrod, J. F.; Samuel, E. *J. Am. Chem. Soc.* **1994**, *116*, 11562-11563.
- (51) Coutant, B.; Quignard, F.; Choplin, A. *J. Chem. Soc., Chem. Commun.* **1995**, 137-138.
- (52) Imori, T.; Lu, V.; Cai, H.; Tilley, T. D. *J. Am. Chem. Soc.* **1995**, *117*, 9931-9940.

- (53) Aitken, C.; Harrod, J. F.; Gill, U. S. *Can. J. Chem.* **1987**, *65*, 1804-1809.
- (54) Harrod, J. F.; Yun, S. S. *Organometallics* **1987**, *6*, 1381-1387.
- (55) Harrod, J. F.; Ziegler, T.; Tschinke, V. *Organometallics* **1990**, *9*, 897-902.
- (56) Jordan, R. F. *J. Chem. Ed.* **1988**, *65*, 285-289.
- (57) Huang, J.; Rempel, G. L. *Prog. Polym. Sci.* **1995**, *20*, 459-526.
- (58) Möhring, P. C.; Coville, N. J. *J. Organomet. Chem.* **1994**, *479*, 1-29.
- (59) Bochmann, M. *J. Chem. Soc., Dalton Trans.* **1996**, 255-270.
- (60) Jordan, R. F. *Adv. Organomet. Chem.* **1991**, *32*, 325-387 and references cited therein.
- (61) Jordan, R. F.; Bradley, P. K.; LaPointe, R. E.; Taylor, D. F. *New. J. Chem.* **1990**, *14*, 505-511.
- (62) Marks, T. J. *Acc. Chem. Res.* **1992**, *25*, 57-65 and references cited therein.
- (63) Kaminsky, W.; Kopf, J.; Sinn, H.; Vollmer, H.-J. *Angew. Chem., Int. Ed. Engl.* **1976**, *15*, 629-630.
- (64) Kopf, J.; Vollmer, H.-J.; Kaminsky, W. *Cryst. Struct. Commun.* **1980**, *9*, 271.
- (65) Eisch, J. J.; Piotrowski, A. M.; Brownstein, S. K.; Gabe, E. J.; Lee, F. L. *J. Am. Chem. Soc.* **1985**, *107*, 7219-7221.
- (66) Strauss, S. H. *Chem. Rev.* **1993**, *93*, 927-942.
- (67) Yang, X.; Stern, C. L.; Marks, T. J. *J. Am. Chem. Soc.* **1991**, *113*, 3623-3625.
- (68) Temme, B.; Erker, G.; Karl, J.; Luftmann, H.; Frohlich, R.; Kotila, S. *Angew. Chem., Int. Ed. Engl.* **1995**, *34*, 1755-1757.
- (69) Yang, X.; Stern, C.; Marks, T. J. *Angew. Chem., Int. Ed. Engl.* **1992**, *31*, 1375-1377.
- (70) Bochmann, M.; Lancaster, S. J.; Hursthouse, M. B.; Malik, K. M. A. *Organometallics* **1994**, *13*, 2235-2243.
- (71) Pellecchia, C.; Immirzi, A.; Grassi, A.; Zambelli, A. *Organometallics* **1993**, *12*, 4473-4478.

- (72a) Gillis, D. J.; Tudoret, M.-J.; Baird, M. C. *J. Am. Chem. Soc.* **1993**, *115*, 2543-2545.
- (72b) Gillis, D. J.; Quyoum, R.; Tudoret, M.-J.; Wang, Q.; Jeremic, D.; Roszak, A. W.; Baird, M. C. *Organometallics* **1996**, *15*, 3600-3605.
- (73) Pellecchia, C.; Grassi, A.; Immirzi, A. *J. Am. Chem. Soc.* **1993**, *115*, 1160-1162.
- (74) Van der Linden, A.; Schaverien, C. J.; Meijboom, N.; Ganter, C.; Orpen, A. G. *J. Am. Chem. Soc.* **1995**, *117*, 3008-3021.
- (75) Grassi, A.; Pellecchia, C.; Oliva, L.; Laschi, F. *Macromol. Chem. Phys.* **1995**, *196*, 1093-1100.
- (76) Grassi, A.; Zambelli, A.; Laschi, F. *Organometallics* **1996**, *15*, 480-482.
- (77) Temme, B.; Erker, G.; Frohlich, R.; Grehl, M. *Angew. Chem. Int. Ed. Engl.* **1994**, *33*, 1480-1482.
- (78) Temme, B.; Erker, G.; Frohlich, R.; Grehl, M. *J. Chem. Soc., Chem. Commun.* **1994**, 1713-1714.
- (79) Ruwwe, J.; Erker, G.; Frohlich, R. *Angew. Chem. Int. Ed. Engl.* **1996**, *35*, 80-82.
- (80) Willey, G. R.; Butcher, M. L.; McPartlin, M.; Scowen, I. J. *J. Chem. Soc., Dalton Trans.* **1994**, 305-309.
- (81) Roddick, D. M.; Heyn, R. H.; Tilley, D. T. *Organometallics* **1989**, *8*, 324-330.
- (82) Jordan, R. F.; LaPointe, R. E.; Baenziger, N.; Hinch, G. D. *Organometallics* **1990**, *9*, 1539-1545.
- (83) Jordan, R. F.; LaPointe, R. E.; Bajgur, C. S.; Echols, S. F.; Willett, R. *J. Am. Chem. Soc.* **1987**, *109*, 4111-4113.
- (84) Jordan, R. F.; Dasher, W. E.; Echols, S. F. *J. Am. Chem. Soc.* **1986**, *108*, 1718-1719.

- (85) Jordan, R. F.; Bajgur, C. S.; Willett, R.; Scott, B. *J. Am. Chem. Soc.* **1986**, *108*, 7410-7411.
- (86) Crowther, D. J.; Borkowsky, S. L.; Swenson, D.; Meyer, T. Y.; Jordan, R. J. *Organometallics* **1993**, *12*, 2897-2903.
- (87) Jordan, R. F.; Bajgur, C. S.; Dasher, W. E.; Rheingold, A. L. *Organometallics* **1987**, *6*, 1041-1051.
- (88) Crowther, D. J.; Jordan, R. F.; Baenziger, N. C.; Verma, A. *Organometallics* **1990**, *9*, 2574-2580.
- (89) Burk, M. J.; Tumas, W.; Ward, M. D.; Wheeler, D. R. *J. Am. Chem. Soc.* **1990**, *112*, 6133-6135.
- (90) Borkowsky, S. L.; Jordan, R. F.; Hinch, G. D. *Organometallics* **1991**, *10*, 1268-1274.
- (91) Bochmann, M.; Wilson, L. M.; Hursthouse, M. B.; Short, R. L. *Organometallics* **1987**, *6*, 2556-2563.
- (92) Martin, B. D.; Matchett, S. A.; Norton, J. R.; Anderson, O. P. *J. Am. Chem. Soc.* **1985**, *107*, 7952-7963.
- (93) Siedle, A. R.; Newmark, R. A.; Gleason, W. B.; Lamanna, W. M. *Organometallics* **1990**, *9*, 1290-1295.
- (94) Boutonnet, F.; Zablocka, M.; Igau, A.; Majoral, J.-P.; Raynaud, B.; Jaud, J. *J. Chem. Soc., Chem. Commun.* **1993**, 1866-1867.
- (95) Borkowsky, S. L.; Baenziger, N. C.; Jordan, R. F. *Organometallics* **1993**, *12*, 486-495.
- (96) Anderson, J. E.; Sawtelle, S. M. *Inorg. Chem.* **1992**, *31*, 5345-5346.
- (97) Hlatky, G. G.; Turner, H. W.; Eckman, R. R. *J. Am. Chem. Soc.* **1989**, *111*, 2728-2729.
- (98) Grossman, R. B.; Doyle, R. A.; Buchwald, S. L. *Organometallics* **1991**, *10*, 1501-1505.

- (99) Yang, X.; King, W. A.; Sabat, M.; Marks, T. J. *Organometallics* **1993**, *12*, 4254-4258.
- (100) Bochmann, M.; Wilson, L. M. *J. Chem. Soc., Chem. Commun.* **1986**, 1610-1611.
- (101) Eshuis, J. J. W.; Tan, Y. Y.; Teuben, J. H. *J. Mol. Catal., A: Chem.* **1990**, *62*, 277-287.
- (102) Taube, R.; Krukowka, L. *J. Organomet. Chem.* **1988**, *347*, C9-C11.
- (103) Bochmann, M.; Karger, G.; Jaggar, J. J. *J. Chem. Soc., Chem. Commun.* **1990**, 1038-1039.
- (104) Schaverien, C. J. *Organometallics* **1992**, *11*, 3476-3478.
- (105) Uhrhammer, R.; Black, D. G.; Gardner, T. G.; Olsen, J. D.; Jordan, R. F. *J. Am. Chem. Soc.* **1993**, *115*, 8493-8494.
- (106) Negishi, E. In *Comprehensive Organometallic Chemistry*; G. Wilkinson; F. G. A. Stone and E. W. Abel, Ed.; Pergamon: New York, 1982; Vol. 7; p 326.
- (107) Bochmann, M.; Jaggar, A. J.; Nicholls, J. C. *Angew. Chem., Int. Ed. Engl.* **1990**, *29*, 780-782.
- (108) Horton, A. *Organometallics* **1992**, *11*, 3271-3275.
- (109) Bochmann, M.; Cuenca, T.; Hardy, D. T. *J. Organomet. Chem.* **1994**, *484*, C10-C12.
- (110) Straus, D. A.; Zhang, C.; Tilley, T. D. *J. Organomet. Chem.* **1989**, *369*, C13-C17.
- (111) Chien, J. C. W.; Tsai, W.-M.; Rausch, M. D. *J. Am. Chem. Soc.* **1991**, *113*, 8570-8571.
- (112) Bochmann, M.; Lancaster, S. J. *Organometallics* **1993**, *12*, 633-640.
- (113) Coutts, R. S. P.; Kautzner, B.; Wailes, P. C. *Aust. J. Chem.* **1969**, *22*, 1137-1141.

- (114) Seewald, P. A.; White, G. S.; Stephan, D. W. *Can. J. Chem.* **1988**, *66*, 1147-1152.
- (115) Jordan, R. F.; Echols, S. F. *Inorg. Chem.* **1987**, *26*, 383-386.
- (116) Odenkirk, W.; Bosnich, B. *J. Chem. Soc., Chem. Commun.* **1995**, 1181-1182.
- (117) Tornieporth-Oetting, I. C.; White, P. S. *Organometallics* **1995**, *14*, 1632-1636.
- (118) Winter, C. H.; Zhou, X.-X.; Heeg, M. J. *Inorg. Chem.* **1992**, *31*, 1808-1815.
- (119) Maeta, H.; Hashimoto, T.; Hasegawa, T.; Suzuki, K. *Tetrahedron Lett.* **1992**, *33*, 5965-5968.
- (120) Bochmann, M.; Jaggar, A. J.; Wilson, L. M.; Hursthouse, M. B.; Motevalli, M. *Polyhedron* **1989**, *8*, 1838-1843.
- (121) Park, J. W.; Henling, L. M.; Schaefer, W. P.; Grubbs, R. H. *Organometallics* **1990**, *9*, 1650-1656.
- (122) Bochmann, M.; Lancaster, S. J.; Robinson, O. B. *J. Chem. Soc., Chem. Commun.* **1995**, 2081-2082.
- (123) Spence, R. E. v. H.; Piers, W. E. *Organometallics* **1995**, *14*, 4617-4624.
- (124a) Temme, B.; Karl, J.; Erker, G. *Chem. Eur. J.* **1996**, *2*, 919-924.
- (124b) Sun, Y.; Piers, W. E.; Rettig, S. J. *Organometallics* **1996**, *15*, 4110-4112.
- (125) Devore, D. D.; Timmers, F. J.; Hasha, D. L.; Rosen, R. K.; Marks, T. J.; Deck, P. A.; Stern, C. L. *Organometallics* **1995**, *14*, 3132-3134.
- (126) Jordan, R. F.; LaPointe, R. E.; Bradley, P. K.; Baenziger, N. *Organometallics* **1989**, *8*, 2892-2903.
- (127) Alelyunas, Y. W.; Guo, Z.; LaPointe, R. E.; Jordan, R. F. *Organometallics* **1993**, *12*, 544-553.
- (128) Horton, A. D. *J. Chem. Soc., Chem. Commun.* **1992**, 185-187.
- (129) Horton, A. D.; Orpen, A. G. *Angew. Chem., Int. Ed. Engl.* **1992**, *31*, 876-878.
- (130) Horton, A. D.; Orpen, A. G. *Organometallics* **1992**, *11*, 8-10.

- (131) Rottger, D.; Erker, G.; Frohlich, R.; Grehl, M.; Silverio, S. J.; Hyla-Kryspin, I.; Gleiter, R. *J. Am. Chem. Soc.* **1995**, *117*, 10503-10512.
- (132) Rottger, D.; Pflug, J.; Erker, G.; Kotila, S.; Frohlich, R. *Organometallics* **1996**, *15*, 1265-1267.
- (133) Horton, A. D. *Organometallics* **1996**, *15*, 2675-2677.
- (134) Pellecchia, C.; Grassi, A.; Zambelli, A. *J. Chem. Soc., Chem. Commun.* **1993**, 947-949.
- (135) Rottger, D.; Erker, G.; Frohlich, R.; Kotila, S. *Chem. Ber.* **1996**, *129*, 5-9.
- (136) Rottger, D.; Erker, G.; Frohlich, R.; Kotila, S. *Chem. Ber.* **1996**, *129*, 1-3.
- (137) Jordan, R. F.; Guram, A. S. *Organometallics* **1990**, *9*, 2116-2123.
- (138) Jordan, R. F.; Taylor, D. F. *J. Am. Chem. Soc.* **1989**, *111*, 778-779.
- (139) Guram, A. S.; Jordan, R. F. *Organometallics* **1990**, *9*, 2190-2192.
- (140) Guram, A. S.; Jordan, R. F.; Taylor, D. F. *J. Am. Chem. Soc.* **1991**, *113*, 1833-1835.
- (141) Guram, A. S.; Swenson, D. C.; Jordan, R. J. *J. Am. Chem. Soc.* **1992**, *114*, 8991-8996.
- (142) Rodewald, S.; Jordan, R. J. *J. Am. Chem. Soc.* **1994**, *116*, 4491-4492.
- (143) Jordan, R. F.; Taylor, D. F.; Baenziger, N. C. *Organometallics* **1990**, *9*, 1546-1557.
- (144) Bochmann, M.; Wilson, L. M.; Hursthouse, M. B.; Motevalli, M. *Organometallics* **1988**, *7*, 1148-1154.
- (145) Alelyunas, Y. W.; Jordan, R. F.; Echols, S. F.; Borkowsky, S. L.; Bradley, P. K. *Organometallics* **1991**, *10*, 1406-1416.
- (146) Guo, Z.; Swenson, D. C.; Guram, A. S.; Jordan, R. F. *Organometallics* **1994**, *13*, 766-773.
- (147) Guram, A. S.; Guo, Z.; Jordan, R. F. *J. Am. Chem. Soc.* **1993**, *115*, 4902-4903.

- (148) Antonelli, D. M.; Tjaden, E. B.; Stryker, J. M. *Organometallics* **1994**, *13*, 763-765.
- (149) Collins, S.; Koene, B. E.; Ramachandran, R.; Taylor, N. J. *Organometallics* **1991**, *10*, 2092-2094.
- (150) Piers, W. E.; Koch, L.; Ridge, D. S.; MacGillivray, L. R.; Zaworotko, M. *Organometallics* **1992**, *11*, 3148-3152.
- (151) Guo, Z.-Y.; Bradley, P. K.; Jordan, R. F. *Organometallics* **1992**, *11*, 2690-2693.
- (152) Lauher, J. W.; Hoffmann, R. *J. Am. Chem. Soc.* **1976**, *98*, 1729-1742.
- (153) Woo, T. K.; Ziegler, T. *Organometallics* **1994**, *13*, 2252-2261.
- (154) Amorose, D. M.; Lee, R. A.; Petersen, J. L. *Organometallics* **1991**, *10*, 2191-2198.
- (155) Eshuis, J. J.; Tan, Y. Y.; Meetsma, A.; Teuben, J. H.; Renkema, J.; Evens, G. G. *Organometallics* **1992**, *11*, 362-369.
- (156) Bochmann, M.; Jaggar, A. J. *J. Organomet. Chem.* **1992**, *424*, C5-C7.
- (157) Bochmann, M. *Angew. Chem. Int. Ed. Engl.* **1992**, *31*, 1181-1182.
- (158) Horton, A. D.; Frijns, J. H. G. *Angew. Chem., Int. Ed. Engl.* **1991**, *30*, 1152-1154.
- (159) Horton, A. D.; de With, J. *J. Chem. Soc., Chem. Commun.* **1996**, 1375-1376.
- (160) Horton, A. D.; de With, J.; van der Linden, A. J.; van der Weg, H. *Organometallics* **1996**, *15*, 2672-2674.
- (161) Horton, A. D.; Orpen, A. G. *Organometallics* **1991**, *10*, 3910-3918.
- (162) Yang, X.; Stern, C. L.; Marks, T. J. *Organometallics* **1991**, *10*, 840-842.
- (163) Yang, X.; Stern, C. L.; Marks, T. J. *J. Am. Chem. Soc.* **1994**, *116*, 10015-10031.
- (164) Gomez, R.; Green, M. L. H.; Haggitt, J. L. *J. Chem. Soc., Chem. Commun.* **1994**, 2607-2608.

- (165) Jia, L.; Yang, X.; Ishihara, A.; Marks, T. J. *Organometallics* **1995**, *14*, 3135-3137.
- (166) Giardello, M. A.; Eisen, M. S.; Stern, C. L.; Marks, T. J. *J. Am. Chem. Soc.* **1995**, *117*, 12114-12129.
- (167) Deck, P. A.; Marks, T. J. *J. Am. Chem. Soc.* **1995**, *117*, 6128-6129.
- (168) Siedle, A. R.; Newmark, R. A. *J. Organomet. Chem.* **1995**, *497*, 119-125.
- (169) Hlatky, G. G.; Eckman, R. R.; Turner, H. W. *Organometallics* **1992**, *11*, 1413-1416.
- (170) Reed, C. A.; Xie, Z.; Bau, R.; Benesi, A. *Science* **1993**, *262*, 402-404.
- (171) Xie, Z.; Liston, D. J.; Jelinec, T.; Mitro, V.; Bau, R.; Reed, C. A. *J. Chem. Soc., Chem. Commun.* **1993**, 384-386.
- (172) Xie, Z.; Jelinec, T.; Bau, R.; Reed, C. A. *J. Am. Chem. Soc.* **1994**, *116*, 1907-1913.
- (173) Eisch, J. J.; Pombrik, S. I.; Zheng, G.-X. *Organometallics* **1993**, *12*, 3856-3863.
- (174) Eisch, J. J.; Caldwell, K. R.; Werner, S.; Kruger, C. *Organometallics* **1991**, *10*, 3417-3419.
- (175) Wang, Q.; Quyoum, R.; Gillis, D. J.; Tudoret, M.-J.; Jeremic, D.; Hunter, B. K.; Baird, M. C. *Organometallics* **1996**, *15*, 693-703.
- (176) Amor, J. I.; Cuenca, T.; Galakhov, M.; Royo, P. *J. Organomet. Chem.* **1995**, *497*, 127-131.
- (177) Troyanov, S. *J. Organomet. Chem.* **1994**, *475*, 139-147.
- (178) Pellecchia, C.; Immirzi, A.; Zambelli, A. *J. Organomet. Chem.* **1994**, *479*, C9-C11.
- (179) Pellecchia, C.; Immirzi, A.; Pappalardo, D.; Peluso, A. *Organometallics* **1994**, *13*, 3773-3775.
- (180) Wu, Z.; Jordan, R. F.; Petersen, J. L. *J. Am. Chem. Soc.* **1995**, *117*, 5867-5868.

- (181) Pellecchia, C.; Grassi, A.; Zambelli, A. *Organometallics* **1994**, *13*, 298-302.
- (182) Jordan, R. J.; Bradley, P. K.; Baenziger, N. C.; LaPointe, R. E. *J. Am. Chem. Soc.* **1990**, *112*, 1289-1291.
- (183) Guo, Z.; Swenson, D. C.; Jordan, R. F. *Organometallics* **1994**, *13*, 1424-1432.
- (184) Alelyunas, Y. W.; Baenziger, N. C.; Bradley, P. K.; Jordan, R. J. *Organometallics* **1994**, *13*, 148-156.
- (185) Horton, A. D.; Orpen, A. G. *Organometallics* **1992**, *11*, 1193-1201.
- (186a) Lancaster, S. J.; Robinson, O. B.; Bochmann, M.; Coles, S. J.; Hursthouse, M. B. *Organometallics* **1995**, *14*, 2456-2462.
- (186b) Scollard, J. D.; McConville, D. H. *J. Am. Chem. Soc.* **1996**, *118*, 10008-10009.
- (187) Bochmann, M.; Lancaster, S. J. *Angew. Chem., Int. Ed. Engl.* **1994**, *33*, 1634-1637.
- (188a) Lancaster, S. J.; Bochmann, M. *J. Organomet. Chem.* **1995**, *497*, 55-59.
- (188b) Beck, S.; Prosenc, M.-H.; Brintzinger, H.-H.; Goretzki, R.; Herfert, N.; Fink, G. *J. Mol. Cat. A: Chem.* **1996**, *111*, 67-79.
- (189) Lickiss, P. D. *J. Chem. Soc., Dalton Trans.* **1992**, 1333-1338.
- (190) Chojnowski, J.; Stanczyk, W. *Main Group Chemistry News* **1994**, *2*, 6-15.
- (191) Corriu, R. J. P.; Henner, M. *J. Organomet. Chem.* **1974**, *74*, 1-28.
- (192) Speranza, M. *Chem. Rev.* **1993**, *93*, 2933-2980.
- (193) Lambert, J. B.; Kania, L.; Zhang, S. *Chem. Rev.* **1995**, *95*, 1191-1201.
- (194) Cowley, A. H.; Cushner, M. C.; Riley, P. E. *J. Am. Chem. Soc.* **1980**, *102*, 624-628.
- (195) Olah, G. A.; Mo, Y. K. *J. Am. Chem. Soc.* **1971**, *93*, 4942-4943.
- (196) Olah, G. A.; Laali, K.; Farooq, O. *Organometallics* **1984**, *3*, 1337-1340.
- (197) Olah, G. A.; Rasul, G.; Heiliger, L.; Bausch, J.; Prakash, G. K. S. *J. Am. Chem. Soc.* **1992**, *114*, 7737-7742.
- (198) Lew, C. S. Q.; McClelland, R. A. *J. Am. Chem. Soc.* **1993**, *115*, 11516-11520.

- (199) Apeloig, Y.; Stanger, A. *J. Am. Chem. Soc.* **1987**, *109*, 272-273.
- (200) Mayr, H.; Basso, N. *Angew. Chem. Int. Ed. Engl.* **1992**, *31*, 1046-1048.
- (201) Basso, N.; Gorg, S.; Popowski, E.; Mayr, H. *J. Am. Chem. Soc.* **1993**, *115*, 6025-6028.
- (202) Mayr, H.; Basso, N.; Hagen, G. *J. Am. Chem. Soc.* **1992**, *114*, 3060-3066.
- (203) Chojnowski, J.; Fortuniak, W.; Stanczyk, W. *J. Am. Chem. Soc.* **1987**, *109*, 7776-7781.
- (204) Chojnowski, J.; Wilczek, L.; Fortuniak, W. *J. Organomet. Chem.* **1977**, *135*, 13-22.
- (205) Breliere, C.; Carre, F.; Corriu, R.; Mehdi, A.; Man, M. W. C. *J. Chem. Soc., Chem. Commun.* **1994**, 2333-2334.
- (206) Belzner, J.; Schar, D.; Kneisel, B. O.; Herbst-Irmer, R. *Organometallics* **1995**, *14*, 1840-1843.
- (207) Chuit, C.; Corriu, R. J. P.; Reye, C.; Young, J. C. *Chem. Rev.* **1993**, *93*, 1371-1448 and references cited therein.
- (208) Schott, v. G.; Golz, K. *Z. Anorg. Allg. Chem.* **1971**, *383*, 314.
- (209) Schott, v. G.; Golz, K. *Z. Anorg. Allg. Chem.* **1973**, *399*, 7-24.
- (210) Jutzi, P.; Bunte, E.-A. *Angew. Chem., Int. Ed. Engl.* **1992**, *31*, 1605-1607.
- (211) Chuit, C.; Corriu, R. J. P.; Mehdi, A.; Reye, C. *Angew. Chem., Int. Ed. Engl.* **1993**, *32*, 1311-1313.
- (212) Corey, J. Y.; West, R. *J. Am. Chem. Soc.* **1963**, *85*, 4034-4035.
- (213) Carre, F.; Chuit, C.; Corriu, R. J. P.; Mehdi, A.; Reye, C. *Angew. Chem., Int. Ed. Engl.* **1994**, *33*, 1097-1099.
- (214) Wannagat, U.; Liehr, W. *Angew. Chem.* **1957**, *69*, 783-784.
- (215) Lambert, J. B.; Sun, H.-n. *J. Am. Chem. Soc.* **1976**, *98*, 5611-5615.
- (216) Prakash, G. K. S.; Keyaniyan, S.; Aniszfeld, R.; Heiliger, L.; Olah, G. A.; Stevens, R. C.; Choi, H.-K.; Bau, R. *J. Am. Chem. Soc.* **1987**, *109*, 5123-5126.

- (217) Lambert, J. B.; Schulz, W. J. J.; McConnell, J. A.; Schilf, W. J. *Am. Chem. Soc.* **1988**, *110*, 2201-2210.
- (218) Lambert, J. B.; McConnell, J. A.; Schulz, W. J. J. *J. Am. Chem. Soc.* **1986**, *108*, 2482-2484.
- (219) Lambert, J. B.; Schulz, W. J. J. *J. Am. Chem. Soc.* **1983**, *105*, 1671-1672.
- (220) Lambert, J. B.; Kania, L.; Schilf, W.; McConnell, J. A. *Organometallics* **1991**, *10*, 2578-2584.
- (221) Corey, J. Y. *J. Am. Chem. Soc.* **1975**, *97*, 3237-3238.
- (222) Lambert, J. B.; Schilf, W. J. *Am. Chem. Soc.* **1988**, *110*, 6364-6367.
- (223) Olah, G. A.; Field, L. D. *Organometallics* **1982**, *1*, 1485-1487.
- (224) Lambert, J. B.; McConnell, J. A.; Schilf, W.; Schulz, W. J. J. *J. Chem. Soc., Chem. Commun.* **1988**, 455-456.
- (225) Olah, G. A.; Heiliger, L.; Li, X.-Y.; Prakash, G. K. S. *J. Am. Chem. Soc.* **1990**, *112*, 5991-5995.
- (226) Bahr, S. R.; Boudjouk, P. J. *Am. Chem. Soc.* **1993**, *115*, 4514-4519.
- (227) Lambert, J. B.; Zhang, S.; Stern, C. L.; Huffman, J. C. *Science* **1993**, *260*, 1917-1918.
- (228) Lambert, J. B.; Zhang, S. *J. Chem. Soc., Chem. Commun.* **1993**, 383-384.
- (229) Eaborn, C. J. *Organomet. Chem.* **1991**, *405*, 173-177.
- (230) Cremer, D.; Olsson, L.; Ottosson, C.-H. *J. Mol. Struct. (THEOCHEM)* **1994**, *313*, 91-109.
- (231) Olsson, L.; Ottosson, C.-H.; Cremer, D. *J. Am. Chem. Soc.* **1995**, *117*, 7460-7479.
- (232) Arshadi, M.; Johnels, D.; Edlund, U.; Ottosson, C.-H.; Cremer, D. *J. Am. Chem. Soc.* **1996**, *118*, 5120-5131.
- (233) Kira, M.; Hino, T.; Sakurai, H. *J. Am. Chem. Soc.* **1992**, *114*, 6697-6700.
- (234) Lambert, J. B.; Zhang, S.; Ciro, S. M. *Organometallics* **1994**, *13*, 2430-2443.

- (235) Xie, Z.; Bau, R.; Reed, C. A. *J. Chem. Soc., Chem. Commun.* **1994**, 2519-2520.
- (236) Hensen, K.; Zengerly, T.; Pickel, P.; Klebe, G. *Angew. Chem., Int. Ed. Engl.* **1983**, 22, 725-727.
- (237) Xie, Z.; Manning, J.; Reed, R. W.; Rajeev, M.; Boyd, P. D. W.; Benesi, A.; Reed, C. A. *J. Am. Chem. Soc.* **1996**, 118, 2922-2928.
- (238) Xie, Z.; Bau, R.; Benesi, A.; Reed, C. A. *Organometallics* **1995**, 14, 3933-3941.
- (239) Pauling, L. *Science* **1994**, 263, 983-983.
- (240) Schleyer, P. v. R.; Buzek, P.; Muller, T.; Apeloig, Y.; Siehl, H.-U. *Angew. Chem. Int. Ed. Engl.* **1993**, 32, 1471-1473.
- (241a) Olah, G. A.; Rasul, G.; Li, X.-y.; Buchholz, H. A.; Sandford, G.; Prakash, G. K. S. *Science* **1994**, 263, 983-984.
- (241b) Olah, G. A.; Rasul, G.; Prakash, G. K. S. *J. Organomet. Chem.* **1996**, 521, 271-277.
- (242) Olsson, L.; Cremer, D. *Chem. Phys. Lett.* **1993**, 215, 433-443.
- (243) Cacace, F.; Attina, M.; Fornarini, S. *Angew. Chem., Int. Ed. Engl.* **1995**, 34, 654-655.
- (244) Lambert, J. B.; Zhang, S. *Science* **1994**, 263, 984-985.
- (245) Lambert, J. B. personal communication.
- (246) Ruffolo, R.; Decken, A.; Girard, L.; Gupta, H. K.; Brook, M. A.; McGlinchey, M. J. *Organometallics* **1994**, 13, 4328-4335.
- (247) Jacobson, D. B.; Bakhtiar, R. *J. Am. Chem. Soc.* **1993**, 115, 10830-10844.
- (248) Choe, S.-B.; Kanai, H.; Klabunde, K. J. *J. Am. Chem. Soc.* **1989**, 111, 2875-2882.
- (249) Straus, D. A.; Tilley, T. D.; Rheingold, A. L.; Geib, S. J. *J. Am. Chem. Soc.* **1987**, 109, 5872-5873.
- (250) Zhang, C.; Grumbine, S. D.; Tilley, T. D. *Polyhedron* **1991**, 10, 1173-1176.

- (251) Grumbine, S. D.; Chadha, R. K.; Tilley, T. D. *J. Am. Chem. Soc.* **1992**, *114*, 1518-1520.
- (252) Kawano, Y.; Tobita, H.; Shimoi, M.; Ogino, H. *J. Am. Chem. Soc.* **1994**, *116*, 8575-8581.
- (253) Kobayashi, H.; Ueno, K.; Ogino, H. *Organometallics* **1995**, *14*, 5490-5492.
- (254) Grumbine, S. K.; Straus, D. A.; Tilley, T. D.; Rheingold, A. L. *Polyhedron* **1995**, *14*, 127-148.
- (255) Straus, D. A.; Grumbine, S. D.; Tilley, T. D. *J. Am. Chem. Soc.* **1990**, *112*, 7801-7802.
- (256) Straus, D. A.; Zhang, C.; Quimbata, G. E.; Grumbine, S. D.; Heyn, R. H.; Tilley, T. D.; Rheingold, A. L.; Geib, S. J. *J. Am. Chem. Soc.* **1990**, *112*, 2673-2681.
- (257) Lee, K. E.; Arif, A. M.; Gladysz, J. A. *Chem. Ber.* **1991**, *124*, 309-320.
- (258) Grumbine, S. D.; Tilley, T. D.; Rheingold, A. L. *J. Am. Chem. Soc.* **1993**, *115*, 358-360.
- (259) Grumbine, S. D.; Tilley, T. D.; Arnold, F. P.; Rheingold, A. L. *J. Am. Chem. Soc.* **1993**, *115*, 7884-7885.
- (260) Grumbine, S. K.; Tilley, T. D. *J. Am. Chem. Soc.* **1994**, *116*, 5495-5496.
- (261) Grumbine, S. K.; Tilley, T. D. *J. Am. Chem. Soc.* **1994**, *116*, 6951-6952.
- (262) Figge, L. K.; Carroll, P. J.; Berry, D. H. *Angew. Chem., Int. Ed. Engl.* **1996**, *35*, 435-437.
- (263) Figge, L. K.; Carroll, P. J.; Berry, D. H. *Organometallics* **1996**, *15*, 209-215.

CHAPTER 2

An Unusual “Cation-like” Zirconocene Hydrosilyl Complex. Silylium Ligand or a Nonclassically Bonded Si-H?¹

Vladimir K. Dioumaev and John F. Harrod

Chemistry Department, McGill University, Montreal, QC, Canada H3A 2K6

Abstract



The novel zirconocene complexes $[\text{Cp}'_2\text{Zr}(\mu\text{-H})(\text{SiHR})]_2^{2+}[\text{BR}'_n(\text{C}_6\text{F}_5)_{4-n}]_2^{2-}$ ($\text{Cp}' = \text{Cp}, \text{MeCp}, \text{Me}_5\text{Cp}$; $\text{R} = \text{Ph}$ or PhCH_2 ; $\text{R}' = \text{Bu}$ or H) were isolated from silane dehydropolymerization reaction mixtures catalyzed by $\text{Cp}'_2\text{ZrCl}_2/2\text{BuLi}/\text{B}(\text{C}_6\text{F}_5)_3$ or by $[\text{Cp}'_2\text{Zr}(\mu\text{-H})\text{H}]_2/2\text{B}(\text{C}_6\text{F}_5)_3$ combination catalysts. A total structure analysis of these compounds, performed by multinuclear, multidimensional NMR spectroscopy, shows that each zirconocene fragment bears a positive charge, which is delocalized between the metal center and hydrosilane ligand.

2.1 Introduction

We recently reported a new type of cationic catalyst for the dehydrocoupling of primary silanes, which proved to have certain advantages over neutral analogues. Our preliminary results indicated significant positive charge on the silicon ligand.¹ In view of the controversy surrounding the existence of cationic silylium in the condensed phase,²⁻¹² it was of interest to investigate these metal bonded cation-like silylium compounds in more detail. We now report the total structure analysis of the reaction products in solution by multinuclear, multidimensional NMR spectroscopy.

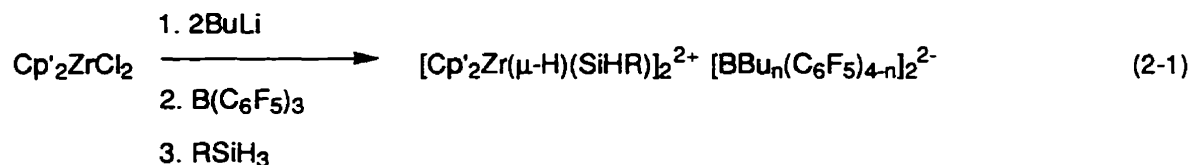
2.2 Results and Discussion

2.2.1 Total Structure Determination Strategy

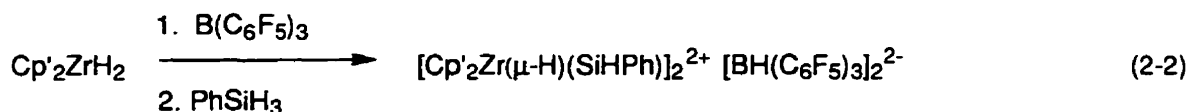
Compound **29a** was synthesized from a mixture of Cp_2ZrCl_2 , BuLi, $\text{B}(\text{C}_6\text{F}_5)_3$ and PhSiH_3 at $-20\text{ }^\circ\text{C}$ (eq 2-1) and was precipitated from toluene-pentane. Attempts were made to obtain an X-ray quality crystal, but this compound always precipitated as an oil from all aromatic and chloroorganic solvents. The oil solidified to a microcrystalline powder upon washing it with pentane and drying under vacuum. The structure of **29a** has been determined by NMR, IR, and UV measurements as $[\text{Cp}_2\text{Zr}(\mu\text{-H})(\text{SiHPh})]_2^{2+}[\text{BBu}_n(\text{C}_6\text{F}_5)_{4-n}]_2^{2-}$.

The ^1H NMR spectrum of **29a** (Figure 2-1) contains five groups of signals, which can be readily assigned to the Ph, SiH, Cp, and $\mu\text{-H-Zr}$ groups in a 5:1:10:1 H ratio together with an alkyl fragment in the aliphatic region of the spectrum. The ^1H chemical shifts (Table 2-1) for most of these signals are quite characteristic and can also be cross-referenced with the ^{13}C chemical shifts of the directly bonded carbons, extracted from a ^1H - ^{13}C HMQC experiment. Indeed, the ^{13}C resonances for the Ph and Cp groups (Table 2-2) appear in the expected regions, while the SiH and ZrH fragments do not show

any H-C correlation, indicating a lack of direct bonding of those protons to any carbon atoms. On the other hand, the SiH proton resonance does show a cross-peak to silicon in the ^1H - ^{29}Si HMQC spectrum ($^1J_{\text{SiH}} = 203.5 \text{ Hz}$), while the ZrH signal shows only a long-range H-Si connectivity ($J_{\text{SiH}} = 32.2 \text{ Hz}$) as expected.



29a $\text{Cp}'_2 = (\text{C}_5\text{H}_5)_2$; $\text{R} = \text{Ph}$
29b $\text{Cp}'_2 = (\text{C}_5\text{H}_5)_2$; $\text{R} = \text{CH}_2\text{Ph}$
29c $\text{Cp}'_2 = (\text{C}_5\text{H}_5)(\text{Me}_5\text{C}_5)$; $\text{R} = \text{Ph}$
29d $\text{Cp}'_2 = (\text{MeC}_5\text{H}_4)_2$; $\text{R} = \text{Ph}$



29e $\text{Cp}' = \text{C}_5\text{H}_4\text{CH}_3$

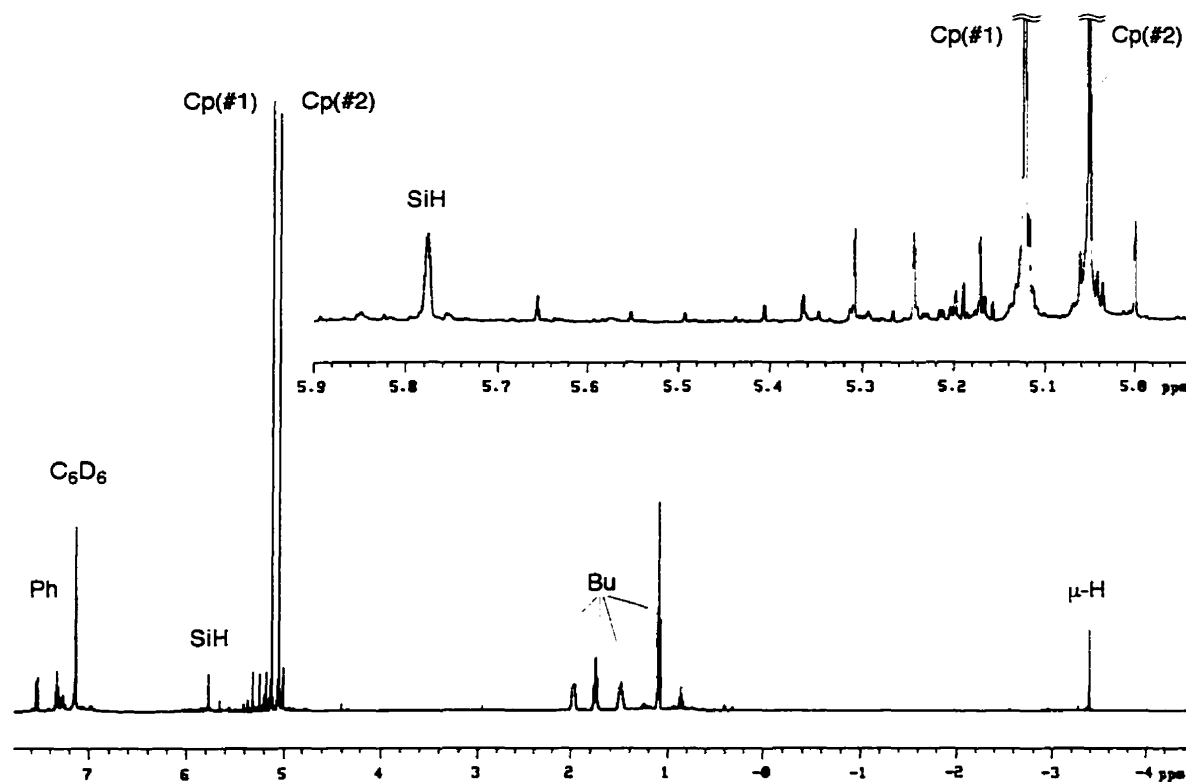


Figure 2-1. ^1H NMR spectrum of **29a** in C_6D_6 .

Table 2-1. ^1H NMR data for **29a-e**^a

	for given compound (solvent)						
	29a (C ₆ D ₆)	29a (C ₂ D ₂ Cl ₄)	29b (C ₇ D ₈)	29c (C ₆ D ₆)	29c (C ₇ D ₈)	29d (C ₆ D ₆)	29e ^b (C ₆ D ₆)
α -Bu	1.96, br m	1.11, br m	1.87, br m	1.99, br s	1.83, br s	1.98, br m	na
β -Bu	1.46, br m	0.76, br m	1.42, m	1.50, m	1.39, m	1.50, br m	na
γ -Bu	1.73, m	1.19, q	1.70, m	1.74, m	1.68, m	1.73, m	na
δ -Bu	1.08, t (7.25)	0.72, t (7.3)	1.08, t (7.3)	1.10, t (7.4)	1.07, t (7.8)	1.08, t (7.3)	na
μ -H	-3.39, s	-2.93, s	-3.90, s	-1.82, -2.85, AX q (15.0)	-1.77, -2.81, AX q (15.0)	-3.12, s	-3.13
Cp	5.12, s	5.71, s	5.12, s	5.16, s	5.15, s	c	c
Cp	5.06, s	5.79, s	5.03, s	5.10, s	5.21, s	c	c
Cp*	na	na	na	1.48, s	1.55, s	na	na
Cp*	na	na	na	1.47, s	1.58, s	na	na
CH ₂ Si	na	na	2.44, d, (5.5)	na	na	na	na
Si-H	5.78, br s	6.17, br s	5.34, m	5.53, br s	5.54, br s	5.83, br s	5.83, br s
<i>o</i> -Ph	7.6-7.4, m	7.8-7.6, m	7.3-6.6, m	7.7-7.5, m	7.72, d, (7.5)	7.66, d, (7.5)	7.54, d, (7.5)
<i>m</i> -Ph	7.0-6.8, m	7.6-7.2, m	7.3-6.6, m	7.3-6.8, m	7.39, t (7.8)	7.32, t (7.7)	7.31, t (7.8)
<i>p</i> -Ph	7.4-7.2, m	7.6-7.2, m	7.3-6.6, m	7.5-7.3, m	7.32, t (7.8)	7.27, t (7.8)	7.28, t (7.8)

^a The chemical shifts are in parts per million, and the figures in parentheses are coupling constants in hertz. The coupling constants for most of the resonances are not reported as the signals are either second order multiplets or are too broad for an accurate value to be determined. Abbreviations: s, singlet; t, triplet; m, multiplet; br s, broad singlet; br m,

broad multiplet; AX q, second order AX quartet; nd, not determined; na, not applicable. All spectra were recorded at +25 °C (except for **29a** in C₂D₂Cl₄, which was recorded at -40 °C).

^b The borate counterion is [HB(C₆F₅)₃]⁻. The B-H signal has a chemical shift of 2.58 ppm (¹J_{BH} = 77.3 Hz, equal intensity quadruplet).

^c The ¹H (this table) and ¹³C (Table 2-2) resonances for the directly bonded H and C nuclei in the MeCp ligand are reported in the same order. The MeCp ¹H signals are all second order multiplets, MeCp resonances are singlets. ¹H chemical shifts (ppm): for **29d**, 5.22, 5.22, 5.07, 5.04, 4.86, 4.86, 4.85, 4.68, 1.71, 1.66; for **29e**, 4.68, 4.83, 4.84, 4.85, 5.03, 5.06, 5.20, 5.20, 1.66, 1.71.

The alkyl group, referred to above, gives rise to four multiplets in the ¹H NMR spectrum and four signals in the ¹³C NMR spectrum. Their relative intensities indicate a linear CH₃CH₂CH₂CH₂ chain, while the chemical shifts and line shapes reveal bonding to quadrupolar boron nuclei.¹³ The ¹H COSY spectrum confirms the presence of a linear butyl fragment, as shown by the one-by-one connectivity pattern of all four resonances, none of which has any COSY connectivities to the rest of the ¹H resonances outside the aliphatic region. Instead, the α-CH₂ of the butyl group exhibits a cross-peak due to the coupling to the boron nucleus in the ¹H-¹¹B HMQC spectrum and can be tentatively assigned to a [BBu_{*n*}(C₆F₅)_{4-*n*}]⁻ borate anion structure. The ¹⁹F NMR spectrum confirms a tetracoordinated borate structure (Table 2-3), which is very different from the spectrum of the starting tricoordinate borane. All ¹⁹F signals can be separated into three distinct groups, either by a ¹⁹F COSY experiment or by a simple intensity reasoning where possible. Each of these groups contains a full set of ortho, meta, and para fluorines, representing different borates, [BBu_{*n*}(C₆F₅)_{4-*n*}]⁻. They can be tentatively assigned by fitting various integer *n* values from 0 to 4 for each set of ¹⁹F resonances so that an average number of Bu groups per borate, calculated this way, is equal to the value obtained from the ratio of ¹H NMR Cp and Bu integrals, assuming that there is one borate per zirconocene as the stoichiometry of the reaction requires. The ¹³C chemical shifts can be

extracted from ^{19}F - ^{13}C HMQC and HMBC experiments (Table 2-4). Reactions leading to redistribution of substituents at the boron center and further proof of the ^{19}F resonances assignment will be reported elsewhere.

Table 2-2. ^{13}C and ^{29}Si NMR data for **29a-e**^a

	for given compound (solvent)						
	29a (C_6D_6)	29a ($\text{C}_2\text{D}_2\text{Cl}_4$)	29b (C_7D_8)	29c (C_6D_6)	29c (C_7D_8)	29d (C_6D_6)	29e ^b (C_6D_6)
α -Bu	23.4	23.2	23.5	23.7	23.2	23.3	na
β -Bu	31.3	30.7	31.1	31.4	31.1	31.2	na
γ -Bu	27.2	27.0	27.2	27.4	27.2	27.2	na
δ -Bu	14.5	14.5	14.3	14.6	14.6	14.4	na
Cp	106.1	106.4	105.5	106.0	107.4	c	c
Cp	105.9	106.1	105.6	106.9	106.6	c	c
Cp*	na	na	na	11.8	11.9	na	na
Cp*	na	na	na	11.7	11.9	na	na
CH_2 -Si	na	na	27.4	na	na	na	na
<i>o</i> -Ph	135.2	135.2	nd	136.2	136.7	135.4	nd
<i>m</i> -Ph	128.0	129.1	nd	128.6	129.0	129.2	nd
<i>p</i> -Ph	128.9	130.9	nd	nd	130.7	130.9	nd
ipso-Ph	nd	135.6	nd	nd	nd	nd	nd
Si-H	105.9 (203.5, 32.2)	110.0 (203.0, nd)	110.9 (203.3, nd)	106.0 (nd)	106.2 (nd)	nd (nd)	101.5 (202.4, nd)

^a The chemical shifts are in parts per million, and the figures in parentheses are J_{SiH} coupling constants in hertz. The multiplicity of the ^{29}Si resonance is unknown as the data were determined indirectly from a 2D ^1H - ^{29}Si HMQC experiment. Abbreviations: nd, not determined; na, not applicable. All spectra were recorded at +25 °C (except for **29a** in $\text{C}_2\text{D}_2\text{Cl}_4$, which was recorded at -40 °C).

^b The borate counterion is $[\text{HB}(\text{C}_6\text{F}_5)_3]^-$.

^c The ¹H (Table 2-1) and ¹³C (this table) resonances for the directly bonded H and C nuclei in MeCp ligands are reported in the same order. ¹³C chemical shifts (ppm): for **29d**, 107.1, 105.2, 107.1, 104.3, 109.1, 107.5, 101.2, 113.1, 14.7, 14.4; for **29e**, 112.6, 100.4, 107.0, 109.2, 103.8, 105.0, 104.8, 104.8, 13.2, 13.2.

Table 2-3. ¹⁹F NMR chemical shifts for [BBu_n(C₆F₅)_{4-n}]⁻ anion^a

	for given compound (solvent)					
	29a (C ₆ D ₆)	29a (C ₂ D ₂ Cl ₄)	29b (C ₇ D ₈)	29c (C ₆ D ₆)	29c (C ₇ D ₈)	29d (C ₆ D ₆)
<i>o</i> -PhF ₂	-139.7, br s	-141.2, br s	-139.5, br s	-139.0, br s	-139.1, br s	-139.6, br s
<i>m</i> -PhF ₂	-166.0, t (20.7)	-167.3, t (19.8)	-166.1, br s	-166.2, br s	-165.4, t (20.5)	-166.1, t (20.0)
<i>p</i> -PhF ₂	-161.7, t (19.5)	-163.5, t (20.3)	-162.0, br s	-162.0, br s	-161.8, t (20.7)	-161.8, t (20.7)
<i>o</i> -PhF ₃	-134.4, d (24.5)	-136.5, d (23.0)	-134.3, br s		-135.7, d (21.2)	
<i>m</i> -PhF ₃	-168.7, t (20.7)	-170.1, t (19.8)	-168.4, br s		-167.6, t (21.1)	
<i>p</i> -PhF ₃	-166.3, t (21.4)	-167.6, t (20.5)	-166.1, br s		-165.2, t (20.5)	
<i>o</i> -PhF ₄			-132.9, br s	-136.4, br s	-135.5, d (21.2)	-134.6, d (21.2)
<i>m</i> -PhF ₄			nd	-167.6, br s	-167.8, t (21.1)	-168.7, t (20.7)
<i>p</i> -PhF ₄			-165.1, br s	-165.3, br s	-165.4, t (20.5)	-166.3, t (20.7)

^a The chemical shifts are reported in parts per million, and the figures in parentheses are the *J*_{FF} coupling constants in hertz. Abbreviations: d, doublet; t, triplet; br s, broad singlet; na, not applicable; nd, not determined. PhF₂, PhF₃, and PhF₄ stand for [BBu₂(C₆F₅)₂]⁻, [BBu₁(C₆F₅)₃]⁻, and [B(C₆F₅)₄]⁻ anions, respectively. All spectra were recorded at +25 °C (except for **29a** in C₂D₂Cl₄, which was recorded at -40 °C).

Table 2-4. ^{13}C NMR chemical shifts for the C_6F_5 groups of the $[\text{BBu}_n(\text{C}_6\text{F}_5)_{4-n}]^-$ anion^a

	for given compound (solvent)		
	29a ($\text{C}_2\text{D}_2\text{Cl}_4$)	29b (C_7D_8)	29c (C_7D_8)
<i>o</i> -PhF ₂	147.6, d m	149.0	148.4
<i>m</i> -PhF ₂	nd	137.4	137.2
<i>p</i> -PhF ₂	138.2, m	139.3	139.1
<i>o</i> -PhF ₃	148.3, d m, (236.7)	nd	149.2
<i>m</i> -PhF ₃	136.1, d m, (226.5)	nd	136.8
<i>p</i> -PhF ₃	137.1, d m, (244.9)	nd	138.0
ipso-PhF ₃	135.3	nd	nd
<i>o</i> -PhF ₄		nd	149.2
<i>m</i> -PhF ₄		nd	136.8
<i>p</i> -PhF ₄		nd	138.0

^a The chemical shifts are reported in parts per million and the figures in parentheses are the $^1J_{\text{CF}}$ coupling constants in hertz. Most of the $^1J_{\text{CF}}$ are unknown as the ^{13}C chemical shifts were determined indirectly from 2D ^{19}F - ^{13}C HMQC experiments. Abbreviations: d, doublet; t, triplet; br s, broad singlet; m, multiplet; d m, doublet of multiplets; na, not applicable; nd, not determined. PhF₂, PhF₃, and PhF₄ stand for $[\text{BBu}_2(\text{C}_6\text{F}_5)_2]^-$, $[\text{BBu}_1(\text{C}_6\text{F}_5)_3]^-$, and $[\text{B}(\text{C}_6\text{F}_5)_4]^-$ anions, respectively. All spectra were recorded at +25 °C (except for 29a in $\text{C}_2\text{D}_2\text{Cl}_4$, which was recorded at -40 °C).

The zirconocene core of the molecule is established from a ^1H COSY experiment. The Cp signals give cross-peaks with the ZrH, which in turn shows connectivities to the SiH and Ph. The proposed structure then is $[\text{Cp}_2\text{Zr}(\mu\text{-H})(\text{SiHPhY})]_x$, where x is the degree of association and Y is a generic substituent which has yet to be identified. It cannot be another zirconocene group as the bonding electrons of zirconium are already exhausted. Elemental analysis of 29a rules out Cl as a possible candidate for Y. On the other hand, the fact that the SiH signal is a simple singlet eliminates all elements with abundant magnetic isotopes (Li, B, and F) from being either directly attached to Si or in the α

position of group Y. The only exception could be Y = H, where both protons (SiH and SiY) are chemically and magnetically equivalent and do not exhibit scalar coupling. Although the SiH signal integrates for one H against two Cp groups, the actual number of protons attached to silicon could be higher as the peak is broad and the apparent integral intensity could be misleading. The possibility of a second proton being bonded to silicon was probed by investigating an analogue $[\text{Cp}_2\text{Zr}(\mu\text{-H})(\text{SiHCH}_2\text{Ph})]_2^{2+}[\text{BBu}_n(\text{C}_6\text{F}_5)_{4-n}]_2^{2-}$ (**29b**) with a benzyl group on silicon instead of phenyl. The methylene protons in the former are clearly a doublet in the ^1H NMR spectrum as expected for a $=\text{Si}(\text{H})\text{CH}_2\text{Ph}$ fragment as opposed to a triplet for a $-\text{Si}(\text{H})_2\text{CH}_2\text{Ph}$ group, which proves that Y is not H. The last two possible candidates for Y, C and Si, are ruled out by 1D ^{29}Si NMR and long-range ^1H - ^{13}C and ^1H - ^{29}Si correlation (HMBC) experiments. The only H(Si) to C cross-peak is to the ipso-carbon of the phenyl ring, which also correlates to the ortho-protons, and the integral intensities confirm that there is only one phenyl group per zirconocene. Furthermore, there is only one peak in the ^{29}Si NMR spectrum, and it is already assigned. Neither are there any long-range H(Si) to Si cross-peaks other than those which belong to the $[\text{Cp}_2\text{Zr}(\mu\text{-H})(\text{SiHPhY})]_x$ fragment. We have thus dismissed all available nuclei as possible candidates for substituent Y. On the other hand, the existence of a borate anion requires the presence of a positive charge somewhere in the molecule to balance the charge. The fourth “substituent Y” on silicon is then a positive charge, and the structure is proposed to be $[\text{Cp}_2\text{Zr}(\mu\text{-H})(\text{SiHPh})]_x^{x+}[\text{BBu}_n(\text{C}_6\text{F}_5)_{4-n}]_x^{x-}$. The degree of association (x) can be measured directly from the NMR spectrum of $[\text{CpCp}^*\text{Zr}(\mu\text{-H})(\text{SiHPh})]_x^{x+}[\text{BBu}_n(\text{C}_6\text{F}_5)_{4-n}]_x^{x-}$ (**29c**). The presence of chemically inequivalent cyclopentadienyl groups (Cp and Cp*) in **29c** results in a diastereotopic relationship between the bridging hydrides, which gives a characteristic *two spin* second order AX quartet. The number of bridging hydrides in **29c** is then two and so is the degree of association. The tendency to dimerize should be even more pronounced in the cases of

the less sterically constrained **29a** and **29b**. The other important conclusion from the diastereotopy in **29c** is that there is at least one chiral center in the molecule. In fact, there are two of them, as the Cp rings in **29a** and **29b** are diastereotopic but the other groups are not. The necessary condition to have pairs of nondiastereotopically related groups in a chiral dimer is to have them related by a symmetry operation.¹⁴ This proves that, although the dimeric molecule possesses chirality, it is still a symmetric dimer and thus must have an even number of chiral centers.

To probe the validity of the structural analysis, a similar compound, $[\text{MeCp}_2\text{Zr}(\mu\text{-H})(\text{SiHPh})]_2^{2+}[\text{BH}(\text{C}_6\text{F}_5)_3]_2^{2-}$ (**29e**), was synthesized by an alternative procedure (eq 2-2) from $[\text{MeCp}_2\text{Zr}(\mu\text{-H})\text{H}]_2$, $\text{B}(\text{C}_6\text{F}_5)_3$, and PhSiH_3 . This synthetic route avoids ambiguities associated with the $\text{Cp}_2\text{ZrCl}_2/2\text{BuLi}$ reagent¹⁵ and furnishes a single borate anion, $[\text{HB}(\text{C}_6\text{F}_5)_3]^-$, which has been reported before.¹⁶ The ^1H and ^{13}C NMR spectra of the zirconocene core of **29e** are almost identical with $[\text{MeCp}_2\text{Zr}(\mu\text{-H})(\text{SiHPh})]_2^{2+}[\text{BBu}_n(\text{C}_6\text{F}_5)_{4-n}]_2^{2-}$ (**29d**), which has been synthesized from a mixture of $\text{MeCp}_2\text{ZrCl}_2$, BuLi , $\text{B}(\text{C}_6\text{F}_5)_3$, and PhSiH_3 .

In view of the controversy surrounding the existence of cationic silylium in the condensed phase,²⁻¹² two caveats are offered with respect to the structure of **29**. Firstly, two mesomeric structures are possible (Figure 2-2), one of them having the positive charge on zirconium, **29'**, the other one on silicon, **29''**. Secondly, a stabilizing interaction with the borate ion and/or solvent cannot be excluded (mesomer **29'''**). The latter interactions, if they exist, must be weak since the solvent (toluene) can be completely removed upon long exposure to high vacuum, and no concentration dependence in the ion pairing in solution for **29a** was detected, *vide infra*.

In the IR spectrum of **29a** a peak is observed at 1216 cm^{-1} , which is absent from the spectrum of a sample of **29a** prepared with PhSiD_3 . This peak is in the region expected for neutral¹⁷⁻²⁶ and cationic²⁷ zirconocene hydrides containing the $\text{Zr}_2(\mu\text{-H})_2$ group. The ν_{SiH} mode appears at 2113 cm^{-1} , in good agreement with the assignment for mesomers

29a'' and **29a'''**.²⁸ If the structure is visualized in terms of mesomer **29a'**, the 2113 cm^{-1} stretch corresponds to a normal, unperturbed SiH. The low frequency for the other stretch reflects a considerable weakening of the second SiH bond. In the well-documented examples of an agostic SiH-Zr²⁹ the frequency is decreased by 100-200 cm^{-1} , whereas in **29a** it is shifted by about 900 cm^{-1} . The IR data thus favors mesomer **29a''** and **29a'''** over **29a'**.

The UV spectrum of **29a** exhibits a weak absorption in toluene at 430 nm ($\epsilon = 165 \text{ dm}^3 \text{ mol}^{-1} \text{ cm}^{-1}$), similar to that observed previously for zirconocene silyl complexes and tentatively assigned as a silyl ligand-to-metal charge-transfer transition.³⁰

From a topological point of view all of the mesomers are identical as they contain the same symmetry elements and can be schematically drawn as **29''''** (Figure 2-2). The two chiral silicon atoms and the two possible (cis- and trans-) orientations of the Cp and Cp* ligands give rise to four diastereomers for **29c** (Table 2-5). Compounds **29a** and **29b** can only form two diastereomers as all Cp groups are chemically equivalent. Table 2-5 summarizes the symmetry point groups for all diastereomers and the spatial relationships between potentially diastereotopic groups stemming from them.¹⁴

Both diastereomers of **29a** and **29b** have diastereotopic Cp groups as reflected in the observed NMR spectra. Unfortunately, it is not possible to establish which isomer is actually formed as the only difference between them is that the SiH and the bridging hydride fragments are enantiotopic in one of them and equivalent in the other. Both of these structures give rise to the same NMR multiplicity pattern. On the other hand the NMR spectrum of **29c** is more informative and can be assigned to only two out of four possible stereoisomers, as the other two do not possess diastereotopic groups (Table 2-5). One of the two diastereomers can be discarded on steric grounds (Figure 2-3, (*S,R*)- or (*R,S*)-*cis*-**29c**) as it has both Cp* groups on the same side of the bisectorial plane. The other diastereomer ((*S,S*)- or (*R,R*)-*trans*-**29c**) is almost identical to the structure of the neutral silyltitanocene dimer, which was studied earlier by single crystal X-ray

diffraction.³¹ It is not clear why the phenyl groups in this compound adopt a cis arrangement, but at least it proves that there is no significant repulsion between them. Besides, the larger covalent radius of zirconium should further reduce steric interactions between cis phenyl groups and between phenyl and cyclopentadienyl groups. Another possible explanation is that the structure of **29c** could be closer to the mesomeric form **29c'''** (Figure 2-2), which has at least a restricted rotation about the Si-Zr axis and does not have to have the two phenyls in a cis arrangement to be (*S,S*)- or (*R,R*)-*trans*-**29c**. The ²⁹Si NMR chemical shift for **29c** is in good agreement with the nonplanar geometry of the silicon ligand of mesomer **29c'''**, as compared with the data for organic^{2,3,32-34} and organometallic³⁵ “cation-like” silylium compounds reported previously. It is also favored by the *J*_{SiH} coupling constants, which differ by an order of magnitude for the Si-H and Si-(μ-H) bonds (203.5 and 32.2 Hz, respectively). The coupling constant of 32.2 Hz is very close to a normal HSi-Zr-H ³*J*_{SiH} value,^{36,37} which would be expected for **29c''** and **29c'''**. On the other hand, this value is also within the range for compounds containing nonclassical, or agostic, metal-SiH bonds.^{38,39} This suggests that the mesomer structure **29c'** is feasible as well, although most of the known nonclassical metal-SiH compounds exhibit much higher scalar coupling.^{29,36,40-46}

A NOESY experiment is in excellent agreement with the proposed mesomer structures **29c'** and **29c''**. Each of the bridging hydrides exhibits a cross-correlation to a different pair of Cp and Cp* ligands (Figure 2-4), which can be rationalized in terms of distorted Zr-H-Zr or inherently asymmetrical Zr-Si-H-Zr bridges. Indeed, the frontier orbitals of zirconocene are in the bisectorial plane of the sandwich. The bridging hydrides are thus constrained to be in close proximity to that plane, so that the NOEs between μ-H and the cyclopentadienyl groups of the same CpCp*Zr moiety are approximately equal. Experimentally observed pairs of NOE cross-peaks (μ-H(#1) to Cp(#1) and Cp*(#1); μ-H(#2) to Cp(#2) and Cp*(#2)) thus represent the left and the right sides of the bridged dimer with respect to the (μ-H)-(μ-H) axis. The SiH and Ph groups have NOEs with other

pairs of Cp and Cp* (Figure 2-5), confirming that they appear on different sides of the bisectorial plane as predicted from the topological analysis.

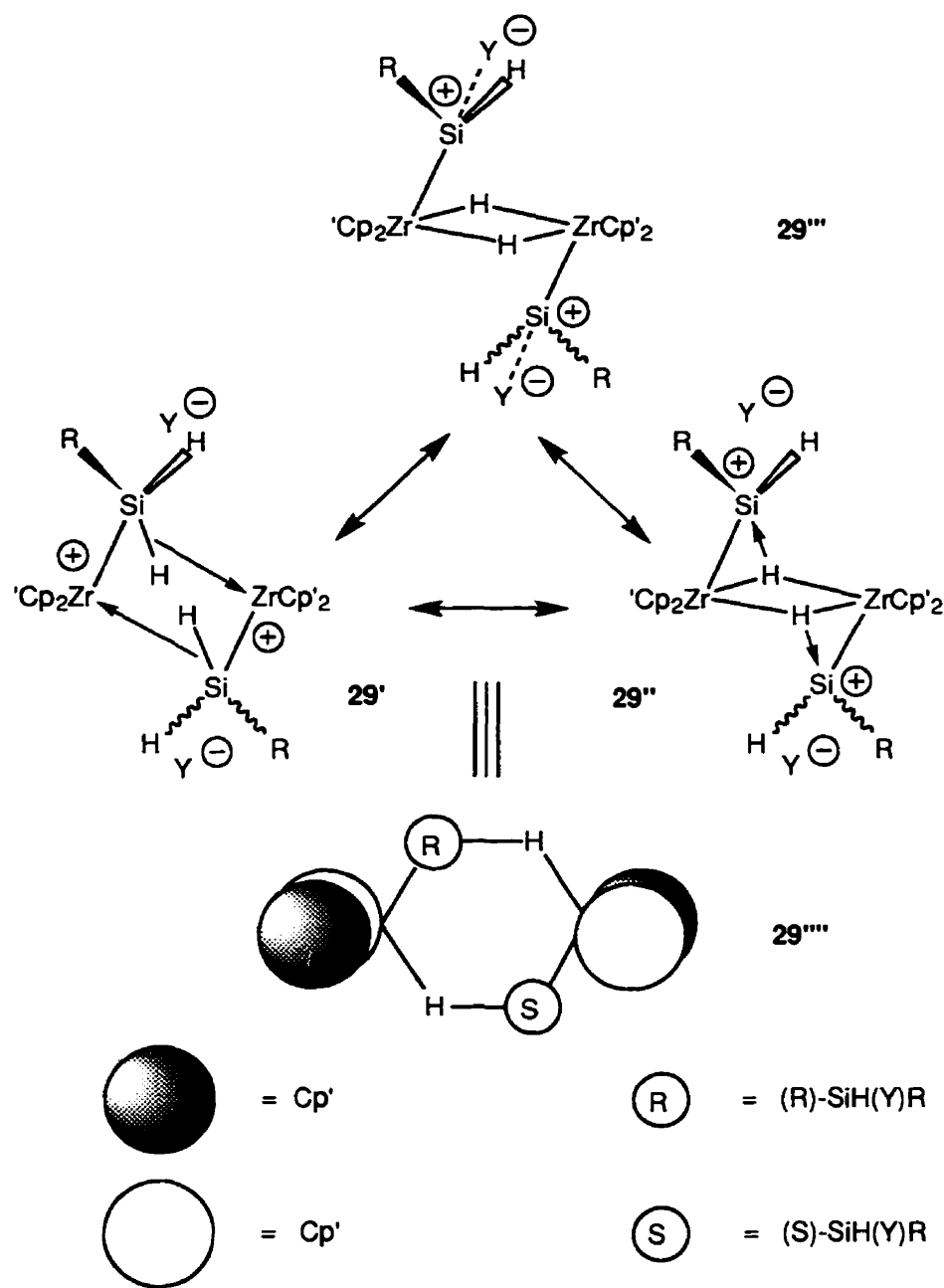


Figure 2-2. Proposed mesomer structures for **29a-e** and their topological representation.

Table 2-5. Spatial relationship of the Cp, Cp*, μ -H and Si ligands in **29a**, **29b** and **29c**

Diastereomer	μ -H	Si-H	diagonal Cp's	top/bottom Cp's	left/right Cp's
(<i>S,S</i>)- or (<i>R,R</i>)- <i>trans</i> - 29c	ni ^a diast	ni diast	ni diast	chemically inequivalent	
(<i>S,S</i>)- or (<i>R,R</i>)- <i>cis</i> - 29c	C_2 equiv	C_2 equiv	chemically inequivalent		C_2 equiv
(<i>S,R</i>)- or (<i>R,S</i>)- <i>trans</i> - 29c	S_2 enant	S_2 enant	S_2 enant	chemically inequivalent	
(<i>S,R</i>)- or (<i>R,S</i>)- <i>cis</i> - 29c	ni dias	ni diast	chemically inequivalent		ni diast
(<i>S,S</i>)- or (<i>R,R</i>)- 29a or 29b	C_2 equiv	C_2 equiv	ni diast		C_2 equiv
(<i>S,R</i>)- or (<i>R,S</i>)- 29a or 29b	S_2 enant	S_2 enant	S_2 enant	ni diast	
achiral ^b <i>trans</i> - 29c	S_2 enant	S_2 enant	S_2 enant	chemically inequivalent	
achiral ^b <i>cis</i> - 29c	C_2 equiv	C_2 equiv	chemically inequivalent		C_2 equiv

^a ni, not interchangeable by any symmetry operation; diast, diastereotopic; enant, enantiotopic; equiv, equivalent; C_2 -axes of rotation; S_2 -axes of rotation-inversion; cis, both Cp* ligands are on one side of the bisectorial plane; trans, on opposite sides. "Diagonal", "top/bottom", and "left/right" ligand labels are given with respect to the bisectorial plane.

^b planar silicon cation with no chiral center on it.

No NOE was detected between the butyl group of the borate anion and any proton of the cation, although the relaxation times for the butyl protons (except for the α -CH₂) are of the same order as those for the SiH and μ -H protons, which makes any short cation-anion contacts in **29c**''' (Figure 2-2) unlikely. There is no evidence for any cation-anion interactions in the ¹⁹F NMR spectra either, which casts further doubt on the

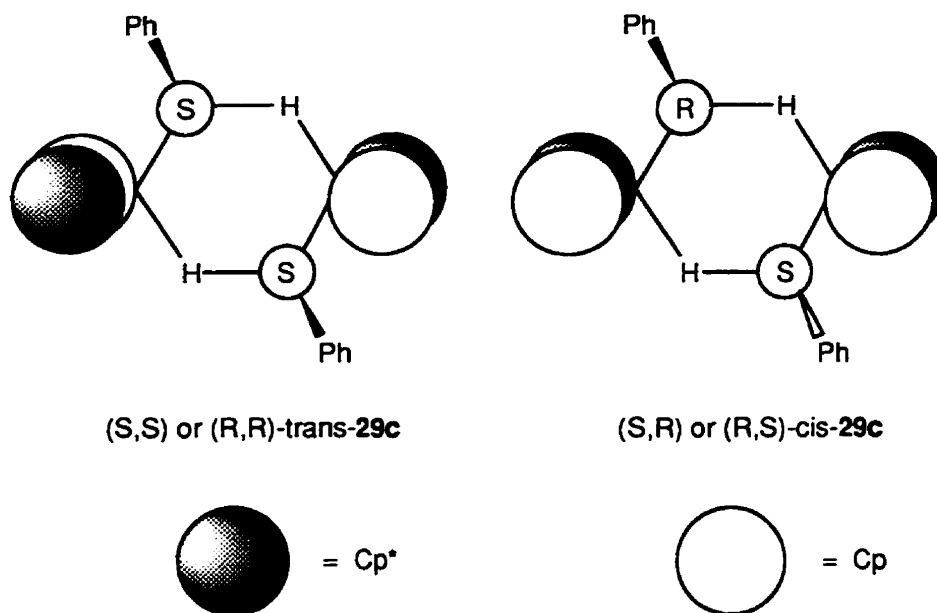


Figure 2-3. Topological representation of all isomers of **29c**, which agree with the results of the NOESY experiment. Cis stands for an arrangement of both Cp ligands on one side of the bisectorial plane; trans, on opposite sides.

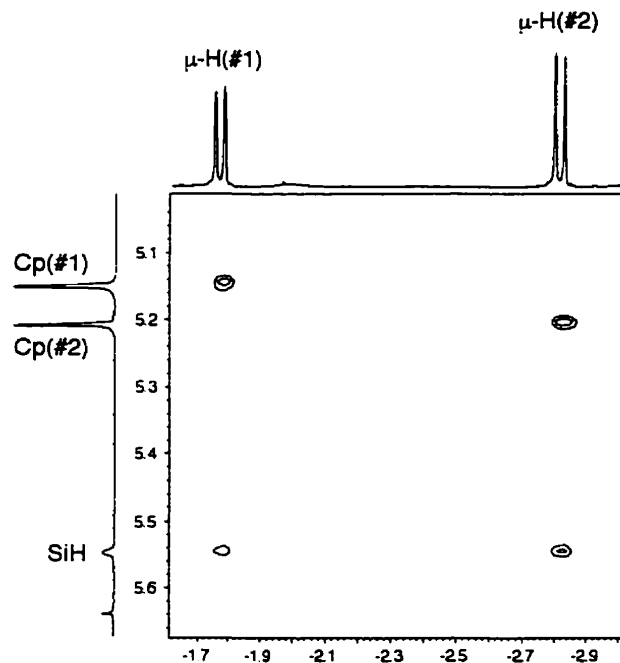


Figure 2-4. Fragment of an ^1H NOESY plot for **29c** which shows that each of the bridging hydrides exhibits a cross-correlation to a different Cp ligand, which can be rationalized in terms of distorted Zr-H-Zr or inherently asymmetric Zr-Si-H-Zr bridges.

structure **29c'''**. Although the number of ^{19}F resonances is doubled when a sample of **29c** in C_7D_8 is cooled to $-20\text{ }^\circ\text{C}$, it is not due to coordination. If a borate really coordinates through one of the F atoms, a significant upfield shift is expected for the latter⁴⁷ and the ratio of integrals for the coordinated/free pentafluorophenyl groups $[(\text{C}_6\text{F}_5)_{\text{coord}}\text{BBu}_n(\text{C}_6\text{F}_5)_{3-n}]^-$ should be strictly $1/(3-n)$. Besides, if the coordination occurs through ortho or meta fluorines,¹⁶ the pentafluorophenyl group loses C_2 symmetry and the spin system changes from $\text{AA}'\text{MM}'\text{X}$ to ABMNX . None of these changes occur in the cooled samples of **29c**. The multiplicity of the spectrum indicates that all pentafluorophenyls within the borate are C_2 symmetrical and equivalent in a broad temperature range (-40 to $+40\text{ }^\circ\text{C}$ for $\text{C}_2\text{D}_2\text{Cl}_4$ and -90 to $+40\text{ }^\circ\text{C}$ for C_7D_8). Careful inspection of the sample revealed that the spectral changes are due to the formation of a second liquid phase (**29c**- C_7D_8 liquid clathrate⁴⁸) upon cooling below $-10\text{ }^\circ\text{C}$. The second phase solidifies upon further cooling to -60 to $-90\text{ }^\circ\text{C}$, and the ^{19}F spectrum simplifies accordingly (Figure 2-6).

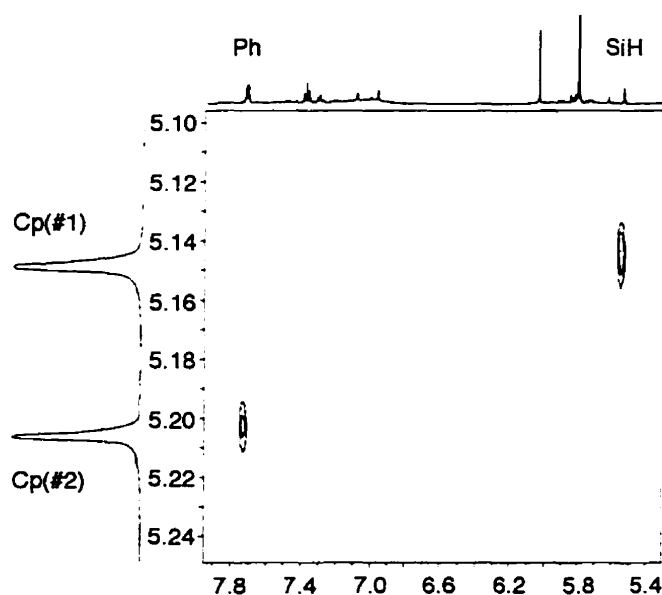


Figure 2-5. Fragment of an ^1H NOESY plot for **29c** which shows that the SiH and Ph groups have NOEs with different Cp ligands, confirming that they appear on different sides of the bisectorial plane (Figure 3, (*S,S*)- or (*R,R*)-*trans*-**29c** structure).

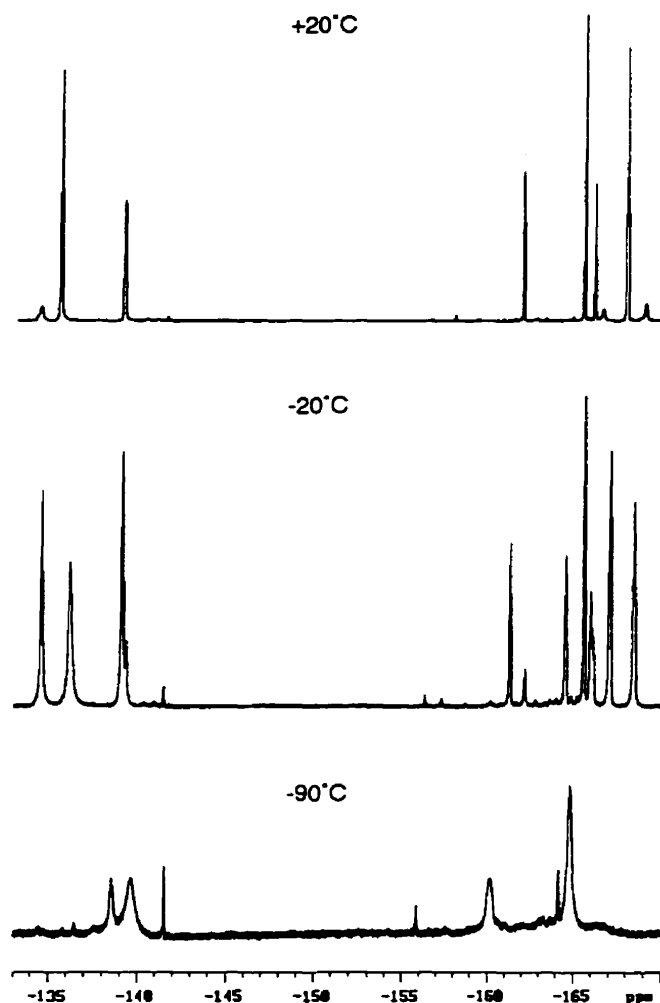


Figure 2-6. Variable temperature ^{19}F NMR spectra for compound **29c** in C_7D_8 . The number of ^{19}F resonances is doubled when the sample is cooled to -20°C , due to the formation of a second liquid phase (**29c**- C_7D_8 clathrate). The clathrate phase solidifies upon further decrease of temperature (-90°C), and the ^{19}F spectrum simplifies accordingly.

It can thus be concluded that **29c** is a racemic mixture of (*S,S*) and (*R,R*)-*trans*-**29c** isomers, which can be best visualized either as mesomer **29c'** or **29c''**. The SiH coupling constants and the IR data for **29a** suggest that **29c''** corresponds most closely to the true structure of **29c**. The real structure, however, might be a hybrid of both

mesomeric extremes, with the positive charge shared between Zr and Si atoms, as indicated by the NMR data.

This charge delocalization can be the source of the surprising stability of the “silylium-like” cation in this case. High-level *ab initio* calculations show that the poor stability of silylium ions in the condensed phase is mainly due to the inefficiency of the hyperconjugative and inductive stabilization of Si^+ by hydrocarbon substituents (Me) as compared to the same effects for C^+ .⁴⁹⁻⁵² The hyperconjugation is decreased because the energy difference and spatial separation between the pseudo- $\pi(\text{Me})$ and $2p\pi(\text{Si}^+)$ orbitals results in poor overlap. The inductive effect of the alkyl groups destabilizes R_3Si^+ as C is more electronegative than Si.⁴⁹⁻⁵² On the other hand, the mesomeric form **29''** can have a much better stabilization than trialkylsilylium because of the inductive effect of Zr, which is more electropositive than C and Si, and because of the better hyperconjugation between a Zr-H bond and an unoccupied Si^+ orbital. The latter should be facilitated by the larger size of the Zr- compared to C-centered orbitals. Such hyperconjugation leads to an increase in the Zr-Si bond order, and it is of interest to note that recent calculations on $(\text{CO})_5\text{Cr}=\text{SiR}_2$ ($\text{R}_2 = \text{H}_2, \text{Me}_2, \text{F}_2, \text{Cl}_2, \text{Me}(\text{OMe})$) compounds indicate that substantial contributions to bonding can arise from π -overlaps in transition metal-silicon bonds.⁵³ Indeed, stable metal-silylene complexes with strong $\text{M}=\text{Si}$ double bonds are well-known,⁵⁴ and their electronic structure can be described adequately.⁵⁵ In the cases of Tilley's base-stabilized⁵⁶⁻⁶¹ and base-free⁶²⁻⁶⁸ cationic silylene compounds, the π -bond is weaker due to the positive charge on the metal, and the structure could be a hybrid of two mesomers, $[\text{M}^+=\text{Si}]$ and $[\text{M}-\text{Si}^+]$. It should be emphasized that in compounds **29a-e** there are no d-electrons on the metal, as opposed to cationic silylene complexes, and there is no possibility of multiple bonding.

2.2.2 ^{29}Si NMR Studies of Ion Pairs in Solution

Perhaps the most useful tool for studying the share of the silicon atom in positive charge delocalization is ^{29}Si NMR spectroscopy;^{69,70} at the same time it is the source of the most controversial discussions.^{8-10,71-73} If there is a partial positive charge on silicon and it exists as an ion pair in solution, then the ^{29}Si chemical shift and $^1J_{\text{SiH}}$ coupling constant should be sensitive to the tightness of the ion pair, which in turn is concentration dependent. This type of concentration dependence study requires high dilution, which usually leads to contamination with traces of moisture and oxygen from the solvents. The silylium cation can then degrade, forming Si-O bonds giving rise to deceptively low field chemical shifts. These can then be misinterpreted as less tightly bonded ion pairs or free ions.

In our experiments we used a technique designed to keep the amount of hydrolysis products relative to the sample very low (see experimental section). To enhance the ^{29}Si NMR signals, an inverse detection (HMQC) was used, which improved the detection limit by 2 orders of magnitude. This allowed coverage of a concentration range in which up to 98% of the free ions of $\text{R}_3\text{Si}^+\text{ClO}_4^-$ ($\text{R} = \text{Ph}, \text{Me}$) were previously claimed to exist.⁷⁴ It was impossible to test this concentration range by direct detection ^{29}Si NMR techniques due to the low receptivity.⁷³ As can be seen from the results (Figure 2-7), neither the ^{29}Si chemical shift nor the $^1J_{\text{SiH}}$ coupling constant is significantly dependent on concentration. This suggests that **29a** either exists as free ions in the whole range of concentrations studied or as completely associated tight ion pairs. The former is incompatible with anion stabilized silylium **29a'''** but compatible with the zirconium cation **29a'**, or the internally stabilized silylium **29a''**. The latter is unlikely since even more polarizing cationic titanocene complexes, with the more coordinative AlCl_4^- counterion, ionize extensively in chloroalkane solutions.⁷⁵ Still further evidence in favor of negligible bonding between anion and cation is the identity of the NMR parameters for the anion in **29a** to those of

$[\text{Ph}_3\text{C}]^+[\text{BBu}_2(\text{C}_6\text{F}_5)_2]^-$ and of the parameters for the anion in **29e** to those of $[\text{Cp}^*\text{ZrH}][\text{BH}(\text{C}_6\text{F}_5)_3]$.¹⁶

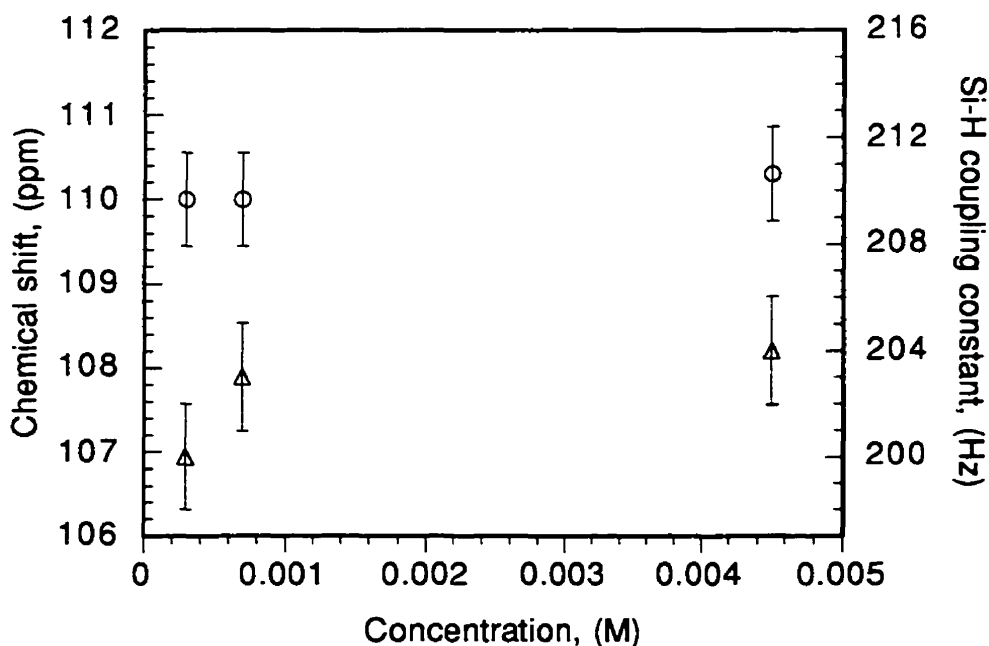


Figure 2-7. ^{29}Si chemical shift (o) and the $^1J_{\text{SiH}}$ coupling constant (Δ) versus concentration plots for **29a**. The sample does not exhibit any ion pairing effects in the studied range of concentrations.

The very existence of silylium compounds has been challenged^{4,5} as, in all the known examples, there are weak bonding contacts between R_3Si^+ and another group (S)^{2,3,10,32-34} and the positive charge was calculated to be localized mainly on that group rather than on Si.^{4,49-52} However, the ability of compounds $[\text{R}_3\text{Si}\cdots(\text{S})]^+[\text{X}]^-$ to ionize in halocarbon solvents is beyond any doubt,^{2,10,32,34} and even if the resulting $[\text{R}_3\text{Si}\cdots(\text{S})]^+$ ions have no silylium character, the ^{29}Si NMR chemical shifts should still be sensitive to that type of ion pairing.⁴⁹

2.2.3 Ion Exchange Reaction

An attempt to probe the charge delocalization between Zr and Si in **29** by reaction with CsF did not give a clear result. Reaction of **29a** and CsF in THF proceeded vigorously, and a number of unidentified products were formed (at least six major peaks in the Cp region). However, an ^1H - ^{29}Si coupled HMQC experiment revealed only one Si-containing product in the reaction mixture ($\delta = -42.5$ ppm, $^1J_{\text{SiH}} = 172.5$ Hz, $J_{\text{FH}} = 14.2$ Hz). The concentration was not high enough to obtain a 1D ^{29}Si NMR spectrum and the resolution in the ^1H - ^{29}Si HMQC experiment was not high enough to resolve the F-Si coupling constant. Failure to resolve this peak places an upper limit of 20 Hz on any J_{FH} . Even though, the information was insufficient to identify the full structure of this product, the values for J_{FH} and J_{SiF} are characteristic enough to favor a structure containing $\text{HSi}[\text{Zr}]\text{F}$ rather than $[\text{Zr}]\text{-Si(H)F}$ ($^2J_{\text{HSiF}}$ coupling constants are usually in the range of 45-65 Hz,⁷⁶ and $^1J_{\text{SiF}}$ are never as low as 20 Hz.⁷⁷)

Other attempted ion exchange reactions, with MeLi or with $[\text{NBu}_4]\text{F}$, gave even more inconclusive results.

2.3 Conclusions

Novel zirconocene complexes **29a-e** were isolated from silane dehydropolymerization reaction mixtures catalyzed by $\text{Cp}'_2\text{ZrCl}_2/2\text{BuLi}/\text{B}(\text{C}_6\text{F}_5)_3$ or by $[\text{Cp}'_2\text{Zr}(\mu\text{-H})\text{H}]_2/2\text{B}(\text{C}_6\text{F}_5)_3$ combination catalysts. In the absence of X-ray quality crystals, a total structure analysis of these compounds was performed by multinuclear, multidimensional NMR spectroscopy. A 3D structure, unambiguously determined by a set of homo- (COSY, TOCSY and NOESY) and heterocorrelation (HMQC and HMBC) experiments, shows that each zirconocene fragment bears a positive charge, which is delocalized between the metal center and the hydrosilane ligand. Ion exchange reactions

with CsF indicate that much of the positive charge is localized on Zr. However, it is likely that the positive charge is really delocalized between Zr and Si and cannot be assigned to only one particular atom. The structures of **29a-e** are best visualized as a hybrid of two mesomeric forms **29'** and **29''**, which can be formally described either as zirconocene with an internally stabilized silylium ligand or cationic zirconocene with an α -agostic (or nonclassically bonded) Si-H. A lack of concentration dependence for the ^{29}Si NMR chemical shifts and $^1\text{J}_{\text{SiH}}$ coupling constants is in agreement with this interpretation.

2.4 Experimental Section

2.4.1 Materials and Methods

All operations were performed in Schlenk-type glassware on a dual-manifold Schlenk line, equipped with flexible stainless steel tubing, or in an argon-filled M.Braun Labmaster 130 glovebox (<0.05 ppm H_2O). Argon was purchased from Matheson (prepurified for the glovebox and ultrahigh purity (UHP) for the vacuum line) and was used as received. Hydrocarbon solvents (protio- and deuteriobenzene, and toluene, pentane, and hexanes) were dried and stored over Na/K alloy, benzophenone, and 18-crown-6 in Teflon-valved bulbs and were vacuum transferred prior to use. THF was vacuum transferred from sodium benzophenone ketyl. Halogenated solvents and silanes (1,1,2,2-tetrachloroethane- d_2 , $\text{C}_6\text{F}_5\text{Br}$, PhSiH_3 , and $\text{PhCH}_2\text{SiH}_3$) were degassed and stored over molecular sieves. Cp_2ZrCl_2 , $\text{Me}_5\text{C}_5\text{H}$, ZrCl_4 , C_6D_6 , C_7D_8 , 1,1,2,2-tetrachloroethane- d_2 , $\text{C}_6\text{F}_5\text{Br}$, CsF, PhC(O)Ph , 18-crown-6, BCl_3 (1.0 M in heptane), n-BuLi (1.6 M in hexanes), CpNa (2.0 M solution in THF), and CDCl_3 were purchased from Aldrich and used as received unless stated otherwise.

The compounds $(\text{MeCp})_2\text{ZrCl}_2$,⁷⁸ $[(\text{MeCp})\text{Zr}(\mu\text{-H})\text{H}]_2$,¹⁸ $\text{CpCp}^*\text{ZrCl}_2$,⁷⁹ $\text{B}(\text{C}_6\text{F}_5)_3$,⁸⁰ and RSiH_3 (R = Ph and PhCH_2)⁸¹ were prepared according to literature procedures.

2.4.2 Physical and Analytical Measurements

NMR spectra were recorded on a Varian Unity 500 (FT, 500 MHz for ^1H), Varian XL-200, or Varian Gemini-200 (FT, 200 MHz for ^1H) spectrometers. Chemical shifts for ^1H and ^{13}C spectra were referenced using internal solvent references and are reported relative to tetramethylsilane. ^{11}B , ^{19}F , and ^{29}Si spectra were referenced to external $\text{Et}_2\text{O}\cdot\text{BF}_3$, CF_3COOH , and $\text{Si}(\text{CH}_3)_4$, respectively. Quantitative NMR measurements were performed using residual solvent protons as internal references. IR and UV spectra were recorded on Bruker IFS-48 (FT) and HP-8452A (FT) spectrometers, respectively. Elemental analyses were performed by Oneida Research Services, Inc., Whitesboro, New York.

All NMR samples were prepared in an NMR-tube assembly, consisting of one or more 2 mL round-bottom flasks fitted with a Teflon valve to which an NMR tube was fused at an angle of 45° . Components of an NMR sample were loaded separately, when necessary, in each of the flasks and were mixed in appropriate order by transferring from one flask of choice to the other by tilting of the entire apparatus. A sample was treated with small quantities (0.1-0.2 mL) of a deuterated solvent of choice. The solvent was then evaporated, and the evaporation-vacuum transfer cycle was repeated to remove any residual traces of nondeuterated solvent. A fresh portion of the same deuterated solvent (0.6-0.7 mL) was then vacuum transferred into the assembly, and the solution was carefully decanted into the side NMR tube. The top part of the tube was washed by touching it with a swab of cotton wool soaked with liquid nitrogen, which causes condensation of the solvent vapors on the inner walls. The sample was then frozen and flame sealed.

2.4.3.1 $[\text{Cp}_2\text{Zr}(\mu\text{-H})(\text{SiHPh})]_2^{2+}[\text{BBu}_n(\text{C}_6\text{F}_5)_{4-n}]_2^{2-}$ (29a),¹ Low Temperature Synthesis

Part A Cp_2ZrCl_2 (0.219 g, 0.75 mmol) and $(\text{C}_6\text{F}_5)_3\text{B}$ (0.384 g, 0.75 mmol) were loaded into separate Schlenk tubes in the glovebox. On the vacuum line, toluene was vacuum transferred into both tubes (8 mL each). The Cp_2ZrCl_2 was suspended in toluene at $-41\text{ }^\circ\text{C}$ (CH_3CN -dry ice bath), and a 2.5 M solution of BuLi in hexanes (0.6 mL, 1.50 mmol) was added. The mixture was stirred at $-41\text{ }^\circ\text{C}$ for 1 h. The color gradually changed from white to light yellow. The toluene solution of $(\text{C}_6\text{F}_5)_3\text{B}$ was cooled to $-41\text{ }^\circ\text{C}$ and was slowly transferred by cannula into the butylated zirconocene solution. A brown-red oil was formed almost instantaneously. The reaction mixture was protected from light with aluminum foil and was left stirring for 30 min. PhSiH_3 (0.56 mL, 4.50 mmol) was then added, and the stirring was continued for a further 3 h while the solution was allowed to warm gradually to room temperature. The solvent was partially evaporated (leaving 1-2 mL), and pentane was vacuum transferred into the tube, causing precipitation of a yellow slurry. The brown mother liquor was removed, and the bright yellow residue was washed with two additional portions of pentane (2x10 mL) and dried under vacuum to furnish a yellow microcrystalline powder.

Part B The yellow solid was redissolved in toluene (300 mL) and was left standing for 3 days in the dark to allow precipitation of LiCl . The brownish-yellow mother liquor was carefully separated from the white precipitate and evaporated almost to dryness. The resulting slurry was washed with a 5% solution of toluene in pentane (2x10 mL) and with pure pentane (2x10 mL). The resulting yellow powder was dried under high vacuum for 2 days; yield 57 %. IR (powder, cm^{-1}): 1216 (ν_{ZrH}), 2113 (ν_{SiH}). UV-vis (toluene, nm ($\text{dm}^3\text{ mol}^{-1}\text{ cm}^{-1}$)): λ (ϵ) 335 (3190), 430 (165). Anal. Calcd for $\text{C}_{76}\text{H}_{52}\text{B}_2\text{F}_{30}\text{Si}_2\text{Zr}_2$: C, 50.84; H, 2.92, N, 0.00; Cl, 0.00. Found: C, 50.45; H, 2.77; N, 0.00; Cl, 0.00. ^{11}B -NMR (C_6D_6 , $25\text{ }^\circ\text{C}$): δ -24.3 and -24.8 (s, $[\text{BBu}_n(\text{C}_6\text{F}_5)_{4-n}]^-$, $n = 0, 2$); ^{11}B -NMR ($\text{C}_2\text{D}_2\text{Cl}_4$, $-40\text{ }^\circ\text{C}$): δ -25.2 (s, $[\text{BBu}(\text{C}_6\text{F}_5)_3]^-$).

2.4.3.2 $[\text{Cp}_2\text{Zr}(\mu\text{-H})(\text{SiHPh})]_2^{2+}[\text{BBu}_n(\text{C}_6\text{F}_5)_{4-n}]_2^{2-}$ (29a), Room Temperature Synthesis

The title complex was synthesized using the same procedure as that for 29a (part A), but all reactions were done at room temperature. The product was dark purple and was contaminated by poly(phenylsilane) and unidentified paramagnetic compounds (crude yield ~75 %).

2.4.3.3 $[\text{Cp}_2\text{Zr}(\mu\text{-H})(\text{SiHCH}_2\text{Ph})]_2^{2+}[\text{BBu}_n(\text{C}_6\text{F}_5)_{4-n}]_2^{2-}$ (29b)

The title complex was synthesized using the same procedure as that for 29a (part A) by the reaction of Cp_2ZrCl_2 (0.073 g, 0.25 mmol), BuLi in hexanes (0.2 mL, 0.50 mmol), $(\text{C}_6\text{F}_5)_3\text{B}$ (0.128 g, 0.25 mmol), and $\text{PhCH}_2\text{SiH}_3$ (0.139 mL, 1.0 mmol) (crude yield ~70 %).

2.4.3.4 $[\text{Cp}'\text{Cp}''\text{Zr}(\mu\text{-H})(\text{SiHPh})]_2^{2+}[\text{BBu}_n(\text{C}_6\text{F}_5)_{4-n}]_2^{2-}$ ($\text{Cp}'\text{Cp}'' = \text{CpCp}^*, (\text{MeCp})_2$) (29c,¹ 29d)

The title compounds were synthesized using the same procedure as that for 29a (part A) by the reaction of $\text{CpCp}^*\text{ZrCl}_2$ (0.136 g, 0.375 mmol) or $(\text{MeCp})_2\text{ZrCl}_2$ (0.120 g, 0.375 mmol) with BuLi in hexanes (0.3 mL, 0.75 mmol), $(\text{C}_6\text{F}_5)_3\text{B}$ (0.202 g, 0.39 mmol), and PhSiH_3 (0.185 mL, 1.5 mmol) (crude yield ~70 %). ^{11}B -NMR (C_6D_6 , 25 °C): for 29c, δ -24.4 (s, $[\text{B}(\text{C}_6\text{F}_5)_4]^-$), δ -24.5 (br s, $[\text{BBu}_n(\text{C}_6\text{F}_5)_{4-n}]^-$, $n = 0, 1, 2$); for 29d, δ -24.6 (br s, $[\text{BBu}_n(\text{C}_6\text{F}_5)_{4-n}]^-$, $n = 0, 2$).

2.4.3.5 $[(\text{MeCp})_2\text{Zr}(\mu\text{-H})(\text{SiHPh})]_2^{2+}[\text{BH}(\text{C}_6\text{F}_5)_3]_2^{2-}$ (29e)

$[(\text{MeCp})\text{Zr}(\mu\text{-H})\text{H}]_2$ (0.025 g, 0.05 mmol) and $(\text{C}_6\text{F}_5)_3\text{B}$ (0.056 g, 0.11 mmol) were loaded into separate flasks of the double flask NMR assembly, *vide supra*, in the glovebox, and toluene was then vacuum transferred into both flasks (2 mL each). The apparatus was immersed in an acetone-dry ice bath (-78 °C), the reagents were mixed

together, and the mixture was stirred for 30 min at -78 °C and for 3 h at room temperature. The color gradually changed from white to light yellow and light purple. The solvent was removed under vacuum, and the residue was washed with pentane (2x5 mL). A fresh portion of toluene (5 mL) was vacuum transferred into the flask, and PhSiH₃ (0.05 mL, 0.40 mmol) was added. The reaction mixture was protected from light with aluminum foil and was left stirring overnight. The solvent was partially removed (leaving 0.5-1 mL), and pentane was vacuum transferred into the flask, causing precipitation of a yellow solid. The clear mother liquor was removed, and the residue was washed with an additional portion of pentane (5 mL). The sample was dried under high vacuum, and an NMR sample was prepared as described above.

NMR data for [BH(C₆F₅)₃]⁻ (C₆D₆, 25 °C). ¹¹B-NMR: δ -25.6 (s). ¹³C-NMR: δ 148.2 (*o*-C₆F₅), 138.6 (*p*-C₆F₅), 136.8 (*m*-C₆F₅). ¹⁹F-NMR: δ -139.1 (d, *J*_{FF} = 15 Hz, *o*-C₆F₅), -163.1 (t, *J*_{FF} = 20.5 Hz, *p*-C₆F₅), -167.2 (br t, *m*-C₆F₅). The rest of the NMR data for **29e** are reported in Tables 2-1 and 2-2.

2.4.3.6 ²⁹Si NMR Studies of Ion Pairing in Solution

In the drybox, **29a** (0.0045 g, 0.0025 mmol) and 1,1,2,2-tetrachloroethane-*d*₂ (0.55 mL) were loaded in an NMR container, attached to a Teflon valve, and flame sealed under vacuum. To minimize the danger of side reactions, the measurements were performed at -40 °C immediately after the preparation of the sample.

A special NMR tube with a small, pendant bulb at the top was used to prepare highly diluted samples. The shape of the apparatus allowed it to be inserted in the standard 5 mm probe of the NMR spectrometer. Most of the original sample was poured into the bulb by tilting the NMR tube. The solvent was then vacuum transferred back into the tube, leaving the nonvolatile materials in the bulb. A single tilting-vacuum transfer cycle allowed at least a 10-fold dilution. No new impurities were introduced no matter how many dilution cycles were done, since the apparatus was flame sealed. The concentration

changes were readily estimated by comparison of the residual solvent proton integrals (constant throughout the experiment) with those of the Cp ligands of **29a**. The dilution-measurement cycles were done until the detection limit for ^{29}Si nuclei was reached.

2.4.3.7 Reaction of **29a** with CsF

CsF (0.003 g, 0.02 mmol) and **29a** (0.009 g, 0.005 mmol) were charged in the NMR assembly, *vide supra*, in the glovebox. On the vacuum line, THF was then vacuum transferred (1 mL) and the mixture was left stirring for 3 h. The color of the reaction mixture changed from yellow to black. The solvent was evaporated under vacuum, and an NMR sample was prepared in C_6D_6 .

NMR (C_6D_6 , 25 °C). ^1H -NMR: δ 7.85 (m, Ph), 7.35, (m, Ph) 7.20 (m, Ph), 6.00 (s, Cp), 5.28 (s, Cp), 5.27 (s, Cp), 5.15 (s, Cp), 4.94 (s, Cp), 4.93 (s, Cp), 4.85 (d, $J_{\text{HF}} = 14.2$ Hz, SiH), 1.83 (m, α -Bu), 1.68 (m, γ -Bu), 1.44 (m, β -Bu), 1.08 (t, $^2J_{\text{HH}} = 7.3$ Hz, δ -Bu), -5.55 (s, μ -H).

^{19}F -NMR for $[\text{BBu}_2(\text{C}_6\text{F}_5)_2]^-$, δ -135.8 (d, $J_{\text{FF}} = 20.2$ Hz, *o*- C_6F_5), -164.0 (t, $J_{\text{FF}} = 20.5$ Hz, *p*- C_6F_5), -167.8 (t, $J_{\text{FF}} = 20.5$ Hz, *m*- C_6F_5); for $[\text{BBu}_1(\text{C}_6\text{F}_5)_3]^-$, δ -134.0 (d, $J_{\text{FF}} = 20.2$ Hz, *o*- C_6F_5), -165.7 (t, $J_{\text{FF}} = 20.4$ Hz, *p*- C_6F_5), -168.4 (t, $J_{\text{FF}} = 20.5$ Hz, *m*- C_6F_5); for $[\text{B}(\text{C}_6\text{F}_5)_4]^-$, δ -132.5 (d, $J_{\text{FF}} = 20.2$ Hz, *o*- C_6F_5), -165.9 (t, $J_{\text{FF}} = 20.6$ Hz, *p*- C_6F_5), -168.6 (t, $J_{\text{FF}} = 20.5$ Hz, *m*- C_6F_5), -133.2 (d, $J_{\text{FF}} = 20.2$ Hz). ^{29}Si -NMR: δ -42.5 ($J_{\text{HSi}} = 172.5$ Hz, SiH).

No reaction occurred when CsF and **29a** were mixed in C_6D_6 .

Acknowledgment

Financial support for this work from the NSERC of Canada and Fonds FCAR du Québec is gratefully acknowledged.

References

- (1) Part of this work was previously communicated. Dioumaev, V. K.; Harrod, J. F. *Organometallics* **1994**, *13*, 1548-1550.
- (2) Lambert, J. B.; Zhang, S.; Stern, C. L.; Huffman, J. C. *Science* **1993**, *260*, 1917-1918.
- (3) Reed, C. A.; Xie, Z.; Bau, R.; Benesi, A. *Science* **1993**, *262*, 402-404.
- (4) Olah, G. A.; Rasul, G.; Li, X.-y.; Buchholz, H. A.; Sandford, G.; Prakash, G. K. S. *Science* **1994**, *263*, 983-984.
- (5) Pauling, L. *Science* **1994**, *263*, 983-983.
- (6) Lambert, J. B.; Zhang, S. *Science* **1994**, *263*, 984-985.
- (7) Reed, C. A.; Xie, Z. *Science* **1994**, *263*, 985-986.
- (8) Lickiss, P. D. *J. Chem. Soc., Dalton Trans.* **1992**, 1333-1338.
- (9) Chojnowski, J.; Stanczyk, W. *Main Group Chemistry News* **1994**, *2*, 6-15.
- (10) Lambert, J. B.; Kania, L.; Zhang, S. *Chem. Rev.* **1995**, *95*, 1191-1201.
- (11) Speranza, M. *Chem. Rev.* **1993**, *93*, 2933-2980.
- (12) Corriu, R. J. P.; Henner, M. *J. Organomet. Chem.* **1974**, *74*, 1-28.
- (13) Skrzypczak-Jankun, E.; Cheesman, B. V.; Zheng, B.; Lemert, R. M.; Asthana, S.; Srebnik, M. *J. Chem. Soc., Chem. Commun.* **1994**, 127-128.
- (14) Mislow, K.; Raban, M. In *Topics in Stereochemistry*; ; N. L. Allinger and E. L. Eliel, Ed.; Wiley: New York, 1967; Vol. 1, pp 1-38.
- (15) Dioumaev, V. K.; Harrod, J. F., submitted to *Organometallics*.
- (16) Yang, X.; Stern, C.; Marks, T. J. *Angew. Chem., Int. Ed. Engl.* **1992**, *31*, 1375-1377.
- (17) Gell, K. I.; Posin, B.; Schwartz, J.; Williams, G. M. *J. Am. Chem. Soc.* **1982**, *104*, 1846-1855.
- (18) Jones, S. B.; Petersen, J. L. *Inorg. Chem.* **1981**, *20*, 2889-2894.

- (19) Weigold, H.; Bell, A. P.; Willing, R. I. *J. Organomet. Chem.* **1974**, *73*, C23-C24.
- (20) Wailes, P. C.; Weigold, H. *J. Organomet. Chem.* **1970**, *24*, 405-411.
- (21) Pez, G. P.; Putnik, C. F.; Suib, S. L.; Stucky, G. D. *J. Am. Chem. Soc.* **1979**, *101*, 6933-6937.
- (22) Wailes, P. C.; Weigold, H.; Bell, A. P. *J. Organomet. Chem.* **1972**, *43*, C29-C31.
- (23) Kautzner, B.; Wailes, P. C.; Weigold, H. *J. Chem. Soc., Chem. Commun.* **1969**, 1105-1105.
- (24) Wailes, P. C.; Weigold, H. *J. Organomet. Chem.* **1970**, *24*, 405-411.
- (25) Wailes, P. C.; Weigold, H.; Schwartz, J.; Jung, C. *Inorg. Synth.* **1979**, *19*, 223-227.
- (26) Erker, G.; Kropp, K.; Kruger, C.; Chiang, A.-P. *Chem. Ber.* **1982**, *115*, 2447-2460.
- (27) Luinstra, G. A.; Rief, U.; Prosenc, M. H. *Organometallics* **1995**, *14*, 1551-1552.
- (28) Szymanski, H. A.; Erickson, R. E. *Infrared Band Handbook*; 2nd ed.; IFI/Plenum: New York, 1970; Vol. 1.
- (29) Procopio, L. J.; Carroll, P. J.; Berry, D. H. *J. Am. Chem. Soc.* **1994**, *116*, 177-185.
- (30) Woo, H.-G.; Heyn, R. H.; Tilley, T. D. *J. Am. Chem. Soc.* **1992**, *114*, 5698-5707.
- (31) Aitken, C. T.; Harrod, J. F.; Samuel, E. *J. Am. Chem. Soc.* **1986**, *108*, 4059-4066.
- (32) Lambert, J. B.; Zhang, S.; Ciro, S. M. *Organometallics* **1994**, *13*, 2430-2443.
- (33) Xie, Z.; Liston, D. J.; Jelinec, T.; Mitro, V.; Bau, R.; Reed, C. A. *J. Chem. Soc., Chem. Commun.* **1993**, 384-386.
- (34) Lambert, J. B.; Zhang, S. *J. Chem. Soc., Chem. Commun.* **1993**, 383-384.

- (35) Choe, S.-B.; Kanai, H.; Klabunde, K. J. *J. Am. Chem. Soc.* **1989**, *111*, 2875-2882.
- (36) Schubert, U. *Adv. Organomet. Chem.* **1990**, *30*, 151-187.
- (37) Tilley, T. D. In *Chemistry of Organic Silicon Compounds*; ; S. Patai and Z. Rappoport, Ed.; Wiley: New York, 1991, pp 246-364.
- (38) Spaltenstein, E.; Palma, P.; Kreutzer, K. A.; Willoughby, C. A.; Davis, W. M.; Buchwald, S. L. *J. Am. Chem. Soc.* **1994**, *116*, 10308-10309.
- (39) Luo, X.-L.; Kubas, G. J.; Burns, C. J.; Bryan, J. C.; Unkefer, C. J. *J. Am. Chem. Soc.* **1995**, *117*, 1159-1160.
- (40) Scharrer, E.; Chang, S.; Brookhart, M. *Organometallics* **1995**, *14*, 5686-5694.
- (41) Scharrer, E.; Brookhart, M. *J. Organomet. Chem.* **1995**, *497*, 61-71.
- (42) Ohff, A.; Kosse, P.; Baumann, W.; Tillack, A.; Kempe, R.; Gorls, H.; Burlakov, V. V.; Rosenthal, U. *J. Am. Chem. Soc.* **1995**, *117*, 10399-10400.
- (43) Lemke, F. R. *J. Am. Chem. Soc.* **1994**, *116*, 11183-11184.
- (44) Luo, X.-L.; Kubas, G. J.; Bryan, J. C.; Burns, C. J.; Unkefer, C. J. *J. Am. Chem. Soc.* **1994**, *116*, 10312-10313.
- (45) Schubert, U.; Scholz, G.; Muller, J.; Ackermann, K.; Worle, B. J. *J. Organomet. Chem.* **1986**, *306*, 303-326.
- (46) Colomer, E.; Corriu, R. J. P.; Marzin, C.; Vioux, A. *Inorg. Chem.* **1982**, *21*, 368-373.
- (47) Horton, A. D.; Orpen, A. G. *Organometallics* **1991**, *10*, 3910-3918.
- (48) Atwood, J. L. In *Coordination Chemistry of Aluminum*; ; G. H. Robinson, Ed.; VCH: New York, 1993, Chapter 6, pp 197-232.
- (49) Olsson, L.; Ottosson, C.-H.; Cremer, D. *J. Am. Chem. Soc.* **1995**, *117*, 7460-7479.
- (50) Cremer, D.; Olsson, L.; Ottosson, C.-H. *J. Mol. Struct. (THEOCHEM)* **1994**, *313*, 91-109.

- (51) Olsson, L.; Cremer, D. *Chem. Phys. Lett.* **1993**, *215*, 433-443.
- (52) Schleyer, P. v. R.; Buzek, P.; Muller, T.; Apeloig, Y.; Siehl, H.-U. *Angew. Chem. Int. Ed. Engl.* **1993**, *32*, 1471-1473.
- (53) Jacobsen, H.; Ziegler, T. *Organometallics* **1995**, *14*, 224-230.
- (54) Zybail, C. E.; Liu, C. *Synlett* **1995**, *7*, 687-699, and references cited therein.
- (55) Cundary, T. R.; Gordon, M. S. *Organometallics* **1992**, *11*, 3122-3129.
- (56) Straus, D. A.; Tilley, T. D.; Rheingold, A. L.; Geib, S. J. *J. Am. Chem. Soc.* **1987**, *109*, 5872-5873.
- (57) Zhang, C.; Grumbine, S. D.; Tilley, T. D. *Polyhedron* **1991**, *10*, 1173-1176.
- (58) Grumbine, S. D.; Chadha, R. K.; Tilley, T. D. *J. Am. Chem. Soc.* **1992**, *114*, 1518-1520.
- (59) Kawano, Y.; Tobita, H.; Shimoi, M.; Ogino, H. *J. Am. Chem. Soc.* **1994**, *116*, 8575-8581.
- (60) Kobayashi, H.; Ueno, K.; Ogino, H. *Organometallics* **1995**, *14*, 5490-5492.
- (61) Grumbine, S. K.; Straus, D. A.; Tilley, T. D.; Rheingold, A. L. *Polyhedron* **1995**, *14*, 127-148.
- (62) Straus, D. A.; Grumbine, S. D.; Tilley, T. D. *J. Am. Chem. Soc.* **1990**, *112*, 7801-7802.
- (63) Straus, D. A.; Zhang, C.; Quimbata, G. E.; Grumbine, S. D.; Heyn, R. H.; Tilley, T. D.; Rheingold, A. L.; Geib, S. J. *J. Am. Chem. Soc.* **1990**, *112*, 2673-2681.
- (64) Lee, K. E.; Arif, A. M.; Gladysz, J. A. *Chem. Ber.* **1991**, *124*, 309-320.
- (65) Grumbine, S. D.; Tilley, T. D.; Rheingold, A. L. *J. Am. Chem. Soc.* **1993**, *115*, 358-360.
- (66) Grumbine, S. D.; Tilley, T. D.; Arnold, F. P.; Rheingold, A. L. *J. Am. Chem. Soc.* **1993**, *115*, 7884-7885.
- (67) Grumbine, S. K.; Tilley, T. D. *J. Am. Chem. Soc.* **1994**, *116*, 5495-5496.
- (68) Grumbine, S. K.; Tilley, T. D. *J. Am. Chem. Soc.* **1994**, *116*, 6951-6952.

- (69) Olah, G. A.; Rasul, G.; Heiliger, L.; Bausch, J.; Prakash, G. K. S. *J. Am. Chem. Soc.* **1992**, *114*, 7737-7742.
- (70) Olah, G. A.; Field, L. D. *Organometallics* **1982**, *1*, 1485-1487.
- (71) Prakash, G. K. S.; Keyaniyan, S.; Aniszfeld, R.; Heiliger, L.; Olah, G. A.; Stevens, R. C.; Choi, H.-K.; Bau, R. *J. Am. Chem. Soc.* **1987**, *109*, 5123-5126.
- (72) Olah, G. A.; Heiliger, L.; Li, X.-Y.; Prakash, G. K. S. *J. Am. Chem. Soc.* **1990**, *112*, 5991-5995.
- (73) Lambert, J. B.; Kania, L.; Schilf, W.; McConnell, J. A. *Organometallics* **1991**, *10*, 2578-2584.
- (74) Lambert, J. B.; Schilf, W. *J. Am. Chem. Soc.* **1988**, *110*, 6364-6367.
- (75) Eisch, J. J.; Pombrik, S. I.; Zheng, G.-X. *Organometallics* **1993**, *12*, 3856-3863.
- (76) Frankiss, S. G. *J. Phys. Chem.* **1967**, *71*, 3418-3421.
- (77) *Recent Advances in Silicon-29 NMR Spectroscopy*; Williams, E. A., Ed.; Annual reports on NMR spectroscopy.; Academic: London, 1983; Vol. 15, pp p 276.
- (78) Samuel, E. *Bull. Soc. Chim. Fr.* **1966**, 3548-3564.
- (79) Wolczanski, P. T.; Bercaw, J. E. *Organometallics* **1982**, *1*, 793-799.
- (80) Massey, A. G.; Park, A. J. *J. Organomet. Chem.* **1964**, *2*, 245-250.
- (81) Finholt, A. E.; Bond, A. C. J.; Wilzbach, K. E.; Schlesinger, H. I. *J. Am. Chem. Soc.* **1947**, *69*, 2692-2696.

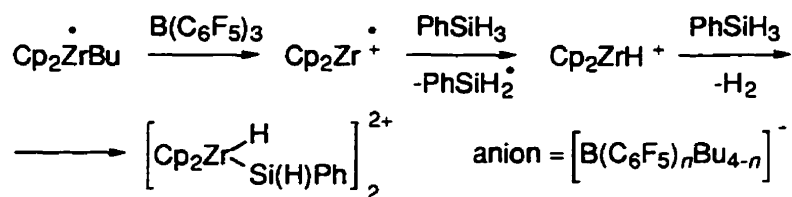
CHAPTER 3

Studies of the Formation and Decomposition Pathways for Some Cationic Zirconoceneydridosilyl Complexes

Vladimir K. Dioumaev and John F. Harrod

Chemistry Department, McGill University, Montreal, QC, Canada, H3A 2K6

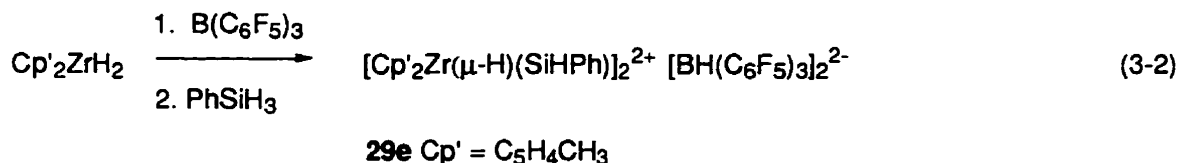
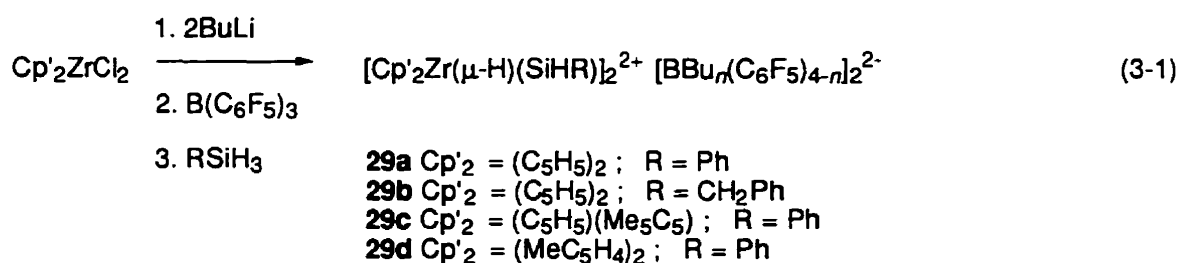
Abstract



Reactions and intermediates leading to zirconocene complexes $[\text{Cp}'_2\text{Zr}(\mu\text{-H})(\text{SiHR})]_2^{2+}[\text{BR}'_n(\text{C}_6\text{F}_5)_{4-n}]_2^{2-}$ ($\text{Cp}'=\text{Cp}$, MeCp , Me_5Cp ; $\text{R}=\text{Ph}$ or PhCH_2 ; $\text{R}'=\text{Bu}$ or H .) **29a-e** were investigated *in situ* by NMR and EPR studies and by trapping unstable intermediates with PMe_3 . Two novel Zr^{III} complexes, $[\text{Cp}_2\text{Zr}^{\text{III}}]^+[\text{BBu}_n(\text{C}_6\text{F}_5)_{4-n}]^-$, **33**, and $[\text{Cp}_2\text{Zr}^{\text{III}}(\text{PMe}_3)_2]^+[\text{BBu}_n(\text{C}_6\text{F}_5)_{4-n}]^-$, **36**, were identified by EPR spectroscopy. The unstable, diamagnetic compound $[\text{Cp}_2\text{Zr}^{\text{IV}}\text{Bu}]^+[\text{BBu}_n(\text{C}_6\text{F}_5)_{4-n}]^-$, **30**, was identified by ^1H - ^1H COSY and ^1H - ^{13}C HMQC experiments at -20°C . Redistribution of borate butyl and pentafluorophenyl ligands was found to occur by a direct boron to boron migration and not by a metal assisted mechanism. The latter was ruled out by an independent synthesis of expected reaction intermediates for both reaction pathways ($[\text{Ph}_3\text{C}][\text{BBu}(\text{C}_6\text{F}_5)_3]$, $[\text{Cp}_2\text{Zr}(\text{C}_6\text{F}_5)]^+[\text{BBu}_n(\text{C}_6\text{F}_5)_{4-n}]^-$ and $[\text{Cp}_2\text{Zr}(\text{C}_6\text{F}_5)(\mu_3\text{-HB}(\text{C}_6\text{F}_5)_3)]_2$) and an investigation of their model redistribution reactions by NMR spectroscopy.

3.1 Introduction

Coordination catalysts for silane polymerization are currently of scientific and technological interest because silicon-containing polymers have significant potential as materials for ceramic precursors for electronics, and integrated optics.¹⁻⁶ Transition metal catalysts offer an unprecedented control over the stereochemistry of the polymeric products and the cyclic/linear chain selectivity.⁷⁻¹⁰ On the other hand there is still room for improvement in the catalyst design to produce polysilanes with molecular chains long enough to ensure good mechanical properties. Most of the progress in this field is based on studies of the reaction intermediates and mechanisms involving neutral Cp_2MR_2 ($\text{M}=\text{Ti}$, Zr , Hf , $\text{R}=\text{alkyl}$, H , silyl) compounds.¹⁰⁻¹⁵ We recently reported a novel type of cationic catalyst for the dehydrocoupling of primary silanes, which proved to have certain advantages over neutral analogs.^{16,17} The unusual structure of the species isolated from the reaction mixture, **29** (eq 3-1 and 3-2),¹⁸ prompted us to investigate the chemistry of this system more thoroughly. We now report studies of the formation pathways and reactivity of the reaction products in solution using multinuclear, multidimensional NMR spectroscopy and EPR spectroscopy.



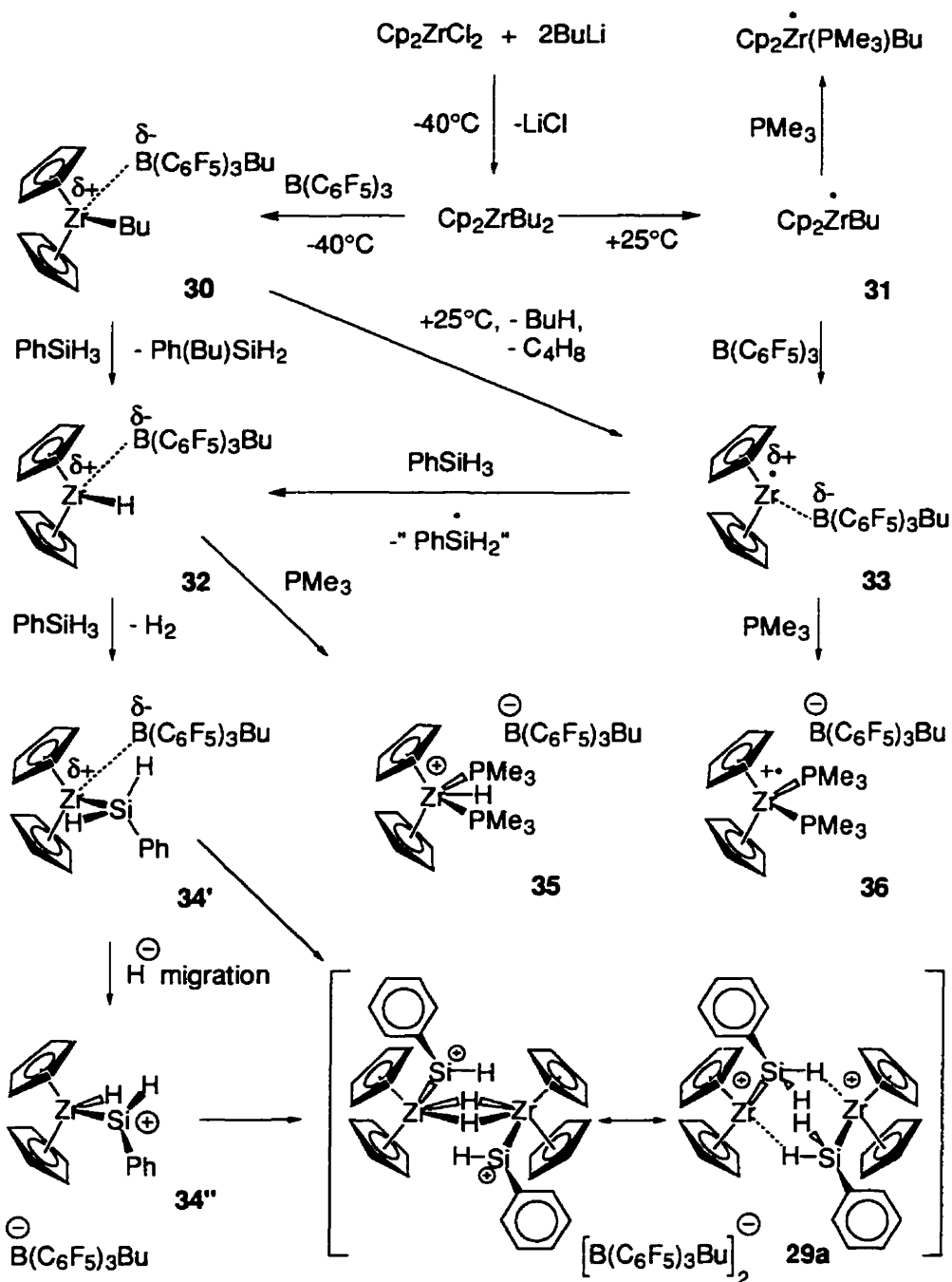
3.2 Results and discussion

3.2.1 Formation pathway for **29**

Mixtures of neutral Cp_2MX_2 metallocenes ($\text{M}=\text{Ti, Zr, Hf}$; $\text{X}=\text{Me, H}$) and primary silanes were studied earlier and analogs of compounds **29** were isolated from them.^{12,19-22} However, the combination catalyst $\text{Cp}'_2\text{ZrCl}_2/2\text{BuLi}/\text{B}(\text{C}_6\text{F}_5)_3$ behaves differently from Cp_2ZrX_2 ($\text{X}=\text{Me, H}$) in that it has a better selectivity for the production of long linear polymer chains. An even more intriguing observation is the fact that the $\text{Cp}_2\text{ZrCl}_2/2\text{BuLi}/\text{B}(\text{C}_6\text{F}_5)_3$ mixture has a totally different silane dehydrocoupling performance than an almost identical combination catalyst $\text{Cp}_2\text{ZrMe}_2/\text{B}(\text{C}_6\text{F}_5)_3$, which is virtually inactive.¹⁶ To obtain further insight into the nature of the reaction intermediates and to improve the molecular weights of the products of the dehydrocoupling reaction we investigated reactions leading to compound **29a**.

3.2.1.1 Low temperature reaction

Reaction of BuLi with Cp_2ZrCl_2 at low temperature leads to a rapid and quantitative conversion (as observed by NMR spectroscopy) to Cp_2ZrBu_2 and LiCl (Scheme 3-1).^{23,24} Addition of $\text{B}(\text{C}_6\text{F}_5)_3$ results in butyl group transfer from zirconium to boron and the formation of a number of cationic zirconocenes. This step is quantitative in borate as observed by ^{19}F NMR, but the fate of the metallocene fragment is more ambiguous. One of the products is $[\text{Cp}_2\text{ZrBu}]^+$, **30**, as identified by ^1H COSY and ^1H - ^{13}C HMQC experiments, but the other zirconocene related NMR signals are not characteristic enough for a firm assignment. A sigma bond metathesis reaction with one equivalent of PhSiH_3 converts most of those compounds into $[\text{Cp}_2\text{ZrH}]^+$, **32**. The latter was not observed directly in the reaction mixture but can be either trapped as a previously characterized phosphine adduct **35**²⁵ or can be synthesized independently and further reacted with

Scheme 3-1 Reactions and intermediates in the $\text{Cp}_2\text{ZrCl}_2/2\text{BuLi}/\text{B}(\text{C}_6\text{F}_5)_3/\text{PhSiH}_3$ system

PhSiH_3 (eq 3-2).¹⁸ The second equivalent of PhSiH_3 leads to $[\text{Cp}_2\text{ZrSi}(\text{H})_2\text{Ph}]^+$, **34'**, which can either dimerize or undergo silicon to metal hydride migration accompanied by

dimerization (a similar hydride migration from silicon to a cation-like iridium center was reported by Bergman *et al.* and confirms that silicon can lose electron density in favor of a metal cation²⁶). Both paths would lead to mesomeric structures of the same compound **29a**, and the byproducts are silanes, polyphenylsilanes and dihydrogen.¹⁸

Interestingly, when the precatalyst is synthesized at low temperature, the yield and the molecular weights of polysilanes are low. In addition the isolated and purified compounds **29** do not catalyze the dehydrocoupling reaction to any significant extent. However, the catalytic activity can be increased appreciably if the precatalyst is synthesized at room temperature.

3.2.1.2 Room temperature reaction

Reaction of BuLi with Cp_2ZrCl_2 in toluene at room temperature results in reduction of zirconium with formation of a number of Cp_2ZrR metallocenes as observed by EPR (Scheme 3-1).²⁴ The main product is Cp_2ZrBu , **31**, which gives an apparent triplet ($g=1.9961$, t, $a(\text{H})=2.4$ G, $a(\text{Zr})<9$ G) due to the coupling to the α -methylene fragment.²⁴ It can be trapped as a phosphine complex $\text{Cp}_2\text{ZrBu}(\text{PMe}_3)$, which appears as a doublet of unresolved multiplets ($g=1.9955$, d, $a(\text{P})=20.6$ G, $a(\text{Zr})=16.25$ G, $a(\text{H})<2$ G).²⁴ The steric bulk of the butyl ligand allows only one PMe_3 molecule to enter the coordination sphere. Reaction of Cp_2ZrBu with $\text{B}(\text{C}_6\text{F}_5)_3$ furnishes $[\text{Cp}_2\text{Zr}]^+[\text{BBu}(\text{C}_6\text{F}_5)_3]^-$, **33**, which gives rise to a single line in the EPR spectrum ($g_{\text{iso}}=1.9972$ at RT, s, $a(\text{Zr})=12.3$ G; $g_x=1.9970$, $g_y=1.9900$, $g_z=2.0075$ at -150 °C) (Figure 3-1). The low value for the $a(\text{Zr})$ is in good agreement with the electron deficient structure **33**.²⁷ It is of interest, that the calculated $g_{\text{averaged}}=1.9982$ for the frozen solution sample is considerably different from the g_{iso} for the sample in solution. It indicates, that **33** may exist as a mixture of species in solution (probably solvent separated and tight ion pairs, see below) and the equilibrium shifts upon cooling. Further, the high value for g_y indicates the presence of a strong

π -donor ligand in the bisectorial plane of the sandwich.²⁸ Indeed, in group 4 $\text{Cp}_2\text{M}^{\text{III}}\text{X}$ complexes g_y primarily depends on the HOMO-LUMO ($1a_1 \rightarrow b_2$) energy gap, where the HOMO, nonbonding $1a_1$, is largely d_{z^2} (in the Dahl-Petersen coordination system) and is fairly insensitive to the σ -donor properties of X. On the other hand, LUMO, b_2 , is mainly d_{xz} and acts as a π -acceptor. Hence, the energy gap is governed by the π -donor ability of the X ligand.²⁸ In the case of **33** there is no directly attached ligand X and such a π -donation can only be the result of a tight contact with the solvent, counter ion, or a Cp of another metallocene. Given the ability of such ionic compounds to form liquid clathrates (or solvent separated ion pairs),^{18,29} a tight contact with the toluene solvent is the most likely explanation. It also accounts for the discrepancies in the $g_{\text{averaged}}/g_{\text{iso}}$ values.

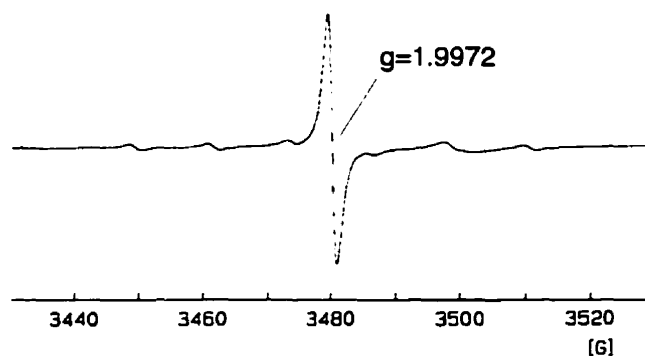


Figure 3-1. The EPR spectrum of the clathrate of $[\text{Cp}_2\text{Zr}]^+[\text{BBu}_n(\text{C}_6\text{F}_5)_{4-n}]^-$ in toluene.

Compound **33** could, in principle, also be synthesized by reaction of Cp_2ZrBu and $[\text{Ph}_3\text{C}]^+[\text{BBu}_n(\text{C}_6\text{F}_5)_{4-n}]^-$, but the major EPR active product in this case is $\text{Ph}_3\text{C}^\bullet$ ($g=2.0021$, m). Alternatively, thermal (+25 °C) decomposition of **30** gives **33** as the final, thermodynamic product (eq 3-3). It is formed at the expense of two more unstable compounds, which can be detected at the early stages of decomposition ($g=1.9964$, s, $a(\text{Zr})=7.1$ G and $g=1.9860$, s, $a(\text{Zr})=25.8$ G, Figure 3-2). The former complex is also formed during photolysis of **29a**, *vide infra*. It is even more electron

deficient than **33** and can be tentatively assigned to the tight ion pair form of **33**, which has a cation-anion interaction, but no strongly coordinated solvent. Due to the interference of the second compound, interpretation of the frozen glass EPR spectrum was not accurate enough to test this assignment, but such a coordination of fluorophenylborates has been previously reported to occur either through F atoms,³⁰⁻³² or through another ligand of the borate anion, [BR(C₆F₅)₃]⁻ (R = Me,³²⁻³⁸ CH₂Ph³⁹⁻⁴¹).

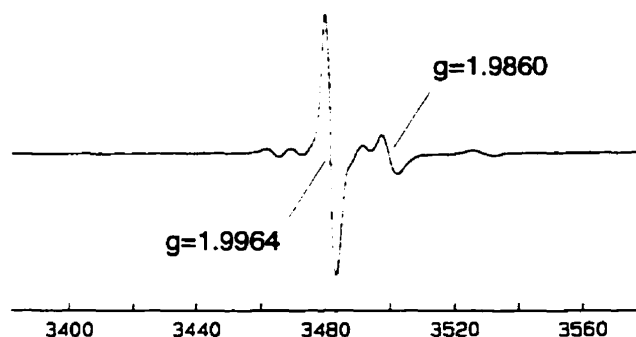
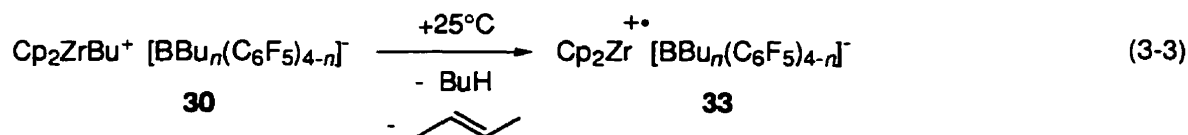


Figure 3-2. An EPR spectrum of the thermal decomposition products of **30** in toluene. The main peak is tentatively assigned to [Cp₂Zr]⁺[BBu_n(C₆F₅)_{4-n}]⁻.



Compound **33** readily abstracts hydrogen from PhSiH₃ leading to the same product **32** as the low temperature path. The rest of the steps are the same for both temperatures. The obvious difference between the low and room temperature synthesis and the key to the catalytic performance is the presence of low oxidation state compound **33** in the latter. If silane is in excess, the room temperature synthesis furnishes **29a** as the final product only when all PhSiH₃ is consumed. Addition of a fresh portion of silane does not reinitiate the dehydrocoupling reaction. It is thus clear that production of **29a** is a sterile branch of the

catalytic cycle. When the reaction is still in progress, **34** is consumed in a productive cycle fast enough to preclude irreversible formation of its dimer **29a**.

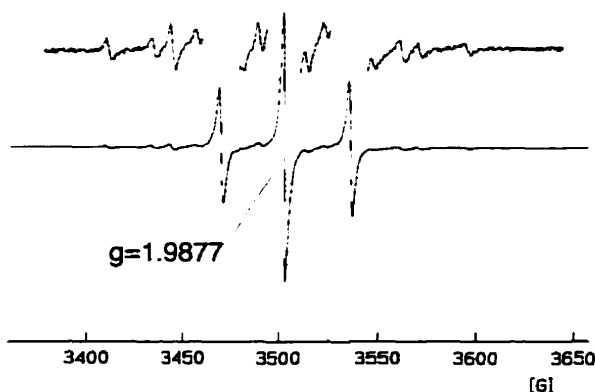


Figure 3-3. The EPR spectrum of $[\text{Cp}_2\text{Zr}(\text{PMe}_3)_2]^+[\text{BBu}_n(\text{C}_6\text{F}_5)_{4-n}]^-$ in C_6D_6 .

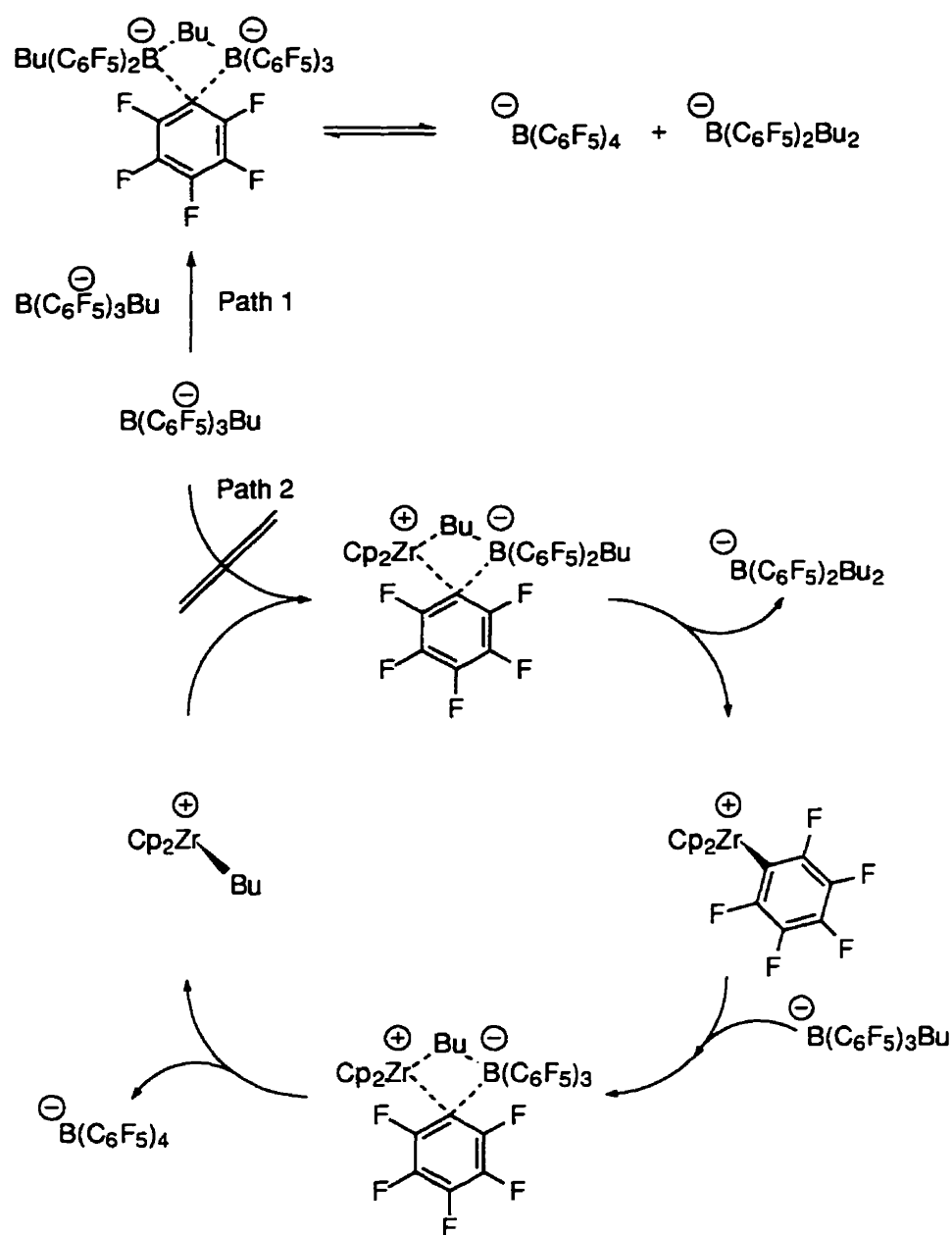
Further support for the structure of **33** was provided by trapping it with PMe_3 . The product, **36**, can be readily identified by EPR spectroscopy ($g=1.9877$, t ; $a(\text{P})=33.0$ G, $a(\text{Zr})=23.4$ G, Figure 3-3). The multiplicity of the signal and the value of $a(\text{P})$ clearly indicate a bisphosphine adduct, $\text{Cp}_2\text{ZrX}(\text{PMe}_3)_2$, while the lack of any observable hyperfine coupling to X (bandwidth < 3 G) and the presence of borate anion (^1H NMR spectroscopy) suggest that 'substituent X' is a positive charge, which is in good agreement with the electron count for **36**. Indeed, if X is a two-electron donor ligand, $\text{Cp}_2\text{ZrX}(\text{PMe}_3)_2$ is a 19e complex, whereas a zero-electron donor (positive charge) gives a more reasonable 17e configuration and more space to accommodate two phosphines. To the best of our knowledge there is only one other reported example of a stable zirconocene(III) cation-radical in condensed phase, $((\text{Me}_3\text{SiCp})_2\text{Zr}^{\text{III}}(\text{dmpe})^+\text{BF}_4^-$; $g=1.9871$, $a(\text{P})=26.5$ G)⁴² although titanocene analogs ($\text{Cp}_2\text{Ti}^{\text{III}}(\text{L})_2^+$, where L = PMe_3 , THF, MeCN, $\text{H}_2\text{NCH}_2\text{CH}_2\text{NH}_2$, $\text{Me}_2\text{NCH}_2\text{CH}_2\text{NMe}_2$, and 2,2-bipyridyl) are well known.⁴³⁻⁴⁸

3.2.2 Ligand Redistribution

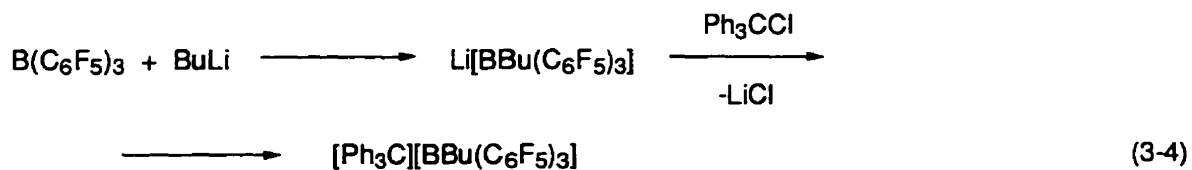
The chemistry of the borate counter-ion has so far been neglected in the discussion. However, the structure and reactivity of the borate anion proved to be more complicated than originally expected. Indeed, a number of anions with a general formula $[\text{BBu}_n(\text{C}_6\text{F}_5)_{4-n}]^-$ are actually formed (as observed by ^{19}F NMR) instead of a single monobutylborate. In view of the large number of publications involving $\text{B}(\text{C}_6\text{F}_5)_3$ and $[\text{B}(\text{C}_6\text{F}_5)_3]^-$ it is surprising that there are no reported precedents for this type of redistribution.

Boron ligand redistribution is likely to occur by one of two mechanisms. It can either occur by a direct boron to boron migration (Scheme 3-2, path 1) or can be metal-assisted (Scheme 3-2, path 2). Tetrahaloborates were reported to participate in ligand exchange via dissociation, followed by an $\text{S}_{\text{N}}2$ attack of the halide on another borate molecule.⁴⁹ Such a dissociation step is unlikely to occur in case of $[\text{BBu}_n(\text{C}_6\text{F}_5)_{4-n}]^-$ as neither Bu nor C_6F_5 is a good leaving group. To the best of our knowledge no alkyl or aryl boron to boron bridges or ligand redistribution have ever been reported, while boron to metal ligand transfer reactions^{32,37,50-56} and bridging structures^{32-34,36} are well known. If the ligand redistribution follows the metal-assisted path, there should be a reversible formation of $\text{Cp}_2\text{Zr}(\text{C}_6\text{F}_5)^+$. To probe the feasibility of this path the synthesis of cationic and cation-like $\text{Cp}_2\text{Zr}(\text{C}_6\text{F}_5)^+$ was attempted (Scheme 3-3). The complex $[\text{Cp}_2\text{Zr}(\text{C}_6\text{F}_5)]^+[\text{BBu}_n(\text{C}_6\text{F}_5)_{4-n}]^-$ proved to be unstable and decomposed immediately via abstraction of a perfluorophenyl group from the borate anion to form $\text{B}(\text{C}_6\text{F}_5)_3$, $\text{Cp}_2\text{Zr}(\text{C}_6\text{F}_5)_2$ and other decomposition products. Although the latter were not identified, the $\text{Zr}(\text{C}_6\text{F}_5)$ fragment was detected in all of them. It is thus clear, that the C_6F_5 group was not transferred from Zr to B in this case.

Another analog of $\text{Cp}_2\text{Zr}(\text{C}_6\text{F}_5)^+$, the cation-like $[\text{Cp}_2\text{Zr}(\text{C}_6\text{F}_5)(\mu_3\text{-HB}(\text{C}_6\text{F}_5)_3)]_2$, can be easily synthesized starting from $[\text{Cp}_2\text{Zr}(\text{C}_6\text{F}_5)(\mu\text{-H})]_2$ and $\text{B}(\text{C}_6\text{F}_5)_3$. The product



Scheme 3-2 Conceivable ligand redistribution pathways for $[\text{BPh}_n\text{Bu}_{4-n}]^-$ anions



is stable in aromatic solvents at room temperature. Judging by the ^1H chemical shift (-0.95 ppm) for the $\mu\text{-H}$ and the absence of a measurable H-B coupling (although the signal is significantly broadened by the B-H interaction), the Zr-H-Zr fragment is mainly preserved and the newly formed B-H bond is long and weak. However, the ^{19}F NMR spectrum exhibits a characteristic pattern for a tetracoordinated borate, which is very different from the spectrum of the starting tricoordinated borane. It can be thus concluded that the Lewis acid weakly coordinates to a Zr-H bond forming a cation-like compound but in the non-polar medium the product is a $\text{Zr}(\mu\text{-H})_2\text{Zr}$ dimer. No Zr to B group transfer occurred, either at ambient, or at elevated temperatures. A minor decomposition occurred by the abstraction of a pentafluorophenyl group from the borate anion as was the case with cationic $[\text{Cp}_2\text{Zr}(\text{C}_6\text{F}_5)]^+[\text{BBu}_n(\text{C}_6\text{F}_5)_{4-n}]^-$. The low reactivity of the cation-like compound can be attributed to its dimeric structure. In an attempt to cleave the dimer, the reaction was repeated in THF. Unfortunately, the main product was $\text{Cp}_2\text{Zr}(\text{C}_6\text{F}_5)(\text{OBU})$, which results from THF ring opening by the strongly acidic Zr center. No Zr to B ligand transfer was observed in this case either.

A similar reactivity pattern was reported by Marks and coworkers, who observed that ligand transfer is readily reversible when the group is Me but not when it is C_6F_5 .^{32,34} The above data strongly suggest that zirconium does not participate in the redistribution of the borate ligands in the present case. Besides, neither $\text{Cp}_2\text{Zr}(\text{C}_6\text{F}_5)^+$ nor $\text{Cp}_2\text{Zr}(\text{C}_6\text{F}_5)_2$ was detected among the products of equation 3-1.

To test the alternative pathway a synthesis of $[\text{Ph}_3\text{C}][\text{BBu}(\text{C}_6\text{F}_5)_3]$ was attempted (eq 3-4). Interestingly, $[\text{Ph}_3\text{C}][\text{BBu}(\text{C}_6\text{F}_5)_3]$ is only present in substantial quantities in freshly prepared samples. $[\text{Ph}_3\text{C}][\text{BBu}_2(\text{C}_6\text{F}_5)_2]$ and $[\text{Ph}_3\text{C}][\text{B}(\text{C}_6\text{F}_5)_4]$, whose presence was confirmed by ^{19}F NMR spectroscopy, are formed quite rapidly upon storage of the solutions. The redistribution pathway can be analyzed by ^{19}F NOESY experiments. In some cases there is an extra set of ^{19}F NMR resonances in addition to the signals due to the bis- tris- and tetrakis(pentafluorophenyl)borates (Figure 3-4). These peaks are in slow

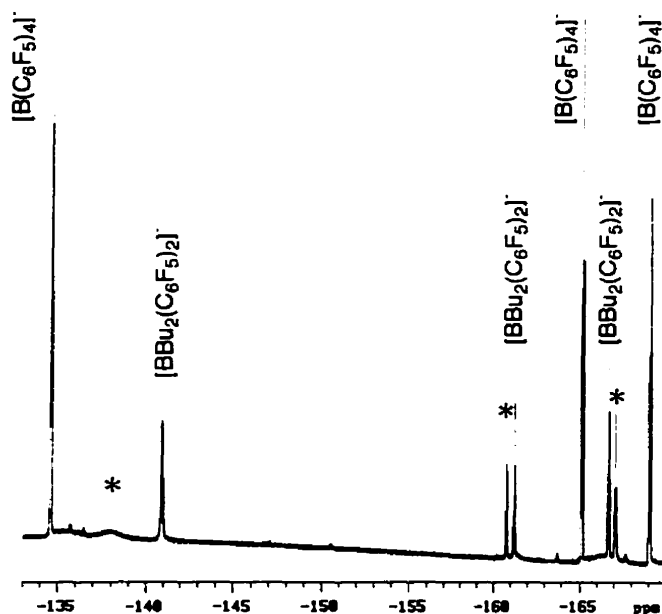


Figure 3-4. An ^{19}F NMR spectrum of $[\text{Ph}_3\text{C}][\text{BBu}_n(\text{C}_6\text{F}_5)_{4-n}]$ in C_6D_6 . There is an extra set of ^{19}F NMR resonances, marked by an asterisk, in addition to the signals due to the $[\text{Ph}_3\text{C}][\text{BBu}_2(\text{C}_6\text{F}_5)_2]$ and $[\text{Ph}_3\text{C}][\text{B}(\text{C}_6\text{F}_5)_4]$, which is in slow dynamic exchange with the former. The extra set of ^{19}F NMR signals is not due to $[\text{Ph}_3\text{C}][\text{BBu}(\text{C}_6\text{F}_5)_3]$ and can be tentatively attributed to the postulated bridging diborate compound $[\text{Ph}_3\text{C}]_2[\text{B}_2\text{Bu}_4(\text{C}_6\text{F}_5)_4]$.

dynamic exchange with the $[\text{Ph}_3\text{C}][\text{BBu}_2(\text{C}_6\text{F}_5)_2]$ signals, as can be seen from the 'out-of-phase' NOE peaks arising from F nuclei of different borates. This indicates a slow intermolecular ligand exchange process (Scheme 3-2, Path 1). The regular 'in phase' intramolecular NOEs for the neighboring fluorine atoms within the C_6F_5 ring can be observed as well. This process is irreversible, it accelerates at elevated temperatures and stops when only $[\text{Ph}_3\text{C}][\text{BBu}_2(\text{C}_6\text{F}_5)_2]$ and $[\text{Ph}_3\text{C}][\text{B}(\text{C}_6\text{F}_5)_4]$ are present in the system. The extra set of ^{19}F NMR signals is not likely to belong to $[\text{Ph}_3\text{C}][\text{BBu}_3(\text{C}_6\text{F}_5)]$ in a degenerate exchange with $[\text{Ph}_3\text{C}][\text{BBu}_2(\text{C}_6\text{F}_5)_2]$, since there is no evidence of exchange with the other borates on the same time scale, nor are the other borates exchanging with

each other. A more likely explanation is that these peaks belong to the postulated bridging diborate compound $[\text{Ph}_3\text{C}]_2[\text{Bu}_2(\text{C}_6\text{F}_5)\text{B}(\mu\text{-C}_6\text{F}_5)_2\text{BBu}_2(\text{C}_6\text{F}_5)]_2$. The lack of any spectral difference between bridging and terminal C_6F_5 groups in it can be rationalized in terms of coalescence due to the intramolecular dynamic exchange. Bridging and terminal meta- and para- C_6F_5 signals are similar and nearly coincide within pairs. They are thus only slightly broadened. On the other hand, the ortho- C_6F_5 resonances can be significantly affected by bridging, if any agostic interactions are involved, and the coalescence peak of the bridging-terminal pair can be broad accordingly. Although this assignment is tentative, the experiment itself clearly demonstrates that perfluorophenylborates can and do undergo redistribution without any external assistance or catalysis.

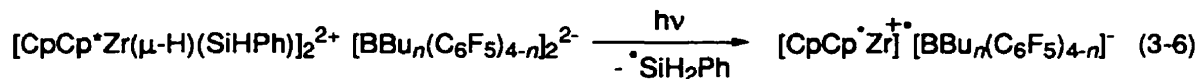
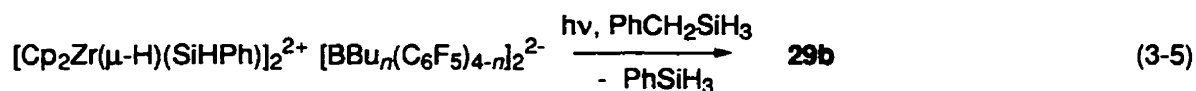
Alternatively, the redistribution reaction might have been catalyzed by traces of residual $\text{B}(\text{C}_6\text{F}_5)_3$. This is unlikely to be the main pathway, as the extra set of peaks and their time dependence, *vide supra*, becomes very difficult to explain. The intermediate cannot be a $\text{BBu}_n(\text{C}_6\text{F}_5)_{4-n} \cdot \text{B}(\text{C}_6\text{F}_5)_3$ adduct, since its irreversible decay must yield a borane and a borate in equal amounts, but no borane was detected.

3.2.3 Reactivity, Thermal and Photolytic Degradation of 29a

Compound **29a** is surprisingly stable towards oxygen and moisture, its solutions do not show any decomposition for at least 1 hour when exposed to air. Under anaerobic conditions it reacts with benzylsilane in a matter of hours when irradiated with a daylight fluorescent lamp (eq 3-5), but no reaction occurred in the dark.

Marks and coworkers recently reported that some of the cationic zirconocenes with tetrakis(pentafluorophenyl)borate anions decompose at elevated temperatures by abstraction of fluoride or pentafluorophenyl by zirconium as well as by CH activation of the Cp ligand or aromatic hydrocarbon solvent, which precludes their use in high temperature processes.³² The low stability was attributed to the cationic charge on zirconium and to an

open coordination sphere. It was of interest to study the thermal stability of **29a**, which also contains similar borate anions but has the positive charge delocalized between Zr and Si.¹⁸ As a result of this charge delocalization **29a** proved to be much more thermally stable. At room temperature solid samples or solutions in hydrocarbon solvents have been stored for years in the absence of light without noticeable decomposition. At higher temperatures (above +60 °C) decomposition occurs in a matter of minutes with the major pathway being the decomposition of the Bu-B bond, with formation of $\text{BH}_n(\text{C}_6\text{F}_5)_{4-n}$ anions.^{31,32} Prolonged heating caused pentafluorophenyl but not fluoride abstraction by zirconium and further decomposition to species which were not identified.



The same Bu-B bond cleavage can occur upon irradiation of the sample with a daylight fluorescent lamp. It also causes Zr(IV) to Zr(III) reduction accompanied by elimination of PhSiH_3 and formation of a number of radical species. The first EPR signal to appear upon irradiation is a broad and featureless singlet ($g=2.0036$). Such a high g value cannot be due to a zirconocene. In view of this, and the absence of observable satellite peaks this signal is tentatively attributed to a silicon centered radical. A second EPR signal appears either simultaneously or shortly after the first one, and grows at its expense in the dark. This signal is due to **33** ($g=1.9964$, s , $a(\text{Zr})=7.1$ G), *vide supra*. It is gradually replaced by another peak, assigned in section 3.2.1.2 to an inner sphere solvated form of **33** ($g=1.9972$, s , $a(\text{Zr})=12.3$ G). These redox transformations are reversible and a slow oxidative addition of silane to **33** regenerates **29a** when the sample is left in the dark for 1-2 months. It is of interest that similar spectral transformations have

been reported for the Cp_2ZrCl_2 -MAO system.⁵⁷ A $\text{Cp}_2\text{Zr}(\mu\text{-Cl})_2\text{MAO}$ cation-like complex ($g=1.998$, $a(\text{Zr})=7$ G), formed adducts with ethylene and styrene ($g=1.998$, $a(\text{Zr})=12$ G and $g=1.998$, $a(\text{Zr})=13$ G respectively). Although the changes in the $a(\text{Zr})$ value have been attributed to the formation of a $\text{Cp}(\text{Cl})\text{Zr}(\mu\text{-Cl})_2\text{MAO}$ complex,⁵⁷ an adduct with an olefin seems to be a more likely explanation. Firstly, such an olefin adduct accounts for the differences between the ethylene and styrene experiments. Secondly, a loss of a Cp is unlikely to be reversible, whereas formation of two forms of **33** is.

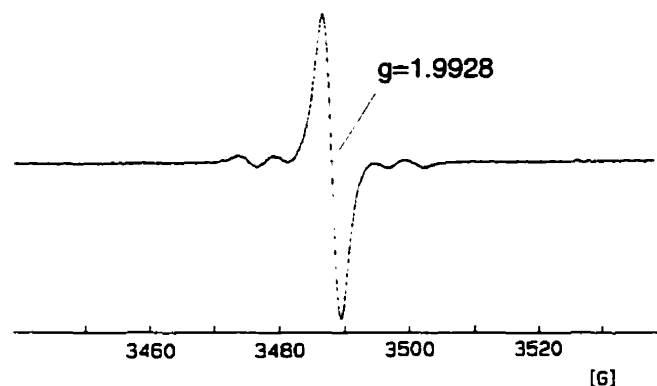
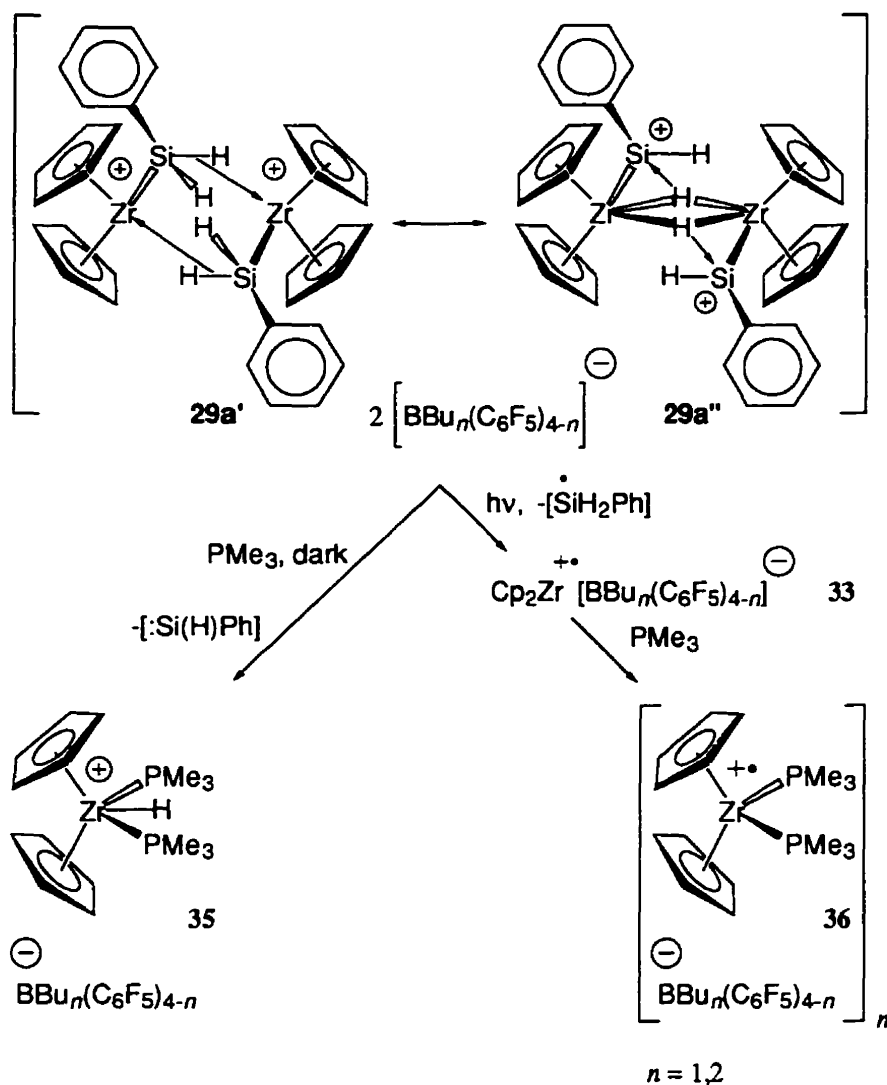


Figure 3-5. The EPR spectrum of $[\text{CpCp}^*\text{Zr}]^+\bullet[\text{BBu}_n(\text{C}_6\text{F}_5)_{4-n}]^-$ in toluene.

$[\text{CpCp}^*\text{Zr}(\mu\text{-H})(\text{SiHPh})]_2^{2+}[\text{BBu}_n(\text{C}_6\text{F}_5)_{4-n}]_2^{2-}$, **29c**, also undergoes photolytic decomposition (eq 3-6). But in this case a single product is formed ($g_{\text{iso}}=1.9928$ at RT, Figure 3-5, s, $a(\text{Zr})=5.1$ G; $g_x=1.9915$, $g_y=1.9845$, $g_z=2.0060$ at -150 °C). The difference between g_{iso} and the value of 1.9940 calculated for g_{ave} together with the relatively high value of g_y indicates some π stabilization in this compound, although the effect is less pronounced than in **33**, as both $a(\text{Zr})$ and g_y are higher in the latter (*vide supra*). Such a stabilization can be either attributed to a cation-anion interaction, as discussed above, or to an agostic interaction between Zr and one of the Me groups of the Cp^* ligand, which blocks a coordination site and precludes tight coordination of toluene. Although formation of an insoluble clathrate of **29c** and its derivatives is observed under

some conditions, it did not occur in the above mentioned EPR sample, which remained homogeneous.



Scheme 3-4 The routes for the dark and photoreaction of **29a** with PMe_3

When a preirradiated sample of **29a** was treated with PMe_3 , all of the resonances described above disappeared (Scheme 3-4) and were replaced by the triplet EPR signal of **36**. Quantitative measurement of the concentration of **36** from its EPR signal showed it to account for about 3 % of the total Zr. The other product of this reaction exhibits broad and

featureless ^1H NMR resonances in the Cp and PMe_3 regions which precluded an accurate characterization. It is tentatively assigned as a dimer $[\text{Cp}_2\text{Zr}^{\text{III}}(\text{PMe}_3)_x]_2^{2+}[\text{BR}_n(\text{C}_6\text{F}_5)_{4-n}]_2^{2-}$ ($\text{R}=\text{Bu}$ or H), the signals of which are broadened due to a fast exchange with its paramagnetic monomer **36**.

The reaction of **29a** with PMe_3 took a different course in the dark. The major product (up to 50 %) of this reaction is **35**, not **36**. The latter is formed in only trace amounts (less than 1 %).

3.3 Conclusions

Formation of $[\text{Cp}'_2\text{Zr}(\mu\text{-H})(\text{SiHR})]_2^{2+}[\text{BBu}_n(\text{C}_6\text{F}_5)_{4-n}]_2^{2-}$ ($\text{Cp}'=\text{Cp}$, MeCp , Me_5Cp ; $\text{R}=\text{Ph}$ or PhCH_2) **29a-d** from Cp_2ZrCl_2 , BuLi , $\text{B}(\text{C}_6\text{F}_5)_3$ and PhSiH_3 occurs at room temperature via a redox reaction, or at $-20/-40$ °C via a constant oxidation state σ -bond metathesis process. The borate counterion, $[\text{BBu}(\text{C}_6\text{F}_5)_3]^-$, initially formed in a zirconium to boron group transfer reaction, further undergoes boron to boron redistribution and thermal or photolytic decomposition to furnish $[\text{BR}'_n(\text{C}_6\text{F}_5)_{4-n}]$ ($\text{R}=\text{Bu}$ or H). Compounds **29a-e** are stable under anaerobic conditions at room temperature in the dark, but undergo fast decomposition at elevated temperatures ($+60$ °C) or in the presence of light. They are moderately stable to air and moisture, but long exposure causes hydrolysis.

3.4 Experimental Section

3.4.1 Materials and Methods

General experimental techniques and solvent purifications were described earlier.¹⁸ All operations were performed in Schlenk-type glassware on a dual-manifold Schlenk line, equipped with flexible stainless steel tubing, or in an argon-filled M.Braun Labmaster 130 glovebox (<0.05 ppm H_2O). Argon was purchased from Matheson (prepurified for the

glovebox and UHP for the vacuum line) and was used as received. Hydrocarbon solvents (protio- and deuterio- benzene and toluene, pentane and hexanes) were dried and stored over Na/K alloy, benzophenone and 18-crown-6 in Teflon-valved bulbs and were vacuum transferred prior to use. THF was vacuum transferred from sodium benzophenone ketyl. Halogenated solvents and silanes (1,1,2,2-tetrachloroethane- d_2 , C_6F_5Br , $PhSiH_3$ and $PhCH_2SiH_3$) were degassed and stored over molecular sieves. Cp_2ZrCl_2 , $[Cp_2Zr(H)Cl]_2$, Me_5C_5H , $ZrCl_4$, C_6D_6 , C_7D_8 , 1,1,2,2-tetrachloroethane- d_2 , C_6F_5Br , Ph_3CCl , $PhC(O)Ph$, 18-crown-6, BCl_3 (1.0 M in heptane), $n-BuLi$ (2.5 M in hexanes), PMe_3 (1.0 M in toluene), $CpNa$ (2.0 M solution in THF), magnesium powder and $CDCl_3$ were purchased from Aldrich and used as received unless stated otherwise.

The compounds $(MeCp)_2ZrCl_2$,⁵⁸ $[(MeCp)Zr(\mu-H)H]_2$,⁵⁹ $CpCp^*ZrCl_2$,⁶⁰ $B(C_6F_5)_3$,⁶¹ $[Ph_3C]^+[B(C_6F_5)_4]^-$,⁶² and $RSiH_3$ ($R = Ph$ and $PhCH_2$)⁶³ were prepared according to literature procedures.

3.4.2 Physical and Analytical Measurements

NMR spectra were recorded on a Varian Unity 500 (FT, 500 MHz for 1H), Varian XL-200 or Varian Gemini-200 (FT, 200 MHz for 1H) spectrometers. Chemical shifts for 1H and ^{13}C spectra were referenced using internal solvent references and are reported relative to tetramethylsilane. ^{19}F and ^{31}P spectra were referenced to external CF_3COOH and PMe_3 samples respectively. Quantitative NMR measurements were performed using residual solvent protons as internal references. EPR spectra were recorded on a Bruker ESP 300E (X-band) spectrometer and were referenced to external DPPH. Quantitative EPR measurements were performed with an external standard of TEMPO of known concentration. Mass spectra were recorded on a KRATOS MS25RFA spectrometer equipped with a KRATOS DS90 data system. Elemental analyses were performed by Oneida Research Services, Inc., Whitesboro, New York. The photochemical experiments

were performed using a general purpose 9 W compact daylight fluorescent bulb (Sylvania, model number F9DTT/27K) with an output primarily in the 350 through 650 nm spectral region.⁶⁴

All NMR samples were prepared in an NMR-tube assembly, consisting of one or more 5 mL round-bottom flasks fitted with a Teflon valve to which an NMR tube was fused at an angle of 45°. Components of a NMR sample were loaded separately, when necessary, in each of the flasks and were mixed in appropriate order by transferring from one flask of choice to the other by tilting of the entire apparatus. A sample was treated with small quantities (0.1-0.2 mL) of a deuterated solvent of choice. The solvent was then evaporated and the evaporation-vacuum transfer cycle was repeated to remove any residual nondeuterated solvent. A fresh portion of the same deuterated solvent (0.6-0.7 mL) was then vacuum transferred into the assembly and the solution was carefully decanted into the side NMR-tube. The top part of the tube was washed by touching it with a swab of cotton wool soaked with liquid nitrogen, which cause condensation of the solvent vapors on the inner walls. The sample was then frozen and flame sealed.

3.4.3.1 Low Temperature reaction of Cp_2ZrBu_2 with $\text{B}(\text{C}_6\text{F}_5)_3$

Cp_2ZrCl_2 (0.073g, 0.25 mmol), $(\text{C}_6\text{F}_5)_3\text{B}$ (0.128 g, 0.25 mmol) and a 2.5 M solution of BuLi in hexanes (0.2 mL, 0.50 mmol) were loaded in separate flasks of a triple flask NMR assembly, *vide supra*. The flask with BuLi was isolated from the rest of the assembly by a Teflon valve and the hexanes were removed under vacuum. Toluene- d_8 was then vacuum transferred into that flask (0.1-0.2 mL). The evaporation-vacuum transfer cycle was repeated twice to remove any residual hexanes and a final fresh portion of toluene- d_8 (0.8-1 mL) was vacuum transferred into the assembly. The entire apparatus was then immersed in a CH_3CN -dry ice bath (-41°C) and the solution of BuLi was mixed with Cp_2ZrCl_2 . The mixture was stirred at -41°C for 1 h and the cold yellow solution was then mixed with $(\text{C}_6\text{F}_5)_3\text{B}$ and stirred for another 30 min at -41°C . A yellow-brownish oil was

formed almost instantaneously. The residue was allowed to settle for 30 min at -41 °C and the mother liquor was decanted into the NMR-tube. The sample was frozen and flame sealed under vacuum.

$[\text{Cp}_2\text{ZrBu}]^+[\text{BBu}_n(\text{C}_6\text{F}_5)_{4-n}]^-$: NMR (C_6D_6 , -20 °C) ^1H δ 5.69 (s, Cp), 1.82 (m, α -BuB), 1.68 (m, γ -BuB), 1.40 (m, β -BuZr), 1.35 (m, γ -BuZr), 1.32 (m, β -BuB), 1.06 (t, δ -BuB), 0.86 (masked by BuH peak, δ -BuZr), 0.38 (m, α -BuZr). ^{13}C (from ^1H - ^{13}C HMQC) δ 113.2 (Cp), 50.8 (α -BuZr), 36.1 (β -BuZr), 31.5 (β -BuB), 27.4 (γ -BuB), 24.1 (γ -BuZr), 23.7 (α -BuB), 14.3 (δ -BuB), 11.6 (δ -BuZr). ^{19}F δ $[\text{BBu}_2(\text{C}_6\text{F}_5)_2]^-$: -139.9 (br s, *o*- C_6F_5), -161.3 (br s, *p*- C_6F_5), -165.7 (br s, *m*- C_6F_5); $[\text{BBu}_1(\text{C}_6\text{F}_5)_3]^-$: -137.9 (br s, *o*- C_6F_5), -163.7 (br s, *p*- C_6F_5), -166.6 (br s, *m*- C_6F_5). The resonances of residual $\text{Cp}_2\text{ZrBu}_2^{24}$ and butane are not listed.

3.4.3.2 Quenching $\text{Cp}_2\text{ZrBu}_2\text{-B}(\text{C}_6\text{F}_5)_3\text{-PhSiH}_3$ mixture with PMe_3

A mixture of $\text{Cp}_2\text{ZrBu}_2\text{-B}(\text{C}_6\text{F}_5)_3$ (0.25 mmol) was prepared in toluene as described above. PhSiH_3 (0.13 mL, 1.0 mmol) was then added and stirring was continued for a further 2 h while the solution was allowed to warm gradually to 0 °C. A 1.0 M toluene solution of PMe_3 (1.0 mL, 1.0 mmol) was added. The mixture was left stirring for 1 h and an NMR/EPR sample was prepared as described above:

$[\text{Cp}_2\text{ZrH}(\text{PMe}_3)_2]^+[\text{BBu}_n(\text{C}_6\text{F}_5)_{4-n}]^-$ NMR (C_6D_6 , 25 °C) ^1H δ 4.88 (t, $J_{\text{HP}}=2.3$ Hz, Cp), 2.05 (m, α -Bu), 1.78 (q, γ -Bu), 1.57 (m, β -Bu), 1.12 (t, $^2J_{\text{HH}}=7.4$ Hz, δ -Bu), 0.66 (t, $^2J_{\text{HP}}=104.1$ Hz, HZr), 0.60 (equal intensity t, $J_{\text{HP}}=4.0$ Hz, Me_3P); ^{13}C δ 101.7 (Cp), 17.8 (Me_3P); ^{31}P δ 0.8 (104 Hz, Me_3P).

$[\text{Cp}_2\text{Zr}^{\text{III}}(\text{PMe}_3)_2]^+[\text{BBu}_n(\text{C}_6\text{F}_5)_{4-n}]^-$ NMR (C_6D_6 , 25 °C) ^1H δ 2.05 (m, α -Bu), 1.78 (q, γ -Bu), 1.57 (m, β -Bu), 1.12 (t, $^2J_{\text{HH}}=7.4$ Hz, δ -Bu). EPR (C_6D_6 , 25 °C) $g=1.9877$ (t, $a(\text{P})=33.0$ G, $a(\text{Zr})=23.4$ G).

3.4.3.3 Reaction of Cp_2ZrBu with $\text{B}(\text{C}_6\text{F}_5)_3$

Cp_2ZrBu was synthesized from Cp_2ZrCl_2 (0.0365 g, 0.125 mmol) and BuLi (0.1 mL of 2.5 M solution in hexanes, 0.25 mmol) in 5 mL of toluene (1 day at RT).²⁴ $(\text{C}_6\text{F}_5)_3\text{B}$ (0.064 g, 0.125 mmol) was added and an EPR sample was frozen and flame sealed under vacuum.

EPR (toluene, +25 °C): $g=1.9964$ (br s, $a(\text{Zr})=7.1$ G), $g=1.9972$ (s, $a(\text{Zr})=12.3$ G).

3.4.3.4 Reaction of Cp_2ZrBu with $[\text{Ph}_3\text{C}]^+[\text{BBu}_n(\text{C}_6\text{F}_5)_{4-n}]^-$ (average $n=1$)

Cp_2ZrBu (0.125 mmol) was synthesized in 5 mL of toluene as described above. $[\text{Ph}_3\text{C}]^+[\text{BBu}_n(\text{C}_6\text{F}_5)_{4-n}]^-$ (0.101 g, 0.125 mmol) was added and stirred for 5 min. The color changed from brown-red to light yellow. An EPR sample was frozen and flame sealed under vacuum.

EPR (toluene, +25 °C): Ph_3C^+ $g=2.0021$ (m) and poorly resolved $g=1.9972$ (s, $a(\text{Zr})=12.3$ G).

3.4.3.5 Thermal degradation of 30

An EPR sample of $\text{Cp}_2\text{ZrBu}_2\text{-B}(\text{C}_6\text{F}_5)_3$ was prepared as described above in toluene. The sample was allowed to warm to room temperature, while the changes were monitored by EPR.

Early decomposition stage (1 to 30 min), EPR (toluene, +25 °C): $g=1.9860$ (s, $a(\text{Zr})=25.8$ G), $g=1.9964$ (br s, $a(\text{Zr})=7.1$ G), $g=1.9972$ (s, $a(\text{Zr})=12.3$ G).

Late decomposition stage (1 to 30 days), EPR (toluene, +25 °C): $g_{\text{iso}}=1.9972$ (s, $a(\text{Zr})=12.3$ G); (-150 °C) $g_x=1.9970$, $g_y=1.9900$, $g_z=2.0075$.

3.4.3.6 Reaction of $[\text{Cp}_2\text{Zr}^{\text{III}}]^+[\text{BBu}_n(\text{C}_6\text{F}_5)_{4-n}]^-$ with PhSiH_3 ¹⁸

Cp_2ZrCl_2 (0.219 g, 0.75 mmol) and $(\text{C}_6\text{F}_5)_3\text{B}$ (0.384 g, 0.75 mmol) were loaded into separate Schlenk tubes in the glovebox. Toluene was vacuum transferred into both tubes (8 mL each). The Cp_2ZrCl_2 was suspended in toluene at -41°C (CH_3CN -dry ice bath) and a 2.5 M solution of BuLi in hexanes (0.6 mL, 1.50 mmol) was added. The mixture was stirred at room temperature for 1 h. The color changed from white to brown. The toluene solution of $(\text{C}_6\text{F}_5)_3\text{B}$ was transferred by cannula into the butylated zirconocene solution. A brown-red oil was formed almost instantaneously. The reaction mixture was protected from light with aluminum foil and was left stirring for 1 h. PhSiH_3 (0.56 mL, 4.50 mmol) was then added and the stirring was continued for a further 3 h. The solvent was partially evaporated (leaving 1-2 mL) and pentane was vacuum transferred into the tube causing precipitation of a purple slurry. The brown mother liquor was removed and the residue was washed with two additional portions of pentane (2x10 mL) and dried under vacuum to furnish a microcrystalline powder. The product was dark purple and mainly contained **29a**, contaminated by polyphenylsilane and traces of highly colored, unidentified, zirconocene compounds (crude yield ~75 %).

3.4.3.7 $[\text{Cp}_2\text{Zr}^{\text{III}}(\text{PMe}_3)_2]^+[\text{BBu}_n(\text{C}_6\text{F}_5)_{4-n}]^-$ (36)

Cp_2ZrBu (0.75 mmol) was synthesized in 10 mL of toluene as described above. A solution of $(\text{C}_6\text{F}_5)_3\text{B}$ (0.384 g, 0.75 mmol) in 10 mL of toluene was added via syringe and the mixture was stirred 1 h. A 1.0 M toluene solution of PMe_3 (2.0 mL, 2.0 mmol) was added and the sample was used for EPR analysis without further purification.

EPR (toluene, $+25^\circ\text{C}$), $g=1.9877$ (t; $a(\text{P})=33.0\text{ G}$, $a(\text{Zr})=23.4\text{ G}$)

3.4.3.8 $[\text{Ph}_3\text{C}]^+[\text{BBu}_n(\text{C}_6\text{F}_5)_{4-n}]^-$, (average $n=1$)

In the glovebox, toluene (0.5 mL), $(\text{C}_6\text{F}_5)_3\text{B}$ (0.128 g, 0.25 mmol) and a 2.5 M solution of BuLi in hexanes (0.100 mL, 0.25 mmol) were loaded in a Schlenk tube. A

white precipitate was formed and the mixture was left stirring for 1 hour. Ph_3CCl (0.077 g, 0.0275 mmol) was then added and the reaction was continued for another h. The mother liquor was transferred to the NMR assembly and the product was precipitated upon addition of pentane (3 ml). The supernatant was removed by syringe and the red-brown solid was collected and washed with two portions of pentane (2x2 mL). An NMR sample was prepared in benzene- d_6 .

NMR (C_6D_6 , +25 °C) ^1H δ 7.35 (m, Ph), 7.06 (m, Ph), 6.98 (m, Ph).

$[\text{Ph}_3\text{C}]^+[\text{B}(\text{C}_6\text{F}_5)_4]^-$ ^{19}F δ -134.6 (br s, *o*- C_6F_5), -165.1 (t, 21.4 Hz, *p*- C_6F_5), -169.1 (t, 17.4 Hz, *m*- C_6F_5); ^{13}C δ 148.5 (*o*- C_6F_5), 136.4 (*m*- C_6F_5), 138.4 (*p*- C_6F_5).

$[\text{Ph}_3\text{C}]^+[\text{BBu}(\text{C}_6\text{F}_5)_3]^-$ ^{19}F δ -135.3 (br s, *o*- C_6F_5), -163.5 (t, 20.7 Hz, *p*- C_6F_5), -166.4 (br s, *m*- C_6F_5)

$[\text{Ph}_3\text{C}]^+[\text{BBu}_2(\text{C}_6\text{F}_5)_2]^-$ ^{19}F δ -140.9 (br s, *o*- C_6F_5), -161.2 (t, 19.8 Hz, *p*- C_6F_5), -166.7 (t, 19.0 Hz, *m*- C_6F_5)

$[\text{Ph}_3\text{C}]^+_2[\text{B}_2\text{Bu}_n(\text{C}_6\text{F}_5)_{8-n}]^{2-}$ ^{19}F δ -138.0 (br s, *o*- $[\text{B}_2\text{Bu}_n(\text{C}_6\text{F}_5)_{8-n}]^{2-}$), -160.8 (t, 20.7 Hz, *p*- $[\text{B}_2\text{Bu}_n(\text{C}_6\text{F}_5)_{8-n}]^{2-}$), -167.1 (br s, *m*- $[\text{B}_2\text{Bu}_n(\text{C}_6\text{F}_5)_{8-n}]^{2-}$).

3.4.3.9 $\text{Cp}_2\text{Zr}(\text{C}_6\text{F}_5)_2$

This procedure differs from that reported by Chaudhari and Stone⁶⁵ in that a Grignard reagent was used instead of aryllithium. Mg powder (0.097 g, 4.00 mmol) was loaded in a Schlenk flask and was dried under vacuum at 60 °C. THF (15 mL) was vacuum transferred into the flask and $\text{C}_6\text{F}_5\text{Br}$ (0.50 mL, 4 mmol) was added to the cooled (-78 °C) suspension. The reaction mixture was allowed to warm gradually and was left stirring for 6 h at room temperature. The color of the mixture changed from colorless to light yellow and then brownish as soon as the solution reached room temperature. The solution was recooled (-78 °C) and transferred via cannula to a Schlenk flask containing Cp_2ZrCl_2 (0.526 g, 1.8 mmol). The reaction mixture was stirred for 24 h at room temperature to give a dark green solution. The solvent was evaporated, the residue was

redissolved in toluene (25 mL) and recrystallized from toluene/pentane (25/25 mL). A greenish-white solid was collected by filtration and sublimed at 120-150 °C / 0.01-0.001 Torr to furnish white crystalline product: yield 0.320 g, 46 %.

NMR (C_6D_6 , +25 °C) ^1H δ 5.72 (s, Cp); ^{19}F δ -120.5 (br s, *o*- C_6F_5), -157.8 (t, 19.9 Hz, *p*- C_6F_5), -164.5 (m, *m*- C_6F_5); ^{13}C δ 136.5 (*m*- C_6F_5), 139.8 (*p*- C_6F_5). MS (EI, ion source 200 °C, 70 eV, direct inlet 100 °C), [m/z (relative intensity)]: 554 (M^+ , 15), 239 (25), 220 (20), 193 (45), 175 (40), 168 (100).

3.4.3.10 $[\text{Cp}_2\text{Zr}(\text{C}_6\text{F}_5)(\mu\text{-H})]_2$

Mg powder (0.049 g, 2.00 mmol) was loaded in a Schlenk flask and was dried under vacuum at 60 °C. THF (15 mL) was vacuum transferred into the flask and $\text{C}_6\text{F}_5\text{Br}$ (0.25 mL, 2 mmol) was added to the cooled (-78 °C) suspension. The reaction mixture was allowed to warm gradually and was left stirring for 3 h at room temperature. The color of the mixture changed from colorless to light yellow and then brownish as soon as the solution reached room temperature. The cold (-78 °C) solution was transferred via cannula to a Schlenk flask containing $\text{Cp}_2\text{Zr}(\text{H})\text{Cl}$ (0.468 g, 1.8 mmol) and the reaction mixture was stirred for 24 h at room temperature. The mother liquor was then removed and the residue was redissolved in hot THF (35 mL). Hot toluene (15 mL) was added and the mixture was allowed to cool to room temperature. A white crystalline product was collected by filtration, washed with pentane and dried under vacuum: yield 64 %. Anal. Calcd for $\text{C}_{16}\text{H}_{11}\text{F}_5\text{Zr}$: C, 49.34; H, 2.85. Found: C, 49.16; H, 2.74.

NMR (C_6D_6 , +25 °C) ^1H δ 5.59 (s, Cp), -1.92 (q, 6.5 Hz, $\mu\text{-H}$); ^{19}F δ -107.0 (d, 27.3 Hz, *o*- C_6F_5), -160.8 (t, 19.8 Hz, *p*- C_6F_5), -164.7 (t, 19.8 Hz, *m*- C_6F_5).

3.4.3.11 Reaction of $[\text{Cp}_2\text{Zr}(\text{C}_6\text{F}_5)(\mu\text{-H})]_2$ with $\text{B}(\text{C}_6\text{F}_5)_3$ in C_6D_6

In the glovebox, $[\text{Cp}_2\text{Zr}(\text{C}_6\text{F}_5)\text{H}]_2$ (0.008 g, 0.01 mmol), $\text{B}(\text{C}_6\text{F}_5)_3$ (0.010 g, 0.02 mmol) and C_6D_6 were loaded in an NMR tube assembly, *vide supra*. The sample

was then frozen and flame sealed. $\text{Cp}_2\text{Zr}(\text{C}_6\text{F}_5)_2$ was identified by a comparison to an authentic sample, *vide supra*. The estimated yields, by integration of the Cp peaks, of $[\text{Cp}_2\text{Zr}(\text{C}_6\text{F}_5)(\mu_3\text{-HB}(\text{C}_6\text{F}_5)_3)]_2$ and $\text{Cp}_2\text{Zr}(\text{C}_6\text{F}_5)_2$ are 95 and 4 % respectively.

$[\text{Cp}_2\text{Zr}(\text{C}_6\text{F}_5)(\mu_3\text{-HB}(\text{C}_6\text{F}_5)_3)]_2$: NMR (C_6D_6 , +25 °C) ^1H δ 5.49 (s, Cp), -0.95 (br s, $\mu\text{-H}$); ^{13}C δ 148.2 (*o*-BH(C_6F_5) $_3^-$), 146.6 (*o*-Zr(C_6F_5)), 140.5 (*p*-BH(C_6F_5) $_3^-$), 140.2 (*p*-Zr(C_6F_5)), 137.6 (*m*-BH(C_6F_5) $_3^-$), 137.4 (*m*-Zr(C_6F_5)), 114.7 (Cp); ^{19}F δ -164.9 (t, 22.8 Hz, *m*-BH(C_6F_5) $_3^-$), -163.5 (m, *m*-Zr(C_6F_5)), -157.2 (t, 21.4 Hz, *p*-BH(C_6F_5) $_3^-$), -156.8 (t, 20.0 Hz, *p*-Zr(C_6F_5)), -137.1 (br s, *o*-BH(C_6F_5) $_3^-$), -114.0 (br s, *o*-Zr(C_6F_5)).

3.4.3.12 Reaction of $[\text{Cp}_2\text{Zr}(\text{C}_6\text{F}_5)(\mu\text{-H})]_2$ with $\text{B}(\text{C}_6\text{F}_5)_3$ in THF

In the glovebox, $[\text{Cp}_2\text{Zr}(\text{C}_6\text{F}_5)\text{H}]_2$ (0.008 g, 0.01 mmol) and $\text{B}(\text{C}_6\text{F}_5)_3$ (0.010 g, 0.02 mmol) were loaded in an NMR tube assembly, *vide supra*. THF (5 mL) was vacuum transferred into the assembly and the reaction mixture was left stirring for 2 h at room temperature. The solvent was removed under vacuum and an NMR sample was prepared as described above.

$\text{Cp}_2\text{Zr}(\text{C}_6\text{F}_5)(\text{OBu})$: NMR (C_6D_6 , +25 °C) ^1H δ 5.74 (s, Cp), 3.87 (t, 6.5 Hz, $\alpha\text{-OBu}$), 1.33 (quintet, 7.0 Hz, $\beta\text{-OBu}$), 1.22 (sextet, 7.7 Hz, $\gamma\text{-OBu}$), 0.89 (t, 7.5 Hz, $\delta\text{-OBu}$); ^{13}C δ 111.2 (Cp), 75.2 ($\alpha\text{-OBu}$), 22.5 ($\gamma\text{-OBu}$), 17.9 ($\beta\text{-OBu}$), 13.1 ($\delta\text{-OBu}$); ^{19}F δ -114.0 (br s, *o*- C_6F_5), -159.9 (t, 19.8 Hz, *p*- C_6F_5), -165.3 (t, 19.8 Hz, *m*- C_6F_5).

3.4.3.13 Reaction of $[\text{Cp}_2\text{Zr}(\text{C}_6\text{F}_5)(\mu\text{-H})]_2$ with $[\text{Ph}_3\text{C}]^+[\text{BBu}_n(\text{C}_6\text{F}_5)_{4-n}]^-$

In the glovebox, $[\text{Cp}_2\text{Zr}(\text{C}_6\text{F}_5)\text{H}]_2$ (0.008 g, 0.01 mmol), $[\text{Ph}_3\text{C}]^+[\text{BBu}_n(\text{C}_6\text{F}_5)_{4-n}]^-$ (average $n=1$) (0.017 g, 0.03 mmol) and C_6D_6 were loaded in an NMR tube and the sample was sealed with a rubber septum. The NMR tube was stored in an argon filled container, and all NMR measurements were done within 1 h after the

sample was removed from the container. The products were identified by a comparison to authentic samples of $[\text{Ph}_3\text{C}]^+[\text{BBu}_n(\text{C}_6\text{F}_5)_{4-n}]^-$ and $\text{B}(\text{C}_6\text{F}_5)_3$.

$\text{B}(\text{C}_6\text{F}_5)_3$: NMR (C_6D_6 , +25 °C) ^{19}F δ -131.5 (br s, *o*- C_6F_5), -144.2 (br s, *p*- C_6F_5), -162.6 (br s, *m*- C_6F_5); ^{13}C δ 148.4 (*o*- C_6F_5), 145.2 (*p*- C_6F_5), 137.7 (*m*- C_6F_5).

3.4.3.14 Reaction of 29a with $\text{PhCH}_2\text{SiH}_3$

In the glove box, **29a** (0.017 g, 0.01 mmol), $\text{PhCH}_2\text{SiH}_3$ (0.004 mL, 0.03 mmol) and toluene-*d*₈ (0.6 mL) were loaded in an NMR tube assembly and flame sealed. All manipulations were done either in the dark or with the sample being protected by aluminum foil. The mixture was periodically analyzed by NMR spectroscopy but no changes occurred even after 4 months of storage in the dark.

The same sample was then exposed to a daylight fluorescent lamp for 4 h. The color of the solution changed from light yellow to red-brown and a 60 % conversion of **29a** into **29b** occurred as monitored by NMR. The product was identified by comparison to an independently synthesized sample of **29b**.¹⁸

3.4.3.15 Thermal Degradation of 29a

A sample of **29a** in C_6D_6 was flame sealed in an NMR tube which was heated at +60 °C for 4 h. The light yellow solution turned red-brown and deposition of an oily precipitate occurred. The $[\text{BH}(\text{C}_6\text{F}_5)_3]^-$ moiety was identified by comparison to an independently synthesized sample of **29e**.¹⁸

3.4.3.16 Photolytic Degradation of 29a

A sample of **29a** in C_6D_6 was flame sealed in an NMR tube and exposed to a daylight fluorescent lamp for 7 days. The light yellow solution turned red-brown and deposited an oily solid.

NMR (C_6D_6 , +25 °C) 1H δ 7.40-7.00 (m, $PhSiH_3$), 5.90 (br s, Cp), 4.22 (s, $PhSiH_3$), 1.88 (equal intensity quadruplet, $^1J_{BH}=85$ Hz), 1.20 (m, β -BuH), 0.85 (t, α -BuH).

EPR (C_6D_6 , +25 °C), $g=1.9964$ (br s, $a(Zr)=7.1$ G), $g=1.9972$ (s, $a(Zr)=12.3$ G), $g=2.0036$ (br s).

3.4.3.17 Photolytic Degradation of 29c

A sample of **29c** in toluene was flame sealed in an NMR tube, which was exposed to a daylight fluorescent lamp for 5 min. The light yellow solution turned purple but no precipitation occurred.

EPR (toluene, +25 °C), $g_{iso}=1.9925$ (s, $a(Zr)=5.1$ G)

(toluene, -150 °C), $g_x=1.9915$, $g_y=1.9845$, $g_z=2.0060$

3.4.3.18 Reaction of 29a with PMe_3

3.4.3.18.1 Dark reaction

29a (0.009 g, 0.005 mmol) was loaded in an NMR assembly. The reaction mixture was protected from light with aluminum foil. Whenever manipulations required removal of the protective foil, the lights in the laboratory were switched off. Toluene was then vacuum transferred (1 mL) and a 1.0 M toluene solution of PMe_3 (0.050 mL, 0.05 mmol) was added. The mixture was left stirring for 24 h, but no visible changes occurred. An NMR/EPR sample was prepared as described above:

$[Cp_2ZrH(PMe_3)_2]^+[BBu_n(C_6F_5)_{4-n}]^-$, concentration=0.005 M (approximately 50 % of the starting [Zr]). The rest of the products (another 50 % of the starting [BBu]) also contain the $[BBu_n(C_6F_5)_{4-n}]^-$ moiety.

Quantitative EPR measurements were always performed on a freshly prepared sample. A number of experiments were done with different acquisition parameters (modulation and microwave power) to ensure that there was no saturation of the signal.

The other acquisition parameters were compensated for by a system normalization constant and were usually kept constant for both the unknown and the standard sample measurements:

$[\text{Cp}_2\text{Zr}^{\text{III}}(\text{PMe}_3)_2]^+[\text{BBu}_n(\text{C}_6\text{F}_5)_{4-n}]^-$, concentration=0.00006 M (less than 1 % of the starting [Zr])

3.4.3.18.2 Photoreaction

29a (0.009 g, 0.005 mmol) was loaded in an NMR assembly. Toluene was then vacuum transferred (1 mL) and the reaction mixture was irradiated with a 9 W daylight fluorescent light for 24 h. This was accompanied by a color change of the mixture from yellow to dark brown. A 1.0 M toluene solution of PMe_3 (0.050 mL, 0.05 mmol) was added and the mixture was left stirring for 24 h in the dark. An NMR/EPR sample was prepared as described above. The Cp and PMe_3 signals of $[\text{Cp}_2\text{ZrH}(\text{PMe}_3)_2]^+[\text{BBu}_n(\text{C}_6\text{F}_5)_{4-n}]^-$ were detected but constituted less than 1 % of the starting [Zr]. The rest of the resonances were lost in broad featureless bands at 6.4-5.2 and 1.4-0.2 ppm. The overall detectable concentration of $[\text{BBu}_n(\text{C}_6\text{F}_5)_{4-n}]^-$ was less than 1 % of the starting [BBu].

$[\text{Cp}_2\text{Zr}(\text{PMe}_3)_2]^+[\text{BH}_n(\text{C}_6\text{F}_5)_{4-n}]^-$ EPR (C_6D_6 , 25 °C) $g=1.9886$ (t, $a(\text{P})=33.2$ G, $a(\text{Zr})=23.4$ G). Concentration=0.00025 M (approximately 3 % of the starting [Zr])

Acknowledgment

Financial support for this work from the NSERC of Canada and Fonds FCAR du Québec is gratefully acknowledged.

References

- (1) *Inorganic and Organometallic Polymers*; Zeldin, M.; Wynne, K. J.; Allcock, H. R., Ed.; American Chemical Society: Washington, DC, 1988.
- (2) Mark, J. E.; Allock, H. R.; West, R. C. In *Inorganic Polymers* Prentice Hall: Englewood Cliffs, 1992; pp 186-236.
- (3) *Silicon-Based Polymer Science: A Comprehensive Resource*; Ziegler, J. M.; Fearon, F. W. G., Ed.; American Chemical Society: Washington, DC, 1990.
- (4) West, R. *J. Organomet. Chem.* **1986**, *300*, 327-346.
- (5) Miller, R. D.; Michl, J. *Chem. Rev.* **1989**, *89*, 1359-1410.
- (6) Ziegler, J. M. *Mol. Cryst. Liq. Cryst.* **1990**, *190*, 265-282.
- (7) Gauvin, F.; Harrod, J. F. *Can. J. Chem.* **1990**, *68*, 1638-1640.
- (8) Banovetz, J. P.; Stein, K. M.; Waymouth, R. M. *Organometallics* **1991**, *10*, 3430-3432.
- (9) Harrod, J. F. In *Inorganic and Organometallic Polymers with Special Properties*; R. M. Laine, Ed.; Kluwer Academic: Dordrecht, 1992; Vol. 206; pp 87-98.
- (10) Tilley, T. D. *Acc. Chem. Res.* **1993**, *26*, 22-29.
- (11) Samuel, E.; Harrod, J. F. *J. Am. Chem. Soc.* **1984**, *106*, 1859-1860.
- (12) Aitken, C. T.; Harrod, J. F.; Samuel, E. *J. Am. Chem. Soc.* **1986**, *108*, 4059-4066.
- (13) Harrod, J. F. In *Inorganic and Organometallic Polymers*; M. Zeldin; K. J. Wynne and H. R. Allcock, Ed.; American Chemical Society: Washington DC, 1988; pp 89-100.
- (14) Woo, H.-G.; Tilley, T. D. *J. Am. Chem. Soc.* **1989**, *111*, 3757-3758.
- (15) Woo, H.-G.; Tilley, T. D. *J. Am. Chem. Soc.* **1989**, *111*, 8043-8044.
- (16) Dioumaev, V. K.; Harrod, J. F. *Organometallics* **1994**, *13*, 1548-1550.
- (17) Dioumaev, V. K.; Harrod, J. F. *J. Organomet. Chem.* **1996**, *521*, 133-143.
- (18) Dioumaev, V. K.; Harrod, J. F. *Organometallics* **1996**, *15*, 3859-3867.

- (19) Aitken, C.; Harrod, J. F.; Samuel, E. *Can. J. Chem.* **1986**, *64*, 1677-1679.
- (20) Mu, Y.; Aitken, C.; Cote, B.; Harrod, J. F.; Samuel, E. *Can. J. Chem.* **1991**, *69*, 264-276.
- (21) Takahashi, T.; Hasegawa, M.; Suzuki, N.; Saburi, M.; Rousset, C. J.; Fanwick, P. E.; Negishi, E.-i. *J. Am. Chem. Soc.* **1991**, *113*, 8564-8566.
- (22) Harrod, J. F.; Mu, Y.; Samuel, E. *Can. J. Chem.* **1992**, *70*, 2980-2984.
- (23) Negishi, E.; Takahashi, T. *Acc. Chem. Res.* **1994**, *27*, 124-130 and references cited therein.
- (24) Dioumaev, V. K.; Harrod, J. F., submitted to *Organometallics*.
- (25) Jordan, R. F.; Bajgur, C. S.; Dasher, W. E.; Rheingold, A. L. *Organometallics* **1987**, *6*, 1041-1051.
- (26) Burger, P.; Bergman, R. G. *J. Am. Chem. Soc.* **1993**, *115*, 10462-10463.
- (27) Samuel, E. *Inorg. Chem.* **1983**, *22*, 2967-2970.
- (28) Lukens, J., W.W.; Smith III, M. R.; Andersen, R. A. *J. Am. Chem. Soc.* **1996**, *118*, 1719-1728.
- (29) Atwood, J. L. In *Coordination Chemistry of Aluminum*; G. H. Robinson, Ed.; VCH: New York, 1993; pp 197-232.
- (30) Yang, X.; Stern, C. L.; Marks, T. J. *Organometallics* **1991**, *10*, 840-842.
- (31) Yang, X.; Stern, C.; Marks, T. J. *Angew. Chem., Int. Ed. Engl.* **1992**, *31*, 1375-1377.
- (32) Yang, X.; Stern, C. L.; Marks, T. J. *J. Am. Chem. Soc.* **1994**, *116*, 10015-10031.
- (33) Yang, X.; Stern, C. L.; Marks, T. J. *J. Am. Chem. Soc.* **1991**, *113*, 3623-3625.
- (34) Deck, P. A.; Marks, T. J. *J. Am. Chem. Soc.* **1995**, *117*, 6128-6129.
- (35) Giardello, M. A.; Eisen, M. S.; Stern, C. L.; Marks, T. J. *J. Am. Chem. Soc.* **1995**, *117*, 12114-12129.

- (36) Bochmann, M.; Lancaster, S. J.; Hursthouse, M. B.; Malik, K. M. A. *Organometallics* **1994**, *13*, 2235-2243.
- (37) Gomez, R.; Green, M. L. H.; Haggitt, J. L. *J. Chem. Soc., Chem. Commun.* **1994**, 2607-2608.
- (38) Gillis, D. J.; Tudoret, M.-J.; Baird, M. C. *J. Am. Chem. Soc.* **1993**, *115*, 2543-2545.
- (39) Pellecchia, C.; Grassi, A.; Immirzi, A. *J. Am. Chem. Soc.* **1993**, *115*, 1160-1162.
- (40) Pellecchia, C.; Immirzi, A.; Grassi, A.; Zambelli, A. *Organometallics* **1993**, *12*, 4473-4478.
- (41) Pellecchia, C.; Grassi, A.; Zambelli, A. *Organometallics* **1994**, *13*, 298-302.
- (42) Cardin, D. J.; Lappert, M. F.; Raston, C. L. *Chemistry of organo-zirconium and -hafnium compounds*; Ellis Horwood: Chichester, 1986.
- (43) Seewald, P. A.; White, G. S.; Stephan, D. W. *Can. J. Chem.* **1988**, *66*, 1147-1152.
- (44) Borkowsky, S. L.; Baenziger, N. C.; Jordan, R. F. *Organometallics* **1993**, *12*, 486-495.
- (45) Merola, J. S.; Campo, K. S.; Gentile, R. A.; Modrick, M. A. *Inorg. Chim. Acta* **1989**, *165*, 87-90.
- (46) Coutts, R. S. P.; Kautzner, B.; Wailes, P. C. *Aust. J. Chem.* **1969**, *22*, 1137-1141.
- (47) Green, M. L. H.; Lucas, C. R. *J. Chem. Soc., Dalton Trans.* **1972**, 1000-1003.
- (48) Samuel, E.; Vedel, J. *Organometallics* **1989**, *8*, 237-241.
- (49) Lockhart, J. C. *Chem. Rev.* **1965**, *65*, 131-151.
- (50) Siedle, A. R.; Newmark, R. A. *J. Organomet. Chem.* **1995**, *497*, 119-125.
- (51) Aresta, M.; Quaranta, E.; Tommasi, I.; Derien, S.; Dunach, E. *Organometallics* **1995**, *14*, 3349-3356.

- (52) de Rege, F. M. G.; Buchwald, S. L. *Tetrahedron* **1995**, *51*, 4291-4296.
- (53) Quintanilla, R.; Cole, T. E. *Tetrahedron* **1995**, *51*, 4297-4308.
- (54) Marsella, J. A.; Caulton, K. G. *J. Am. Chem. Soc.* **1982**, *104*, 2361-2365.
- (55) Siegmann, K.; Pregosin, P. S.; Venanzi, L. M. *Organometallics* **1989**, *8*, 2659-2664.
- (56) Albano, P.; Aresta, M.; Manassero, M. *Inorg. Chem.* **1980**, *19*, 1069-1072.
- (57) Cam, D.; Sartori, F.; Maldotti, A. *Macromol. Chem. Phys.* **1994**, *195*, 2817-2826.
- (58) Samuel, E. *Bull. Soc. Chim. Fr.* **1966**, 3548-3564.
- (59) Jones, S. B.; Petersen, J. L. *Inorg. Chem.* **1981**, *20*, 2889-2894.
- (60) Wolczanski, P. T.; Bercaw, J. E. *Organometallics* **1982**, *1*, 793-799.
- (61) Massey, A. G.; Park, A. J. *J. Organomet. Chem.* **1964**, *2*, 245-250.
- (62) Chien, J. C. W.; Tsai, W.-M.; Rausch, M. D. *J. Am. Chem. Soc.* **1991**, *113*, 8570-8571.
- (63) Finholt, A. E.; Bond, A. C. J.; Wilzbach, K. E.; Schlesinger, H. I. *J. Am. Chem. Soc.* **1947**, *69*, 2692-2696.
- (64) Rabek, J. F. *Experimental Methods in Photochemistry and Photophysics.*; Wiley: Chichester, 1982, pp 55.
- (65) Chaudhari, M. A.; Stone, F. G. A. *J. Chem. Soc. A* **1966**, 838-841.

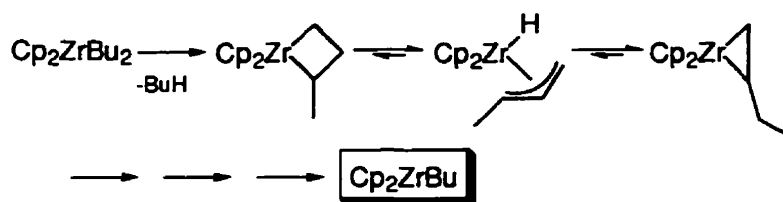
CHAPTER 4

The Nature of the Species Present in the Zirconocene Dichloride-Butyllithium Reaction Mixture

Vladimir K. Dioumaev and John F. Harrod

Chemistry Department, McGill University, Montreal, QC, Canada, H3A 2K6

Abstract

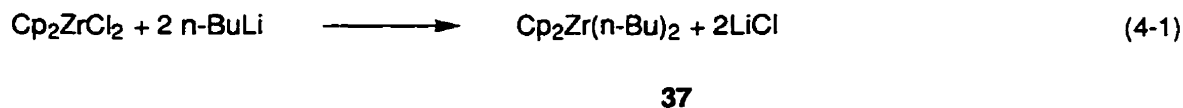


The thermal decomposition of dibutylzirconocene **37** at room temperature affords paramagnetic butylzirconocene(III), **31**, zirconocene(III) hydride, **47**, and diamagnetic butenylzirconocene(IV) hydride dimer, **41a**, and bis-cyclopentadienylzirconia-2-methyl-3-zirconocenylcyclobutane(IV) dimer, **45**. Initially, decomposition furnishes crotylzirconocene(IV) hydride, **39a**, followed by bis-cyclopentadienylzirconia-2-ethylcyclopropane(IV), **38a**, and bis-cyclopentadienylzirconia-3,4-diethylcyclopentane(IV), **40a**, listed in the order of appearance. This order suggests that the primary decomposition reaction is a γ -H abstraction, which leads to the formation of bis-cyclopentadienylzirconia-2-methylcyclobutane(IV) **42a**. The latter was not observed experimentally but is postulated on the basis of secondary products. Reactions leading to the above compounds are discussed from mechanistic and thermochemical points of view.

The reported compounds have been characterized by either EPR or multidimensional, multinuclear NMR spectroscopy. Compound **39a** has also been synthesized independently from zirconocene chloride hydride and crotylmagnesium bromide and undergoes the same rearrangements into **38a** and then **40a**. An allyl analog **39b**, synthesized from zirconocene chloride hydride and allylmagnesium bromide, exhibits the same behavior and rearranges into bis-cyclopentadienylzircona-3,4-dimethylcyclopentane **40b**.

4.1 Introduction

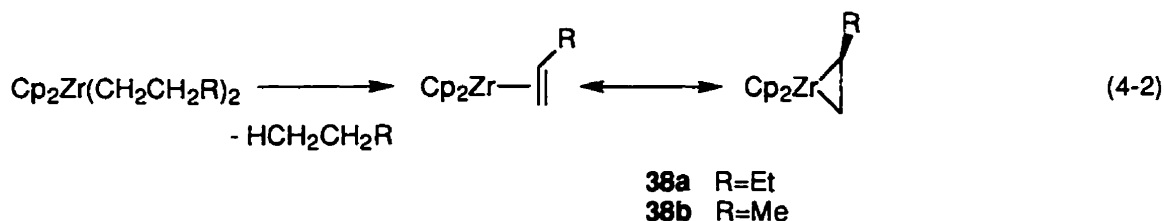
$\text{Cp}_2\text{ZrCl}_2/2\text{RLi}$ ($\text{R}=\text{alkyl}$) reagents have found widespread use in organic synthesis and in catalysis.¹ Despite a long history of study of the chemistry of such systems, the exact nature of the reactive species in solution, at room temperature, remains unclear. The primary reaction is simple and leads to the formation of the dialkylzirconocene **37** (eq 4-1), which in most cases is thermally unstable, but can be characterized in solution at low temperatures by spectroscopic methods.¹



The thermal decomposition reactions of the dialkylzirconocenes are more poorly documented, but it is clear that a number of ill-characterized compounds are formed. Only three reliable conclusions can be drawn from the numerous experiments described in the literature.²⁻⁸ Firstly, the main gaseous product is the corresponding alkane RH , as observed by mass spectroscopy and GC.^{2,8} Continuous heating of the reaction mixture above room temperature, or reaction with alkenes, produces the alkene $\text{R}(-\text{H})$.^{7,8} Secondly, phosphine adducts of alkenezirconocene complexes, $\text{Cp}_2\text{Zr}(\text{RCH}=\text{CH}_2)(\text{PR}'_3)$ ($\text{R}=\text{H}$, Me , Et and Ph ; $\text{PR}'_3=\text{PMe}_3$; $\text{R}=\text{H}$ and Et , $\text{PR}'_3=\text{PPhMe}_2$, PPh_2Me), can be

trapped, isolated from the reaction mixture, and fully characterized.^{3,4} Thirdly, the structural characterization of a phosphine-free titanocene complex, $\text{Cp}^*_2\text{Ti}(\text{CH}_2=\text{CH}_2)$ lends support to the possible existence of zirconocene-alkene complexes, albeit analogous compounds of higher olefins could not be isolated.⁵

It may thus be concluded with some confidence that the dialkylzirconocenes undergo hydrogen abstraction, with liberation of alkane and formation of a zirconocene alkene complex, **38** (eq 4-2). However, the formation of **38** in the absence of phosphine is not unequivocal. Thermally stable titanacyclopentanes, for example, are known to decompose in the presence of phosphines and to form $[\text{Ti}](\text{CH}_2=\text{CH}_2)(\text{PMe}_3)$.⁶ To date, **38** has neither been isolated nor characterized spectroscopically. There have been reports of resonances in the Cp region of the NMR spectra, which can be due to **38** or any other intermediate, but no detailed investigation has been described.⁹⁻¹²



Research in this area is primarily focused on organic products of the Negishi reaction and the fate of zirconocene products, apart from mentioning hypothetical **38**, is usually neglected. In the course of our investigations of silane dehydrocoupling catalysts derived from $\text{Cp}_2\text{ZrCl}_2/2\text{BuLi}/\text{B}(\text{C}_6\text{F}_5)_3$,¹³⁻¹⁵ a number of questions arose which encouraged us to study the chemistry of the $\text{Cp}_2\text{ZrCl}_2/2\text{BuLi}$ system in greater detail. The results of this study are reported herein.

4.2 Results

A mixture of Cp_2ZrCl_2 and BuLi in toluene or THF at -40°C gave a quantitative conversion to a single product, Cp_2ZrBu_2 , identified by its ^1H and ^{13}C NMR spectra (Table 4-1). Assignments of the ^1H and ^{13}C resonances were confirmed by ^1H COSY and ^1H - ^{13}C HMQC experiments. The NMR spectra for the new product were distinctly different from the ones for the starting BuLi.^{16,17}

A cold solution of Cp_2ZrBu_2 (-40°C) was allowed to warm slowly to 20°C until spectral evidence for thermal decomposition was apparent. It was then cooled down (0 through -40°C) to prevent further decomposition. To obtain a larger and more convincing data set, three independent samples for each solvent (toluene and THF) were studied at slightly different temperatures and different warm-up times. Each of the samples was subjected to a number of decomposition-freeze-measurement cycles, and a set of TOCSY, HMQC, COSY and NOESY experiments were performed. In every case a number of compounds were formed. COSY and TOCSY experiments were particularly useful for the identification of the resonances belonging to the same ligand, as both techniques reveal J-coupled protons. TOCSY unambiguously separated ^1H NMR signals in groups, belonging to different ligands, whereas COSY established a chainwise connectivity of the backbone within a ligand. When the J-coupling was too weak to show a cross peak, or when the cross peaks were severely overlapped, the evolution of peak intensities with time gave additional information. ^1H - ^{13}C HMQC data were extremely important to differentiate between allyl, alkenyl and alkyl ligands, as well as to identify methylene groups with magnetically inequivalent protons. When a heavy overlap of signals precluded direct determination of multiplicity and line shape, this information was retrieved in a 1D TOCSY experiment, although accurate coupling constants cannot be extracted this way. Finally, NOESY helped determine a 3D structure and ligand conformations as well as put together structural fragments, which do not exhibit any J-coupling (such as Cp, hydride and

hydrocarbyl ligands belonging to the same Zr center). Decomposition pathways proved to be the same for toluene and THF solutions. The latter has been scrutinized more thoroughly because of a wider use of THF with the $\text{Cp}_2\text{ZrCl}_2/2\text{BuLi}$ system.

Table 4-1. NMR Data

Compound, solvent, temperature	Assignment	^1H δ ppm, multiplicity (coupling constants, Hz) ^a	^{13}C δ ppm
37 , toluene-d ₈ , -20°C	α -Bu	0.31, m	53.9
	β -Bu	1.41, m	35.5
	γ -Bu	1.34, m	30.4
	δ -Bu	1.04, t (6.8)	14.5
	Cp(#1 and 2)	5.6, s	110.3
37 , THF-d ₈ , -20°C	α -Bu	0.23, m	53.7
	β -Bu	1.35, quintet (8.0)	35.7
	γ -Bu	1.06, sextet (7.2)	30.5
	δ -Bu	0.79, t (7.3)	14.2
	Cp(#1 and 2)	6.06, s	111.2
38a THF-d ₈ , -20°C	ZrCH ₂ CHCH ₂ Me	0.02, dd (6.6 and 10.0)	34.9
		0.68, t (6.6)	34.9
	ZrCH ₂ CHCH ₂ Me	1.33, m	57.6
	ZrCH ₂ CHCH ₂ Me	1.42, m	35.0
		1.66, m	35.0
	ZrCH ₂ CHCH ₂ Me	0.96, t (7.1)	20.8
	Cp(#1)	5.50, s	105.2
	Cp(#2)	5.52, s	104.8
39a toluene-d ₈ , -10°C	ZrCH ₂ CH=CHMe	0.78, br. s	35.4
		2.35, br. s	35.4
	ZrCH ₂ CH=CHMe	3.82, ddd (10.8, 11.2, 15.8)	114.3
	ZrCH ₂ CH=CHMe	2.75, br. s	80.9
	ZrCH ₂ CH=CHMe	2.12, br. d (5.6)	21.7
	ZrH	n.d.	n.a.
	Cp(#1)	5.03, br. s	98.8

	Cp(#2)	5.19, br. s	100.8
39a THF-d ₈ , -20°C	ZrCH ₂ CH=CHMe	0.85, br. s	35.8
		2.36, br. s	35.8
	ZrCH ₂ CH=CHMe	4.06, ddd (9.3, 13.7, 15.2)	114.7
	ZrCH ₂ CH=CHMe	2.84, br. s	80.9
	ZrCH ₂ CH=CHMe	2.03, br. d (5.7)	21.6
	ZrH	1.09, br. s	n.a.
	Cp(#1)	5.31, br. s	99.5
	Cp(#2)	5.48, br. s	101.4
40a toluene-d ₈ , 25°C	ZrCH ₂ CHCH ₂ Me	0.41, dd (4.4, 12.2)	46.2
		1.29, t (12.2)	46.2
	ZrCH ₂ CHCH ₂ Me	1.60, m	47.5
	ZrCH ₂ CHCH ₂ Me	1.00, m	30.8
		1.62, m	30.8
	ZrCH ₂ CHCH ₂ Me	0.94, t (7.1)	10.8
	Cp(#1 and 2)	5.84, s	111.5
40a THF-d ₈ , -20°C	ZrCH ₂ CHCH ₂ Me	0.29, dd (4.0, 12.0)	45.5
		1.18, t (12.0)	45.5
	ZrCH ₂ CHCH ₂ Me	1.48, m	47.5
	ZrCH ₂ CHCH ₂ Me	0.72, m	30.6
		1.29, m	30.6
	ZrCH ₂ CHCH ₂ Me	0.68, t (7.0)	10.5
	Cp(#1 and 2)	6.29, s	112.2
40b THF-d ₈ , -40°C	ZrCH ₂ CHMe	0.26, dd (3.5 and 12.2)	51.1
		1.28, t (12.2)	51.1
	ZrCH ₂ CHMe	1.45, m	44.2
	ZrCH ₂ CHMe	0.58, d (5.4)	27.1
	Cp(#1 and 2)	6.28, s	112.3
41a THF-d ₈ , -40°C	ZrCH=CHCH ₂ Me	8.44, d (17.9)	210.5
	ZrCH=CHCH ₂ Me	4.18, ddd (5.9, 7.0, 17.9)	99.8
	ZrCH=CHCH ₂ Me	0.98, m	36.2
		1.90, m	36.2
	ZrCH=CHCH ₂ Me	0.52, t (6.8)	17.4
	Zr-H	-7.80	n.a.

	Cp(#1)	5.92	104.6
	Cp(#2)	5.94	106.2
45 toluene-d ₈ , -10°C	ZrCH ₂ CHCHMe	0.42, dd (7.7 and 12.2)	59.3
		3.06, dd (7.7 and 10.9)	59.3
	ZrCH ₂ CHCHMe	-0.69, ddd (10.9, 12.2, 14.0)	40.6
	ZrCH ₂ CHCHMe	0.68, m	77.2
	ZrCH ₂ CHCHMe	2.04, d (6.7)	31.3
	Zr-H	-6.66, s	n.a.
	Cp(#1)	5.30, s	104
	Cp(#2)	5.325, s	104
	Cp(#3)	5.33, s	104
	Cp(#4)	5.34, s	104
45 THF-d ₈ , 25°C	ZrCH ₂ CHCHMe	0.34, dd (7.6 and 12.6)	59.4
		2.93, dd (7.6 and 10.9)	59.4
	ZrCH ₂ CHCHMe	-0.61, ddd (10.9, 12.6, 14.2)	40.8
	ZrCH ₂ CHCHMe	0.66, m	77.6
	ZrCH ₂ CHCHMe	1.79, d (6.6)	30.7
	Zr-H	-6.55, s	n.a.
	Cp(#1)	5.56, s	104.5
	Cp(#2 and 3)	5.58, s	104.5
	Cp(#4)	5.60, s	105.0

a - The coupling constants for most of the resonances are not reported as the signals are either second order multiplets or are too broad for an accurate value to be determined. s-singlet, t-triplet, m-multiplet, br. s-broad singlet, n.d.-not determined, n.a.-not applicable.

Despite considerable overlap of NMR resonances in the aliphatic region, a number of compounds can be identified. Thus, a characteristic set (-CH₂CH=CHCH₃) of J-coupled (COSY) cross peaks in the ¹H NMR spectrum, (Table 4-1) with the corresponding set of ¹³C resonances, extracted from a ¹H-¹³C HMQC experiment, clearly indicates an crotylzirconocene fragment.¹⁸⁻²⁴ Under certain conditions (the first 10-30

minutes at RT in toluene or the first 10 minutes at RT in THF) this was the main observable metallocene compound in the mixture, apart from the unreacted Cp_2ZrBu_2 , judged by the number of peaks in the Cp regions of the ^1H and ^{13}C spectra (Figure 4-1). The other ligand in this compound is a hydride as can be seen in TOCSY and NOESY experiments. The analogous compound, $\text{Cp}^*_2\text{Zr}(\text{CH}_2\text{CH}=\text{CHCH}_3)\text{H}$, albeit poorly characterized, has been synthesized before by the thermal rearrangement of $\text{Cp}^*_2\text{Zr}(\text{C}(\text{Me})=\text{CH}(\text{Me}))\text{H}$.²⁵

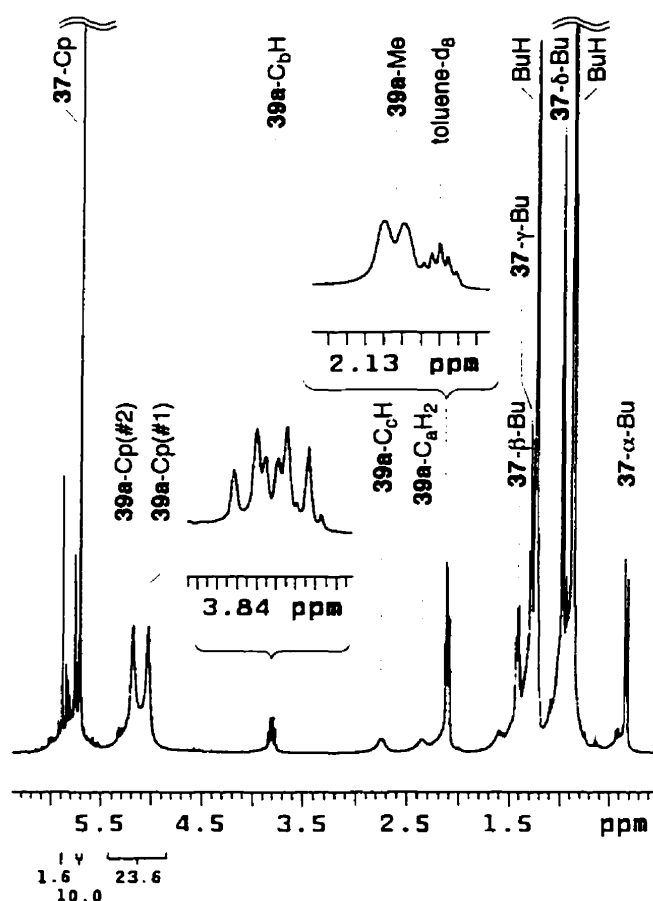


Figure 4-1. An ^1H NMR spectrum of a mixture of **37** and **39a** in toluene- d_8 at $+25^\circ\text{C}$. The Cp, C_aH_2 , C_cH and Me signals of **39a** exhibit dynamic broadening while C_bH is sharp.

The observation of allylic products is not entirely unexpected since the decomposition of alkyl- to allylmetallocenes has been previously raised as a possibility in the context of Ziegler-Natta olefin polymerization catalysis.^{20,26} Formation of a

zirconocene(IV) hydride is of interest as we believe it to be a key step in the redox reactions occurring in the Cp_2ZrBu_2 system, *vide infra*.

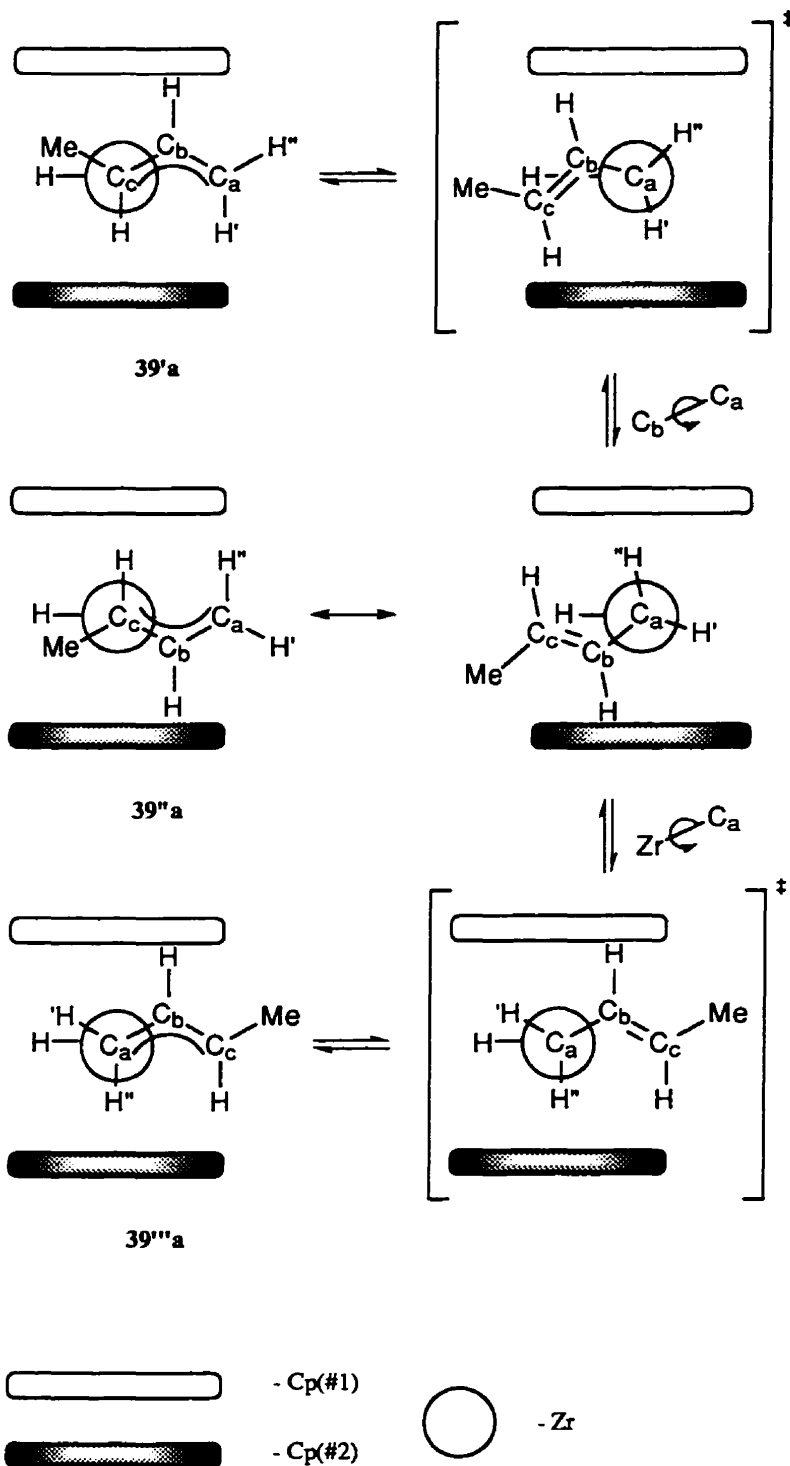


Figure 4-2. Schematic representation of the π - σ - π dynamic processes in **39a**.

It should be noted that the Cp, C_aH₂ and C_cH proton resonances of **39a** are very broad while the Me line is only slightly broadened and the C_bH signal is sharp (Figure 4-1). This broadening stems from a dynamic process which strongly suggests π - σ - π rearrangement with rotation about the C_a-C_b and C_a-Zr bonds (Figure 4-2)^{27,28}. The pairs of diastereotopic Cp and C_aH₂ signals are in exchange and give rise to negative NOE cross peaks. This indicates rotation about the C_a-C_b bond. Such a rotation furnishes two enantiomers, **39'a** and **39''a** (Figure 4-2), which have inverted labels of the diastereotopic Cp rings and crotyl C_aH₂ protons. This process is slow on the NMR time scale and the pairs of dynamically equivalent resonances still appear as separate peaks. The other crotyl resonances should be little affected by this process as they are enantiotopic in the two rotamers, hence their magnetic environment does not change. On the other hand, a π - σ - π rearrangement with rotation about the C_a-Zr bond does change local anisotropy for all proton nuclei as it generates diastereomers (e.g. **39''a** and **39'''a**). This would lead to a doubling of all resonances, or a single set of broad peaks when rotation is fast on the NMR time scale. However, it would not lead to an exchange between the pairs of Cp and C_aH₂ resonances. The relatively narrow linewidth for the Me resonance indicates that this group is influenced by the anisotropic zirconocene core to a much smaller extent due to its remote position. The only proton which is obviously not affected by this process is C_bH as it is in essentially identical magnetic environments in both rotamers. The signals for C_bH in rotamers **39''a** and **39'''a** coincide and do not cause any broadening. The observed resonance is in fact sharp and exhibits well resolved scalar coupling to the rest of the crotyl ligand. The coupling is not averaged by dynamic exchange as one of the processes is slow on the NMR time scale (rotation about the C_a-C_b bond) and the other does not change the spatial relationship of the proton nuclei within the crotyl ligand (rotation about the C_a-Zr bond). Experimentally observed line shapes and NOE cross peaks thus confirm the π - σ - π

rearrangement with a slow, yet observable, rotation about the C_a-C_b bond and a fast one about the C_a-Zr bond.

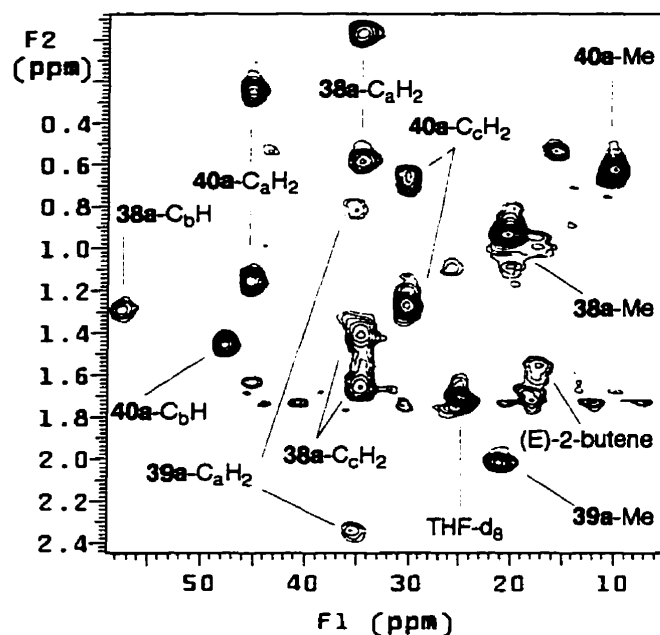
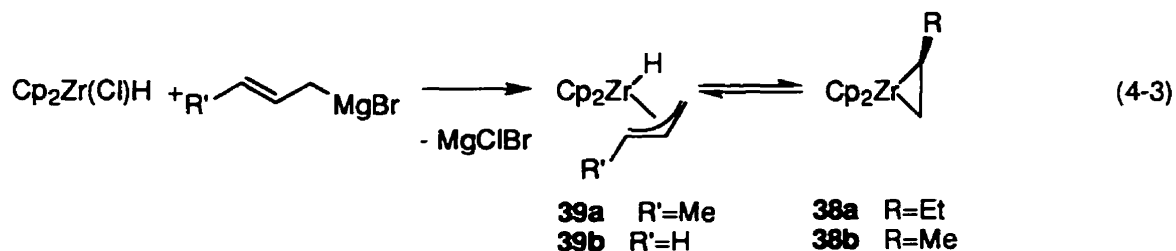


Figure 4-3. An ¹H-¹³C HMQC spectrum of a mixture of **38a**, **39a** and **40a** in THF-d₈ at -40°C. Pairs of cross peaks having a common ¹³C chemical shift belong to diastereotopic methylene groups. A more complete spectrum is shown in Figure 4-21.

The second product formed in the Cp₂ZrCl₂/2 BuLi system is **38a** (Table 4-1), which appears almost simultaneously with **39a** and is derived from it. When **39a** was synthesized independently (eq 4-3), it slowly rearranged into **38a** even at -40°C. The latter compound can be readily assigned by a combination of COSY and HMQC experiments, which reveal a -CH₂CHCH₂CH₃ backbone with two diastereotopic CH₂ groups (Figure

4-3) separated by a CH spacer. This assignment is also supported by TOCSY and NOESY spectra, by integrals and by simultaneous buildup (or decay) of all $\text{CH}_2\text{CHCH}_2\text{CH}_3$ signals with time. The multiplicity of the C_aH_2 group (Figure 4-4) is characteristic of a small cycle with two diastereotopic geminal protons having considerably different coupling constants (gauche and eclipsed) to the same vicinal neighbor. The large difference in the values is typical for rigid rings with little conformational freedom, where the torsion angles are not averaged by free rotation. The ^1H and ^{13}C NMR spectra of **38a** are similar to those of the well characterized phosphine adduct, $\text{Cp}_2\text{Zr}(\text{EtCH}=\text{CH}_2)(\text{PMe}_3)$.^{3,4} To the best of our knowledge, this is the first characterization of this long-postulated intermediate.

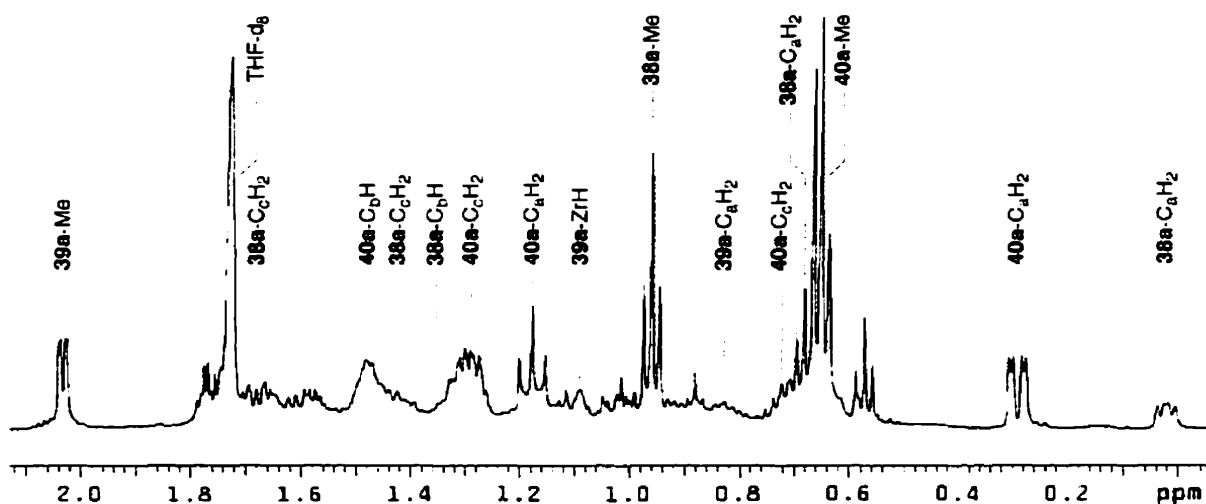


Figure 4-4. An ^1H NMR spectrum of a mixture of **38a**, **39a** and **40a** in THF-d_8 at -20°C . The multiplicity of the C_aH_2 group in **38a** and **40a** is characteristic of a small cycle with two diastereotopic geminal protons having considerably different coupling constants, gauche and eclipsed, to the same vicinal neighbor.

Compounds **38a** and **39a** are in an equilibrium which is significantly shifted towards **38a**, which proves that **38a** cannot be a primary product in the decomposition of **37**. Indeed, if **38a** were formed prior to **39a**, the concentration of the latter would never exceed the concentration of the former. The equilibrium can be observed by NOESY at

0°C. Thus, in addition to the negative NOE cross-peaks, due to the dynamic exchange in the fluxional crotyl complex, *vide supra*, there is another set of negative cross peaks between certain pairs of protons in **38a** and **39a** (Figure 4-5). Dynamic exchange of both C_aH_2 resonances of **39a** with every C_aH_2 signal of **38a** (Figures 4-5 and 4-6) indicates that the process, which scrambles C_aH_2 in **39a** and converts rotamer **39'a** into **39''a** and then into **38''a** (or **39''a**→**39'a**→**38'a**), is sufficiently fast on the NMR time scale to be observed. On the other hand, **38'a** and **38''a** are enantiomers, which have inverted labels of C_aH' and C_aH'' protons. There is, however, no scrambling of the C_aH_2 resonances of **38a**, which means that neither **38'a**→**39'a**→**39''a**→**38''a** nor **38''a**→**39''a**→**39'a**→**38'a** are fast enough to be observable under the same conditions. It should be noted that the hydrogen addition-elimination, which interconverts **38a** and **39a**, is face selective and scrambles proton labels exclusively within C_cH -**38a**/ C_cH -**39a** and C_cH^* -**38a**/ ZrH^* -**39a** pairs. The lack of C_cH -**38a**/ ZrH^* -**39a** and C_cH^* -**38a**/ C_cH -**39a** cross-scrambling indicates that the β -H-elimination, **38a**→**39a**, occurs more readily from the C_cH^* position. This can be explained in terms of steric repulsion between Me and Cp groups, with one rotamer of **38a**, where the Me group points away from both Cp ligands, being significantly lower in energy. The H^*-C_c bond in this rotamer lies almost in the bisectorial plane as required for the elimination to occur.

The observation of such an exchange lends additional support for the assignment of structures **38a** and **39a** as it interlocks similar positions in the skeletons of the two molecules. It also reveals an important feature of the Cp_2ZrBu_2 reagent: there are a number of species present in it, but they are in equilibrium with each other, and if only one compound is consumed in a given reaction, the whole system can evolve towards it. This explains the versatile behavior of the Cp_2ZrBu_2 reagent in various constant- and variable oxidation state reactions, as different reactions can be driven by different species present in that system, even if their concentration is not high.

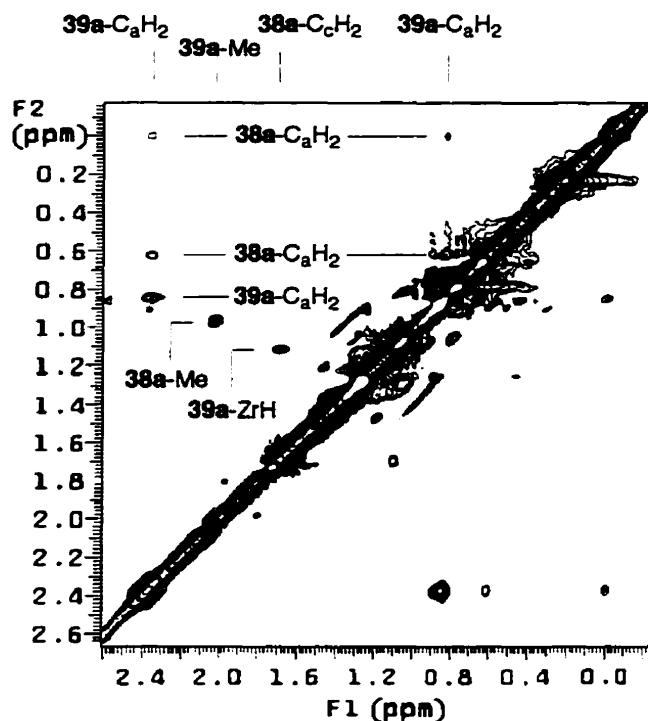


Figure 4-5. An ^1H - ^1H NOESY spectrum (negative contours only) of a mixture of **38a** and **39a** in THF-d_8 at 0°C . Both C_6H_2 resonances of **39a** are in dynamic exchange with each other and with every C_6H_2 signal of **38a**. However, there is no exchange within C_6H_2 and C_6H_2 pairs of **38a**.

Longer decomposition times (several hours at -20 or -40°C , or minutes at RT) lead to the disappearance of **38a** and **39a** and formation of **40a**. A bis-pentamethylcyclopentadienyl (Cp^*) analog of the latter has been previously described by Bercaw *et. al.*²⁵ and further characterized by Marks *et. al.*²⁹ The connectivity pattern in **40a**, readily obtained from a combination of TOCSY, COSY and HMQC experiments, is very similar to **38a** (Figures 4-3 and 4-4). Indeed, the hydrocarbyl skeleton of the former, $(-\text{CH}_2(\text{Et})\text{CH}-\text{CH}(\text{Et})\text{CH}_2-)$, can be viewed as a dimer of the latter. The two halves of the dimer are related by a C_2 symmetry operation, thus only one set of NMR peaks is observed. The zirconacyclopentane **40a**, however, has two features, distinctly different from **38a**: the Cp groups, assigned by NOESY, are equivalent (related by C_2 symmetry)

and integration of Cp versus $-\text{CH}_2\text{CHCH}_2\text{CH}_3$ gives two hydrocarbyls per sandwich. Further, the ^1H and ^{13}C chemical shifts are almost identical to the ones described for the previously prepared Cp* analog.^{25,29}

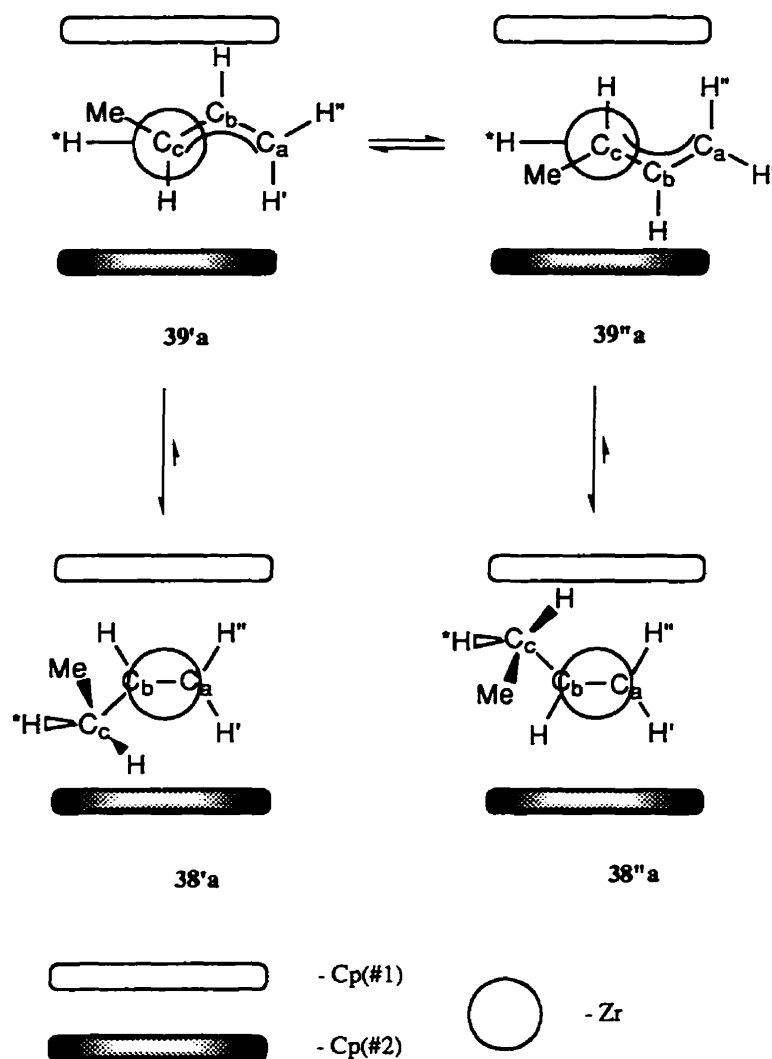


Figure 4-6. Schematic representation of a dynamic exchange between **38a** and **39a**.

Further thermal decomposition leads to the disappearance of **40a** and accumulation of **41a** and **45**. The former is produced in minor quantities but can be readily identified by the characteristic signals of its vinylic group (^1H : 8.44 ppm, d and 4.18 ppm, ddd ; ^{13}C :

210.5 and 99.8 ppm respectively), its $-\text{CH}=\text{CHCH}_2\text{Me}$ backbone (identified by COSY and TOCSY) and its strongly shielded $\mu\text{-H}$ at -7.80 ppm (identified by TOCSY and NOESY). The CH_2 group in **41a** is diastereotopic, reflecting a lack of a mirror plane, which usually coincides with the bisectorial plane in such complexes. Such a reduction of symmetry implies that the vinyl ligand is spatially constrained in some fashion, but none of the experimental data give any indication of what the nature of this constraint is. The other compound, **45**, starts to form at the early stages of decomposition (after the first 20 minutes at RT) and persists for weeks at RT. A TOCSY spectrum shows that one of the ligands in this compound exhibits five well resolved multiplets, which are assigned by COSY and HMQC experiments to a linear $\text{CH}_2\text{CHCHCH}_3$ fragment with saturated C-C bonds. If this is not a carbocycle and has no multiple C-C bonds it has to have three C-Zr bonds. Indeed, the NOESY spectrum proves that this ligand is in a close proximity to four Cp groups (two zirconocene fragments). It also shows that the other ligand is a hydride and the two zirconocenes are bonded to the (α,γ) and β positions of the carbon chain. Figure 4-7a schematically represents a fragment of the 3D structure of **45**, which is based on the previously reported geometry of titanacyclobutanes³⁰ and which explains the observed NOE cross peaks. The steric bulk of the zirconacyclobutane ligand constrains the spatial arrangement of the zirconocene fragments so that their bisectorial planes form a close to zero dihedral angle. That way the zirconacycle lies as close as possible to the bisectorial planes of both zirconocenes. The zirconacyclobutane faces the Cp_2Zr_b wedge with its unsubstituted side so that the Me substituent is in a trans arrangement with Zr_b to minimize steric repulsion. As can be seen from Figure 4-7a, and can be confirmed by simple geometrical estimations, there is only one proton in close proximity to a H-Zr bond. Indeed, the only strong NOE cross peak between hydride and alkyl ligands is between H-Zr and H_b .

The ^{13}C chemical shifts in **45** indicate the same type of structure. Thus, the C_β is in a field too strong for a C nucleus directly bonded to zirconocene and at the same time is

in a field too weak for a C_β nucleus in a metallacyclobutane.³¹⁻³⁴ This is readily explained by competing shielding and deshielding contributions, as C_β shows both characteristics. The C_α and C_γ nuclei, which have only a deshielding contribution of the directly bonded zirconocene, appear in the expected range. The upfield shift of the Zr-H resonance indicates that it occupies a bridging position, while the number and multiplicity of the rest of the signals show that **45** is a symmetric dimer (Figure 4-7b). Finally, the sharp and well resolved resonances of **45** allow for determination of all coupling constants. An excellent fit between the experimental and a simulated spectrum (Figures 4-8a and 4-8b respectively) lends further support to the assignments.

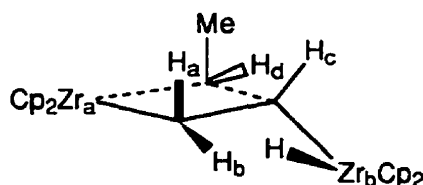


Figure 4-7a. Schematic representation of a fragment of the 3D structure of **45** as determined by NOESY.

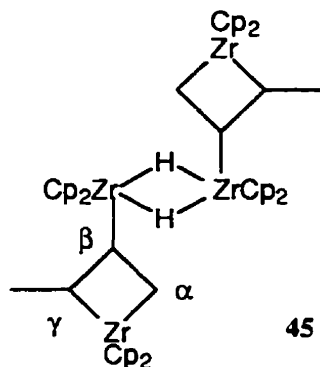
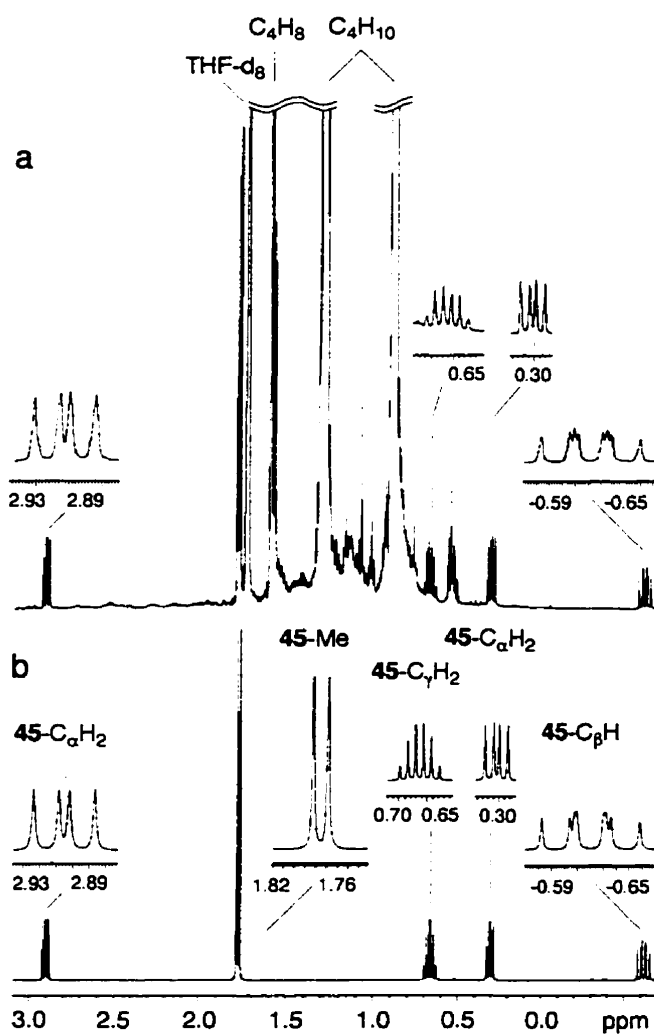


Figure 4-7b. Proposed structure for **45**.

The concentration of **45** gradually increases and it eventually becomes one of the dominant diamagnetic products in the mixture due to its high thermal stability, although its

concentration never exceeds 20% of the initial concentration of **37**. A variety of uncharacterized diamagnetic products are also formed in very minor amounts. Although most of the material remains in solution, the total intensity of all the NMR signals (except butane) decreases at least by a factor of 2, relative to the solvent resonances, in the course of 0.5 to 1 hours at room temperature. Thermal decomposition of **37** is accompanied by a change in color from yellow to black, which is usually an indication of the formation of low oxidation state, paramagnetic Zr^{III} compounds. Indeed, EPR measurements (Figure 4-9) reveal formation of the paramagnetic species, **31**, which gives an apparent triplet in



Figures 4-8a and 4-8b. Experimental and spin simulated ^1H NMR spectrum of **45** respectively.

toluene, due to the hyperfine coupling of the unpaired electron to two protons ($g=1.9961$, $a(H)=2.4$ G). The spectrum is complicated by the presence of some small amounts of other paramagnetic compounds, the signals of which mask the ^{91}Zr satellites of the main signal. Although it is not possible to measure $a(\text{Zr})$ accurately, an upper limit of 9 G can be estimated from the spectrum. The frozen solution EPR spectrum is inconclusive due to the overlap of the main signal with the signals of other compounds. It is worth mentioning that no zero field splitting has been observed.

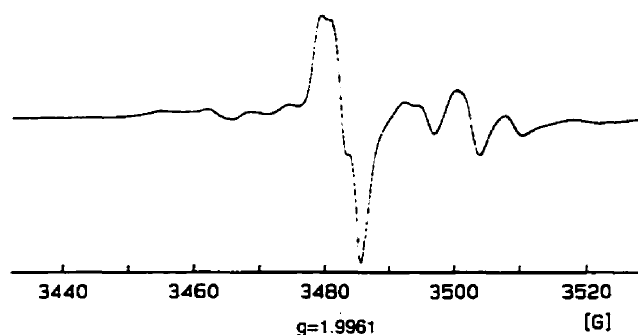


Figure 4-9. An EPR spectrum of a mixture of **31** and unidentified paramagnetic compounds in toluene. The main peak is an apparent triplet due to the hyperfine coupling to the butyl ligand.

When the paramagnetic reaction mixture is quenched with dry HCl (or with DCl in D_2O), $\text{C}_3\text{H}_7\text{CH}_3$ (or $\text{C}_3\text{H}_7\text{CH}_2\text{D}$) is the only volatile product produced, except for traces of butane and butene isomers (less than 1% each). The main NMR detectable zirconium product (>99 %) is Cp_2ZrCl_2 . By NMR integration of the proton spectra, the Cp to $\text{C}_4\text{H}_9\text{D}$ proton ratio is $10:8 \pm 1$. No deuterium labels were detected in the Cp_2ZrCl_2 and no CpZrCl_3 was formed. Because it is known that excess BuLi leads to loss of a Cp group,³⁵ care was taken to insure that there was no excess lithium reagent in the mixture prior to quenching. These observations are crucial as a number of decomposition-reduction reactions have been previously reported, including abstraction of a Cp proton³⁶ and the

loss of one Cp ligand from the sandwich,³⁷ which can not be discriminated by EPR in the case of **31** due to the poor resolution, but can be ruled out based on the NMR results. Possible candidates for the observed EPR spectra are: Cp_2ZrBu , $[\text{Cp}_2\text{ZrBu}]_2$, $[\text{Cp}_2\text{ZrBu}_2]^{-\bullet}$, or $[\text{Cp}_2\text{ZrBu}\cdot\text{Cp}_2\text{ZrR}_2]$, where Cp_2ZrR_2 could be any diamagnetic zirconocene. A dimer $[\text{Cp}_2\text{ZrBu}]_2$ might be either diamagnetic or antiferromagnetic,³⁸ but the latter is inconsistent with the EPR features of **31**. A diamagnetic dimer $[\text{Cp}_2\text{ZrBu}]_2$, on the other hand, although it is not observable by EPR could give the observed broad and featureless NMR spectrum if it is in equilibrium with a paramagnetic monomer. The amount of Zr^{III} directly measured by EPR accounts for about 5% of the total amount of Zr. The radical-anion $[\text{Cp}_2\text{ZrBu}_2]^{-\bullet}$, can be ruled out as the EPR observable species since such electron-rich compounds exhibit much higher $a(\text{Zr})$ and $a(\text{H})$ than **31** does.³⁹⁻⁴¹ Low values for the hyperfine coupling constants such as those presently observed, are usually attributed either to electron-withdrawing substituents⁴² or electron delocalization between two metal centers,⁴³⁻⁴⁵ such as in a $\text{Zr}^{\text{III}}/\text{Zr}^{\text{IV}}$ dimer $[\text{Cp}_2\text{ZrBu}\cdot\text{Cp}_2\text{ZrR}_2]$. The EPR multiplicity for $[\text{Cp}_2\text{ZrBu}\cdot\text{Cp}_2\text{ZrR}_2]$ should be more complicated than a triplet, but with the given resolution and linewidth such a possibility can not be discarded. We thus conclude, that **31** is most probably a diamagnetic dimer $[\text{Cp}_2\text{ZrBu}]_2$ in equilibrium with its paramagnetic monomer or with a paramagnetic dimer $[\text{Cp}_2\text{ZrBu}\cdot\text{Cp}_2\text{ZrR}_2]$. The g-value and the hyperfine constants are in the normal range reported for alkylzirconocenes and titanocenes.^{36,41,46,47} Addition of PMe_3 does not improve the resolution and leads to a simple doubling of the EPR resonances ($\text{Cp}_2\text{ZrBu}(\text{PMe}_3)$: $g=1.9955$, $a(\text{P})=20.6$ G, $a(\text{Zr})=16.25$ G, $a(\text{H})<2$ G in toluene).

The other paramagnetic products (Figure 4-10) are Cp_2ZrH ,^{42,48,49} **47**, ($g=1.9796$, doublet, $a(\text{H})=7.0$ G in THF) and $\text{Cp}_2\text{Zr}(\text{CH}_2\text{CH}=\text{CHMe})$,⁵⁰ a broad unresolved multiplet ($g = 1.9936$ in THF). When toluene is used as a solvent, a more complicated multiplet is observed. Addition of PMe_3 doubles the number of resonances and results in a complicated and intractable spectrum.

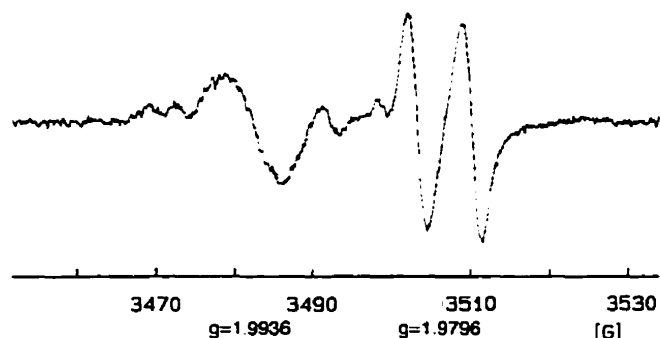


Figure 4-10. An EPR spectrum of a mixture of **47** and $\text{Cp}_2\text{Zr}(\text{CH}_2\text{CH}=\text{CHMe})^{50}$ in THF. The doublet peak is due to the hyperfine coupling to the hydride ligand.

It is worth mentioning that no hydrogen has been detected among the spontaneous decomposition products of **37**. By far the major hydrocarbon product is butane, accompanied by a small amount of cis and trans 2-butene (10-15%), which are formed at the late decomposition stages and are identified by NMR.⁵¹⁻⁵³ Although 1-butene^{53,54} can be detected among the hydrolysis products after HCl or DCl work up, it is not formed when the sample is kept under rigorously anaerobic conditions.

4.3 Discussion

4.3.1 A reaction scheme for decomposition of Cp_2ZrBu_2

The first observable product formed by decomposition of **37** is **39a**. This compound is most unlikely to be a prime decomposition intermediate, since it is hard to imagine any synchronous process, which would lead directly from **37** to **39a**. There must be another intermediate in this transformation. It is usually assumed that decomposition of **37** occurs through β -H abstraction, followed by elimination of butane and formation of **38a**¹. However, the present results show that **38a** itself is formed from **39a**. This particular order can be observed not only in the thermal decomposition of **37** but in an

independent synthesis of **39a**, where a fast rearrangement to **38a** occurs. Therefore, it is highly unlikely that **38a** can be the prime product of decomposition of **37**.

The conclusion that the primary decomposition of Cp_2ZrBu_2 probably occurs by γ - rather than β -H abstraction runs counter to previous opinion. It has been convincingly shown by experiment that β -H abstraction is preferred in the case of $\text{Cp}_2\text{Zr(R)Et}$ compounds.⁵⁵ However, it is likely that the energy difference between α -, β -, and γ -H abstraction is quite small. This is supported by a number of theoretical analyses of agostic intermediates carried out on Ziegler-Natta type systems. Indeed, some of these calculations show the γ -agostic interaction has the lowest energy.⁵⁶⁻⁵⁹ Inspection of molecular models of Cp_2ZrBu_2 shows that β -H abstraction requires a transition state with two flat zirconacycles lying in the same plane and with very little conformational freedom (Figure 4-11a). On the other hand, γ -H abstraction, while still requiring a bicyclic transition state, leaves one ring nonplanar and with the conformational flexibility to absorb steric strain (Figure 4-11b). Thus, it is not unlikely that the change from an ethyl ligand to a more sterically demanding butyl ligand could tilt the reaction pathway in favor of γ -H abstraction. The chain of transformations ($37 \rightarrow \dots \rightarrow 39a \rightarrow 38a$) together with the product, **45** (Scheme 4-1), derived from the postulated zirconacyclobutane suggest that **42a** does exist in this mixture although its concentration and stability are insufficient for a firm identification. This is not surprising as the reaction mixture exhibits a complicated and heavily overlapped NMR spectrum, which only allows identification of the most abundant compounds. An alternative decomposition of **37** with the prime formation of the elusive “ Cp_2Zr ”, accompanied by reductive elimination of octane, can be ruled out at this stage since octane was not detected in the system.

Further decomposition of the postulated **42a** can proceed by β -H abstraction from either the methyl or the methylene group (Scheme 4-1). The former process is a reverse reaction to an olefin insertion into a Zr-H bond, where an olefin is already positioned in the coordination sphere of Zr by a flexible two carbon atom bridge. It is unlikely for such a

β -H abstraction to be thermodynamically or kinetically favorable over the reverse insertion reaction. The β -H abstraction from the methylene group is a similar process except that the bridge is more rigid, which makes the reverse insertion reaction less favorable and the product, **39a**, more stable. Such allyl and metallacyclobutane interconversions are known; e.g. migration of hydrocarbyl fragments from a central metal to a β position of an allyl ligand with formation of zirconacyclobutane has been reported before by Stryker *et al* and is believed to occur via a radical process.^{18,19} A concerted σ -bond metathesis process is a less likely alternative due to an unfavorable geometry of the transition state.^{18,19} Such a rearrangement strongly depends on the nature of the migrating group (e.g. methyl in methyl(allyl)zirconocene does not migrate, whereas allyl in bis-allylzirconocene does)¹⁹ and might proceed in a reverse direction in the case of a hydride as has been reported for the late transition metals.⁶⁰

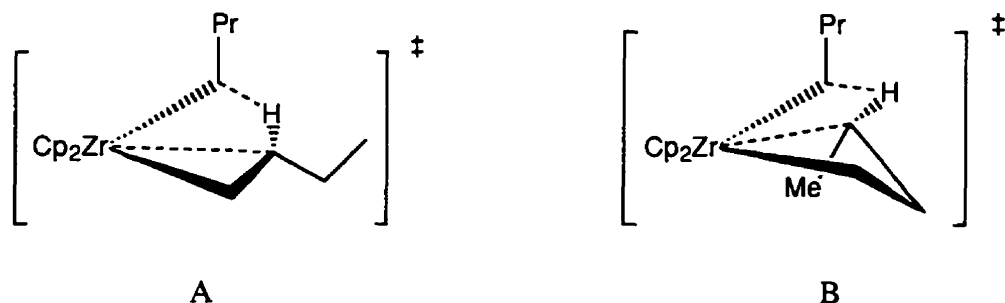
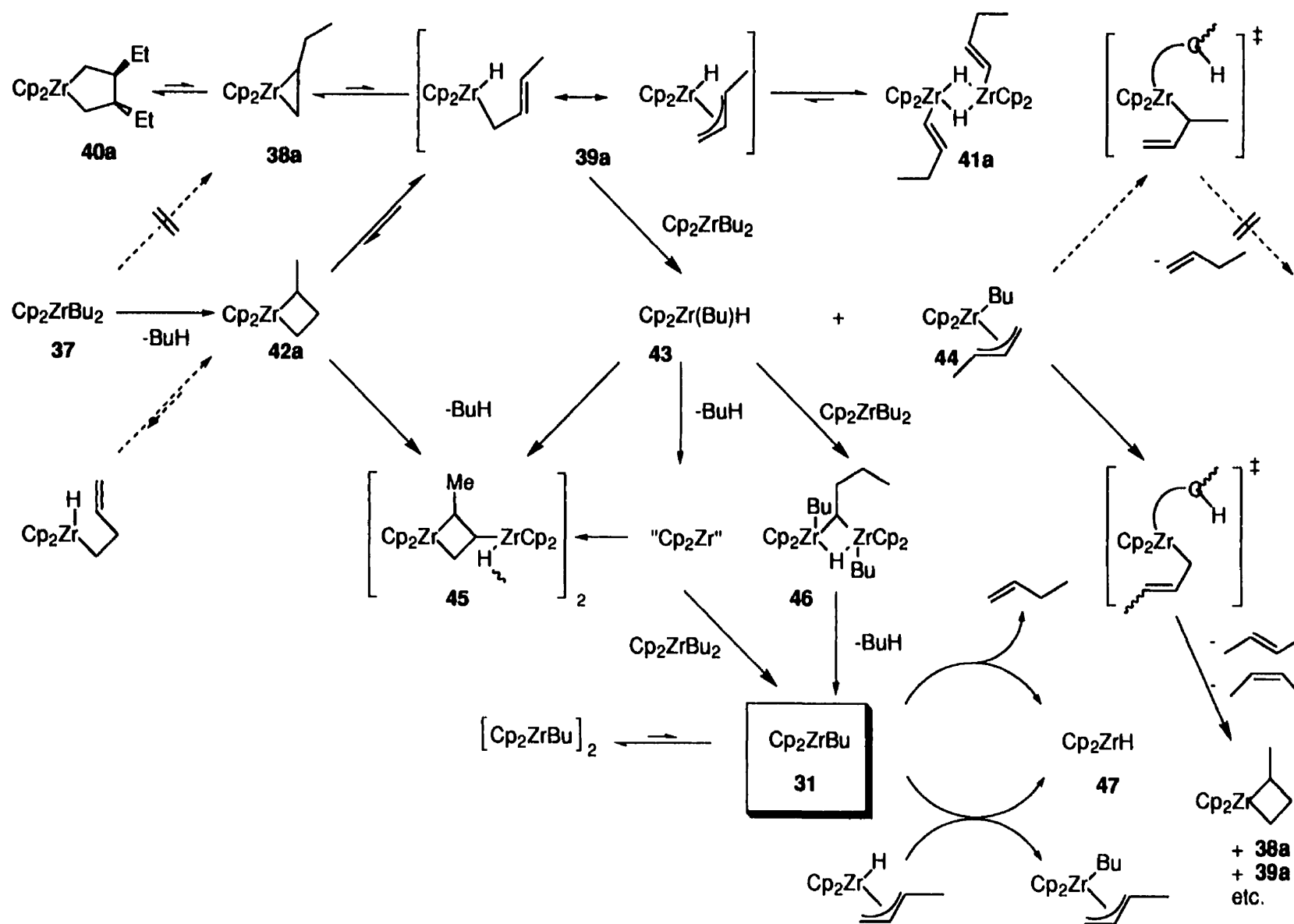


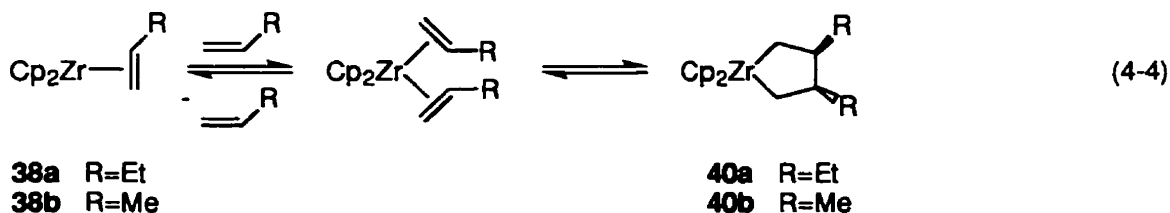
Figure 4-11a and 4-11b. Generic σ -bond metathesis transition states for β - and γ -H abstraction. 4-11a: two flat zirconacycles are lying in the same plane and have no conformational freedom. 4-11b: - still bicyclic, but one of the cycles does not have to be planar and can twist to meet the geometry requirements of the other one.

Finally, **39a** undergoes a slow (at -40°) 1,3-H shift forming **41a**, or an insertion of the olefin (crotyl) into the Zr-H bond forming **38a**, which is the second major observable product in the early stages of decomposition. Similar intramolecular hydrogen migrations, which interconvert metallacyclobutanes, metallacyclopropanes, alkenyl- and

Scheme 4-1 A proposed sequence of reactions occurring during decomposition of Cp_2ZrBu_2

allylmetal hydrides have been previously reported for early- and late transition metals in relation to the catalytic isomerization of olefins.^{25,60,61} A rearrangement between Cp* analogs of **38a** and **39a** has been previously cited as a possible mechanism for isomerization of alkenylzirconocene hydrides, albeit the authors have favored another pathway.²⁵ These processes are most likely reversible although the equilibria are shifted almost entirely towards **38a**. Even though **39a** disappears rapidly, the products in the later stages of decomposition (**45**, **41a**, **31** 2-butene and butane) are more likely to be derivatives of either **42a** or **39a** and cannot be formed directly from **38a**. (e.g. reductive elimination from **38a** should lead to 1-butene, which has not been detected in the absence of hydrolysis)

Although both Cp*₂Zr(CH₂CH=CHCH₃)H, in the presence of 1- or 2-butene,²⁵ and Cp*₂ZrBu₂²⁹ have been reported to produce the Cp* analog of **40a**, a mechanism for the transformation of **38a** or **39a** into **40a** is not immediately clear. Such reactions are usually explained by a simplified approach (eq 4-4),¹ where two olefins first coordinate to the same d² Zr center and then couple together.¹ Given the fact that 1-butene, was not detected in the reaction mixture, we conclude that the mechanism for this process is yet to be defined. However, the simplistic model is still useful for visualization of the reaction pathway and predictions of regio- and stereospecificity.¹ This reaction is reversible,²⁵ and although **40a** is a major kinetic product, it gradually rearranges back to **39a** as the latter slowly but irreversibly participates in other reactions, leading to reductive elimination (Scheme 4-1).



Since the most abundant hydrocarbon product is butane, the major reductive elimination must occur from zirconium center(s) bearing both butyl and hydride ligands. Such a compound, $\text{Cp}_2\text{Zr}(\text{H})\text{Bu}$, **43**, can be formed from **39a** by ligand redistribution with butyl zirconocene. The postulated **43** has not been observed spectroscopically, which is most likely due to its extreme instability. It can either spontaneously lose butane, or form a Zr-H-Zr bridged structure with other sterically non crowded zirconocenes. When **37** is still abundant in the reaction mixture, the newly formed bridge would contain H and Bu fragments in close proximity. A dimer of **39a** and **37** is also a candidate for elimination of BuH. Such compounds are likely to undergo reductive elimination of butane with formation of **31** (Scheme 4-1) and $\text{Cp}_2\text{Zr}(\text{CH}_2\text{CH}=\text{CHMe})$ respectively. Indeed, alkylzirconocene hydrides are known to participate in reductive elimination reactions. The exact mechanism of such eliminations is unknown. It has been postulated to be a unimolecular, two electron process, but experimental observations are further complicated by ligand scrambling and cyclopentadienyl C-H activation processes.⁶²⁻⁶⁴ The latter do not occur in the present case as has been shown by the DCl quenching experiment, *vide supra*.

Reductive elimination could occur from a monomeric alkylzirconocene hydride with formation of " $\text{Cp}_2\text{Zr}^{\text{II}}$ ", as previously postulated.⁶⁵ The " $\text{Cp}_2\text{Zr}^{\text{II}}$ " can undergo further redox comproportionation with Cp_2ZrBu_2 to form Cp_2ZrBu (Scheme 4-1), as has been reported before for $\text{Cp}_2\text{Zr}^{\text{II}}(\text{PMe}_3)_2/\text{Cp}_2\text{Zr}^{\text{IV}}\text{X}_2$.^{66,67} Butylzirconocene(III) is further converted to zirconocene hydride **47** either by H-elimination or ligand exchange with other hydride species. The latter is more plausible, as H-elimination would most likely produce 1-butene, which has not been found. The other elimination products, cis and trans-2-butene, can be accounted for by a similar reductive elimination from **39a** (or its dimer) or a nonreductive H-abstraction from the butyl ligand in $\text{Cp}_2\text{Zr}(\text{crotyl})\text{Bu}$ (Scheme 4-1). Such a reduction of mono- and bis-cyclopentadienyl compounds of titanium and zirconium by the MR_n alkylating agents ($\text{M}=\text{Li}$,⁶⁸ MgBr ,⁶⁹ Al^{70-72}) is a well known, yet poorly understood reaction. It is often discussed in the context of the Ziegler-Natta

polymerization reaction as it is believed to be of relevance to the catalyst deactivation, whereas nonreductive hydrogen- or alkyl eliminations are responsible for chain transfer reactions.^{73,74}

The most thermally stable diamagnetic compound in this mixture and the second most abundant product, **45**, can be formed from **42a** either by insertion of "Cp₂Zr" or by a σ -bond metathesis with **43**. The presence of a zirconacyclobutyl skeleton in **45** lends further support for the existence of its precursor, **42a**, in this mixture.

4.3.2 Some thermochemical aspects of the proposed reaction steps

The observed elimination products and proposed reaction pathways can be rationalized on the basis of the previously reported Zr-H and Zr-C bond disruption enthalpies of similar zirconocenes.^{29,75,76} As has been reported before²⁹ and can be seen from the data in Table 4-2, modest steric effects do not have any significant influence on the BDE values (e.g. Cp₂ZrMe₂, Cp*₂ZrMe₂ and Cp₂*Zr(η^1, η^1 -CH₂CH₂-o-C₆H₄)). This allows the use of the BDEs measured for Zr-alkyl bonds in Cp₂*Zr(η^1, η^1 -CH₂CH₂-o-C₆H₄), Cp₂Zr(n-C₆H₁₃)Cl and Cp₂Zr(cyclo-C₆H₁₃)Cl, as a good approximation for all nonstrained Zr-(sp³-C) bonds, with the proviso that the values for the latter two compounds should be corrected for the effect of chloride ligand. The mean values, reported for compounds Cp₂ZrR₂ with two identical substituents, which have been titrated in a double stage procedure (e.g. Cp₂ZrR₂+2R'OH → Cp₂Zr(OR')R+RH+R'OH → Cp₂Zr(OR')₂+2RH), also need to be corrected to account for the effect of the electron withdrawing substituent (OR') on the BDE in the second stage. Such a correction can be done by assuming D[ZrH]-alkyl-D[ZrH]-H=D[ZrX]-alkyl-D[ZrX]-H, which is derived from a modified version of the bond enthalpy equation of Matcha as suggested by Schock and Marks.²⁹ A correction coefficient has been calculated from the BDEs of Zr-H bonds in Cp₂ZrH₂, for which the separate stage and the mean BDEs are

both available, and is assumed to be approximately the same for all Cp_2ZrR_2 compounds. All BDEs for the nonstrained Zr-alkyl bonds, reported for similar compounds by different authors, exhibit an excellent agreement after correction. Furthermore, a steric strain in the zirconacarbocycles can also be estimated. Thus $\text{Cp}_2^*\text{Zr}(\eta^1, \eta^1\text{-CH}_2\text{CH(Et)CH(Et)CH}_2)$ and $\text{Cp}^*\text{Zr}(\eta^1, \eta^5\text{-C}_5\text{Me}_4\text{CH}_2)$ can be used as examples of strained molecules and their Zr-alkyl BDEs are 7.5 (per Et group) to 19 kcal/mol smaller, reflecting the steric strain. The latter compound can be viewed as an extremely strained cycle and it sets an upper limit for the ring strain energy. The former complex gives a more realistic 7-8 kcal/mole steric strain, arising from nonbonding repulsion of the Et groups and Cp^* rings, whereas the ring strain itself in the 4-membered and larger zirconacarbocycles is fairly small (e.g. a Zr-alkyl BDE in $\text{Cp}_2^*\text{Zr}(\eta^1, \eta^1\text{-CH}_2\text{CH}_2\text{-o-C}_6\text{H}_4)$ is indistinguishable from the values for any nonstrained Zr-alkyl bond as the hydrocarbyl fragment is flat and has neither ring strain nor any significant nonbonding interactions with the Cp^* ligands). In the case of unsubstituted Cp the nonbonding repulsion should be even smaller.

With no accurate experimental data available for zirconacyclopropane or zirconacyclobutane compounds, we have chosen arbitrary steric strain values of 15 and 8 kcal/mol per cycle respectively. Thus the calculated reaction enthalpies should be treated only as rough estimates because the starting BDE values are of limited accuracy. The ΔG_{calcd} can be estimated assuming that the $T\Delta S$ contribution of creating an additional particle near room temperature is ca. -9 ± 3 kcal/mol,²⁹ which adds further uncertainty to our calculations. With all the limitations taken into consideration, this approach can still provide valuable information as most of the reactions in question are estimated to be very endothermic by more than 30 kcal/mol (eq 4-6, 4-7, 4-9 and 4-10), and are unlikely to occur even if there are large errors in the starting BDEs. Calculating interconversions of zirconacyclobutanes, zirconacyclopropanes, alkenyl- and allylmethyl hydrides, on the other hand, would be meaningless as the margin of error for them is higher than the expected effect itself.

Table 4-2. Bond Disruption Enthalpies (kcal/mol)

Bond (compound)	D	D _{corrected}	Ref.
Zr-Me (Cp ₂ ZrMe ₂)	67	62.5 ^a	76
Zr-Me (Cp* ₂ ZrMe ₂)	67	62.5 ^a	29
Zr-H (Cp* ₂ ZrH ₂)	first stage	75	29
	second stage		
Zr-H (Cp ₂ Zr(Cl)H)	87	75 ^c	76
Zr-(sp ³ -C) (Cp ₂ Zr(Cl)-n-C ₆ H ₁₃)	76	64 ^c	76
Zr-(sp ³ -C) (Cp ₂ Zr(Cl)-cyclo-C ₆ H ₁₁)	76	64 ^c	76
Zr-(sp ³ -C) (Cp ₂ *Zr(η ¹ ,η ¹ -CH ₂ CH ₂ -o-C ₆ H ₄))	63.1	63.1	
strained Zr-(sp ³ -C) (Cp ₂ *Zr(η ¹ ,η ¹ -CH ₂ CH(Et)CH(Et)CH ₂))	53.5	49 ^a	29
strained Zr-(sp ³ -C) (Cp*Zr(Ph)(η ¹ ,η ⁵ -C ₅ Me ₄ CH ₂))	45	45 ^d	29
Zr-(sp ² -C) (Cp* ₂ ZrPh ₂)	73	73 ^d	29
Zr-allyl (Cp ₂ Zr(allyl) ⁺), minimal value	D _{Zr-alkyl} + 15		75
sp ³ -C-H (H-CH ₂ CH ₃)	98	98	82
allylic C-H (H-CH ₂ CH=CH ₂)	85	85	82
sp ² -C-H (H-CH=CH ₂)	103	103	82
internal C-C (CH ₃ -CH ₂ CH ₃)	85	85	82
π component of C=C (CH ₂ =CH ₂)	75	75	82
H-H (H ₂)	104	104	82

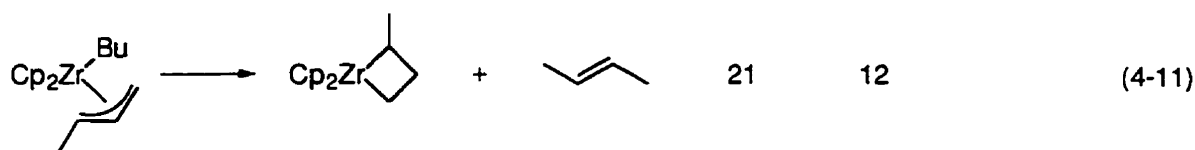
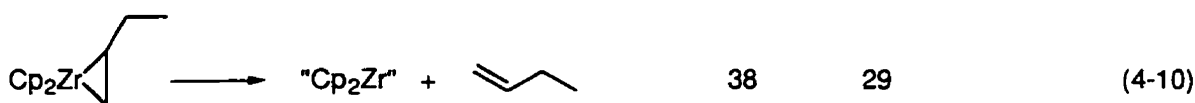
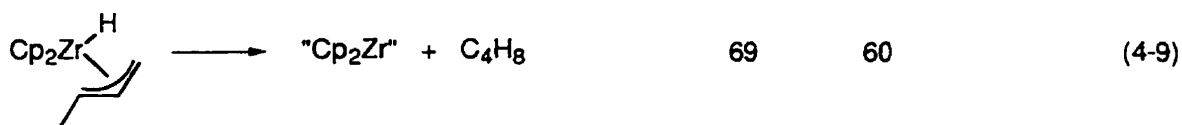
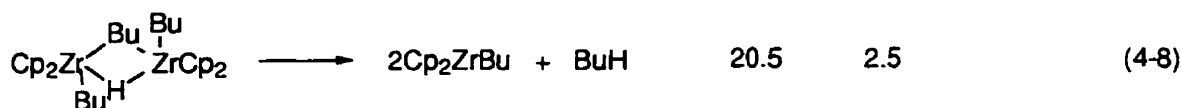
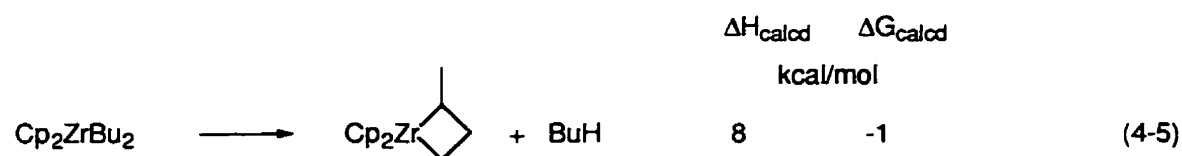
^a The mean values, reported for compounds Cp₂ZrX₂ with two identical substituents, which had been titrated in a double stage procedure (e.g. Cp₂ZrMe₂+ROH → Cp₂Zr(OR)Me+MeH → Cp₂Zr(OR)₂+MeH), were corrected to account for the effect of the electron withdrawing substituent (OR) on the BDE in the second stage. The correction coefficient was estimated from the BDEs of the Zr-H bonds in Cp₂ZrH₂, for which the separate stage and the mean BDEs are both available, and was assumed to be approximately the same for all Cp₂ZrX₂ compounds.

^b Two titration stages had been done separately and do not need any correction.

^c The values, reported for Cp₂Zr(Cl)X, were corrected for the effect of the electron withdrawing ligand (Cl). A correction coefficient was estimated from the difference in the

BDEs of Zr-H bonds in Cp_2ZrH_2 and $\text{Cp}_2\text{Zr}(\text{Cl})\text{H}$ and was assumed to be approximately the same for all $\text{Cp}_2\text{Zr}(\text{Cl})\text{X}$ compounds.

^d Only the first titration stage was performed and the value does not require any correction.



As can be seen from the results of our calculation, the three most favorable elimination processes account for the formation of the major identified or postulated compounds: **42a** (or isomers **38a** and **39a**, eq 4-5), **40a** (eq 4-12), **31** and butane (eq 4-8). The only thermodynamically feasible reductive elimination is the elimination from the

dimeric $[\text{Zr}(\mu\text{-H})(\mu\text{-Bu})\text{Zr}]$ **46** and is due to an entropy gain. Alternative reductive eliminations from monomeric $[\text{Zr}(\text{H})\text{R}]$, **43** and **39a**, or from **38a** are highly endothermic (eq 4-7, 4-9 and 4-10). In the case of $\text{R}=\text{crotyl}$, which is a bulky 4-electron donor ligand, formation of a dimer is unlikely to occur, which makes reductive elimination unfavorable and explains the absence of 1-butene among the products. 2-Butene, on the other hand, can be formed via a thermodynamically more favorable nonreductive route (eq 4-11 and Scheme 4-1). The transition state for the same H-abstraction, which would lead to 1-butene is considerably more constrained (Scheme 4-1), hence 1-butene is not formed. An absence of any observable quantities of dihydrogen or octane among the products is in good agreement with the observed intermediates, proposed decomposition pathway and the thermochemical calculations (eq 4-6).

When the starting compounds are zirconocene chloride hydride and crotylmagnesium bromide, the scrambling-dimerization-reductive elimination sequence is not the major reaction pathway as no hydrocarbyl ligands other than crotyl are available and it is too coordinatively demanding to allow any significant dimerization (e.g. to form the crotyl analog of **46**), *vide supra*. With dimerization being unfavorable, the equilibrium shifts towards the zirconacyclopentane **40a** and zirconacyclobutane **45**, which are kinetically stable for days at room temperature. Reduction of zirconium(IV) does not occur.

4.4 Conclusions

Cp_2ZrBu_2 is unstable with respect to elimination of butane by γ -hydrogen abstraction from the neighboring butyl group, leading to the zirconacyclobutane **42a**. The latter has not been detected directly, but is postulated on the basis of the observed product, **45**, and other reactions in the system. **42a** rearranges to form crotylzirconocene hydride, **39a**, which undergoes further rearrangement to produce the zirconacyclopropane, **38a**,

and the dimeric butenylzirconocene hydride, **41a**. In the early stages of decomposition the most abundant diamagnetic products are **38a** and **39a**. Further thermolysis leads to the formation of **40a**, **41a** and **45**. Compounds **40a**, **41a** and **45** are stable for days at RT, but the first two are in equilibrium with **39a**. When the starting material is Cp_2ZrBu_2 , unconsumed Cp_2ZrBu_2 reacts with **39a** by ligand exchange or dimerization, and reductive elimination occurs to produce zirconocene(III). Compounds **40a** and **41a** are consumed accordingly, to eventually give Cp_2ZrR ($\text{R}=\text{Bu}$, crotyl and H) and other minor paramagnetic compounds. If **39a** is synthesized directly from zirconocene chloride hydride and crotylmagnesium bromide (in the absence of Cp_2ZrBu_2), the ligand exchange-dimerization-reductive elimination sequence is not the major reaction pathway as no hydrocarbyl ligands other than crotyl are available and it is too coordinatively demanding to allow any significant dimerization (e.g. to form the crotyl analog of **46**). With dimerization being unfavorable, the equilibrium shifts towards the zirconacyclopentane **40a**, which is kinetically stable for days at room temperature, and reduction of zirconium does not occur. The thermal instability of many of the key zirconocene intermediates and the suppression of the reduction pathway by unsaturated ligand (e.g. crotyl), provides an explanation for the necessity of adding the unsaturated reactant in Negishi cyclometalations before the mixture is brought to room temperature.¹

Although it has not been possible to identify all of the decomposition products, the very fact that the $\text{Cp}_2\text{ZrCl}_2/2\text{BuLi}$ reagent contains substantial amounts of Zr^{III} is very important. It explains the reactivity origins of the $\text{Cp}_2\text{ZrCl}_2/2\text{BuLi}$ reagent in dehydropolymerization of silanes^{13,14,77-79} and sheds new light on the reaction mechanism.¹⁴

4.5 Experimental

4.5.1 Materials and Methods

All operations were performed in Schlenk-type glassware on a dual-manifold Schlenk line or in an argon-filled M.Braun Labmaster 130 glovebox (<0.05 ppm H₂O). Argon was purchased from Matheson (prepurified for the glovebox and UHP for the vacuum line) and was used as received. The solvents (protio- and deuterio- benzene, toluene and THF) were dried and stored over Na/K alloy, benzophenone and 18-crown-6 in Teflon-valved bulbs and were vacuum transferred prior to use. Crotyl bromide and CDCl₃ were stored over molecular sieves. Cp₂ZrCl₂, [Cp₂Zr(H)Cl]₂, n-BuLi (1.6M in C₆H₁₄), Mg turnings, MeCH=CHCH₂Br, CH₂=CHCH₂MgBr (1.0M in Et₂O), C₆D₆, C₇D₈, C₄D₈O, and CDCl₃ were purchased from Aldrich and used as received unless stated otherwise.

4.5.2 Physical and Analytical Measurements

Grignard reagents and n-BuLi were titrated with a solution of sec-BuOH in xylene, using 2,2'-biquinoline as an indicator.⁸⁰ NMR spectra were recorded on a Varian Unity 500 (FT, 500 MHz for ¹H) spectrometer. Chemical shifts for ¹H and ¹³C spectra were referenced using internal solvent resonances and are reported relative to tetramethylsilane. EPR spectra were recorded on a Bruker ESP 300E (X-band) spectrometer and were referenced to external DPPH. All samples for spectroscopic measurements were flame-sealed in NMR tubes under vacuum. Quantitative EPR measurements were performed with an external standard of TEMPO of known concentration. A number of experiments were done with different acquisition parameters (modulation and microwave power) to ensure that there was no saturation of the signal. The other acquisition parameters were

compensated for by a system normalization constant and were usually kept constant for both the unknown and the standard sample measurements.

4.5.3.1 Preparation of a Cp_2ZrBu_2 NMR sample

A solution of n-BuLi in hexanes (0.10 mL, 0.25 mmol) was syringed into an NMR tube assembly, consisting of two 5 mL round-bottom flasks fitted with a Teflon valve to which an NMR tube has been fused at an angle of 45°. The solvent was removed under vacuum and the residue was redissolved in toluene-d₈ or THF-d₈ (0.1-0.2 mL). The evaporation-vacuum transfer cycle was repeated twice to remove any residual hexanes and a final fresh portion of toluene-d₈ or THF-d₈ (0.6-0.7 mL) was vacuum transferred into the assembly. Cp_2ZrCl_2 (36.5 mg, 0.125 mmol) was loaded in the side-bulb without coming in contact with BuLi. The apparatus was immersed in a CH_3CN -dry ice bath (-41°C) and the reagents were mixed together and stirred for 30 minutes. The cold, light yellow mother liquor was decanted into the cooled NMR tube. The top part of the tube was washed by touching it with a swab of cotton wool soaked with liquid nitrogen, which caused condensation of the solvent vapors on the inner walls. The sample was then frozen, flame sealed and stored at -41°C until it was loaded in the precooled (-40°C) probe of the NMR instrument.

4.5.3.2 Thermal Decomposition of Cp_2ZrBu_2

The first set of NMR measurements (1D ^1H and ^{13}C , COSY and HMQC) was done at -40°C. After that the sample was warmed to +20°C for 10 minutes and was then cooled down to -10°C to prevent further decomposition. 1D ^1H NMR measurements were performed after every 10 minute freeze-thaw cycle until spectral evidence for considerable changes in the sample composition were apparent. A complete set of NMR experiments (1D ^1H and ^{13}C , TOCSY, COSY, HMQC and NOESY) was then performed. The sample was then subjected to another sequence of the freeze-thaw cycles as described above and

another set 1 and 2D NMR measurements. For each set of 2D NMR experiments the acquisition temperature was different (within the 0 through -40°C range), whereas within a set it was constant. The variation of temperature allowed resolution of some of the cross peaks which were otherwise overlapped. For the sample in THF-d₈ the 2D NMR experiments were done after exposing it to +20°C for 0, 0.5, 4 and 9 hrs; for the sample in toluene-d₈ - after 0, 0.2, 3 and 6 hrs.

EPR: Cp₂ZrBu (toluene, +25 °C), g=1.9961 (t, a(H)=2.4 G, a(Zr)<9 G);

(THF, +25 °C), g=1.9936 br.m.

Cp₂ZrH (THF, +25 °C), g=1.9796 (d, a(H)=7.0 G).

4.5.3.3 Cp₂ZrBu(PMe₃)

A solution of Cp₂ZrBu was prepared as follows: Cp₂ZrCl₂ (730 mg, 2.5 mmol) and a stirring bar were loaded in a Schlenk tube and toluene (3 mL) was vacuum transferred onto the solid. The solution was cooled to -41°C and n-BuLi (2.5 M in hexanes, 2 mL, 5.0 mmol) was added by syringe. The mixture was stirred for 1 h at -41°C. This solution was then slowly warmed to ambient temperature, whereupon the color changed from light yellow to brown and then black. After standing for 24 h at +25°C the product was treated with PMe₃ 1.0 M in toluene (5 mL, 5 mmol). EPR and NMR samples were prepared as described above. Practically no NMR signals were detected.

EPR (toluene, +25 °C), g=1.9955 (d, a(P)=20.6 G, a(Zr)=16.25 G, a(H)<2 G).

4.5.3.4 Preparation of MeCH=CHCH₂MgBr

A simplified modification of the previously reported procedure⁸¹ was used. Magnesium turnings (187 mg, 7.7 mmol) and THF (20 ml) were loaded in a Schlenk flask. The mixture was cooled down to 0°C and MeCH₂=CHCHBr (0.72 mL, 7.0 mmol) was added via a syringe. An exothermic reaction occurred and the mixture turned milky gray. It was then stirred for 24 hrs at room temperature, and the precipitate was allowed to settle.

The clear supernatant solution was transferred to a storage flask, part of it was titrated and the rest was used for further reactions.

4.5.3.5 Preparation of a $\text{Cp}_2\text{Zr}(\text{RCH}=\text{CHCH}_2)\text{H}$ ($\text{R}=\text{Me}$, H) NMR sample

A solution of $(\text{CH}_2=\text{CHCHR})\text{MgBr}$ in Et_2O or THF (0.20 mmol) was syringed into the NMR tube assembly described above. The solvent was removed under vacuum, a small amount of THF- d_8 (0.1-0.2 mL) was vacuum transferred, and the sample was thawed out and stirred at 20°C for 5-10 minutes. The evaporation-vacuum transfer cycle was repeated twice to remove any residual protio solvent and a final fresh portion of THF- d_8 (0.6-0.7 mL) was vacuum transferred into the assembly. $[\text{Cp}_2\text{Zr}(\text{H})\text{Cl}]_2$ (51.5 mg, 0.10 mmol) was loaded in the side-bulb without coming in contact with the Grignard reagent. The apparatus was immersed in a CH_3CN -dry ice bath (-41°C) and the reagents were mixed together and stirred for 2 hours at approximately -20°C. The cold, yellow-orange mother liquor was decanted into the cooled NMR tube, frozen, flame sealed and stored at -196°C until it was loaded in the precooled (-40°C) probe of the NMR instrument. NMR experiments were performed at 0, -20 and -40°C.

4.5.3.6 Quenching with HCl or DCl

A solution of Cp_2ZrBu_2 was prepared as follows: Cp_2ZrCl_2 (730 mg, 2.5 mmol) and a stirring bar were loaded in a Schlenk tube and toluene (3 mL) was vacuum transferred onto the solid. The solution was cooled to -41°C and $n\text{-BuLi}$ in hexanes (2 mL of 1.6 M solution) was added by syringe. The mixture was stirred for 1 h at -41°C. This solution was then slowly warmed to ambient temperature, whereupon the color changed from light yellow to brown and then black. It was left for 24 h at +25°C; then an aliquot of the solution was transferred into a side bulb of the NMR tube assembly, described above, and the solvent was evaporated off. Any residual solvent was removed by two evaporation-vacuum transfer cycles with 0.2 mL portions of C_6D_6 . (In the case of the

DCl/D₂O reagent an additional portion of C₆D₆ was vacuum transferred and left frozen in the NMR tube.) A solution of dry HCl gas in CDCl₃ (sample 1) or DCl in D₂O (sample 2) was syringed into the second side bulb of the NMR tube assembly and frozen. The assembly was put under vacuum and sealed with a Teflon valve. The acid solution was allowed to thaw out and mix with the Cp₂ZrBu₂ decomposition products.

In the case of the HCl/CDCl₃ reagent everything was transferred into the NMR tube, frozen, sealed and used for quantitative NMR measurements of the ratio of Cp versus other hydrocarbon protons.

In the case of the DCl/D₂O reagent the gases and volatile liquids were condensed at -196°C (most of D₂O was left behind) into the NMR tube, which was then flame sealed (samples 1 and 2). The remaining solids were dried in vacuum and dissolved in CDCl₃ (sample 3).

¹³C{H} NMR (C₆D₆, sample 1): 13.91 (s, CH₃), 25.13 (s, CH₂).

¹³C{H} NMR (C₆D₆, sample 2): 13.62 (t, ¹J_{CD}=18.8 Hz, CH₂D), 13.92 (s, CH₃), 25.06 (t, ³J_{CD}=0.4 Hz, CH₂CH₂CH₂D), 25.12 (t, ²J_{CD}=0.8 Hz, CH₂CH₂D).

¹H NMR (CDCl₃, sample 3), 6.37 (s, Cp₂ZrCl₂).

Acknowledgment

Financial support for this work from the NSERC of Canada and Fonds FCAR du Québec is gratefully acknowledged.

References

- (1) Negishi, E.; Takahashi, T. *Acc. Chem. Res.* **1994**, *27*, 124-130 and references cited therein.
- (2) Lewis, D. P.; Whitby, R. J.; Jones, R. V. H. *Tetrahedron* **1995**, *51*, 4541-4550.
- (3) Takahashi, T.; Murakami, M.; Kunishige, M.; Saburi, M.; Uchida, Y.; Kozawa, K.; Uchida, T.; Swanson, D. R.; Negishi, E. *Chem. Lett.* **1989**, 761-764.
- (4) Binger, P.; Muller, P.; Benn, R.; Rufinska, A.; Gabor, B.; Kruger, C.; Betz, P. *Chem. Ber.* **1989**, *122*, 1035-1042.
- (5) Cohen, S. A.; Auburn, P. R.; Bercaw, J. E. *J. Am. Chem. Soc.* **1983**, *105*, 1136-1143.
- (6) Hill, J. E.; Fanwick, P. E.; Rothwell, I. P. *Organometallics* **1992**, *11*, 1771-1773.
- (7) Chang, B.-H.; Tung, H.-S.; Brubaker, C. H. J. *Inorg. Chim. Acta* **1981**, *51*, 143-148.
- (8) Kesti, M. R.; Waymouth, R. M. *Organometallics* **1992**, *11*, 1095-1103.
- (9) Negishi, E.; Cederbaum, F. E.; Takahashi, T. *Tetrahedron Lett.* **1986**, *27*, 2829-2832.
- (10) Negishi, E.; Holmes, S. J.; Tour, J. M.; Miller, J. A.; Cederbaum, F. E.; Swanson, D. R.; Takahashi, T. *J. Am. Chem. Soc.* **1989**, *111*, 3336-3346.
- (11) Hoveyda, A. H.; Morken, J. P. *J. Org. Chem.* **1993**, *58*, 4237-4244.
- (12) Didiuk, M. T.; Johannes, C. W.; Morken, J. P.; Hoveyda, A. H. *J. Am. Chem. Soc.* **1995**, *117*, 7097-7104.
- (13) Dioumaev, V. K.; Harrod, J. F. *Organometallics* **1994**, *13*, 1548-1550.
- (14) Dioumaev, V. K.; Harrod, J. F. *J. Organomet. Chem.* **1996**, *521*, 133-143.
- (15) Dioumaev, V. K.; Harrod, J. F. *Organometallics* **1996**, *15*, 3859-3867.
- (16) Bauer, W.; Clark, T.; Schleyer, P. v. R. *J. Am. Chem. Soc.* **1987**, *109*, 970-977.

- (17) Bauer, W.; Schleyer, P. v. R. *J. Am. Chem. Soc.* **1989**, *111*, 7191-7198.
- (18) Tjaden, E. B.; Casty, G. L.; Stryker, J. M. *J. Am. Chem. Soc.* **1993**, *115*, 9814-9815.
- (19) Tjaden, E. B.; Stryker, J. M. *J. Am. Chem. Soc.* **1993**, *115*, 2083-2085.
- (20) Jeske, G.; Lauke, H.; Mauermann, H.; Swepston, P. N.; Schumann, H.; Marks, T. J. *J. Am. Chem. Soc.* **1985**, *107*, 8091-8103.
- (21) Hanzawa, Y.; Harada, S.; Nishio, R.; Taguchi, T. *Tetrahedron Lett.* **1994**, *35*, 9421-9424.
- (22) Dimmock, P. W.; Whitby, R. J. *J. Chem. Soc., Chem. Commun.* **1994**, 2323-2324.
- (23) Balaich, G. J.; Hill, J. E.; Waratuke, S. A.; Fanwick, P. E.; Rothwell, I. P. *Organometallics* **1995**, *14*, 656-665.
- (24) Gordon, G. J.; Whitby, R. J. *Synlett* **1995**, 77-78.
- (25) McDade, C.; Bercaw, J. E. *J. Organomet. Chem.* **1985**, *279*, 281-315.
- (26) Dorf, U.; Engel, K.; Erker, G. *Angew. Chem. Int. Ed. Engl.* **1982**, *21*, 914-915.
- (27) Vrieze, K. In *Dynamic Nuclear Magnetic Resonance Spectroscopy*; L. M. Jackman and F. A. Cotton, Ed.; Academic: New York, 1975; pp 441.
- (28) Trost, B.; Vranken, D. L. V. *Chem. Rev.* **1996**, *96*, 395-422.
- (29) Schock, L. E.; Marks, T. J. *J. Am. Chem. Soc.* **1988**, *110*, 7701-7715.
- (30) Lee, J. B.; Gajda, G. J.; Schaefer, W. P.; Howard, T. R.; Ikariya, T.; Straus, D. A.; Grubbs, R. H. *J. Am. Chem. Soc.* **1981**, *103*, 7358-7361.
- (31) Seetz, J. W. F. L.; Heisteeg, B. J. J. V. d.; Schat, G.; Akkerman, O. S.; Bickelhaupt, F. *J. Mol. Cat.* **1985**, *28*, 71-83.
- (32) Feldman, J.; Schrock, R. R. *Prog. Inorg. Chem.* **1991**, *39*, 35-42.
- (33) Straus, D. A.; Grubbs, R. H. *J. Mol. Cat.* **1985**, *28*, 9-25.
- (34) Gilliom, L. R.; Grubbs, R. H. *Organometallics* **1986**, *5*, 721-724.
- (35) Kondakov, D.; Negishi, E.-i. *J. Chem. Soc., Chem. Commun.* **1996**, 963-964.

- (36) Klei, E.; Teuben, J. H. *J. Organomet. Chem.* **1980**, *188*, 97-107.
- (37) Van der Weij, F. W.; Scholtens, H.; Teuben, J. H. *J. Organomet. Chem.* **1977**, *127*, 299-304.
- (38) Xin, S.; Harrod, J. F.; Samuel, E. *J. Am. Chem. Soc.* **1994**, *116*, 11562-11563.
- (39) Samuel, E.; Guery, D.; Vebel, J.; Basile, F. *Organometallics* **1985**, *4*, 1073-1077.
- (40) Fakhr, A.; Mugnier, Y.; Gautheron, B.; Laviron, E. *Nouv. J. de Chim.* **1986**, *10*, 601-605.
- (41) Cardin, D. J.; Lappert, M. F.; Raston, C. L. *Chemistry of organo-zirconium and -hafnium compounds.*; Ellis Horwood: Chichester, 1986.
- (42) Samuel, E. *Inorg. Chem.* **1983**, *22*, 2967-2970.
- (43) Samuel, E.; Harrod, J. F. *J. Am. Chem. Soc.* **1984**, *106*, 1859-1860.
- (44) Gauvin, F.; Britten, J.; Samuel, E.; Harrod, J. F. *J. Am. Chem. Soc.* **1992**, *114*, 1489-1491.
- (45) Bazhenova, T. A.; Kulikov, A. V.; Shestakov, A. F.; Shilov, A. E.; Antipin, M. Y.; Lyssenko, K. A.; Struchkov, Y. T.; Makhaev, V. D. *J. Am. Chem. Soc.* **1995**, *117*, 12176-12180.
- (46) Klei, E.; Telgen, J. H.; Teuben, J. H. *J. Organomet. Chem.* **1981**, *209*, 297-307.
- (47) Williams, G. M.; Schwartz, J. *J. Am. Chem. Soc.* **1982**, *104*, 1122-1124.
- (48) Bajgur, C. S.; Jones, S. B.; Petersen, J. L. *Organometallics* **1985**, *4*, 1929-1936.
- (49) Wolf, J. M. d. W.; Meetsma, A.; Teuben, J. H. *Organometallics* **1995**, *14*, 5466-5468.
- (50) Soleil, F.; Choukroun, R.; Frances, J. M. In *XIth International Symposium on Organosilicon Chemistry*; Montpellier, France, 1996; pp .
- (51) Pople, J. A.; Schneider, W. G.; Bernstein, J. H. *High resolution nuclear magnetic resonance.*; McGraw-Hill Book: New York , 1959, pp 236-238.
- (52) Rummens, F. H. A.; Kaslander, L. *Can. J. Spec.* **1972**, *17*, 99-102.

- (53) Breitmaier, E.; Voelter, W. *Carbon-13 NMR spectroscopy: high resolution methods and applications in organic chemistry and biochemistry.*; 3d ed.; VCH: New York, 1987.
- (54) Bothner-By, A. A.; Naar-Colin, C. *J. Am. Chem. Soc.* **1961**, *83*, 231-236.
- (55) Negishi, E.; Nguyen, T.; Maye, J. P.; Choueiri, D.; Suzuki, N.; Takahashi, T. *Chem. Lett.* **1992**, 2367-2370.
- (56) Meier, R. J.; van Doremaele, G. H. J.; Iarlori, S.; Buda, F. *J. Am. Chem. Soc.* **1994**, *116*, 7274-7281.
- (57) Woo, T. K.; Ziegler, T. *Organometallics* **1994**, *13*, 2252-2261.
- (58) Fan, L.; Harrison, D.; Woo, T. K.; Ziegler, T. *Organometallics* **1995**, *14*, 2018-2026.
- (59) Margl, P.; Lohrenz, J. C. W.; Ziegler, T.; Blochl, P. E. *J. Am. Chem. Soc.* **1996**, *118*, 4434-4441.
- (60) Tulip, T. H.; Ibers, J. A. *J. Am. Chem. Soc.* **1979**, *101*, 4201-4211.
- (61) Ohff, A.; Burlakov, V. V.; Rosenthal, U. *J. Mol. Catal., A: Chem.* **1996**, *105*, 103-110.
- (62) McAlister, D. R.; Erwin, D. K.; Bercaw, J. E. *J. Am. Chem. Soc.* **1978**, *100*, 5966-5968.
- (63) Wielstra, Y.; Gambarotta, S.; Meetsma, A.; Spek, A. L. *Organometallics* **1989**, *8*, 2948-2952.
- (64) Miller, F. D.; Sanner, R. D. *Organometallics* **1988**, *7*, 818-825.
- (65) Alt, H.; Rausch, M. D. *J. Am. Chem. Soc.* **1974**, *96*, 5936-5937.
- (66) Gambarotta, S.; Chiang, M. Y. *Organometallics* **1987**, *6*, 897-899.
- (67) Wielstra, Y.; Gambarotta, S.; Meetsma, A.; Boer, J. L. d. *Organometallics* **1989**, *8*, 250-251.
- (68) You, Y.; Wilson, S. R.; Girolami, G. S. *Organometallics* **1994**, *13*, 4655-4657.
- (69) Martin, H. A.; Jellinek, F. *J. Organomet. Chem.* **1968**, *12*, 149-161.

- (70) Bueschges, U.; Chien, J. C. W. *J. Polym. Sci., Polym. Chem. Ed.* **1989**, *27*, 1525-1538.
- (71) Chien, J. C. W.; Salajka, Z.; Dong, S. *Macromolecules* **1992**, *25*, 3199-3203.
- (72) Cam, D.; Sartori, F.; Maldotti, A. *Macromol. Chem. Phys.* **1994**, *195*, 2817-2826.
- (73) Chien, J. C. W.; Wang, B.-P. *J. Polym. Sci., Polym. Chem. Ed.* **1990**, *28*, 15-38.
- (74) Huang, J.; Rempel, G. L. *Prog. Polym. Sci.* **1995**, *20*, 459-526.
- (75) Christ, C. S.; Eyler, J. R.; Richardson, D. E. *J. Am. Chem. Soc.* **1990**, *112*, 4778-4787.
- (76) Diogo, H. P.; de Alencar Simoni, J.; Minas de Piedade, M. E.; Dias, A. R.; Martinho-Simoes, J. A. *J. Am. Chem. Soc.* **1993**, *115*, 2764-2774.
- (77) Corey, J. Y.; Huhmann, J. L.; Zhu, X.-H. *Organometallics* **1993**, *12*, 1121-1130.
- (78) Corey, J. Y.; Zhu, X.-H. *Organometallics* **1992**, *11*, 672-683.
- (79) Shaltout, R. M.; Corey, J. Y. *Tetrahedron* **1995**, *51*, 4309-4320.
- (80) Watson, S. C.; Eastham, J. F. *J. Organomet. Chem.* **1967**, *9*, 165.
- (81) Whitesides, G. M.; Nordlander, J. E.; Roberts, J. D. *Disc. Faraday Soc.* **1962**, *34*, 185-190.
- (82) Gordon, A. J.; Ford, R. A. *The chemist's companion: a handbook of practical data, techniques, and references.*; John Wiley and Sons: New York, 1972, pp 112-113.

CHAPTER 5

A Photo-Redox Mechanism For The Reaction Of 'Cation-like' Zirconocene With Primary Silanes

Vladimir K. Dioumaev and John F. Harrod

Chemistry Department, McGill University, Montreal, QC, Canada, H3A 2K6

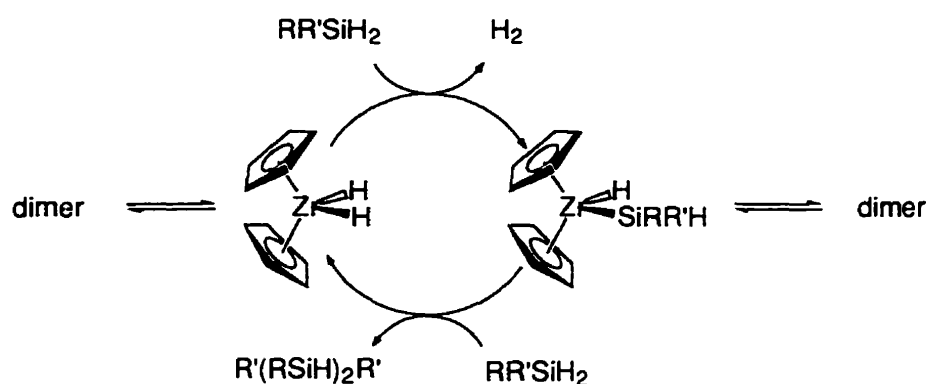
Abstract

A kinetic study of the reaction of $[\text{Cp}_2\text{Zr}(\text{SiHPh})(\mu\text{-H})]_2^{2+}[\text{BBu}_n(\text{C}_6\text{F}_5)_{4-n}]_2^{2-}$ with benzylsilane was carried out using a combination of NMR and EPR spectroscopy. The role of the paramagnetic intermediate, $[\text{Cp}_2\text{Zr}^{\text{III}}]^+[\text{BBu}_n(\text{C}_6\text{F}_5)_{4-n}]^-$, was investigated. The rate law and analysis of intermediates supports a new Zr(IV)/Zr(III) redox mechanism. In this mechanism, Zr(IV) silyl species generate Zr(III) and silyl radicals by homolytic dissociation. Zr(IV)H is regenerated by abstraction of H from SiH by Zr(III) and the cycle is completed by a Zr(IV)H/SiH σ -bond metathesis to regenerate Zr(IV) silyl.

5.1 Introduction

Extensive research efforts have recently been focused on the application of group 4 catalysts for the formation of Si-Si bonds from hydrosilanes.¹⁻⁵ However, the molecular weights of polysilanes formed in dehydrocoupling reactions are still too low or marginal for most industrial applications. An understanding of the mechanisms of such reactions is thus imperative for further progress in this area.

The most widely accepted mechanism, formulated by Tilley and coworkers, consists of a two step σ -bond metathesis process with fixed oxidation state for the metal (Scheme 5-1).⁴⁻⁸ This mechanism is based on kinetic and structural studies of stable, monomeric silyl zircono- and hafnocenes.^{6,7} Both steps in the sequence can be reversible, which explains the depolymerization reaction. Application of the σ -bond metathesis model leads to a significant improvement in the reaction performance.⁵ Thus, the balance of polymerization and depolymerization reactions was discussed in relation to the steric and electronic effects of silane and cyclopentadienyl substituents on the transition states.⁵



Scheme 5-1 The Tilley σ -bond metathesis mechanism for reactions of silanes with early transition silylmetallocenes⁵ ($R = \text{Ar}$ or Alk ; $R' = \text{H}$ or $(\text{SiHR})_n\text{H}$)

The same mechanism was extended to lanthanide and scandium catalysts on the basis of kinetic experiments and nonlocal density functional calculations.⁹⁻¹¹ It should be pointed out that the results of the calculations are not unequivocal since both steps of the sequence were calculated to be endothermic by 3 and 10 kJ mol^{-1} , respectively, and chain scission should prevail. It should be stressed, however, that the calculations were for the special case of SiH_4 and Zr-SiH_3 , while it is well known that substitution can effect SiH bond energies by more than 10 kJ mol^{-1} .

Investigations of titanocene catalysts reported by Harrod *et al* suggest that the reaction mechanism may be more diverse. A number of mono- and dimetallic reduced

Ti(III) and mixed oxidation state Ti(III)/(IV) and Ti(II)/(III) compounds were isolated and structurally characterized.¹²⁻¹⁹ The relation of these compounds to the active catalytic species has not been clearly established, but they are formed in high yields without significant decrease of the catalyst efficiency, and they interconvert with each other. This suggests that M(III) species may be intermediates in the catalytic cycle. In the case of other group 4 metal catalyzed reactions of silanes, germanes, and stannanes, intense colors, indicative of the formation of lower oxidation state species, have also been observed, although no investigation of their role has been reported to date.²⁰⁻²³ A number of reaction schemes have been proposed, including metal-silylene and silyl radical mechanisms.^{1,24,25} A silylene-based mechanism, studied kinetically and with the use of density functional theory, was concluded to be feasible, however, again, the results were not unequivocal.^{25,26} Formation of silylene, although endothermic by 40 kJ mol⁻¹, proceeds with a moderate kinetic barrier and is followed by an exothermic, -48 kJ mol⁻¹, silane insertion step.²⁶ A strong argument against a silylene mechanism is that it requires two available covalent bonds on the metal, whereas Tilley's studies clearly demonstrated catalytic activity with CpCp'M(R)Cl (M = Zr, Hf and R = H, SiR₃ or alkyl) complexes, which have only one reactive bond.^{4,6,7} The possibility of a propagation of polysilicon chains by the coupling of silyl radicals was mentioned briefly in conjunction with the metal-silylene mechanism and was not tested experimentally.²⁵

We have recently reported a new cation-like catalyst for the dehydrocoupling of silanes (Cp'Cp''₂ZrCl₂/2BuLi/B(C₆F₅)₃, where Cp' and Cp'' are substituted cyclopentadienyl, indenyl or tetrahydroindenyl ligands).^{27,28} A significant increase in the molecular weights of polysilanes produced by this catalyst,^{27,28} together with a number of qualitative trends and observations for this and similar catalysts,²⁸⁻³¹ encouraged us to extend our mechanistic studies of this system. A stoichiometric reaction of this catalyst system with silanes yields isolable non-catalytic dimers containing the

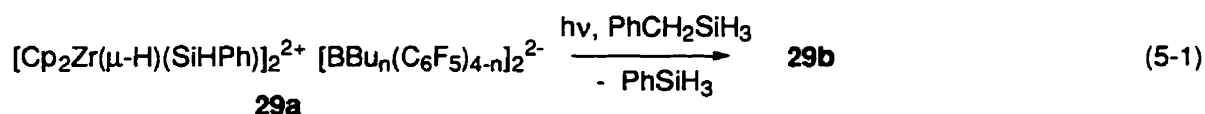
$[\text{Cp}_2\text{Zr}(\text{SiHR})(\mu\text{-H})]_2^{2+}$ ion. This paper describes a kinetic study of a model photochemical metathesis reaction between $[\text{Cp}_2\text{Zr}(\text{SiHPh})(\mu\text{-H})]_2^{2+}$ and $\text{PhCH}_2\text{SiH}_3$.

5.2 Results and Discussion

5.2.1 The Hydrosilane Exchange Reaction

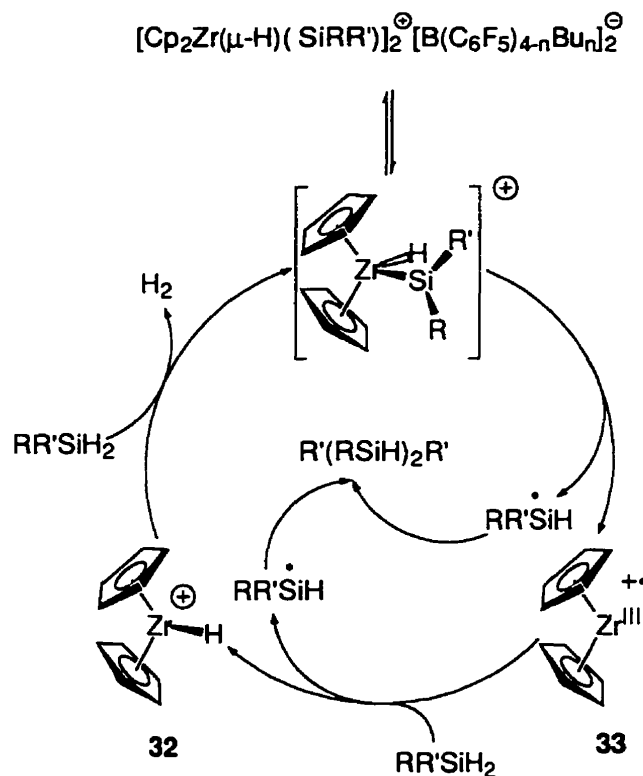
Treatment of $[\text{Cp}_2\text{Zr}(\mu\text{-H})(\text{Si}(\text{H})\text{Ph})]_2^{2+}[\text{BBu}_n(\text{C}_6\text{F}_5)_{4-n}]_2^{2-}$, **29a**, with an excess of benzylsilane at room temperature in toluene solution gives $[\text{Cp}_2\text{Zr}(\mu\text{-H})(\text{Si}(\text{H})\text{CH}_2\text{Ph})]_2^{2+}[\text{BR}'_n(\text{C}_6\text{F}_5)_{4-n}]_2^{2-}$, **29b**, and phenylsilane (eq 5-1).³¹ This reaction only occurs in sun- or regular fluorescent light. Once initiated, the reaction ceases if the light source is removed, showing it to be photochemical rather than photocatalytic. The quantum yield was measured to be 0.96 ± 0.16 . Monochromatic irradiation of the sample revealed that the observed photochemistry is due to light with a wavelength < 440 nm. It gives rise to a number of EPR signals, *vide infra*, and a color change from colorless to yellow-brown. Both the color and the EPR signal intensities depend on the time of exposure and the intensity of the light source. Virtually all of compound **29a** can be converted into NMR silent reduced products by irradiation. However, placing the product in the dark results in a slow reversion to the starting materials.³¹ The decrease in the concentration of **29a** upon irradiation (in the absence of silane) is equal to the concentration changes for **29a** upon the same irradiation time in the presence of benzylsilane. The decay of **29a** in the absence of benzylsilane is not accompanied by formation of any new NMR observable zirconocene species. Interestingly, such a preirradiated sample furnishes **29b** when treated with benzylsilane *in the dark*. The yield of **29b** in this case is at first (2 hours after addition of silane) lower than in the photochemical reaction of **29a** with benzylsilane, but the concentration of **29b** slowly grows in the dark (weeks of storage) until it equals that obtained when the irradiation is performed in the presence of benzylsilane. It is thus clear that the photolysis

of **29a** leads to the formation of an NMR silent compound, which further reacts with benzylsilane to furnish NMR observable **29b**. Unfortunately, the buildup of this intermediate, monitored by EPR measurements, does not quantitatively parallel the decay of **29a**, *vide infra*. Similar behavior was reported by Tilley *et al* for neutral silylzirconocenes and hafnocenes. In his case, the EPR peak intensities were low and the silane exchange reaction proceeded slowly, even in the dark.^{6,32} The quantum yield of 1.0 was attributed to the generation of unidentified reactive species, such as an isomeric M(IV) complex, a long-lived excited state, or a reduced M(III) intermediate. The first explanation was favored as it conforms to the constant oxidation state mechanism, and the relevance of the EPR active species to the catalytic process was questioned.^{6,32} In our case, however, the photochemical transformation is unequivocally a part of the reaction cycle, since no changes occurred in the dark over a period of 1 year, whereas the results of the photochemical reaction are noticeable even after 1 minute of irradiation. In addition, the hypothetical reactive intermediate in this case cannot be "an isomeric M(IV) complex, or a long-lived excited state" because its NMR silent nature does not conform to the former, and its half-life time (at least 2 weeks) is too long for the latter.



The presence of Zr(III) intermediates and the light sensitivity can be rationalized in terms of a redox mechanism, which is illustrated in Scheme 5-2. The principal difference between Scheme 5-1 and this mechanism is the reductive elimination step, which leads to cationic Zr(III) species **33** and silyl radicals. The former abstracts hydrogen from a neutral silane molecule, thus generating another silyl radical. The fate of silyl radicals is either dimerization, which leads to formation of a Si-Si bond or abstraction of hydrogen (or deuterium) from the solvent (toluene-d₈) or another silane molecule.^{33,34} Deuterium

abstraction from toluene, although endothermic by 5-8 kcal/mol, could be driven by its high concentration to give a monodeuterosilane and benzyl radicals. The latter can couple together and terminate the chain. Hydrogen abstraction from another silane molecule is more thermodynamically favorable, but leads to a nonproductive transfer reaction, which can go on in a chainwise fashion. It can be terminated by recombination with a zirconium- or silane-based radical. Recombination with a silyl radical would contribute to the dehydrocoupling reaction while recombination with a Zr(III) leads to a silane exchange reaction. When the solvent is a good proton donor (toluene as compared to benzene), the main route is the formation of $\text{PhSi}(\text{H})_2\text{D}$, whereas in benzene, $(\text{PhSiH}_2)_2$ and $\text{Ph}(\text{H})_2\text{Si-Si}(\text{H})_2(\text{CH}_2\text{Ph})$ are also formed in substantial quantities.

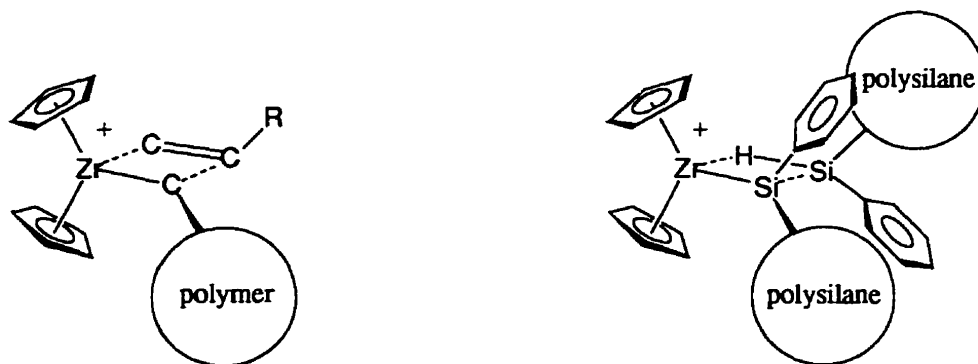


Scheme 5-2 A proposed redox mechanism for reactions of silanes with ‘cation-like’ silylzirconocenes⁶⁰ (R=Ar or Alk; R'=H or (SiHR)_nH)

In a control experiment, photolysis of deuterated $[\text{Cp}_2\text{Zr}(\mu\text{-D})(\text{Si}(\text{D})\text{Ph})_2]^{2+}[\text{BR}'_n(\text{C}_6\text{F}_5)_{4-n}]^{2-}$ was conducted in C_6D_6 in the presence and absence of $\text{PhCH}_2\text{SiH}_3$. In the presence of silane, deuterium and proton labels were scrambled in all silane and disilane products, indicating that the radical transfer from one silane to another occurs much faster than the Si-Si bond formation. In the absence of silane, on the other hand, virtually no scrambling occurred in the disilanes, and retention of deuterium labels in the monosilane products was also much higher. It can be concluded, that in the presence of silanes, the dehydrocoupling proceeds in three stages: (1) generation of silyl radicals; (2) a considerable number of nonproductive chain transfer acts; and (3) recombination of two silyl radicals.

The result of adding redox steps to the catalytic cycle (Scheme 5-2 vs. 5-1) is that the reaction avoids an unfavorable transition state in which a polysilyl ligand coordinated to zirconium is required to react with free polysilane. Such a transition state is inevitable in the constant oxidation state mechanism at high silane conversions, but is severely sterically congested for randomly coiled polysilane chains. The steric demands of metallocene catalysts have been intensively studied for the Ziegler-Natta polymerization where the chain growth occurs via a transition state with an olefin approaching a Zr-polyolefin bond.^{35,36} The only olefins which can sterically fit in the metallocene wedge in such a transition state are ethylene and propylene. Higher terminal and cyclic olefins can be copolymerized with ethylene or propylene but their incorporation in the polymer is not high and rapidly decreases with an increase in the monomer size.^{35,37} Bulkier monomers, e.g. styrene, require nonmetallocene catalysts.³⁵ It should be noted that the per unit steric demands of poly(phenylsilane) are substantially higher than polystyrene as the former has a phenyl substituent on every atom of the polymer backbone. Such considerations cast serious doubts on the possibility of fitting two polysilane random coils in the coordination sphere of zirconocene (Scheme 5-3). In the case of the proposed redox mechanism (Scheme 5-2), the only σ -bond metathesis step is the reaction of $[\text{Cp}_2\text{ZrH}]^+[\text{BBu}_n(\text{C}_6\text{F}_5)_{4-n}]^-$, **32**, with

polysilane. This step is more feasible as a bulky polysilane approaches a sterically noncrowded Zr-H bond.



hydrogen atoms are not shown

Scheme 5-3 A schematic representation of the σ -bond metathesis transition states for the polymerizations of propylene and phenylsilane respectively. The metallocene catalysts are too sterically congested to accommodate two bulky ligands in the metallocene wedge, which casts serious doubts on the possibility of a transition state with two polysilane random coils in the coordination sphere of zirconium

The proposed redox mechanism has some analogies in the literature. Oxidative addition - reductive elimination cycles for zirconocene³⁸⁻⁴³ and titanocene⁴⁴⁻⁴⁸ catalysts are well documented. Silicon radicals are also known intermediates in catalytic cycles.^{34,49,50}

5.2.2 Kinetic Study Using NMR Spectroscopy

A kinetic study was carried out on a model reaction of **29a** with benzylsilane under pseudo-first-order rate conditions for silane (eq 5-1). In the first series of experiments, the concentration of **29a** was varied from 0.0038 to 0.00095 M and the initial concentration of benzylsilane was 0.37 M. Plots of the $\ln(-[29a]_0 d[29a]/dt)$ vs. $\ln([29a])$, although somewhat scattered, show first-order behavior in zirconocene (Figure 5-1). The scattering of the data points can be attributed to the poor precision of fitting a polynomial to a small data set. The goodness of fit can be improved significantly by using a linear fitting

procedure, e.g. imposing the first-order constraints from the very beginning and producing linear plots of $\ln([29a]/[29a]_0)$ vs. time and k_{observed} vs. $1/[29a]_0$ (Figures 5-2a and 5-2b).

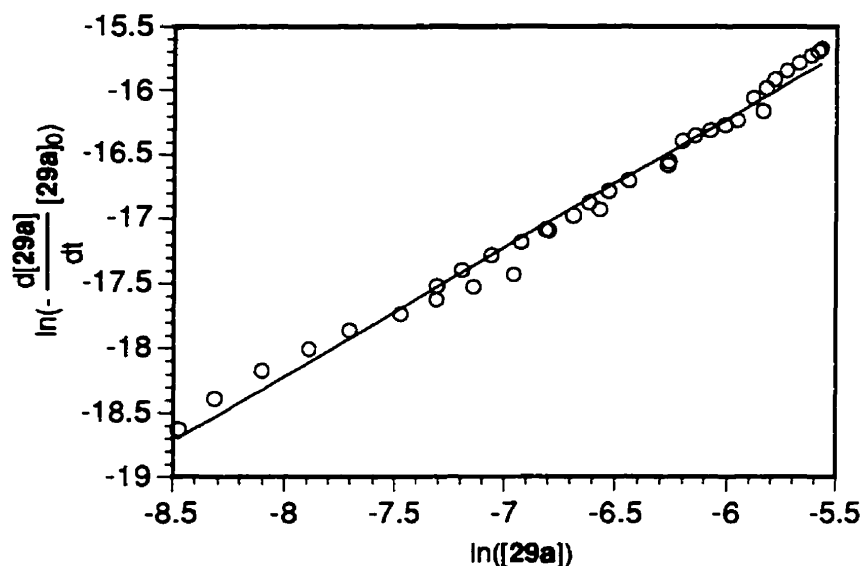


Figure 5-1. A kinetic plot for the reaction of **29a** with benzylosilane as a function of rate vs. concentration of **29a**, which shows a first-order behavior in **29a**. Initial $[\text{PhCH}_2\text{SiH}_3] = 0.37 \text{ M}$. The line $y = -10.2(0.3) + 0.99(0.04)x$ represents the least-squares fit to the data points (the quantities in parentheses are the 95% confidence limits; $R^2 = 0.987$).

Another series of experiments was performed with a constant starting concentration of **29a**, 0.0039 M, while varying the concentration of benzylosilane from 1.20 to 0.10 M. The $\ln(-\text{initial rate})$ vs. $\ln([\text{PhCH}_2\text{SiH}_3])$ plot exhibits zero-order in silane (Figure 5-3).

Finally, a series of identical samples ($[29a] = 0.0057 \text{ M}$; $[\text{PhCH}_2\text{SiH}_3] = 0.14 \text{ M}$) were used for kinetic measurements, where the light intensity was varied by means of neutral density filters. The reaction rate shows a first-order dependence on the light intensity (Figure 5-4, the slope of the log-log plot is $0.89(0.05)$). A combination of all these experiments yields the rate law of eq 5-2.

$$d[29a]/dt = -k(10^{-a})[\text{PhCH}_2\text{SiH}_3]^0[29a]/[29a]_0 = -k_{\text{observed}}[29a] \quad (5-2)$$

$[29a]_0$ - concentration at time = 0,

a - optical density of a filter

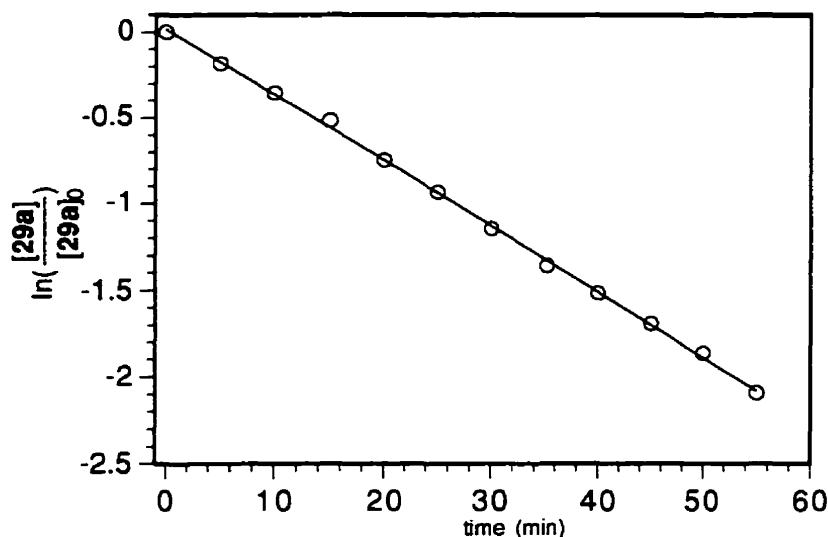


Figure 5-2a. Kinetic plot for the reaction of **29a** with benzylsilane as a function of concentration of **29a** vs. time, which shows a first-order behavior in **[29a]**. Initial **[29a]** = 0.00095 M; **[PhCH₂SiH₃]** = 0.37 M. The line $y = 0.02(0.02) - 3.81(0.07) \times 10^{-2}x$ represents the least-squares fit to the data points (the quantities in parentheses are the 95% confidence limits; $R^2 = 0.999$).

A model sequence of reactions, which explains the observed products and intermediates, is shown in Scheme 5-4. These reactions are either directly observed, or based on reasonable precedents. They furnish a system of nonlinear differential equations, which can not be solved analytically with the given number of measurable variables. Fortunately, the zero-order behavior in benzylsilane suggests that the rate limiting step occurs within the first two stages of the sequence, which significantly simplifies its analytical treatment. The concentration of PhSiH_2^{\bullet} is negligible, hence the conversion of

M_1 into $[\text{Cp}_2\text{Zr}^{\text{III}}] + [\text{BBu}_n(\text{C}_6\text{F}_5)_{4-n}]^-$, **33**, can be considered irreversible. The first two steps of Scheme 5-4, reversible dissociation of **29a** and homolysis of the Zr-Si bond, are virtually independent of the rest of the sequence. The only reverse link between these two parts of the scheme is the reaction of **32** with PhSiH_3 . The rate of this reaction can be considered negligible due to the extremely low concentration of PhSiH_3 compared to $\text{PhCH}_2\text{SiH}_3$. The rate of disappearance of **29a** can then be described in a simplified manner (eq 5-3).

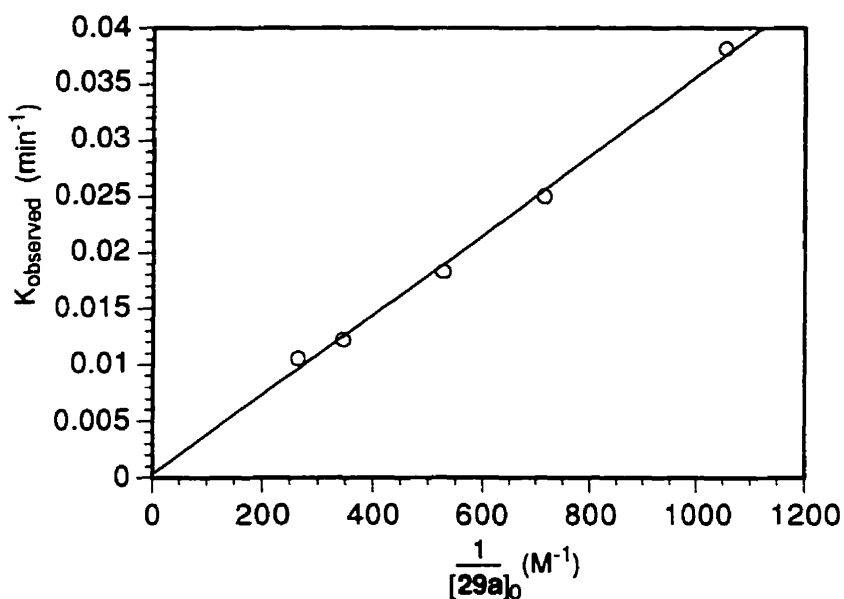
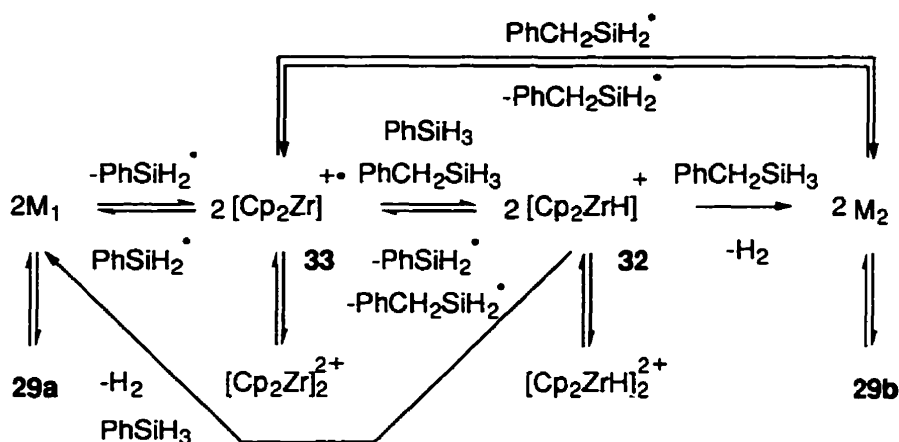


Figure 5-2b. Kinetic plot for the reaction of **29a** with benzylsilane as a function of k_{observed} vs. initial concentration of **29a**, which shows an inverse dependence on $[\text{29a}]_0$. Initial $[\text{PhCH}_2\text{SiH}_3] = 0.37 \text{ M}$. The line $y = 0.000(0.001) + 3.5(0.2) \times 10^{-5}x$ represents the least-squares fit to the data points (the quantities in parentheses are the 95% confidence limits; $R^2 = 0.996$).

A critical question with respect to eq 5-3 is the step, or steps, which involve light. Although dimeric zirconocene hydrides undergo dissociation to monomer and reduction upon photolysis, the actual photolytic step is unknown.⁵¹ To the best of our knowledge



Scheme 5-4 A complete kinetic description of the reaction of **29a** with benzylsilane

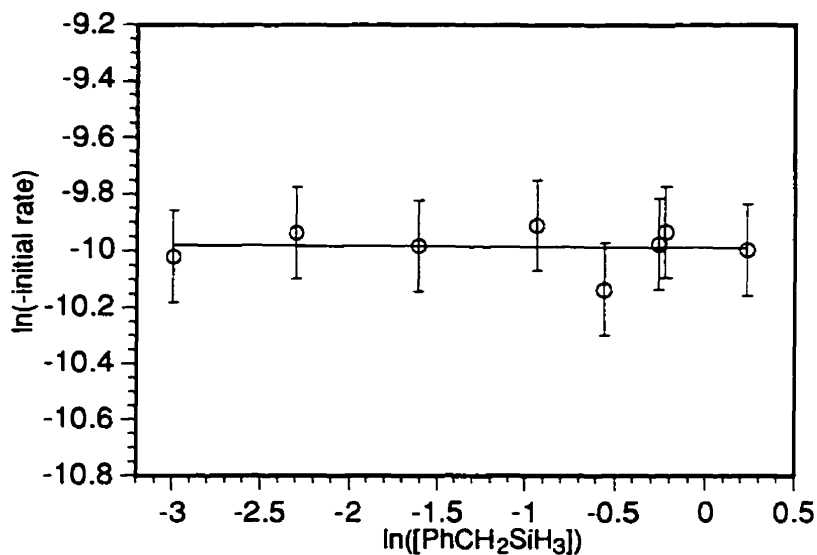
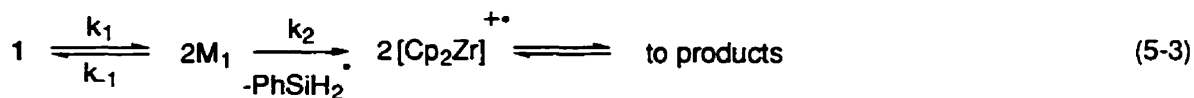


Figure 5-3. Kinetic plot for the reaction of **29a** with benzylsilane as a function of initial rate vs. concentration of benzylsilane, which shows a zero-order behavior in $[PhCH_2SiH_3]$. Initial $[PhCH_2SiH_3] = 0.0039$ M. The bars indicate an $\ln(5\%) = 1.6\%$ error. The line $y = -9.99(0.07) - 0.00(0.04)x$ represents the least-squares fit to the data points (the quantities in parentheses are the 95% confidence limits).



M_1 = monomer of **29a**

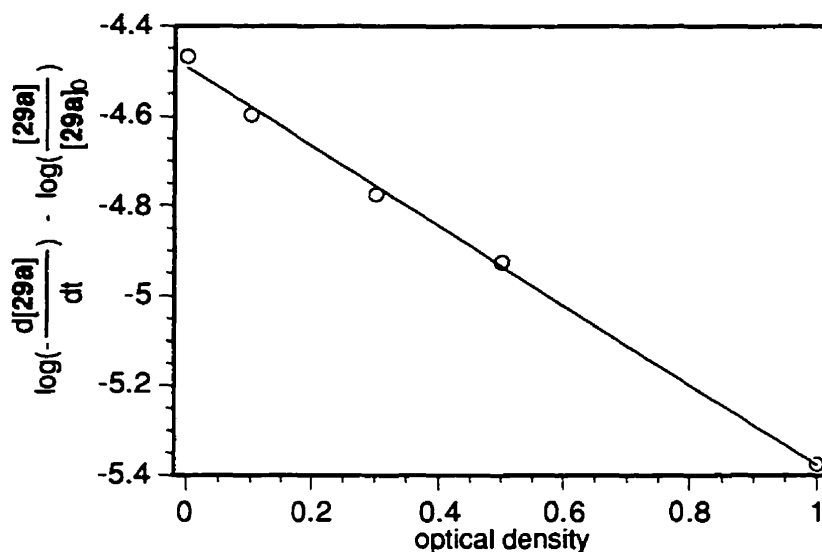


Figure 5-4. Kinetic plot for the reaction of **29a** with benzylsilane as a function of rate vs. optical density of the filters, which shows a first-order behavior in light intensity. Initial $[29a] = 0.0057$ M; $[\text{PhCH}_2\text{SiH}_3] = 0.14$ M. The line $y = -4.49(0.02) - 0.89(0.05)x$ represents the least-squares fit to the data points (the quantities in parentheses are the 95% confidence limits; $R^2 = 0.997$).

there are no reported precedents for any photochemical cleavage of zirconocene hydride dimers, but photolytic reductive elimination for monomeric early transition metallocenes is well documented.⁵²⁻⁵⁶ Besides, photochemical reaction of silylhafnocenes with hydrosilanes was also reported for monomeric starting compounds.³² However, if the reductive elimination step is photochemical, an analytical treatment of the system shown in

equation 5-3 (see experimental part for detail) gives a rate law which does not conform with the experimental data (eq 5-11 vs. 5-2), whereas the first step being photochemical does (eq 5-7 vs. 5-2). The quantum yield also points to the first step being photochemical. Indeed, if the two monomer molecules, produced in the photolytic dissociation step have similar energy due to a fast thermal equilibration, both of them would further participate in the reaction and furnish **29b**. Thus, absorption of a single photon per dimer should be observed (quantum yield = 1), whereas a photochemical reductive elimination should result in a one photon absorption per monomer, i.e. two photons per dimer molecule (quantum yield = 0.5). Further, if the monomer-dimer equilibrium were a fast thermal reaction, one would expect the presence of both monomers (derived from **29a** and **29b**) in the reaction mixture and formation of the mixed zirconocene dimer, $[\text{Cp}_2\text{Zr}(\text{Si}(\text{H})\text{Ph})(\mu\text{-H})_2(\text{Si}(\text{H})\text{CH}_2\text{Ph})\text{ZrCp}_2]^{2+}[\text{BR}'_n(\text{C}_6\text{F}_5)_{4-n}]_2^{2-}$, accordingly. The absence of mixed dimers lends additional support to the assignment of the first step as photochemical.

5.2.3 Semiquantitative Kinetic Study Followed by EPR Spectroscopy

A pure sample of **29a** in toluene-*d*₈ was photolyzed and the build up of Zr(III) concentration was monitored by EPR spectroscopy. The plot of the integral intensity of the EPR peaks vs. photolysis time is roughly linear at the beginning, and the production rate for Zr(III) species was calculated to be close to the rates for reaction of **29a** with benzylsilane. This illustrates that the reductive elimination step is not a minor side reaction but is an essential part of the reaction mechanism. However, at longer photolysis periods the generation of EPR observable Zr(III) species reaches saturation, and the buildup of EPR signals no longer matches the decrease in the NMR measurable concentration of **29a**. The apparent lack of mass balance in this system can be explained by a reversible formation of $[\text{Zr}(\text{III})]_n$, where *n* is an even number, most likely 2. Such a compound has an even number of electron spins and can be diamagnetic, but a fast equilibrium with the

paramagnetic monomer would broaden any NMR resonances and render them poorly detectable. Indeed, when a sample of **29a** was photolyzed for a long time, extremely broad and featureless NMR resonances were observed.³¹ In addition, reversible formation of a dimer (or any inert $[\text{Zr(III)}]_n$) explains why the reaction of benzylsilane with a preirradiated sample of **29a** is much slower than the reaction of benzylsilane with **29a** upon irradiation, *vide supra*.

Such a monomer-dimer equilibrium for **33** can frustrate any EPR-based quantitative measurements. For example, although the oxidative addition step, which follows reductive elimination (Scheme 5-2), can be directly observed as a decay of the EPR signals of **33**, it was not possible to evaluate it quantitatively. Compound **33** is present in two forms, as tight- and solvent separated ion pairs.³¹ Their signals appear as an overlapped and unresolved pair of EPR singlets, $g=1.9964$ $a(\text{Zr})=7.1$ G and $g=1.9972$ $a(\text{Zr})=12.3$ G, which interconvert with each other and gradually decay with different rates. In addition, there is another weak unresolved signal in the spectrum, $g=2.0036$, possibly due to the silane radicals,³¹ whose decay also influences the intensity of the signals of **33**. An attempt was made to measure an overall decay rate, assuming that both forms of **33** obey the same rate law with similar rate constants. Any contribution from the line at $g=2.0036$ was assumed to be negligible as its intensity is weak. The plots of $\ln([\text{Zr(III)}])$ vs. time for the reaction of **29a** with benzylsilane exhibited linear behavior as expected for a first-order reaction in $[\text{Zr(III)}]$, and the goodness of fit within any given experiment was acceptable. However, $\ln(\text{rate})$ vs. $\ln([\text{Zr(III)}])$ or $\ln(\text{rate})$ vs. $\ln([\text{PhCH}_2\text{SiH}_3])$ plots, obtained from a combination of different samples and experiments, showed poor reproducibility and did not allow any conclusions to be drawn. The deviations of the rate constants, obtained from the same sample in different trials, are statistically significant, which means that the starting assumptions are invalid, mostly due to the reversible formation of dimer **33**, and quantitative kinetic study by the present method is not possible.

5.3 Conclusions

The dimeric zirconocene hydride with a cation-like silylium ligand, **29a**, reductively eliminates a silyl radical upon exposure to light of $\lambda < 440$ nm, producing paramagnetic **33**. Intermediate **33** further reacts with benzylsilane to furnish **29b**. An overall transformation of **29a** into **29b** is explained in terms of a new redox mechanism (Scheme 5-2).

The quantum yield and the rate law observed by NMR spectroscopy support the first step of the redox mechanism - photolytic dissociation of **29a**, which in turn undergoes a fast reductive elimination and forms **33**. This reductive elimination step is supported by quantitative NMR and qualitative EPR measurements, but quantitative EPR analysis is frustrated by a variety of parallel processes and can not be used to test the underlying hypotheses.

The presence of all postulated reaction intermediates was proved spectroscopically. Compounds **29a** and **29b** have been exhaustively characterized by multinuclear, multidimensional NMR spectroscopy.²⁹ Compounds **32** and **33** were trapped with trimethylphosphine, as described elsewhere, and their adducts were characterized by NMR and EPR spectroscopy, respectively.³¹ Compound **33** was also characterized *in situ* by EPR spectroscopy.³¹

The two mechanisms (Scheme 5-1 and 5-3), despite their differences, have one common step which is the constant oxidation state σ -bond metathesis reaction (the bottom part of the cycle in Scheme 5-1 and the conversion of **32** to **29b** in Scheme 5-2). It is conceivable that under some circumstances these steps could be a bottle neck and the observed rate law for the entire cycle would thus reveal exclusively the information on the constant oxidation state reaction. In this case, the two mechanisms would be kinetically indistinguishable, which might explain the seeming disparity between the present results

and the kinetic study reported by Tilley *et al.*^{6,7} The other possible explanation is that the introduction of a positive charge on the Zr-Si complex radically alters its reactivity pattern.

5.4 Experimental Section

5.4.1 Materials and Methods

All operations were performed in Schlenk-type glassware on a dual-manifold Schlenk line, equipped with flexible stainless steel tubing, or in an argon-filled M.Braun Labmaster 130 glovebox (<0.05 ppm H₂O). Argon was purchased from Matheson (prepurified for the glovebox and UHP for the vacuum line) and used as received. Hydrocarbon solvents (protio- and deuterio- toluene) were distilled from Na/K alloy-benzophenone and stored in the glovebox. Silanes (PhSiH₃ and PhCH₂SiH₃) were synthesized according to the literature,⁵⁷ degassed, and stored over molecular sieves in the glovebox. Cp₂ZrCl₂, C₇D₈, C₆F₅Br, PhC(O)Ph, BCl₃ (1.0 M in heptane), n-BuLi (1.6 M in hexanes) were purchased from Aldrich and used as received, unless stated otherwise. Compound **29a** was prepared by a previously published method.^{27,29}

5.4.2 Physical and Analytical Measurements

NMR spectra were recorded on a Varian Unity 500 (FT, 500 MHz for ¹H) spectrometer. Chemical shifts for ¹H spectra were referenced using internal solvent references and are reported relative to tetramethylsilane. Quantitative NMR measurements were performed using residual solvent protons as internal references. Long repetition delay, 15 s (at least 5T₁), was used to ensure complete magnetization relaxation and correct peak integration. EPR spectra were recorded on a Bruker ESP 300E (X-band) spectrometer and were referenced to external DPPH. Quantitative EPR measurements were performed with an external standard of TEMPO of known concentration. A number of

experiments were done with different acquisition parameters (modulation and microwave power) to ensure that there was no saturation of the signal. The other acquisition parameters were compensated for by a system normalization constant and were usually kept constant for both the unknown and the standard sample measurements.

For the quantitative photochemical experiments, a general purpose 9 W compact daylight fluorescent bulb (Sylvania, model number F9DTT/27K) with an output primarily in the 300 through 750 nm spectral region was used.⁵⁸ The lamp was placed in a homemade housing, equipped with a holder for an NMR tube (65 mm from the light source) and a window for a photofilter. The entire assembly was compact enough to fit in the thermostat of a gas chromatograph (HP 5890), which was used to control the reaction temperature to an accuracy of ± 0.3 °C. For quantum yield measurements, the light intensity entering the photolysis cell (an NMR tube) through the bandpass filter (Corning CS-7-59) was determined by using the Reinecke's salt actinometer.⁵⁸ A typical photon flux into the photochemical cell was $(2.6 \pm 0.4) \cdot 10^{-5}$ einstein \cdot L⁻¹ \cdot min⁻¹.

5.4.3.1 Reactions Followed by NMR

All NMR samples were prepared in an NMR-tube assembly, consisting of an NMR tube fused to a Teflon valve. The samples were prepared in semidarkness, in the glovebox. A fractional dilution of stock solutions of **29a** and benzylsilane in toluene-*d*₈ was used to ensure concentration accuracy. The samples were loaded in the NMR-tube assembly, removed from the glovebox, frozen, evacuated and flame sealed in the dark. The following series were prepared:

#1: [PhCH₂SiH₃] = 0.37 M; [**29a**] = 0.0038, 0.0029, 0.0019, 0.0014 and 0.00095 M

#2: [**29a**] = 0.0039 M; [PhCH₂SiH₃] = 1.20, 0.80, 0.60, 0.40, 0.20 and 0.10 M

#3: Five identical samples of [**29a**] = 0.0057 M; [PhCH₂SiH₃] = 0.14 M.

The samples were kept in the thermostat for 10 minutes prior to irradiation (series #1 at 27.7 °C, #2 at 26.7 °C and #3 at 30.0 °C), then photolyzed for 5 minutes before

transfer to the NMR probe, which was kept at the same temperature. No changes were detected in the sample when the irradiation was off. This irradiation-measurement cycle was repeated for every kinetic data point. The data was then plotted as concentration vs. time and a second-order polynomial fit procedure was applied to obtain the rate information.

5.4.3.2 Reactions Followed by EPR

The photolytic EPR experiments were done either with the 9 W Sylvania lamp described above or with a Hg-Xe high pressure arc, Hanovia 977B0010 520310, equipped with a water jacket to filter IR radiation, and a GM 252 Schoeffel Monochromator (Schoeffel Instruments Co., Westwood, N.J., USA). The samples were prepared as described above and the concentrations were verified by NMR measurements. The two lamps, and different irradiation periods, were used to generate different concentrations of Zr(III) species. The decay of the EPR signals was monitored and the concentration was plotted vs. time. A second-order polynomial fit was applied to obtain the rate values. The following series was prepared:

[**29a**] = 0.0039 M; [PhCH₂SiH₃] = 0.80, 0.60, 0.50, 0.40, 0.20, 0.10 and 0.05 M

5.4.3.3 Rate Law

If the first step is the rate limiting photochemical reaction, the overall rate law is simply the rate of the dimer dissociation:

$$d[\mathbf{29a}]/dt = -\Phi(10^{-a})I_{\mathbf{29a}^*} \quad (5-4)$$

where Φ is the quantum yield, a the optical density of a filter, and $I_{\mathbf{29a}^*}$ the fraction of visible light ($\lambda < 440$ nm), absorbed by **29a**.

$$I_{\mathbf{29a}^*} = I\epsilon_{\mathbf{29a}}[\mathbf{29a}]/\sum \epsilon_i[i] \quad (5-5)$$

where ϵ_i is the extinction coefficient of the i th component and I is the fraction of visible light absorbed by the sample. Since the only compounds, which have significant

concentrations in the mixture and absorption bands in the specified spectral region, are **29a** and **29b** ($[29a] + [29b] \equiv [29a]_0$), and since they have similar extinction coefficients:

$$I_{29a}^* \equiv I[29a]/([29a] + [29b]) \equiv I[29a]/[29a]_0 \quad (5-6)$$

Finally,

$$d[29a]/dt = -\Phi(10^{-a})I[29a]/[29a]_0 \quad (5-7)$$

If the second step is the rate limiting photochemical reaction, the system shown in eq 3 can be treated as a classical pre-equilibrium case.⁵⁹

$$k_1[29a] = k_{-1}[M_1]^2, \text{ or } M_1 = (k_1[29a]/k_{-1})^{0.5} \quad (5-8)$$

$$\text{and } d[M_1]/dt = -\Phi(10^{-a})I[M_1]/[29a]_0 \quad (5-9)$$

Since there are two molecules of M_1 produced from each molecule of **29a**:

$$d[29a]/dt = -0.5d[M_1]/dt \quad (5-10)$$

Combining equations 5-8, 5-9 and 5-10 furnishes

$$d[29a]/dt = -0.5\Phi(10^{-a})I[M_1]/[29a]_0 = -0.5\Phi(10^{-a})I(k_1/k_{-1})^{0.5}[29a]^{0.5}/[29a]_0 \quad (5-11)$$

Acknowledgment

Financial support for this work from the NSERC of Canada and Fonds FCAR du Québec is gratefully acknowledged.

References

- (1) Harrod, J. F. In *Inorganic and Organometallic Polymers*; M. Zeldin; K. J. Wynne and H. R. Allcock, Ed.; American Chemical Society: Washington DC, 1988; pp 89-100.
- (2) Harrod, J. F.; Mu, Y.; Samuel, E. *Polyhedron* **1991**, *10*, 1239-1245.
- (3) Harrod, J. F. In *Inorganic and Organometallic Polymers with Special Properties*; R. M. Laine, Ed.; Kluwer Academic: Dordrecht, 1992; Vol. 206; pp 87-98.
- (4) Tilley, T. D. *Comments Inorg. Chem.* **1990**, *10*, 37-51.
- (5) Tilley, T. D. *Acc. Chem. Res.* **1993**, *26*, 22-29.
- (6) Woo, H.-G.; Tilley, T. D. *J. Am. Chem. Soc.* **1989**, *111*, 3757-3758.
- (7) Woo, H.-G.; Tilley, T. D. *J. Am. Chem. Soc.* **1989**, *111*, 8043-8044.
- (8) Tilley, T. D.; Woo, H.-G. *Polym. Prepr., Am. Chem. Soc. Div. Polym. Chem.* **1990**, *31*, 228-229.
- (9) Forsyth, C. M.; Nolan, S. P.; Marks, T. J. *Organometallics* **1991**, *10*, 2543-2545.
- (10) Radu, N. S.; Tilley, T. D. *J. Am. Chem. Soc.* **1995**, *117*, 5863-5864.
- (11) Ziegler, T.; Folga, E. *J. Organomet. Chem.* **1994**, *478*, 57-65.
- (12) Samuel, E.; Harrod, J. F. *J. Am. Chem. Soc.* **1984**, *106*, 1859-1860.
- (13) Aitken, C. T.; Harrod, J. F.; Samuel, E. *J. Am. Chem. Soc.* **1986**, *108*, 4059-4066.
- (14) Samuel, E.; Mu, Y.; Harrod, J. F.; Dromzee, Y.; Jeannin, Y. *J. Am. Chem. Soc.* **1990**, *112*, 3435-3439.
- (15) Gauvin, F.; Britten, J.; Samuel, E.; Harrod, J. F. *J. Am. Chem. Soc.* **1992**, *114*, 1489-1491.
- (16) Harrod, J. F.; Mu, Y.; Samuel, E. *Can. J. Chem.* **1992**, *70*, 2980-2984.
- (17) Britten, J.; Mu, Y.; Harrod, J. F.; Polowin, J.; Baird, M. C.; Samuel, E. *Organometallics* **1993**, *12*, 2672-2676.

- (18) Woo, H. G.; Harrod, J. F.; Henique, J.; Samuel, E. *Organometallics* **1993**, *12*, 2883-2885.
- (19) Xin, S.; Harrod, J. F.; Samuel, E. *J. Am. Chem. Soc.* **1994**, *116*, 11562-11563.
- (20) Aitken, C.; Harrod, J. F.; Samuel, E. *Can. J. Chem.* **1986**, *64*, 1677-1679.
- (21) Corey, J. Y.; Zhu, X.-H. *Organometallics* **1992**, *11*, 672-683.
- (22) Coutant, B.; Quignard, F.; Choplin, A. *J. Chem. Soc., Chem. Commun.* **1995**, 137-138.
- (23) Imori, T.; Lu, V.; Cai, H.; Tilley, T. D. *J. Am. Chem. Soc.* **1995**, *117*, 9931-9940.
- (24) Aitken, C.; Harrod, J. F.; Gill, U. S. *Can. J. Chem.* **1987**, *65*, 1804-1809.
- (25) Harrod, J. F.; Yun, S. S. *Organometallics* **1987**, *6*, 1381-1387.
- (26) Harrod, J. F.; Ziegler, T.; Tschinke, V. *Organometallics* **1990**, *9*, 897-902.
- (27) Dioumaev, V. K.; Harrod, J. F. *Organometallics* **1994**, *13*, 1548-1550.
- (28) Dioumaev, V. K.; Harrod, J. F. *J. Organomet. Chem.* **1996**, *521*, 133-143.
- (29) Dioumaev, V. K.; Harrod, J. F. *Organometallics* **1996**, *15*, 3859-3867.
- (30) Dioumaev, V. K.; Harrod, J. F., submitted to *Organometallics*.
- (31) Dioumaev, V. K.; Harrod, J. F., submitted to *Organometallics*.
- (32) Woo, H.-G.; Heyn, R. H.; Tilley, T. D. *J. Am. Chem. Soc.* **1992**, *114*, 5698-5707.
- (33) Gaspar, P. P.; Haizlip, A. D.; Choo, K. Y. *J. Am. Chem. Soc.* **1972**, *94*, 9032-9037.
- (34) Chatgililoglu, C. *Chem. Rev.* **1995**, *95*, 1229-1251.
- (35) Möhring, P. C.; Coville, N. J. *J. Organomet. Chem.* **1994**, *479*, 1-29.
- (36) Huang, J.; Rempel, G. L. *Prog. Polym. Sci.* **1995**, *20*, 459-526.
- (37) Kaminsky, W.; Spiehl, R. *Makromol. Chem.* **1989**, *190*, 515-526.
- (38) Knight, K. S.; Waymouth, R. M. *J. Am. Chem. Soc.* **1991**, *113*, 6268-6270.

- (39) Uesaka, N.; Mori, M.; Okamura, K.; Date, T. *J. Org. Chem.* **1994**, *59*, 4542-4547.
- (40) Knight, K. S.; Waymouth, R. M. *Organometallics* **1994**, *13*, 2575-2577.
- (41) Wischmeyer, U.; Knight, K. S.; Waymouth, R. M. *Tetrahedron Lett.* **1992**, *33*, 7735-7738.
- (42) Knight, K. S.; Wang, D.; Waymouth, R. M.; Ziller, J. J. *Am. Chem. Soc.* **1994**, *116*, 1845-1854.
- (43) Kablaoui, N. M.; Buchwald, S. L. *J. Am. Chem. Soc.* **1996**, *118*, 3182-3191.
- (44) Berk, S. C.; Grossman, R. B.; Buchwald, S. L. *J. Am. Chem. Soc.* **1994**, *116*, 8593-8601.
- (45) Berk, S. C.; Grossman, R. B.; Buchwald, S. L. *J. Am. Chem. Soc.* **1993**, *115*, 4912-4913.
- (46) Fischer, J. M.; Piers, W. E.; Batchilder, S. D. P.; Zaworotko, M. J. *J. Am. Chem. Soc.* **1996**, *118*, 283-284.
- (47) Kablaoui, N. M.; Hicks, F. A.; Buchwald, S. L. *J. Am. Chem. Soc.* **1996**, *118*, 5818-5819.
- (48) Cavallaro, C. L.; Schwartz, J. J. *J. Org. Chem.* **1996**, *61*, 3863-3864.
- (49) Walsh, R. *Acc. Chem. Res.* **1981**, *14*, 246-252.
- (50) Dang, H.-S.; Roberts, B. R. *Tetrahedron Lett.* **1995**, *36*, 2875-2878.
- (51) Bajgur, C. S.; Jones, S. B.; Petersen, J. L. *Organometallics* **1985**, *4*, 1929-1936.
- (52) Geoffroy, G. L.; Wrighton, M. S. In *Organometallic Photochemistry* AP: New York, 1979; pp 300-325.
- (53) Alt, H.; Rausch, M. D. *J. Am. Chem. Soc.* **1974**, *96*, 5936-5937.
- (54) Wielstra, Y.; Gambarotta, S.; Meetsma, A.; Spek, A. L. *Organometallics* **1989**, *8*, 2948-2952.
- (55) Miller, F. D.; Sanner, R. D. *Organometallics* **1988**, *7*, 818-825.

- (56) Cardin, D. J.; Lappert, M. F.; Raston, C. L. *Chemistry of organo-zirconium and -hafnium compounds*.; Ellis Horwood: Chichester, 1986.
- (57) Finholt, A. E.; Bond, A. C. J.; Wilzbach, K. E.; Schlesinger, H. I. *J. Am. Chem. Soc.* **1947**, *69*, 2692-2696.
- (58) Rabek, J. F. *Experimental Methods in Photochemistry and Photophysics*.; Wiley: Chichester, 1982, pp 55.
- (59) Atkins, P. W. In *Physical chemistry*; 3rd ed. W. H. Freeman: New York, 1986; pp 705-706.
- (60) Dioumaev, V. K.; Harrod, J. F. *XXVIII Organosilicon Symposium*; Gainesville, Florida, USA, 1995, pp B-23.

CHAPTER 6

A Systematic Analysis of the Structure-Reactivity Trends for some “Cation-Like” Early Transition Metal Catalysts for Dehydropolymerization of Silanes^{1†}

Vladimir K. Dioumaev and John F. Harrod

Chemistry Department, McGill University, Montreal, QC, Canada, H3A 2K6

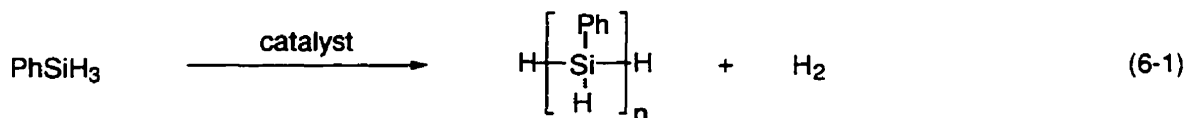
Abstract

The use of “cation-like” metallocene combination catalysts ($\text{Cp}'_2\text{MCl}_2 - 2\text{BuLi} - \text{B}(\text{C}_6\text{F}_5)_3$; $\text{Cp}' = \eta^5\text{-cyclopentadienyl}$, or substituted $\eta^5\text{-cyclopentadienyl}$; $\text{M} = \text{Ti, Zr, Hf, U}$) for dehydropolymerization of silane significantly improves the polymer molecular weight. For example, under the same conditions a $\text{Cp}(\text{C}_5\text{Me}_5)\text{ZrCl}_2/2\text{BuLi}$ catalyst gives $M_n=1890$, while a $\text{Cp}(\text{C}_5\text{Me}_5)\text{ZrCl}_2/2\text{BuLi}/\text{B}(\text{C}_6\text{F}_5)_3$ gives $M_n=7270$. The influence of various factors (steric and electronic effects of the cyclopentadienyl ligands, the nature of the metal, temperature, solvent, concentration and structure of silane) on the build up of polysilane chains are systematically analyzed.

[†] Dedicated to Professor Robert Corriu in recognition of his outstanding contributions to organosilicon chemistry and for the inspiration his work has given us.

6.1 Introduction

Synthetic routes to polysilanes are of scientific and technological interest as these polymers have a great potential in the field of advanced materials for electronics and integrated optics.²⁻⁷ Wurtz-like coupling of halosilanes with molten alkali metals is currently the most useful industrial method.⁴⁻⁷ An alternative, less hazardous synthetic strategy is a catalytic dehydropolymerization of silanes discovered by Harrod *et al* (eq 6-1).⁸ Transition metal catalysts offer some control over the stereochemistry of the polymeric products and the cyclic/linear chain selectivity⁹⁻¹² as well as a greater tolerance towards functional groups, which can be incorporated in the polymer.¹³⁻¹⁵ The major drawback of this route is the low molecular weight of polymers¹² which affects mechanical and optical properties. A considerable improvement in polysilane molecular weight has been achieved over the past decade by a combination of both: an extensive blind screening of various neutral early transition metallocenes^{12,16} as well as studies of the reaction intermediates and mechanisms.^{8,17-20}



Although the mechanism of the dehydrocoupling reaction is still under discussion, the most widely accepted one is a constant oxidation state σ -bond metathesis^{12,19,20} with a transition state similar to that postulated for Ziegler-Natta olefin polymerization. Much of the progress in the field has been based on the results of experimental measurements and theoretical calculations performed for the Ziegler-Natta catalysts.

The highly active olefin polymerization catalysts are believed to be 14-electron cationic Cp_2MR^+ complexes of group 4 or actinide metals or the neutral $\text{Cp}_2\text{M}'\text{R}$ isoelectronic compounds of group 3 or lanthanide metals.^{21,22} Their activity is attributed to

the high degree of electronic and steric unsaturation, which should be an important factor for dehydrogenative silane polymerization as well. There are a number of strategies to synthesize cationic Ziegler-Natta catalysts, which can be used in polymerization of silanes. The earlier versions of those catalysts contain a large excess of alkylaluminumoxane,²² the presence of which might lead to unwanted side reactions in silane polymerization. Recently developed and well characterized homogeneous cationic and “cation-like” group 4 and actinide metallocene catalysts for olefin polymerization,^{23,24} which make use of stoichiometric amounts of $B(C_6F_5)_3$ or $[Ph_3C]^+[BR_4]^-$ (where $[BR_4]^-$ is arylborate or carborane) as a cocatalyst, proved to be also active silane dehydrocoupling catalysts.^{1,25} Furthermore, the catalysts containing the $[BR(C_6F_5)_3]^-$ anion are often reluctant to form crystals, producing oils instead,²⁶⁻²⁸ which is an important property as the dehydropolymerization reaction proceeds in a low polar and highly viscous medium where solubility could be a limiting factor. Although Imori and Tilley reported no improvements using a $Cp'_2MR_2 - [NHR_3]^+[BR_4]^-$ system²⁵, in our experience the $Cp'_2MR_2 - B(C_6F_5)_3$ catalysts have certain advantages over neutral Cp'_2MR_2 catalysts.¹ The above mentioned considerations prompted us to investigate the factors influencing performance of $Cp'_2MR_2 - B(C_6F_5)_3$ and $[Ph_3C]^+[BR_4]^-$ systems toward dehydropolymerization in more detail.

6.2 Results and discussion

The results of a number of dehydrocoupling reactions are summarized in Tables 6-1 and 6-2. A conventional way to evaluate dehydropolymerization catalyst performance is to compare molecular weights of the final products. Molecular weight distributions were estimated by gel permeation chromatography (GPC), calibrated versus polystyrene standards. At high conversion, the molecular weight of a polysilane sample has a bimodal distribution with the low molecular weight fraction being a mixture of cyclic silanes (approximately 5-8 Si based on the GPC retention time) and a high molecular weight

fraction assumed to be linear polymers. In Tables 6-1 and 6-2 only the molecular weight of the high molecular weight fractions are reported, since the low molecular weight fraction always has the same weight within the accuracy of the measurements. Further, averaging the weights of the two fractions often masks the actual trends in the linear chain growth and could be misleading, especially when the weights differ by two orders of magnitude. For cases where the bimodal distribution is not well resolved, there is a certain ambiguity in determining the cut-off point and thus, the calculated molecular weights are somewhat arbitrary. When the molecular weights were too low to show any evidence of the second distribution mode, the entire peak area was used in the calculations and the ratio for the linear versus cyclic oligomers was not determined. These molecular weights are not strictly comparable to the weights of the linear fractions alone. The apparent weight of the latter is significantly higher, although the actual difference between the samples might be almost negligible. For example, samples with a linear polymer fraction of an $M_w=900$, $M_n=700$, or a nonresolved cyclic and linear fraction of $M_w<500$, $M_n<500$ give essentially identical chromatograms.

Table 6-1. Some results for the polymerization of phenylsilane in toluene^a

Catalyst	time	% conversion	M_w	M_n	% linear
1. $\text{Cp}_2\text{ZrCl}_2/2\text{BuLi}$	0.2 h	95	670	600	n.d.
2.	10 d	>99	2450	2080	55
3. $\text{Cp}_2\text{ZrCl}_2/2\text{BuLi}/\text{B}(\text{C}_6\text{F}_5)_3$	4 d	>99	3800	2770	85
4.	10 d	>99	4320	3010	85
5. $(\text{MeCp})_2\text{ZrCl}_2/2\text{BuLi}$	3 d	>99	2400	1800	60
6. $(\text{MeCp})_2\text{ZrCl}_2/2\text{BuLi}/\text{B}(\text{C}_6\text{F}_5)_3$	4 h	70	1100	810	80
7.	3 d	>99	4650	3180	90
8.	10 d	>99	5150	2840	90
9. $(\text{Me}_5\text{C}_5)_2\text{ZrCl}_2/2\text{BuLi}/\text{B}(\text{C}_6\text{F}_5)_3^b$	0.5 h	10	dimer		
10.	20 h	80	Dimer and trimer		

11.	10 d	85	Dimer, trimer and tetramer		
12.	10 d+1 d ^c	>99	Mostly trimer and tetramer		
13. Cp ₂ ZrMe ₂ /B(C ₆ F ₅) ₃	4 d	<5	<500	<500	n.d.
14. Cp ₂ ZrMe ₂ /B(C ₆ F ₅) ₃	10 d ^c	>99	2080	1290	65
15. B(C ₆ F ₅) ₃ ^d	0	n.a.	2450	2080	50
16.	8 d	n.a.	2450	2080	50
17. Cp ₂ TiCl ₂ /2BuLi /B(C ₆ F ₅) ₃	1 d	80	780	510	n.d. ^e
18.	10 d	95	1050	620	n.d. ^e
19. Cp ₂ HfCl ₂ /2BuLi/B(C ₆ F ₅) ₃	1 d	10	<500	<500	n.d.
20.	10 d	95	1220	710	60
21. (Me ₅ C ₅) ₂ UCl ₂ /2BuLi/B(C ₆ F ₅) ₃ ^b	2 h	20	Mostly dimer		
22.	10 d	40	<500	<500	n.d.

^a Reactions at 20 °C in a 1:1 monomer/toluene ratio (v/v), and a catalyst concentration of 5 mol %, except where stated otherwise. The molecular weights (in Daltons) are calibrated with respect to polystyrene standards and the values are estimated to be reliable to within $\pm 5\%$. Where possible the low molecular weight cyclic products were excluded from the calculations of M_w and M_n . MeCp = methylcyclopentadienyl.

^b In this case product analysis is based on ¹H-NMR spectra.

^c The temperature is 60 °C.

^d This is a blank reaction in which the substrate was a pre-prepared polyphenylsilane. It establishes that polymer is inert to the presence of the borane alone.

^e A considerable amount of Ph₂SiH₂ was detected.

The data in Tables 6-1 and 6-2 show that, the presence of B(C₆F₅)₃ leads to a considerable improvement in the molecular weights and yields of linear polymer produced (entries 1-8 of Table 6-1; entries 1-3 and 10-14 of Table 6-2, Figures 6-1a and 6-1b). Perhaps, the most important feature of this catalytic system is that there is no depolymerization reaction observed. This contrasts with most neutral metallocene catalysts which were reported to depolymerize the long linear chains to produce cyclic compounds.¹² For any polycondensation reaction, high molecular weights can only be

achieved at extremely high (higher than 99.9%) conversions and it is thus mandatory to have the reaction going exclusively in one direction.

Table 6-2. Some results for the polymerization of phenylsilane in neat monomer^a

Catalyst	time	% con- version	M _w	M _n	% linear
1. Cp ₂ ZrCl ₂ /2BuLi	1 d	>99	3000	1860	75
2.	10 d	>99	2930	1880	75
3. Cp ₂ ZrCl ₂ /2BuLi/B(C ₆ F ₅) ₃	10 d	>99	4990	2670	90
4. (MeCp) ₂ ZrCl ₂ /2BuLi/B(C ₆ F ₅) ₃	10 d	>99	5640	3020	90
5. (Ind) ₂ ZrCl ₂ /2BuLi/B(C ₆ F ₅) ₃	12 d	>99	4840	2730	80
6. (EBI)ZrCl ₂ /2BuLi/B(C ₆ F ₅) ₃	10 d	>99	1080	910	n.d.
7. (THI) ₂ ZrCl ₂ /2BuLi/B(C ₆ F ₅) ₃	12 d	95	<500	<500	n.d.
8. [(Me ₃ Si)Cp] ₂ ZrCl ₂ /2BuLi/B(C ₆ F ₅) ₃	3 h	<5	<500	<500	n.d.
9. [(Me ₃ Si)Cp] ₂ ZrCl ₂ /2BuLi/B(C ₆ F ₅) ₃	10 d	>99	10910	4150	95
10. Cp(Me ₅ C ₅)ZrCl ₂ /2BuLi	1 d	>99	3300	1980	80
11. Cp(Me ₅ C ₅)ZrCl ₂ /2BuLi	10 d	>99	3220	1890	80
12. Cp(Me ₅ C ₅)ZrCl ₂ /2BuLi/B(C ₆ F ₅) ₃	0.2 h	90	2570	1560	90
13.	3.5 h	95	9640	4800	90
14.	1 d	>99	13790	7270	90
15. Cp(Me ₅ C ₅)ZrCl ₂ /2BuLi/2B(C ₆ F ₅) ₃	1 d	80	980	700	n.d.
16. Cp(Me ₅ C ₅)ZrCl ₂ /2BuLi/B(C ₆ F ₅) ₃ ^b	1.5 h	95	5330	3160	95
17	7 d	>99	10700	5550	95
18. Cp(Me ₅ C ₅)ZrCl ₂ /2BuLi/B(C ₆ F ₅) ₃ ^c	1 d	95	1600	1140	90
19.	17 d	>99	2710	1640	90
20. Cp(Me ₅ C ₅)ZrCl ₂ /2BuLi/B(C ₆ F ₅) ₃	3 h	95	5640	3330	90
21.	3 h + 1 d ^d	>99	5640	3320	90
22.	3 h + 30 d ^d	>99	3910	2250	90
23. Cp(Me ₅ C ₅)ZrCl ₂ /2BuLi/B(C ₆ F ₅) ₃	3 h	95	6450	3410	90
24.	3 h + 1 d ^e	>99	5090	3320	90

25.	3 h + 30 d ^e	>99	3690	1850	45
26. Cp(Me ₅ C ₅)ZrCl ₂ /2BuLi/B(C ₆ F ₅) ₃	0.5 h + 0.5 h ^f	95	8600	3100	90
27.	1 d ^f	>99	12000	3900	90
28.	10 d ^f	>99	3480	1880	80
29. Cp ₂ ZrMe ₂ /4PhSiH ₃ /B(C ₆ F ₅) ₃ ^g	10 d	>99	2380	1540	80
30. Cp ₂ ZrMe ₂ /4PhSiH ₃ /[Ph ₃ C][B(C ₆ F ₅) ₄] ^g	10 d	>99	870	530	n.d.
31. [(MeCp) ₂ ZrH ₂] ₂ /B(C ₆ F ₅) ₃	7 d	0			
32. [(MeCp) ₂ ZrH ₂] ₂ /[Ph ₃ C][B(C ₆ F ₅) ₄]	7 d	0			
33. Cp ₂ ZrMe ₂ /[Ph ₃ C][B(C ₆ F ₅) ₄]	30 d	>99	680	520	n.d.
34. (MeCp) ₂ ZrCl ₂ /2BuLi/4PhSiH ₃ / [Ph ₃ C][B(C ₆ F ₅) ₄] ^g	30 d	>99	660	470	n.d.
35. Cp ₂ ZrCl ₂ /2BuLi /B(C ₆ F ₅) ₃ ^h	10 d	>99	<500	<500	n.d.
36. Cp(Me ₅ C ₅)ZrCl ₂ /2BuLi /B(C ₆ F ₅) ₃ ^h	10 d	>99	<500	<500	n.d.
37. Cp(Me ₅ C ₅)ZrCl ₂ /2BuLi/B(C ₆ F ₅) ₃ ⁱ	5 d	25	<500	<500	n.d.
38. Cp ₂ HfCl ₂ /2BuLi /B(C ₆ F ₅) ₃	10 d ^j	>99	8030	3780	95
39.	1.5 h ^k	>99	5030	2580	90
40.	2 d ^k	>99	4910	2790	85
41. Cp(Me ₅ C ₅)HfCl ₂ /2BuLi /B(C ₆ F ₅) ₃	1 d ^j	>99	4510	1840	95
42.	10 d ^j	>99	4530	2600	95
43.	1 d ^l	>99	2630	1510	90
44.	10 d ^l	>99	8670	3050	85

^a Reactions at 20 °C in neat monomer, and a catalyst concentration of 5 mol %, except where stated otherwise. The molecular weights (in Daltons) are calibrated with respect to polystyrene standards and the values are estimated to be reliable to within $\pm 5\%$. Where possible the low molecular weight cyclic products were excluded from the calculations of M_w and M_n . MeCp = methylcyclopentadienyl, THI=4,5,6,7-tetrahydroindenyl, EBI=ethylene-1,2-bis[1-indenyl], Ind = indenyl.

^b 1 mol % catalyst used in this reaction.

^c Only 0.25 mol % catalyst used in this reaction.

^d Small amount of toluene was added; the PhSiH₃/toluene ratio is ca 5/1.

^e Small amount of 1,2-dichloroethane was added; the PhSiH₃/C₂H₄Cl₂ ratio is ca 5/1.

^f PhSiMe₃ was used as a solvent. (1:1 (v/v) to PhSiH₃)

^g The reagents were mixed in the same order as they appear in the table.

^h PhCH₂SiH₃ was polymerized instead of PhSiH₃.

ⁱ (n-C₆H₁₃)SiH₃ was polymerized instead of PhSiH₃.

^j Before addition of B(C₆F₅)₃ and PhSiH₃, the mixture of Cp'₂HfCl₂ and 2BuLi was stirred for 0.3 hour at 80°C.

^k Polymerization was conducted at 80 °C.

^l Before addition of B(C₆F₅)₃ and PhSiH₃, the mixture of Cp(Me₅C₅)HfCl₂ and 2BuLi was stirred for 1 hour at 108°C.

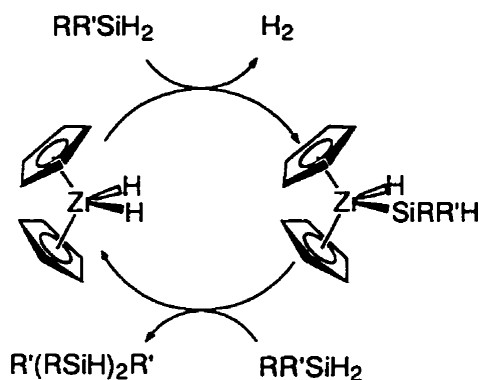
B(C₆F₅)₃ alone does not react either with monomer or with preformed silane polymer (entries 15 and 16 of Table 6-1) on the time scale of a typical polymerization experiment (less than 24 hours for a monomer, 10 days for a polymer), although the broadening of the ¹H NMR resonances indicates some kind of complexation with RSiH₃. When the monomer was exposed to B(C₆F₅)₃ for 8 days, decomposition into a mixture of unidentified products occurred. However, in most polymerization experiments the monomer was more than 99 % consumed within the first 24 hours of the reaction, which sets an upper limit on its exposure to B(C₆F₅)₃. [Ph₃C][B(C₆F₅)₄] is more reactive and causes redistribution of silane monomers, *vide infra*.

6.2.1 Choice of the central metal

A number of Cp'₂MR₂ metallocenes (Cp'₂= two substituted cyclopentadienyl ligands or a bridged substituted bis-cyclopentadienyl moiety, M=Ti, Zr, Hf and U) were screened but only zirconocenes and hafnocenes exhibited selectivity for linear high molecular weight products. Uranocene and titanocene have a very low efficiency both in terms of conversion of the starting monomer and the molecular weight of the final product (entries 17, 18 and 21-22 of Table 6-1). The color of the reaction mixtures indicates

reduction of M^{IV} to M^{III} . Zircono- and hafnocene catalytic systems accumulate large amounts of M^{III} only at the late stages, when most of the primary and secondary SiH bonds have been consumed. The reduced forms of uranium and titanium catalysts, on the other hand, accumulate in the very early stages of polymerization, which can be attributed to the lower reduction potentials for these metals.²⁹ There is no final agreement on the mechanism of the dehydrocoupling reaction, but both the constant oxidation state σ -bond metathesis¹² and the one-electron oxidative addition - reductive elimination mechanisms (Schemes 6-1 and 6-2 respectively) are consistent with the fact that accumulation of the reduced M^{III} species indicates that the catalytic cycle is not functioning properly. Although there is no *a priori* reason why M^{III} species could not undergo σ -bond metathesis, there is at the moment no compelling evidence that they do. Further, the olefin polymerization σ -bond metathesis mechanism regards reduction as an abortive side reaction.^{30,31} On the other hand, in case of one-electron oxidative addition - reductive elimination mechanisms, formation of M^{III} is an important part of the cycle.^{32,33} However, in a high performance one-electron oxidative addition - reductive elimination cycle, M^{III} is expected to be a highly reactive intermediate, not a resting state of the system. The vital importance of the catalyst reduction, which favors the latter mechanism versus σ -bond metathesis, can be illustrated by the behavior of dimethylzirconocene versus dibutylzirconocene. Dibutylzirconocene is unstable at room temperature and undergoes one electron reduction spontaneously. We have observed the decomposition of Cp_2ZrBu_2 , with a half life of ca. 30 min at room temperature, to a mixture of ca. 50% Zr^{III} and 50% Zr^{IV} products by NMR and EPR spectroscopic analysis.³⁴ As a result, the catalyst derived from it does not require any thermal activation. On the other hand, dimethylzirconocene is a stable compound and neither the pure complex, nor its mixture with borane cocatalyst show any evidence for reduction. A mixture of Cp_2ZrMe_2 , $B(C_6F_5)_3$ and $PhSiH_3$ is EPR silent and the performance in dehydropolymerization is extremely poor (entry 13 of Table 6-1). However, when the sample is heated up to 60 °C, the amount of Zr^{III} species increases

significantly, and so does the catalytic activity (entry 14 of Table 6-1). The same trend, although less pronounced, can be observed for hafnocene catalysts. The hafnocene alkyls in general are more stable than zirconocene analogs³⁵ but undergo similar decomposition and reduction reactions at elevated temperatures. Their dehydrocoupling catalytic activity can be increased by heating the catalyst precursor, dibutylhafnocene, for 30-60 minutes at 80-110 °C (entries 38-44 of Table 6-2). Dehydropolymerization itself does not need elevated temperatures, but the unreactive precatalysts need thermal activation to either undergo reduction, or to undergo σ -bond metathesis with the silane substrate. Either, or both types of reaction may be prerequisite to generation of the true catalyst.

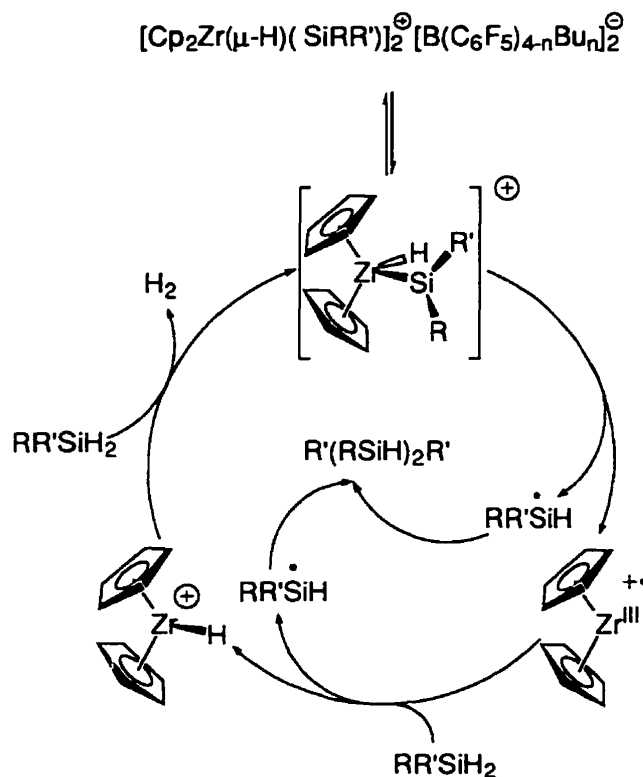


Scheme 6-1 The Tilley σ -bond metathesis mechanism for silane dehydropolymerization¹² ($R=Ar$ or Alk ; $R'=H$ or $(SiHR)_nH$)

From the foregoing, it can be concluded that the relative stability of M^{IV}/M^{III} oxidation states and the energy barrier between them, in regards to dehydropolymerization reaction, are best balanced for zirconocene. The energy barrier is somewhat unfavorable for hafnocene based catalysts and the higher stability of the M^{III} form decreases the activity of urano- and titanocenes. The critical problem with excessive production of the M^{III} forms may be the tendency of these species to form catalytically sterile dimers.

6.2.2 Catalyst preparation strategy

A number of catalyst preparation strategies have been tried. Mixtures of $\text{Cp}'_2\text{ZrMe}_2$ or $[\text{Cp}'_2\text{ZrH}(\mu\text{-H})]_2$ with $\text{B}(\text{C}_6\text{F}_5)_3$ (entry 13 of Table 6-1 and entry 31 of Table 6-2) proved to be poorer catalytic precursors than the $\text{Cp}'_2\text{ZrCl}_2/2\text{BuLi}/\text{B}(\text{C}_6\text{F}_5)_3$ system. The low activity of these precursors can be attributed to the higher stability of the M^{IV} oxidation state. Indeed, when the metallocene was pretreated (exposed to elevated temperatures or reacted with PhSiH_3) to generate some M^{III} species, before introduction of borane, the performance of the catalyst improved significantly (entry 14 of Table 6-1 and entry 29 of Table 6-2).



Scheme 6-2 A tentative one-electron oxidative addition-reductive elimination mechanism for silane dehydropolymerization^{32,33} ($\text{R}=\text{Ar}$ or Alk ; $\text{R}'=\text{H}$ or $(\text{SiHR})_n\text{H}$)

In general, $[\text{Ph}_3\text{C}]^+[\text{BR}_4]^-$ turned out to be a much poorer co-catalyst than $\text{B}(\text{C}_6\text{F}_5)_3$ (entries 30 and 32-34 of Table 6-2). One of the obvious drawbacks of $[\text{Ph}_3\text{C}]^+[\text{BR}_4]^-$ is that it reacts with primary aryl silanes inducing electrophilic redistribution of RSiH_3 into SiH_4 , R_2SiH_2 , R_3SiH and R_4Si . R_2SiH_2 and R_3SiH will either terminate polysilane chain growth, or be unreactive. The SiH_4 acts as a branching agent, causing crosslinking and leading to poorly soluble, intractable products, which are mainly lost during the workup procedure. If any borate cocatalyst is left unreacted in the system, the above mentioned problems can interfere and mask the true performance of the catalyst, generated in this way. In addition, we have confirmed that trityl cation oxidizes catalytically active Zr^{III} species producing trityl radical, which can be observed by EPR spectroscopy. An analogous redox reaction was recently reported for Ti^{III} .³⁶ Imori and Tilley recently reported that a very similar $\{\text{Cp}_2'\text{ZrMe}_2 \text{ or } [\text{Cp}_2'\text{ZrH}_2]_2\}/[\text{NHR}_3]^+[\text{BR}_4]^-$ catalytic system produced high molecular weight polymers.²⁵ It is obvious, that the polymers and conditions reported in the present paper for the $\text{Cp}_2'\text{ZrX}_2/[\text{Ph}_3\text{C}]^+[\text{BR}_4]^-$ combination catalysts are not well optimized but the above mentioned arguments discouraged us from concentrating on this system.

In some cases of coordination catalysis dicationic complexes have certain advantages over monocationic compounds.^{37,38} The dehydropolymerization reaction, however, slowed down significantly (only 80% conversion after 1 day) and decreased the product molecular weights by *an order of magnitude* upon introduction of a second equivalent of borane (entry 15 of Table 6-2). This suggests that the dication complex is completely inactive towards silane polymerization and the observed reaction is driven by a residual monocationic catalyst. The lack of catalytic activity for the dication is consistent with both the constant oxidation state σ -bond metathesis and the one-electron oxidative addition-reductive elimination mechanisms.

6.2.3 Solvent, temperature and concentration effects

As previously reported, the highest rates and degrees of polymerization can be achieved in neat monomer.¹² The obvious drawback of the high concentration conditions is that the reaction mixture completely solidifies at high conversions, which puts an end to the polymerization. On the other hand, the catalyst performance decreases significantly even when a small amount of solvent (usually toluene) is added. This solvent effect may be due to the ability of aromatic solvents to compete with the SiH groups for the catalyst coordination site. This competition will be particularly important for the more hindered terminal SiH₂ groups, whose reaction is required to produce long chains. Tilley and coworkers earlier suggested a number of compromises to overcome these problems.¹² The most attractive idea is a slow bleeding of monomer into the reaction mixture to keep it at least semiliquid. Unfortunately, the known dehydropolymerization catalysts are significantly more active towards monomer-monomer versus monomer-chain coupling. The bleeding of the monomer, thus, results in the build-up of new, short polymer chains instead of propagating the old, long ones. Another approach, a slow introduction of toluene, such that the reaction mixture maintained a slight fluidity, was reported to improve the efficiency of neutral zirconocene catalysts.¹² In the case of the cationic Cp₂'ZrCl₂/BuLi/B(C₆F₅)₃ combination catalyst, however, neither toluene nor dichloroethane improves the efficiency of the catalyst even if they are added at the point when the mixture appears to be solid (entries 20-25 of Table 6-2). Dichloroethane leads to decomposition of the active Zr^{III} catalytic intermediates judging both from the dramatic color change from brown to yellow and the disappearance of EPR signals. In addition, behavior of the catalyst changes in that significant depolymerization can be observed even after 1 day and a large (55%) amount of cyclics is formed after 30 days. The impact of added toluene is much less dramatic; there are no major changes, either in the EPR spectrum or in the color of the sample. The polymerization stops but no depolymerization

is observed after 1 day and very little change occurs even after 30 days. The nature of the solvent influence in this case is obviously different as the solvent merely blocks coordination sites, *vide supra*, but does not decompose the catalyst.

An ideal solvent for the dehydropolymerization should be chemically inert and weakly coordinative, yet polar enough to solubilize the catalyst and the polysilane. The latter requirement is not very strict as the catalyst is soluble enough in relatively nonpolar primary silanes and short chain oligosilanes. Tertiary silanes are known to be inert towards dehydropolymerization presumably because of their steric bulk and inability to coordinate to the metal center.³⁹ Quaternary silanes should be even more weakly coordinative and inert. On the other hand they do not differ much in terms of polarity from the primary silanes and polysilanes. PhSiMe_3 was probed as an inert, sufficiently polar and weakly coordinative solvent candidate (entries 26-28 of Table 6-2). At the early stages (within the first day) the reaction behaves as predicted; the solvent does not interfere with the built up of the long chains and the amount of cyclics does not increase as compared to the neat monomer conditions. The polydispersity index is higher than usual, which indicates, that the low molecular weight oligomers are either less efficiently consumed or are gradually formed again in a depolymerization reaction. The latter prevails at longer (10 days) reaction times. It is not clear, though, whether the depolymerization activity is an inherent property of the catalyst and cannot be avoided, or is a result of insufficient stability of the catalyst and a matter of a proper tuning.

A general way to achieve a higher degree of conversion is to raise the temperature. A number of different experiments with temperatures ranging from 20 to 108°C were performed. The samples were either heated for the entire period of the reaction or only at the early or late stages (entries 12 and 14 of Table 6-1; entries 38-44 of Table 6-2). Unfortunately, with both Zr and Hf catalyst decomposition occurs faster than the built up of the long polymer chains. The decomposed catalyst facilitates the depolymerization reaction and the overall result is a decrease of molecular weight and an increase in the

amount of cyclics (entry 14 of Table 6-1; entries 39 and 40 of Table 6-2 compared to entry 38). The hafnium based catalysts have a better thermal stability but the room temperature reactions still result in higher molecular weight polymers. The thermal instability of the $\text{Cp}_2'\text{HfCl}_2/\text{BuLi}/\text{B}(\text{C}_6\text{F}_5)_3$ combination catalyst is a separate issue from that of the $\text{Cp}_2'\text{HfBu}_2$ precursor.³⁵ In the preparation of the combination catalyst, the $\text{Cp}_2'\text{HfBu}_2$ has to be thermally decomposed before the addition of the $\text{B}(\text{C}_6\text{F}_5)_3$ and the PhSiH_3 (entries 38 and 41-44 of Table 6-2 compared to entries 19 and 20 of Table 6-1). This procedure then gives a catalyst which is active at room temperature.

Another drawback of the dehydropolymerization reaction is the relatively high concentration of the catalyst. Most of the reactions were performed with 5 molar % of catalyst. This amount can be cut down to 1 molar % without any major loss in molecular weight but an attempt to further decrease the concentration to 0.25 molar % was not successful (entries 16-19 of Table 6-2). This is due, in part, to the poisoning impurities in the monomer such as water and oxygen, as reliable drying techniques (Na/K alloy, NaH, LiAlH_4 or benzophenone ketyl) cannot be used. The other source of this concentration limit is the reaction itself, which is almost thermoneutral^{40,41} and most of it occurs in a very viscous medium. It is hard to expect high catalyst turnover frequency under these conditions as diffusion is restricted and the energy gain is small.

6.2.4 Fine tuning of the steric and electronic effects of the cyclopentadienyl ligands

In an attempt to avoid the depolymerization reaction and find a better catalyst a number of zircono- and hafnocene complexes were screened for dehydropolymerization activity. The general order of reactivity parallels those reported for neutral analogs by Harrod's and by Tilley's groups,^{12,18} namely $(\text{C}_5\text{Me}_5)_2\text{Zr} \equiv (\text{THI})_2\text{Zr} < (\text{EBI})\text{Zr} < \text{Cp}_2\text{Zr} \equiv$

$(\text{Ind})_2\text{Zr} < (\text{MeCp})_2\text{Zr} < \text{Cp}_2\text{Hf} \equiv (\text{C}_5\text{Me}_5)(\text{Cp})\text{Hf} < (\text{Me}_3\text{SiCp})_2\text{Zr} < (\text{C}_5\text{Me}_5)(\text{Cp})\text{Zr}$ (THI = 4,5,6,7-tetrahydroindenyl, EBI = ethylene-1,2-bis[1-indenyl], Ind = indenyl). This order indicates that steric effects are definitely dominating. While sterically overcrowded zirconocenes do not furnish any polymer at all (entries 9-12 of Table 6-1 and entry 7 of Table 6-2), undercrowded catalysts, although they are highly active, do not produce high molecular weight products (entries 3, 4 and 6-8 of Table 6-1; entries 3 and 4 of Table 6-2). The latter is usually attributed to the tendency of monomeric zirconocenes to form inactive dimers. $[(\text{Me}_3\text{SiCp})_2\text{Zr}]$ and $[(\text{C}_5\text{Me}_5)(\text{Cp})\text{Zr}]$ based catalysts proved to be a good compromise, they are bulky enough to be stable, yet not overcrowded enough to prohibit approach of oligomeric substrates (entries 8, 9 and 12-17 of Table 6-2).¹² The constrained geometry catalysts (CGC), which have the two cyclopentadienyls of the sandwich complex connected together by a bridging group, proved to be more reactive towards ethylene polymerization due to the more accessible metal center.²² However, neither the neutral⁴² nor the cationic $[\text{Me}_2\text{E}(\text{CpCp}')\text{M}]$, where $\text{E}=\text{Si}$ or C and $\text{M}=\text{Ti}, \text{Zr}, \text{Hf}$ based catalysts ($\text{Cp}'=\text{Cp}$ or C_5Me_5) reported by Tilley's group,²⁵ showed any advantages in dehydropolymerization. We have studied $(\text{EBI})\text{ZrCl}_2$, which has a more flexible two atom bridge, but it exhibited a much poorer activity than the non bridged $(\text{Ind})_2\text{ZrCl}_2$ (entries 5 and 6 of Table 6-2).

Compared to zirconocene, hafnocene non bridged catalytic systems are much less sensitive to the steric effects of the cyclopentadienyl ligands due to a larger opening of the metallocene wedge.⁴³ Thus, the cheap and commercially available Cp_2HfCl_2 has an efficiency as high as $(\text{C}_5\text{Me}_5)(\text{Cp})\text{HfCl}_2$, and is almost approaching $(\text{C}_5\text{Me}_5)(\text{Cp})\text{ZrCl}_2$ (entries 38 and 44 of Table 6-2).

Electronic effects of substituted cyclopentadienyl ligands are relatively unimportant. Thus, a polyaromatic indenyl has nearly the same performance as cyclopentadienyl and methylcyclopentadienyl based catalysts (entries 3-5 of Table 6-2). The slight decrease in activity of the indenyl based catalyst is probably due to the haptotropic rearrangements,

which were reported for the neutral $(\text{Ind})_2\text{TiMe}_2$ dehydropolymerization catalyst.⁴⁴ Such rearrangements lead to the catalyst dimerization through a bridging polyaromatic ligand as well as a poorly predictable coordination environment due to the η^5 - η^6 slipping of the indenyl.

6.2.5 Dehydropolymerization of other monomers

Attempted polymerizations of $\text{PhCH}_2\text{SiH}_3$ and $(n\text{-C}_6\text{H}_{13})\text{SiH}_3$ lead to low molecular weight products and, in the case of $(n\text{-C}_6\text{H}_{13})\text{SiH}_3$, to low polymerization rates as well (entries 35-37 of Table 6-2). Similar behavior was reported for dehydropolymerization with neutral metallocene catalysts¹¹ and can be rationalized by the variable oxidation state model. According to the model (Figure 6-3) the building of the silicon chains occurs by one electron reductive elimination of silyl radicals from the metal center,³² followed by radical coupling to produce Si-Si bonds.^{45,46} The yield and stability of silyl radicals decreases in the series $\text{PhSiH}_2\cdot > \text{PhCH}_2\text{SiH}_2\cdot > (n\text{-C}_6\text{H}_{13})\text{SiH}_2\cdot$,^{46,47} as does the ability of the silanes to undergo polymerization. To the best of our knowledge, no alternative explanation for the particular activity of PhSiH_3 has been offered in terms of the σ -bond metathesis or any other model.

6.2.6 Fractional precipitation of polysilanes

As can be seen from the molecular weights and the amount of the cyclic compounds (Tables 1 and 2, Figure 6-1b) even the best catalytic systems furnish a low quality polymer. However, the quality of the raw product can be easily improved by fractional precipitation from toluene - petroleum ether solution (Table 6-3, Figure 6-1c). The precipitated polymer was separated from the mother liquor by simple decanting. To illustrate the advantages of this purification technique a low quality starting polymer

($M_w=5000$, $M_n=3000$) was used. No centrifugation or filtering was used to improve the yield. The first, high molecular weight fraction (1:2 toluene - petroleum ether) precipitated rapidly. The lower molecular weight fraction (1:6) was not completely recovered and some of the material was lost suspended in the mother liquor. Although the fractionation technique was not optimized, the experiment illustrates that dehydropolymerization reactions can furnish high quality linear long chain polysilanes.

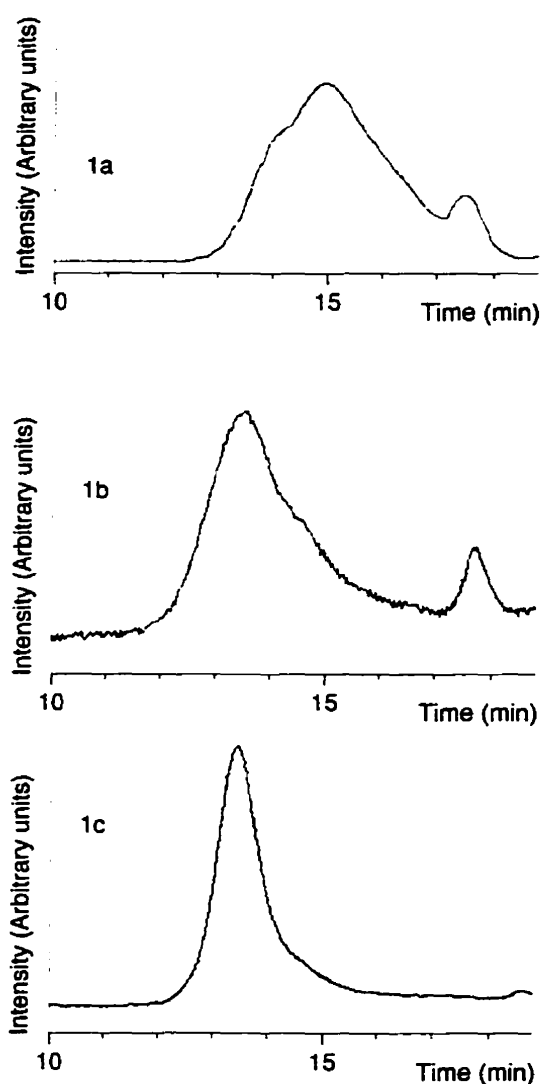


Figure 6-1. GPC traces for oligophenylsilane samples: a) obtained with $\text{Cp}_2\text{ZrCl}_2/2\text{BuLi}/\text{B}(\text{C}_6\text{F}_5)_3$ catalyst after 10 days , b) obtained with $\text{Cp}(\text{Me}_5\text{C}_5)\text{ZrCl}_2/2\text{BuLi}/\text{B}(\text{C}_6\text{F}_5)_3$ catalyst after 1 day, c) improved by fractional precipitation from toluene - petroleum ether.

Table 6-3. Some results for the fractional precipitation of polyphenylsilane^a

toluene/alkane ratio	Yield, %	M _w	M _n	polydispersity index	% linear
1:0 (before fractionation)	-	4910	2790	1.77	85
1:2	24	11900	6620	1.74	100
1:0 (before fractionation)	-	4840	2725	1.78	80
1:2	29	8490	4510	1.88	100
1:6	12 ^b	4590	3030	1.52	100

^a The molecular weights (in Daltons) are calibrated with respect to polystyrene standards and the values are estimated to be reliable to within $\pm 5\%$. The low molecular weight cyclic products were excluded from the calculations of M_w and M_n.

^b This fraction was precipitated from the mother liquor left over after separation of the previous (1:2) fraction.

6.3 Conclusions

Careful optimization of the catalyst structure and reaction conditions leads to higher molecular weight polysilanes (M_w=13800, M_n=7300) in a dehydropolymerization reaction. Catalyst performance can be rationalized in terms of a one-electron oxidative addition - reductive elimination mechanism. The molecular weight of the polymer can be further improved (e.g. from M_w=5000, M_n=2800 to M_w=12000, M_n=6600) by fractional precipitation technique from a toluene-petroleum ether solution.

6.4 Experimental details

6.4.1 General methods

All operations were performed in Schlenk-type glassware on a dual-manifold Schlenk line, equipped with flexible stainless steel tubing, or in an argon-filled M.Braun Labmaster 130 glovebox (<0.05 ppm H₂O). Argon was purchased from Matheson

(prepurified for the glovebox and UHP for the vacuum line) and was used as received. Hydrocarbon solvents (protio- and deuterio- benzene and toluene) were dried and stored over Na/K alloy, benzophenone and 18-crown-6 in Teflon-valved bulbs and were vacuum transferred prior to use. Halogenated solvents and silanes (1,2-dichloroethane, PhSiMe₃, PhSiH₃, (n-C₆H₁₃)SiH₃ and PhCH₂SiH₃) were degassed and stored over molecular sieves. Cp₂ZrCl₂, Cp₂TiCl₂, Cp₂HfCl₂, Me₅C₅H, ZrCl₄, C₆D₆, C₇D₈, 1,2-dichloroethane, C₆F₅Br, PhC(O)Ph, 18-crown-6, BCl₃ (1.0 M in heptane), n-BuLi (2.5 M in hexanes) and CpNa (2.0 M solution in THF) were purchased from Aldrich Chemical Co. and used as received unless stated otherwise. (Me₅C₅)₂ZrCl₂ and PhSiMe₃ were purchased from Strem Chemicals Inc. and United Chemicals respectively.

The compounds Cp₂ZrMe₂,⁴⁸ (MeCp)₂ZrCl₂,⁴⁹ [(MeCp)₂Zr(μ-H)H]₂,⁵⁰ (Me₃SiCp)₂ZrCl₂,⁵¹ Cp(Me₅C₅)ZrCl₂,⁵² (Ind)₂ZrCl₂,⁴⁹ (EBI)ZrCl₂,⁵³ (THI)₂ZrCl₂,⁴⁹ Cp(Me₅C₅)HfCl₂,⁵⁴ (Me₅C₅)₂UCl₂,⁵⁵ B(C₆F₅)₃,⁵⁶ [Ph₃C]⁺[B(C₆F₅)₄]⁻,²⁴ and RSiH₃ (R = Ph, PhCH₂ and n-C₆H₁₃)⁵⁷ were prepared according to literature procedures.

NMR spectra were recorded on a Varian Unity 500 (FT, 500 MHz for ¹H), Varian XL-200 or Varian Gemini-200 (FT, 200 MHz for ¹H) spectrometers. Chemical shifts for ¹H and ¹³C spectra were referenced using internal solvent references and are reported relative to tetramethylsilane. ¹⁹F NMR spectra were referenced to external trifluoroacetic acid. EPR spectra were recorded on a Bruker ESP 300E (X-band) spectrometer and were referenced to external DPPH. The molecular weights of the polysilanes were measured with a Varian 5000 liquid chromatograph equipped with a refractive index detector and Waters TSK G2000 HXL and TSK G4000 HXL columns in series. The chromatograph was calibrated with polystyrene standards and THF was used as an eluent.

All air sensitive NMR samples were prepared in an NMR-tube assembly, consisting of one or more 5 mL round-bottom flasks fitted with a Teflon valve to which an NMR tube has been fused at an angle of 45°. The liquids can be either kept separately in each of the flasks and tubes or can be transferred from one flask of choice to the other by tilting the

entire apparatus. A sample and a stirring bar were loaded in the side flask and treated with a small quantities (0.1-0.2 mL) of a deuterated solvent of choice. The solvent was then evaporated and the evaporation-vacuum transfer cycle was repeated to remove any residual non-deuterated solvents. A fresh portion of the same deuterated solvent (0.6-0.7 mL) was then vacuum transferred into the assembly and the solution was carefully decanted into the side NMR-tube. The top part of the tube was washed by touching it with a piece of cotton wool soaked with liquid nitrogen, which cause condensation of the solvent vapors on the inner walls. The sample was then frozen and flame sealed.

6.4.2.1 Silane polymerization experiments with $\text{Cp}'\text{Cp}''\text{MCl}_2/2\text{BuLi}/\text{B}(\text{C}_6\text{F}_5)_3$ ($\text{M} = \text{Ti, Zr, Hf, U}$) combination catalyst

The metallocene dichlorides (0.125 mmol) and $(\text{C}_6\text{F}_5)_3\text{B}$ (0.125 mmol, 0.064 g) were loaded in separate Schlenk tubes in the glovebox and all further manipulations were performed on a vacuum line. The reaction mixtures were protected from light with aluminum foil. The metallocene dichloride was suspended in 1 mL of toluene at 0°C and a 2.5 M solution of BuLi in hexanes (0.1 mL, 0.25 mmol) was added. The mixture was stirred at room temperature for 30 minutes (for some hafnocene catalysts 60 to 108°C temperatures were applied for 0.3-1 hour). The color gradually changed from light yellow to dark brown. Toluene (5 mL) was added to the $(\text{C}_6\text{F}_5)_3\text{B}$ and the resulting solution was slowly syringed into the butylated metallocene solution. A brown-red oil precipitated (brown-green for $\text{MeCp}_2\text{ZrCl}_2/\text{BuLi}/\text{B}(\text{C}_6\text{F}_5)_3$ and $\text{Cp}(\text{Me}_5\text{C}_5)\text{ZrCl}_2/\text{BuLi}/\text{B}(\text{C}_6\text{F}_5)_3$; black for $\text{Cp}_2\text{TiCl}_2/\text{BuLi}/\text{B}(\text{C}_6\text{F}_5)_3$ and $(\text{EBI})_2\text{ZrCl}_2/\text{BuLi}/\text{B}(\text{C}_6\text{F}_5)_3$). After stirring for another 30 minutes, the solvent was removed in vacuum and the catalyst was spread on the walls of the tube in a thin layer. RSiH_3 or RSiH_3 -toluene mixture ($\text{R} = \text{Ph, PhCH}_2$, or $n\text{-C}_6\text{H}_{13}$) was added and an immediate vigorous evolution of hydrogen started accompanied by a color change from brown to light yellow (titano- and uranocene catalysts did not change color upon addition of silane). In the absence of solvent, the mixture solidified

within the first 1-10 minutes and the brown-red color slowly reappeared. In some cases (see Table 6-2), a specified amount of solvent (toluene, dichloroethane or trimethylphenylsilane) was added within the first 1-3 hours after the addition of silane to keep the reaction mixture liquid. The mixture turned light yellow upon addition of dichloroethane.

Polysilane was worked up in air with minimum exposure to light. The sample was dissolved in toluene and passed through a short plug of dry Florisil to remove catalyst. Toluene was removed under vacuum and solutions for GPC analysis were prepared in THF.

6.4.2.2 Silane polymerization experiments with $\text{Cp}'\text{Cp}''\text{ZrCl}_2/2\text{BuLi}$ combination catalyst

The title polymerization was carried out according to the procedure above except that $\text{B}(\text{C}_6\text{F}_5)_3$ was not used.

6.4.2.3 Silane polymerization experiments with $\text{Cp}_2\text{ZrR}_2/m\text{B}(\text{C}_6\text{F}_5)_3$ or $\text{Cp}'\text{Cp}''\text{ZrR}_2/m[\text{Ph}_3\text{C}][\text{B}(\text{C}_6\text{F}_5)_4]$ ($\text{R}=\text{Me}$ or H and $m=1$ or 2) combination catalyst

The appropriate metallocene (0.125 mmol), toluene (2 mL) and $\text{B}(\text{C}_6\text{F}_5)_3$ or $[\text{Ph}_3\text{C}][\text{B}(\text{C}_6\text{F}_5)_4]$ (0.125 or 0.250 mmol) were loaded in a Schlenk tube in the glovebox and all further manipulations were performed on a vacuum line. The reaction mixtures were protected from light with aluminum foil. After stirring at room temperature for 4 hours, the solvent was removed in vacuum and the catalyst was spread on the walls of the tube in a thin layer. The color of the $\text{Cp}'\text{Cp}''\text{ZrR}_2/[\text{Ph}_3\text{C}][\text{B}(\text{C}_6\text{F}_5)_4]$ mixture was white and the $\text{Cp}_2\text{ZrR}_2/\text{B}(\text{C}_6\text{F}_5)_3$ was green or purple. Phenylsilane was added and the mixture was left stirring in the dark for a specified time period. Polysilane was worked up according to the procedure described above.

6.4.2.4 Silane polymerization experiments with $\text{Cp}_2\text{ZrMe}_2/4\text{PhSiH}_3/\text{B}(\text{C}_6\text{F}_5)_3$ or $\text{Cp}_2\text{ZrMe}_2/4\text{PhSiH}_3/[\text{Ph}_3\text{C}][\text{B}(\text{C}_6\text{F}_5)_4]$ combination catalyst

In the glovebox, Cp_2ZrMe_2 (0.125 mmol, 0.031 g), toluene (2 mL) and PhSiH_3 (0.062 mL, 0.500 mmol) were loaded in a Schlenk tube and the mixture was stirred for 1 hour. Then, $(\text{C}_6\text{F}_5)_3\text{B}$ or $[\text{Ph}_3\text{C}][\text{B}(\text{C}_6\text{F}_5)_4]$ (0.125 mmol) was loaded and all further manipulations were performed on a vacuum line. The solvent was removed in vacuum and the catalyst was spread on the walls of the tube in a thin layer. Phenylsilane was added and the mixture was stirred in the dark for a specified time period (Tables 6-1 and 6-2). Polysilane was worked up according to the procedure described above.

6.4.2.5 Silane polymerization experiment with $(\text{MeCp})_2\text{ZrCl}_2/2\text{BuLi}/4\text{PhSiH}_3/\text{B}(\text{C}_6\text{F}_5)_3$ combination catalyst

The title polymerization was carried out according to the procedure described above except that PhSiH_3 (0.062 mL, 0.500 mmol) was added to the $(\text{MeCp})_2\text{ZrCl}_2/2\text{BuLi}$ mixture after it was allowed to react for 1 hour at room temperature. The mixture was stirred for an additional 1 hour and $\text{B}(\text{C}_6\text{F}_5)_3$ solution in toluene (5 mL) was introduced by a syringe.

6.4.2.6 Fractional separation of polyphenylsilane

A sample of polyphenylsilane (0.300 g) was dissolved in 1.7 mL of dry toluene. Petroleum ether was slowly added from a dropping funnel. Precipitation of the polymer began after approximately 1.5 mL of petroleum ether was added. The white milky suspension was allowed to settle for 0.5 hour. The precipitate was separated by decanting the mother liquor and dried in vacuum. The yields and the molecular weights of different fractions are shown in Table 6-3.

6.4.2.7 Reaction of $B(C_6F_5)_3$ with $RSiH_3$ ($R=Ph$, CH_2Ph)

In the glovebox, $B(C_6F_5)_3$ (0.10 mmol, 0.051 g), $RSiH_3$ (0.01 mmol) and C_6D_6 (0.5 mL) were loaded in an NMR tube assembly and the sample was prepared as described above. No color change occurred. The spectra were acquired after 1 and 24 hours, no changes were observed. Further reaction (8 days) leads to a mixture of at least six compounds (^{19}F NMR), which were not identified.

$R = Ph$, time=24 hours: NMR (C_6D_6 , +25 °C) 1H δ 7.5 (m, Ph), 7.3-7.1 (m, Ph), 4.3 (br s, SiH); ^{19}F δ -131.5 (dt, 21.2, 7.1 Hz, o- C_6F_5), -144.6 (tt, 21.2, 7.1 Hz, p- C_6F_5), -162.8 and -162.9 (tt, m- C_6F_5).

$R = CH_2Ph$, time=24 hours: NMR (C_6D_6 , +25 °C) 1H δ 7.07 (t, Ph), 6.91 (t, Ph), 6.90 (d, Ph), 3.63 (br s, SiH), 1.88 (br s, CH_2); ^{19}F δ -131.5 (d, 21.2 Hz, o- C_6F_5), -144.6 (br s, p- C_6F_5), -162.8 (br s, m- C_6F_5).

6.4.2.8 Reaction of $[Ph_3C][B(C_6F_5)_4]$ with $PhSiH_3$

In the glovebox, $[Ph_3C][B(C_6F_5)_4]$ (0.08 mmol, 0.075 g) and $PhSiH_3$ (ca 8 mmol, 1 mL) were loaded in a Schlenk tube. The color immediately changed from brown-red to light gray. The mixture was stirred for 16 hours, an aliquot was dissolved in C_6D_6 and passed through a short plug of dry Florisil. The components of the mixture were identified by comparison to the 1H NMR spectra of the authentic tri-, di-, and monophenylsilane, the relative amounts were estimated from the integrals to be 32, 46 and 22 % respectively.

1H NMR (C_6D_6 , +25 °C) 1H δ 7.7-7.5 (m, Ph), 7.2-7.0 (m, Ph), 6.00 (br s, Ph_3SiH), 5.07 (br s, Ph_2SiH_2), 4.22 (br s, $PhSiH_3$).

6.4.2.9 Reaction of $B(C_6F_5)_3$ with polyphenylsilane

In the glovebox $B(C_6F_5)_3$ (0.125 mmol, 0.064 g), polyphenylsilane (2.5 mmol, 0.265 g) and toluene (0.25 mL) were charged in a Schlenk tube. No color change occurred.

The mixture was left stirring for 8 days and was worked up according to the same procedure as used for the metallocene-catalyzed polymerization reactions.

Acknowledgment

Financial support for this work from the NSERC of Canada and Fonds FCAR du Québec is gratefully acknowledged. Helpful discussions of this chemistry with Prof. T.D.Tilley are also acknowledged.

References

- (1) Part of this work has appeared as a preliminary communication; Dioumaev, V. K.; Harrod, J. F. *Organometallics* **1994**, *13*, 1548-1550.
- (2) *Inorganic and Organometallic Polymers*; Zeldin, M.; Wynne, K. J.; Allcock, H. R., Ed.; American Chemical Society: Washington, DC, 1988.
- (3) Mark, J. E.; Allcock, H. R.; West, R. C. In *Inorganic Polymers* Prentice Hall: Englewood Cliffs, 1992; pp 186-236.
- (4) *Silicon-Based Polymer Science: A Comprehensive Resource*; Ziegler, J. M.; Fearon, F. W. G., Ed.; American Chemical Society: Washington, DC, 1990.
- (5) West, R. *J. Organomet. Chem.* **1986**, *300*, 327-346.
- (6) Miller, R. D.; Michl, J. *Chem. Rev.* **1989**, *89*, 1359-1410.
- (7) Ziegler, J. M. *Mol. Cryst. Liq. Cryst.* **1990**, *190*, 265-282.
- (8) Aitken, C. T.; Harrod, J. F.; Samuel, E. *J. Am. Chem. Soc.* **1986**, *108*, 4059-4066.
- (9) Gauvin, F.; Harrod, J. F. *Can. J. Chem.* **1990**, *68*, 1638-1640.
- (10) Banovetz, J. P.; Stein, K. M.; Waymouth, R. M. *Organometallics* **1991**, *10*, 3430-3432.
- (11) Harrod, J. F. In *Inorganic and Organometallic Polymers with Special Properties*; R. M. Laine, Ed.; Kluwer Academic: Dordrecht, 1992; Vol. 206; pp 87-98.
- (12) Tilley, T. D. *Acc. Chem. Res.* **1993**, *26*, 22-29.
- (13) Tilley, T. D.; Woo, H.-G. *Polym. Prepr., Am. Chem. Soc. Div. Polym. Chem.* **1990**, *31*, 228-229.
- (14) Banovetz, J. P.; Suzuki, H.; Waymouth, R. M. *Organometallics* **1993**, *12*, 4700-4703.
- (15) Woo, H.-G.; Kim, S.-Y.; Han, M.-K.; Cho, E. J.; Jung, I. N. *Organometallics* **1995**, *14*, 2415-2421.

- (16) Aitken, C.; Barry, J.-P.; Gauvin, F.; Harrod, J. F.; Malek, A.; Rousseau, D. *Organometallics* **1989**, *8*, 1732-1736.
- (17) Samuel, E.; Harrod, J. F. *J. Am. Chem. Soc.* **1984**, *106*, 1859-1860.
- (18) Harrod, J. F. In *Inorganic and Organometallic Polymers*; M. Zeldin; K. J. Wynne and H. R. Allcock, Ed.; American Chemical Society: Washington DC, 1988; pp 89-100.
- (19) Woo, H.-G.; Tilley, T. D. *J. Am. Chem. Soc.* **1989**, *111*, 3757-3758.
- (20) Woo, H.-G.; Tilley, T. D. *J. Am. Chem. Soc.* **1989**, *111*, 8043-8044.
- (21) Jordan, R. F. *J. Chem. Ed.* **1988**, *65*, 285-289.
- (22) Huang, J.; Rempel, G. L. *Prog. Polym. Sci.* **1995**, *20*, 459-526.
- (23) Yang, X.; Stern, C. L.; Marks, T. J. *J. Am. Chem. Soc.* **1991**, *113*, 3623-3625.
- (24) Chien, J. C. W.; Tsai, W.-M.; Rausch, M. D. *J. Am. Chem. Soc.* **1991**, *113*, 8570-8571.
- (25) Imori, T.; Tilley, T. D. *Polyhedron* **1994**, *13*, 2231.
- (26) Pellecchia, C.; Immirzi, A.; Grassi, A.; Zambelli, A. *Organometallics* **1993**, *12*, 4473-4478.
- (27) Pellecchia, C.; Grassi, A.; Zambelli, A. *Organometallics* **1994**, *13*, 298-302.
- (28) Dioumaev, V. K.; Harrod, J. F. *Organometallics* **1996**, *15*, 3859-3867.
- (29) Cotton, F. A.; Wilkinson, G. *Advanced inorganic chemistry*; John Wiley and Sons: New York, 1988.
- (30) Bueschges, U.; Chien, J. C. W. *J. Polym. Sci., Polym. Chem. Ed.* **1989**, *27*, 1525-1538.
- (31) Möhring, P. C.; Coville, N. J. *J. Organomet. Chem.* **1994**, *479*, 1-29.
- (32) Dioumaev, V. K.; Harrod, J. F. *manuscript in preparation*
- (33) Dioumaev, V. K.; Harrod, J. F. *XXVIII Organosilicon Symposium*; Gainesville, Florida, USA, 1995, pp B-23.
- (34) Dioumaev, V. K.; Harrod, J. F., submitted to *Organometallics*.

- (35) Buchwald, S. L.; Kreutzer, K. A.; Fisher, R. A. *J. Am. Chem. Soc.* **1990**, *112*, 4600-4601.
- (36) Grassi, A.; Zambelli, A.; Laschi, F. *Organometallics* **1996**, *15*, 480-482.
- (37) Hollis, T. K.; Bosnich, B. *J. Am. Chem. Soc.* **1995**, *117*, 4570-4581.
- (38) Odenkirk, W.; Bosnich, B. *J. Chem. Soc., Chem. Commun.* **1995**, 1181-1182.
- (39) Corey, J. Y.; Zhu, X.-H. *Organometallics* **1992**, *11*, 672-683.
- (40) Harrod, J. F.; Mu, Y.; Samuel, E. *Polyhedron* **1991**, *10*, 1239-1245.
- (41) King, W. A.; Marks, T. J. *Inorg. Chim. Acta* **1995**, *229*, 343-354.
- (42) Shaltout, R. M.; Corey, J. Y. *Tetrahedron* **1995**, *51*, 4309-4320.
- (43) Shaltout, R. M.; Corey, J. Y.; Rath, N. P. *J. Organomet. Chem.* **1995**, *503*, 205-212.
- (44) Gauvin, F.; Britten, J.; Samuel, E.; Harrod, J. F. *J. Am. Chem. Soc.* **1992**, *114*, 1489-1491.
- (45) Gaspar, P. P.; Haizlip, A. D.; Choo, K. Y. *J. Am. Chem. Soc.* **1972**, *94*, 9032-9037.
- (46) Chatgililoglu, C. *Chem. Rev.* **1995**, *95*, 1229-1251.
- (47) Walsh, R. *Acc. Chem. Res.* **1981**, *14*, 246-252.
- (48) Samuel, E.; Rausch, M. D. *J. Am. Chem. Soc.* **1973**, *95*, 6263-6267.
- (49) Samuel, E. *Bull. Soc. Chim. Fr.* **1966**, 3548-3564.
- (50) Jones, S. B.; Petersen, J. L. *Inorg. Chem.* **1981**, *20*, 2889-2894.
- (51) Lappert, M. F.; Pickett, C. J.; Riley, P. I.; Yarrow, P. I. W. *J. Chem. Soc., Dalton Trans.* **1981**, 805-813.
- (52) Wolczanski, P. T.; Bercaw, J. E. *Organometallics* **1982**, *1*, 793-799.
- (53) Collins, S.; Kuntz, B. A.; Taylor, N. J.; Ward, D. G. *J. Organomet. Chem.* **1988**, *342*, 21-29.
- (54) Rogers, R. D.; Benning, M. M.; Kurihara, L. K. *J. Organomet. Chem.* **1985**, *293*, 51-60.

- (55) Fagan, P. J.; Manriquez, J. M.; Maatta, E. A.; Seyam, A. M.; Marks, T. J. *J. Am. Chem. Soc.* **1981**, *103*, 6650-6667.
- (56) Massey, A. G.; Park, A. J. *J. Organomet. Chem.* **1964**, *2*, 245-250.
- (57) Finholt, A. E.; Bond, A. C. J.; Wilzbach, K. E.; Schlesinger, H. I. *J. Am. Chem. Soc.* **1947**, *69*, 2692-2696.

CHAPTER 7

Conclusions, Contributions to Original Knowledge, and Suggestions for Future Work

This chapter consists of two parts. In the first part, the summary of results and conclusions is presented, as well as the summary of the contributions to original knowledge. In the second part suggestions for future work are made. The conclusions section parallels and, sometimes, repeats individual conclusions made in every chapter (paper), but the general conclusions are more brief and consistent, and put everything in perspective.

7.1 Conclusions and Contributions to Original Knowledge

This thesis is the first detailed and systematic study of the applied and mechanistic aspects of the silane dehydropolymerization reaction catalyzed by cationic early transition metallocene compounds. This problem was dealt with by a combination of spectroscopic techniques, kinetic studies, and trapping of reaction intermediates. The result of such an integrated approach is a new redox mechanism for the dehydropolymerization reaction which explains and predicts the reactivity and selectivity of cationic early transition metal catalysts. The understanding of the structure-reactivity relationship permits improvement of the outcome of the dehydropolymerization reaction, e.g. improvement of the molecular weight of the resulting polymers via design of new and more efficient catalysts. The predictive power of the redox mechanism is reflected in the suggestions for future work section.

An application of a new generation of cationic metallocene catalysts, $\text{Cp}'_2\text{MCl}_2/2\text{BuLi}/\text{B}(\text{C}_6\text{F}_5)_3$, for the dehydropolymerization of silanes was investigated.

The final metallocene products, **29a-e**, isolated from such reaction mixtures, are believed to be dimers of the active catalytic species. Their structure, established by multinuclear, multidimensional NMR spectroscopy, shows that each zirconocene fragment bears a positive charge, which is delocalized between the metal center and the hydrosilane ligand. Reactions leading to their formation were studied in detail. All the postulated intermediates were either observed spectroscopically or trapped and isolated.

The improved activity of the $\text{Cp}'_2\text{ZrCl}_2/2\text{BuLi}/\text{B}(\text{C}_6\text{F}_5)_3$ combination catalyst can be attributed to the highly electrophilic nature of cationic Zr center and a considerable reduction of Zr in the $\text{Cp}'_2\text{ZrCl}_2/2\text{BuLi}$ reagent. The latter result is entirely unexpected both in terms of the widely accepted σ -bond metathesis dehydrocoupling mechanism and the known origins of activity of the $\text{Cp}'_2\text{ZrCl}_2/2\text{BuLi}$ reagent. The chemistry of $\text{Cp}'_2\text{ZrCl}_2/2\text{BuLi}$ was reinvestigated in detail by NMR and EPR spectroscopy, and was rationalized in thermodynamic terms, based on the known bond disruption enthalpy values. The observed products and equilibria cast new light on the diverse behavior of the $\text{Cp}'_2\text{ZrCl}_2/2\text{BuLi}$ reagent in various organic reactions and in the dehydropolymerization of silanes.

The structure of compounds and intermediates, isolated or trapped from the $\text{Cp}'_2\text{ZrCl}_2/2\text{BuLi}$ and $\text{Cp}'_2\text{ZrCl}_2/2\text{BuLi}/\text{B}(\text{C}_6\text{F}_5)_3$ mixtures point towards a new mechanism for the silane dehydrocoupling reaction. The postulated redox mechanism was tested and verified experimentally by quantitative NMR and qualitative EPR measurements as well as kinetic experiments.

Careful optimization of the catalyst structure and reaction conditions, based on the predictions of the one-electron redox mechanism, leads to more active catalysts and higher molecular weight polysilanes. The molecular weight of the polymer can be further improved by fractionation of the polymer.

7.2 Suggestions for Future Work

- According to the proposed redox mechanism, silane (or oligosilane) participates in only one transition state at the metal center, which is coordination of oligosilane to zirconocene hydride (Figure 7-1). The steric constraints in such a transition state are highly asymmetric with respect to the bisectorial plane of the sandwich. It would be of interest to synthesize a new generation of catalysts with a small ligand on one side (Cp, NR_2 , PR_3 and etc.) and a large, flat ligand (any large condensed aromatic compound with a Cp fragment in it) on the other side.

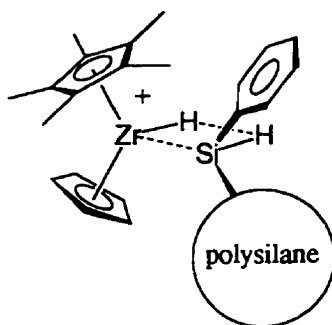


Figure 7-1 A schematic representation of the σ -bond metathesis transition states for the polymerization of phenylsilane

- The proposed redox mechanism suggests that dimerization of the catalyst could be a thermodynamic sink for the dehydrocoupling reaction. It would thus be of interest to immobilize the monomeric catalytic species on a solid surface and prevent dimerization. The monomer versus dimer structural arrangement can be probed by a reaction with PhSiD_3 , followed by solid state ^2H NMR spectroscopy.

The use of heterogeneous catalysts is especially intriguing, as the surface would act as an ultimately large, quasi flat ligand discussed above. In addition, such surface supported catalysts can generate high local concentrations of silyl radicals and increase

the possibility of their productive recombination, even when small amounts of solvent are used along with the liquid monomer. The heterogeneous catalysts are also attractive from the applied point of view, as they can be recovered by mechanical separation from the reaction mixture and recycled.

A simple synthetic path to try is the synthesis of CpZrR_3 (R = neopentyl or any other branched alkyl) from the commercially available CpZrCl_3 and RLi . It can be then deposited on partially deactivated silica gel or glass surface via a metathesis reaction of Zr-R bond with residual $[\text{Si}]\text{OH}$ groups.

- The redox generation of silyl radicals can be achieved by an electrochemical process. The surface of the electrodes can be modified with metallocene- or similar groups, if necessary. Such an electrode would have all the advantages discussed above and at the same time its redox properties would be extremely tunable by simply applying the suitable voltage and cycling pattern.
- The homogeneous polymerization catalysts can be probed for an emulsion polymerization in mixtures of fluorocarbons and toluene. The catalyst should be more soluble in the polar fluorocarbon phase, and a high local concentration of silyl radicals, required for successful coupling, can be achieved in it. The oligosilane nonpolar chains, on the other hand, can be solubilized in the toluene phase, which would keep the reaction mixture from solidifying, and might increase conversions and molecular weights.
- Structural studies of metal stabilized silylium ions should be more successful with carborane anions instead of $[\text{B}(\text{C}_6\text{F}_5)_4]^-$. The products with the former tend to furnish better quality crystals. Secondary silanes with reasonably small substituent (e.g. PhMeSiH_2) should be tried for the single crystal X-ray studies as well. Their adducts

with metallocenes would allow the question of planarity of the metal stabilized silylium ions to be addressed.

- Further kinetic studies can be done by cryogenic flash photolysis techniques, followed by EPR or IR in liquid inert gases. Light sources of high intensity would allow the problem of the first step being rate limiting to be overcome, and would give more insight into the reaction mechanism. The liquid inert gases might allow the ambiguity of the spectrum of solvent-ion adducts and interactions, which complicate kinetic treatment, to be avoided.
- New, bulkier ligands should be synthesized for model kinetic studies to prevent dimerization of metallocene catalysts, as a simple monomeric starting compound should furnish more interpretable kinetic results.

APPENDIX 1

Supplementary Material for Chapter 4

The Nature of the Species Present in the Zirconocene Dichloride - Butyllithium Reaction Mixture

Vladimir Dioumaev and John F. Harrod

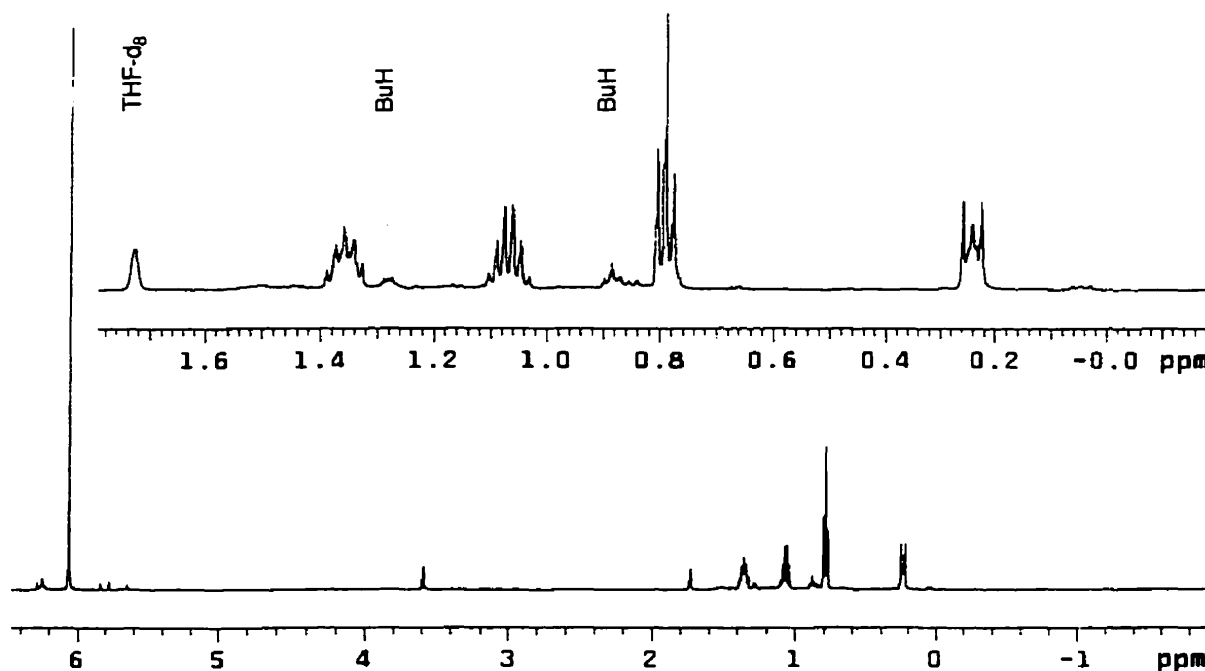


Figure 4-12. The ^1H NMR spectrum of **37** in THF-d₈ at -40°C.

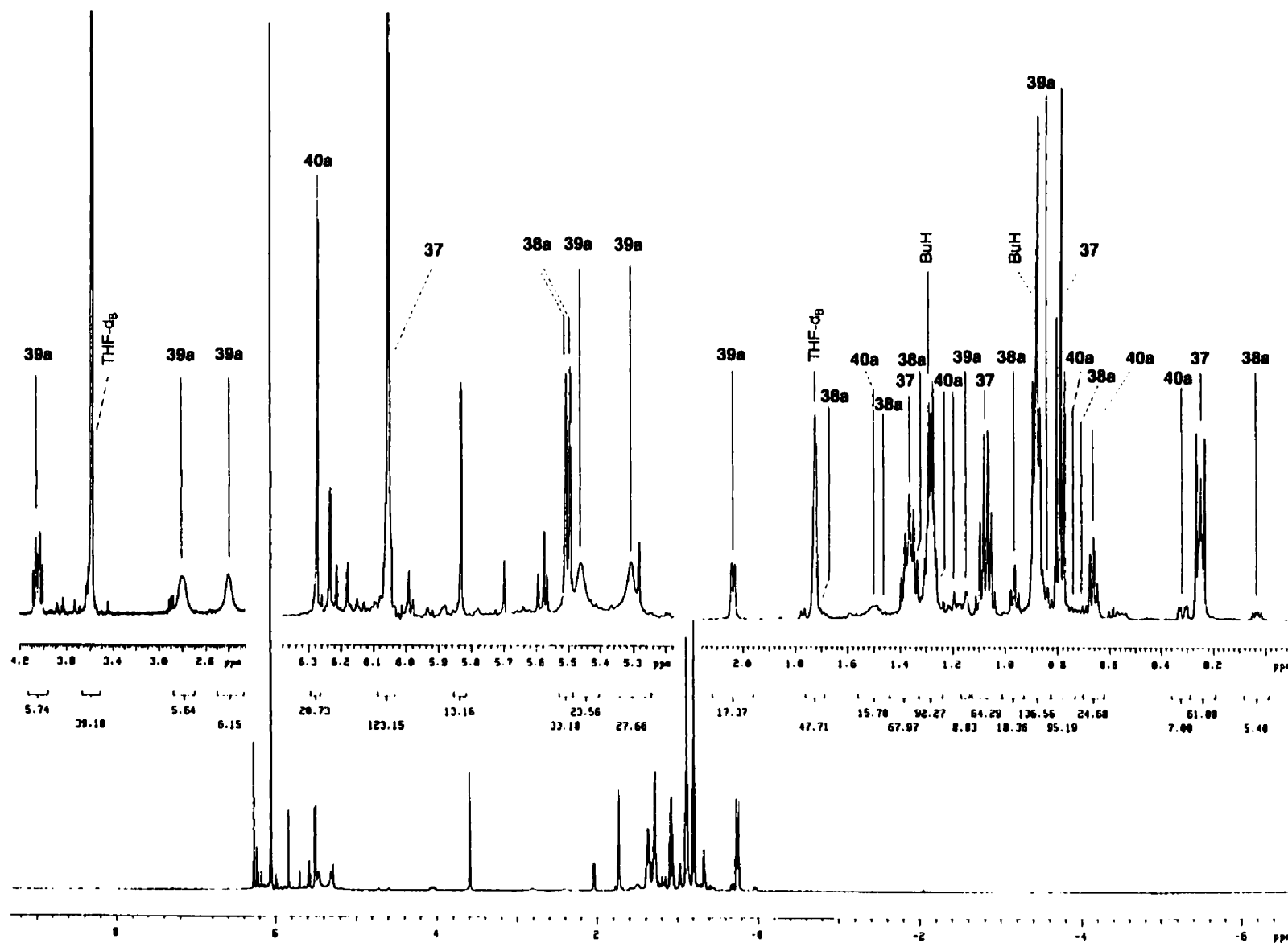


Figure 4-13. An ^1H NMR spectrum of a mixture of 37, 38a, 39a and 40a in THF-d_8 at -40°C .

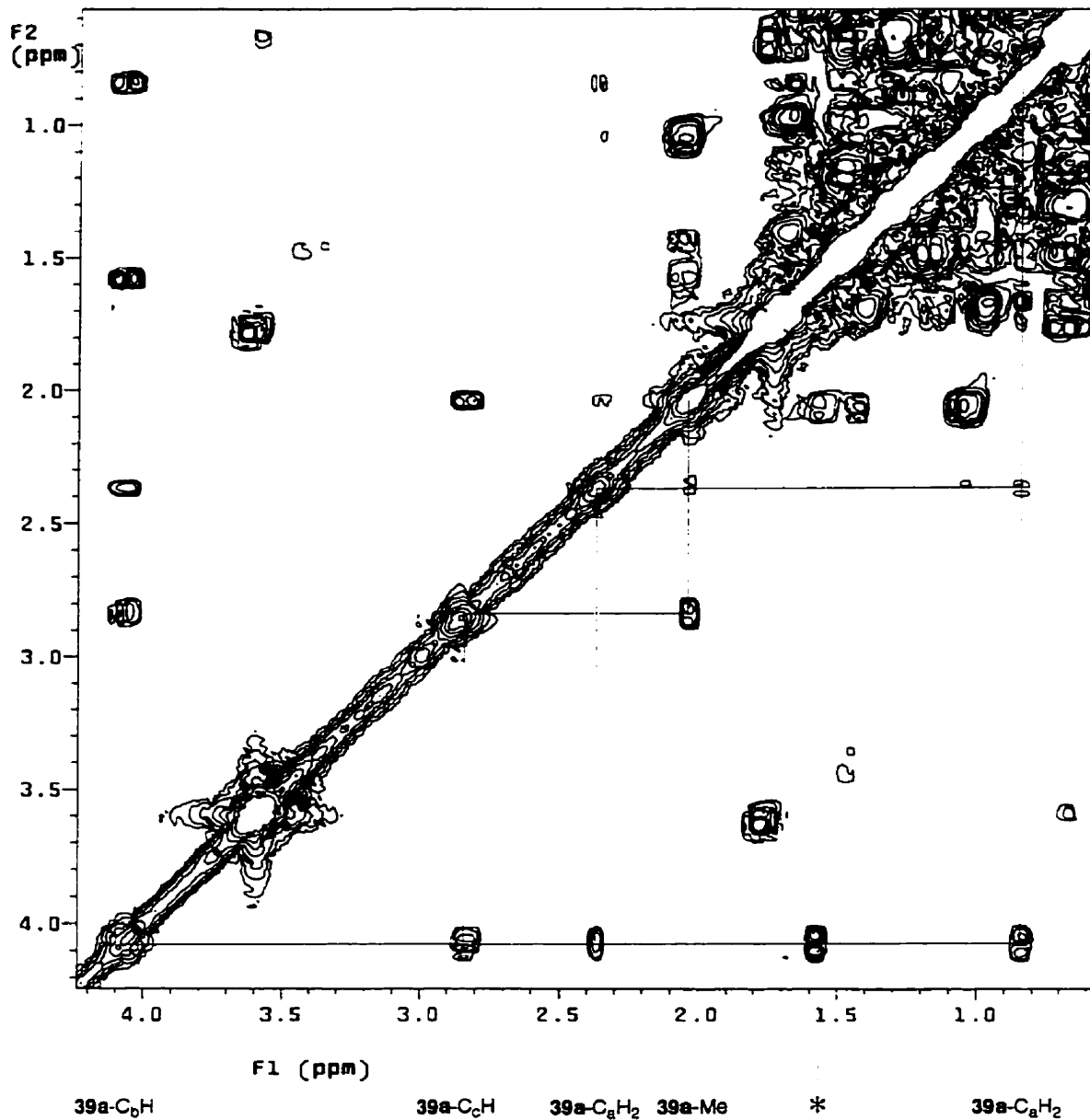


Figure 4-14. A fragment of the ^1H - ^1H COSY spectrum of **39a** in THF-d_8 at -40°C , which shows the connectivity pattern. An asterisk denotes a cross peak of an unknown impurity.

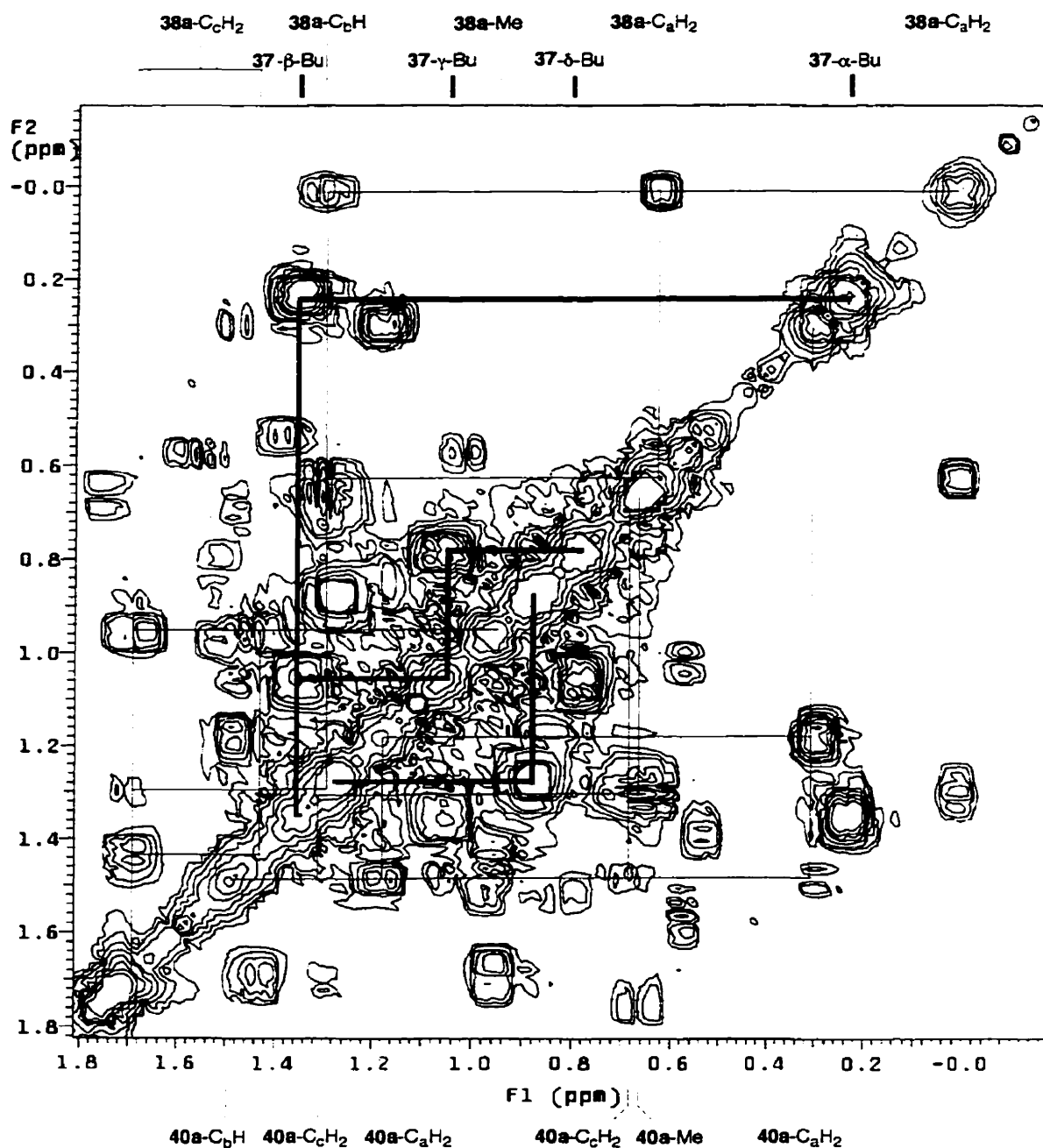


Figure 4-15. A fragment of an ^1H - ^1H COSY spectrum in THF- d_8 at 0°C , which shows a connectivity pattern for **37**, **38a** and **40a**. The tie-lines in the top left half are for **37** (bold) and **38a** (narrow). The tie-lines in the bottom right half are for butane (bold) and **40a** (narrow).

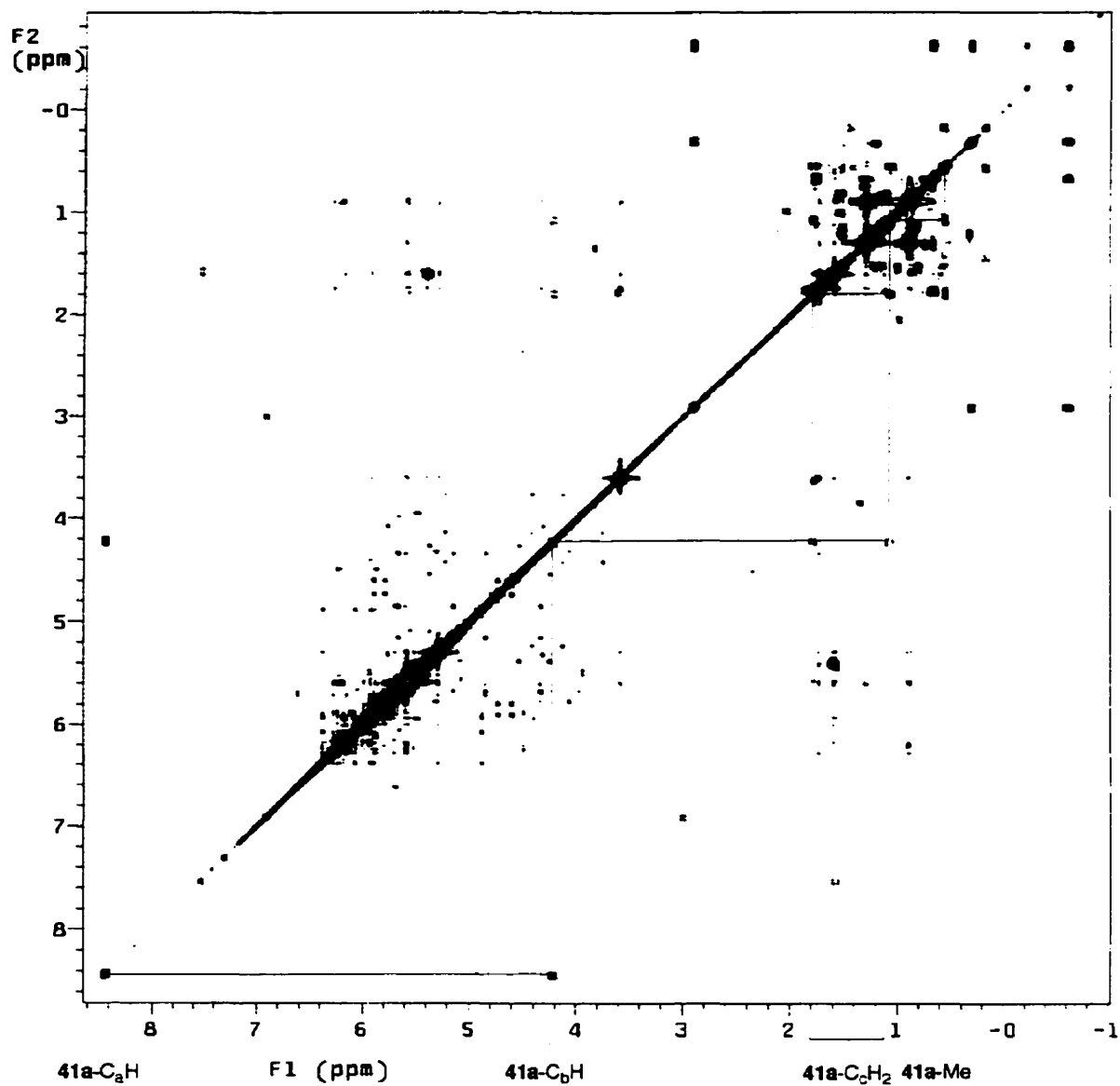


Figure 4-16. A fragment of an ^1H - ^1H COSY spectrum in THF- d_8 at $+25^\circ\text{C}$, which shows a connectivity pattern for **41a**.

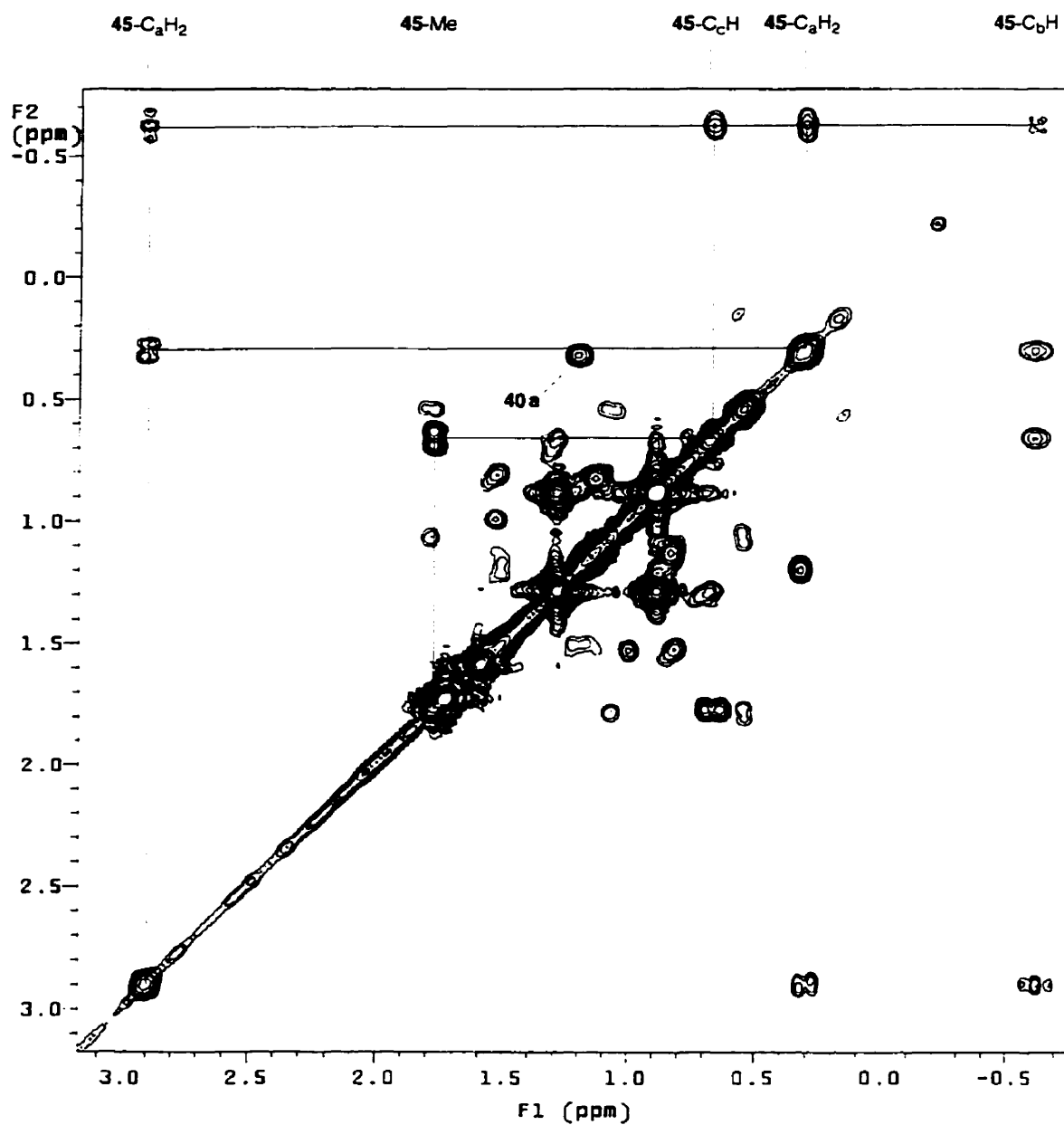


Figure 4-17. A fragment of an ^1H - ^1H COSY spectrum in THF- d_8 at $+25^\circ\text{C}$, which shows a connectivity pattern for **45**.

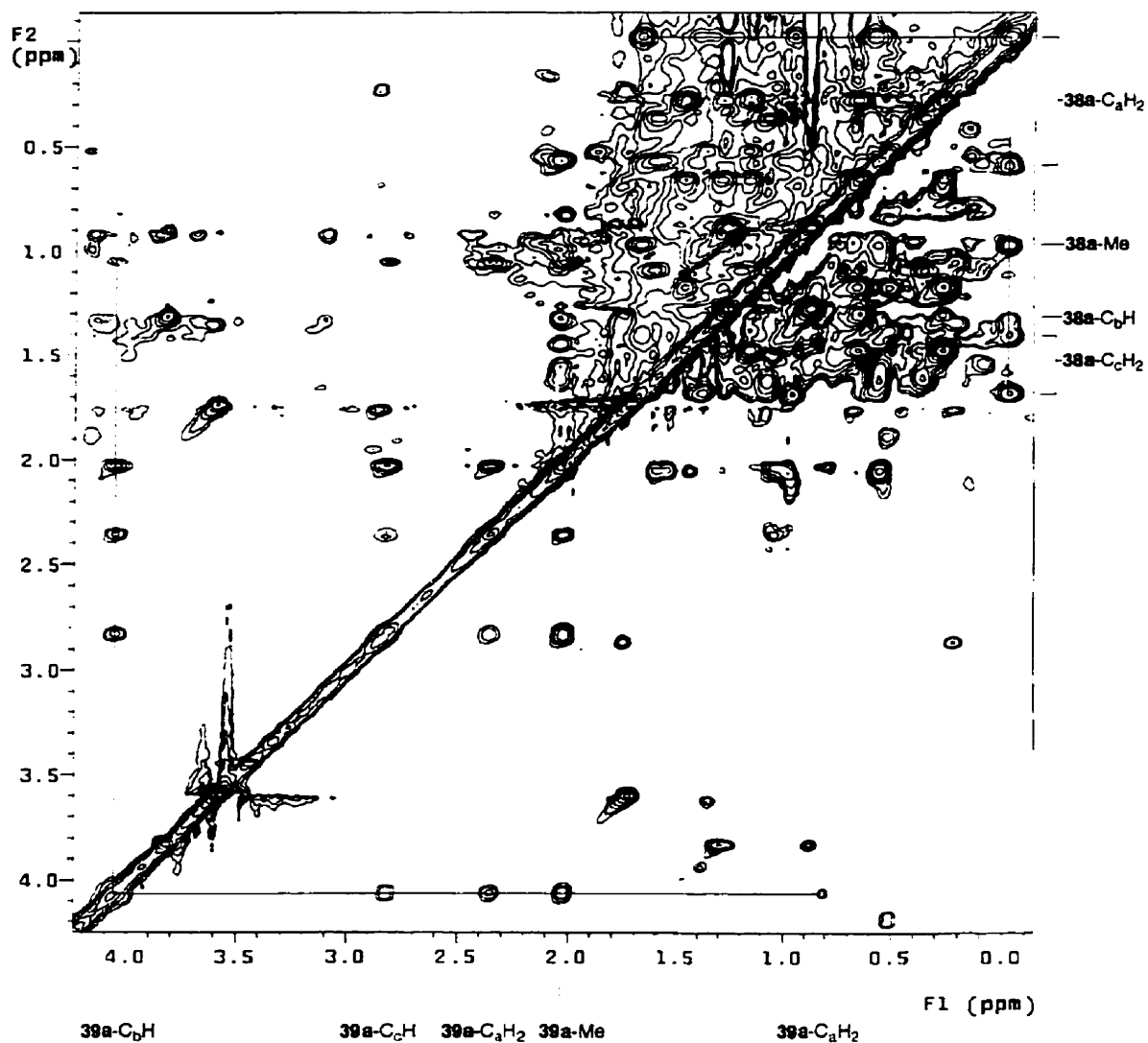


Figure 4-18. A fragment of an ^1H - ^1H TOCSY spectrum in THF- d_8 at -40°C , which shows a connectivity pattern for **38a** and **39a**.

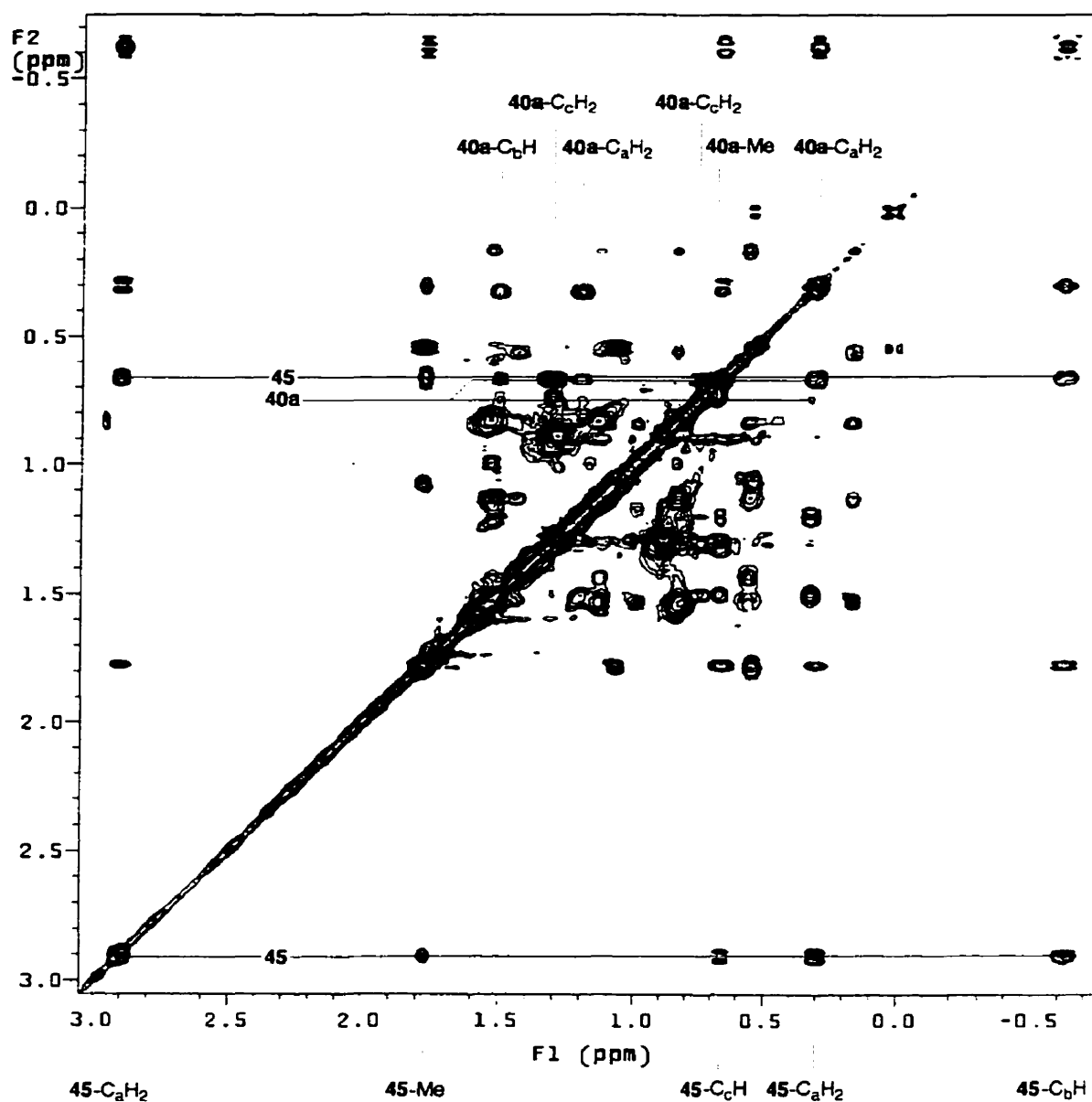


Figure 4-19. A fragment of an ^1H - ^1H TOCSY spectrum in THF- d_8 at $+25^\circ\text{C}$, which shows a connectivity pattern for **40a** and **45**.

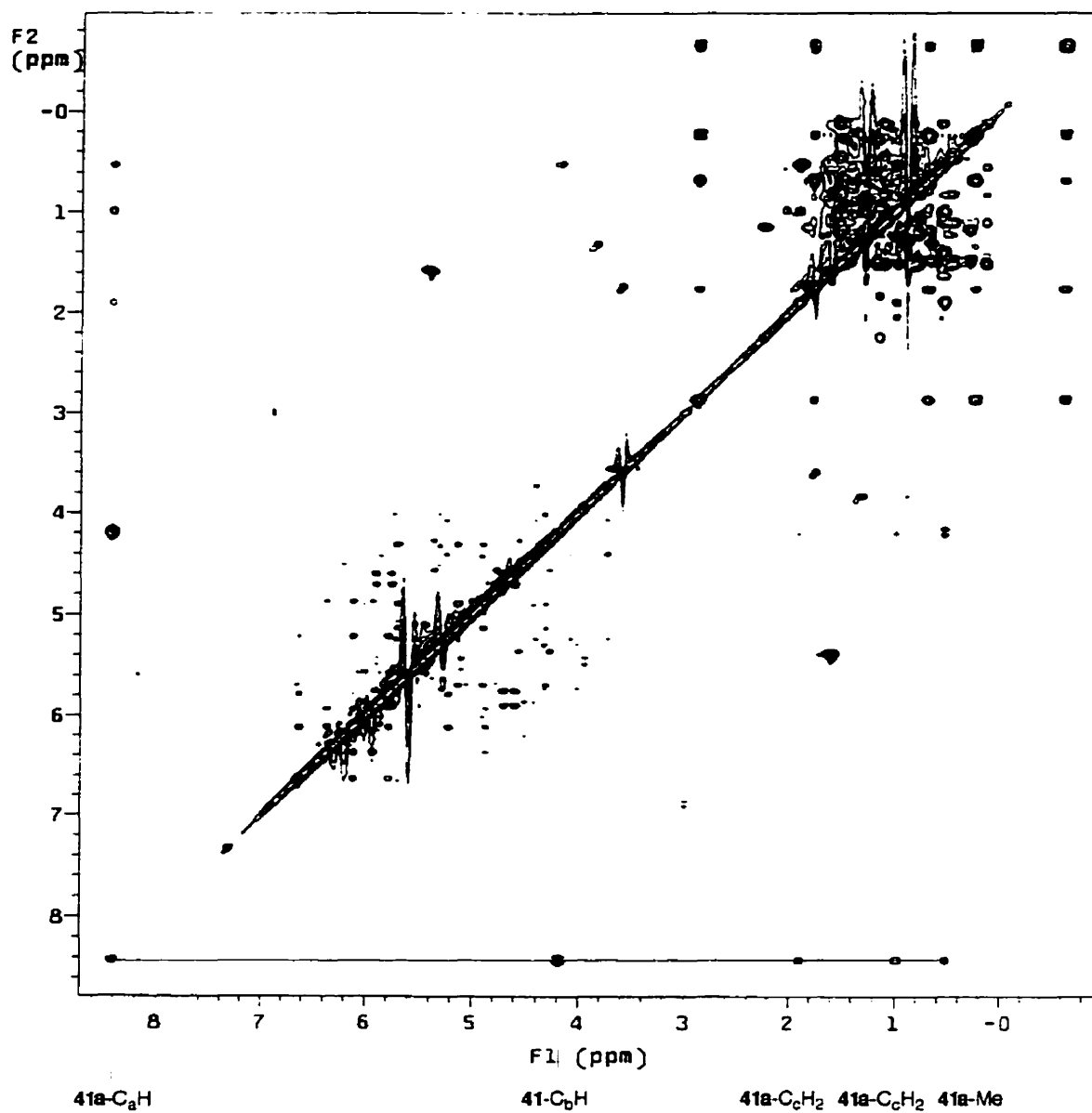


Figure 4-20. A fragment of an ^1H - ^1H TOCSY spectrum in THF- d_8 at -40°C , which shows a connectivity pattern for **41a**.

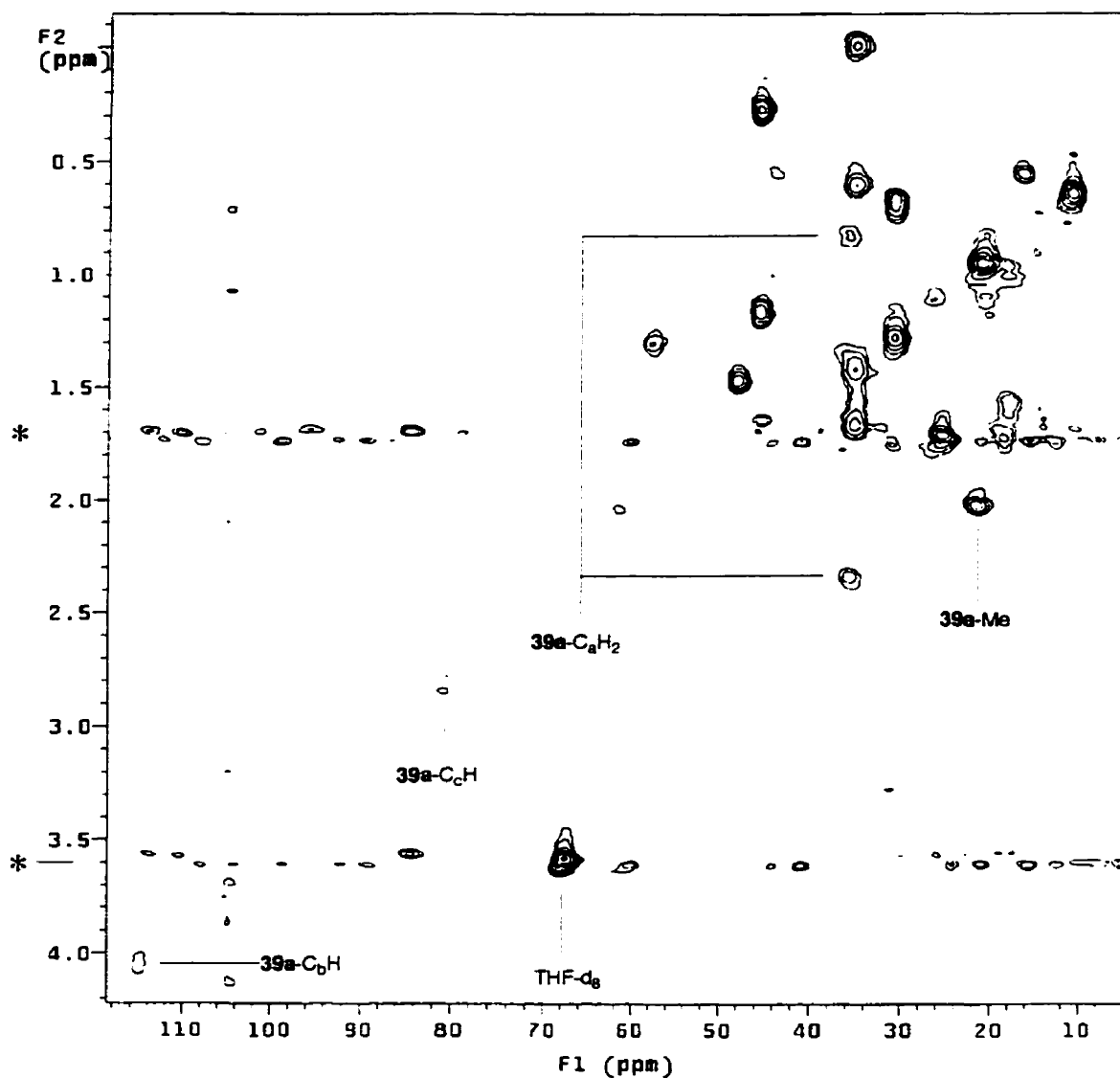


Figure 4-21. A fragment of an ^1H - ^{13}C HMQC spectrum of a mixture of **38a**, **39a** and **40a** in THF- d_8 at -40°C . (The labels for the cross peaks for **38a** and **40a** are given in Figure 4-3). The intensity of allylic resonances is low as the NMR experiment was specifically adjusted for a better sensitivity for aliphatic cross peaks. An asterisk denotes traces of relaxation noise arising from the solvent.

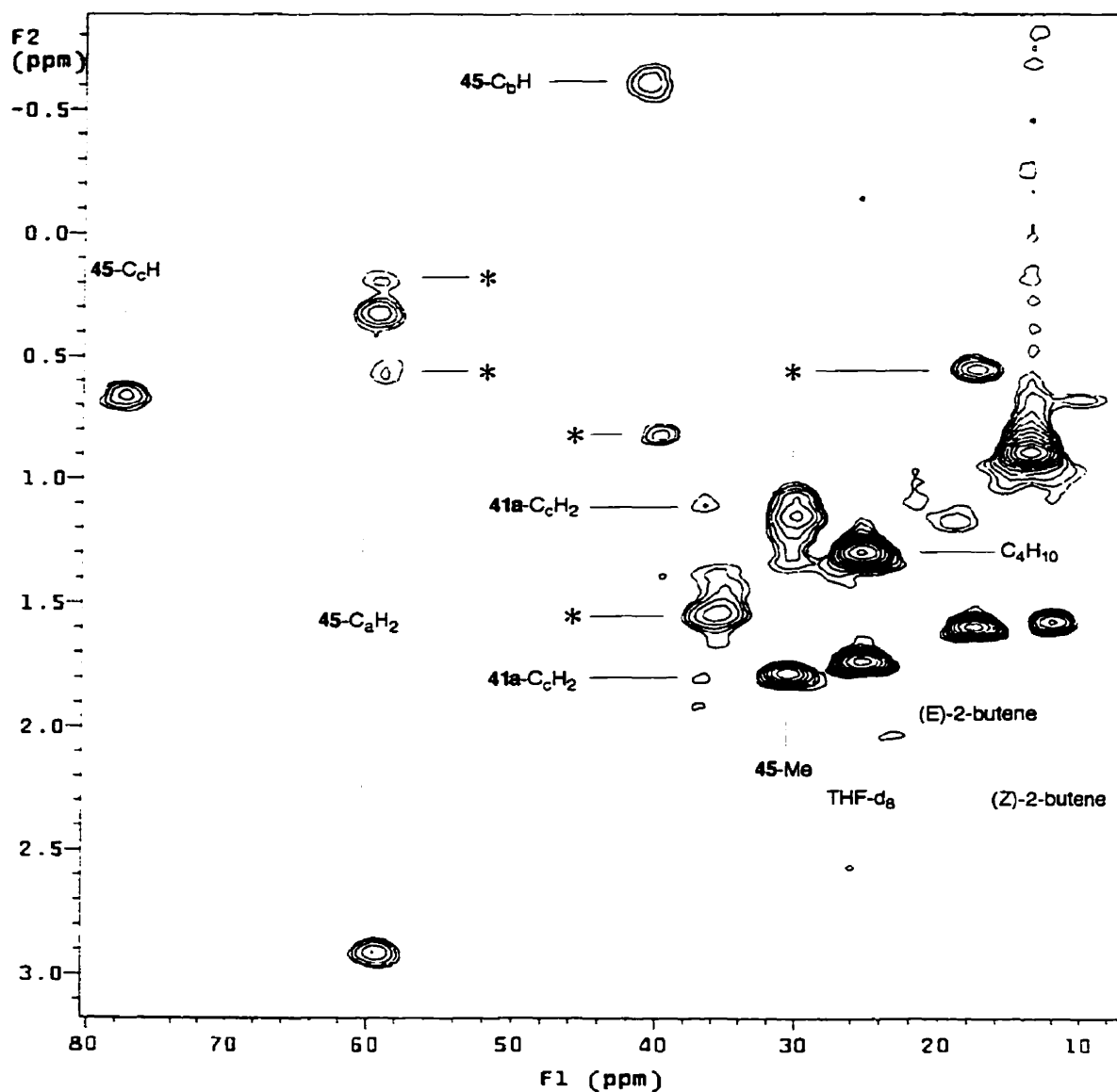


Figure 4-22. A fragment of an ^1H - ^{13}C HMQC spectrum of a mixture of **41a** and **45** in THF- d_8 at +25°C. Pairs of cross peaks having a common ^{13}C chemical shift belong to diastereotopic methylene groups. Cross peaks marked by an asterisk belong to a single ligand, which has not been identified.

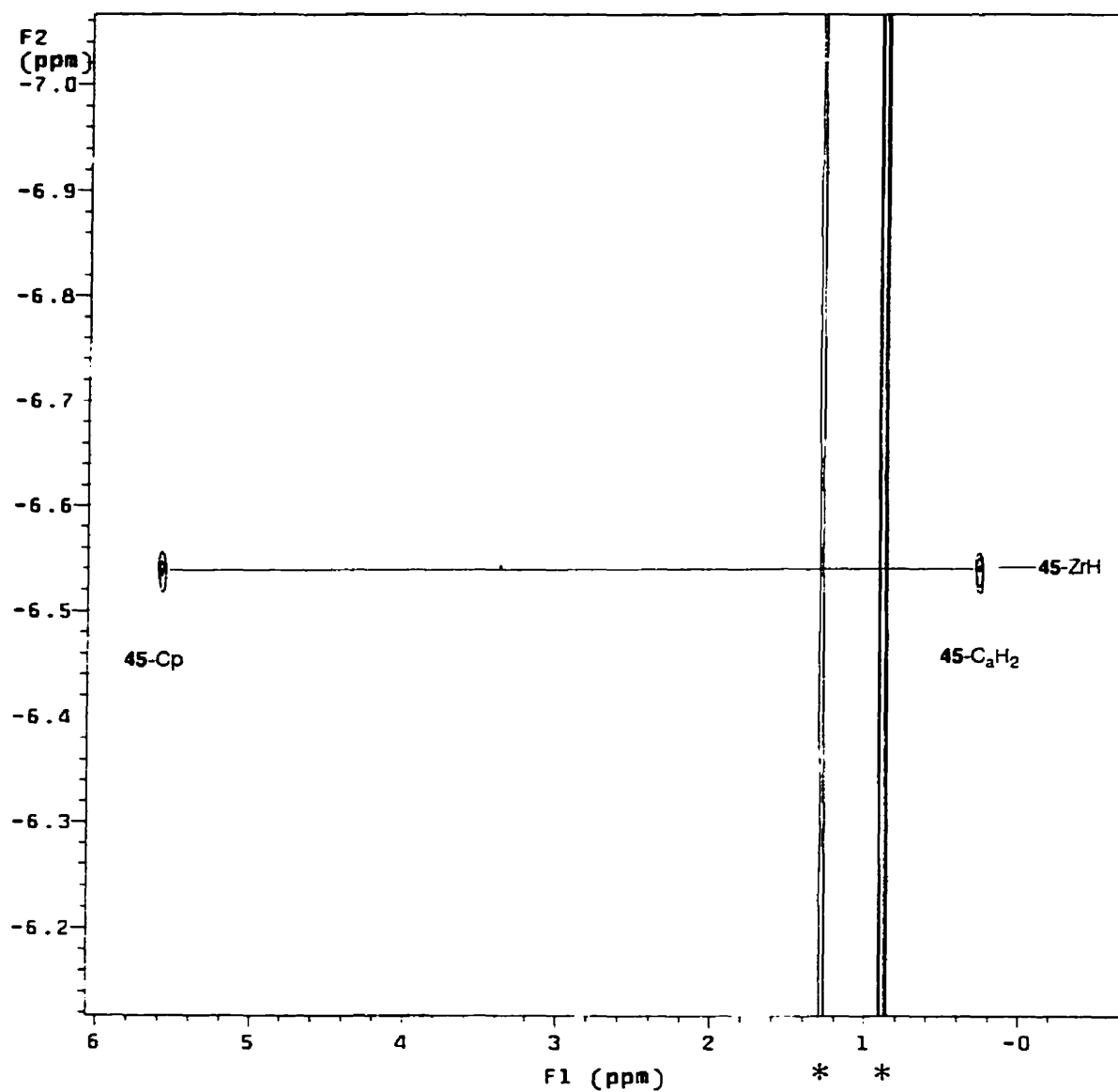
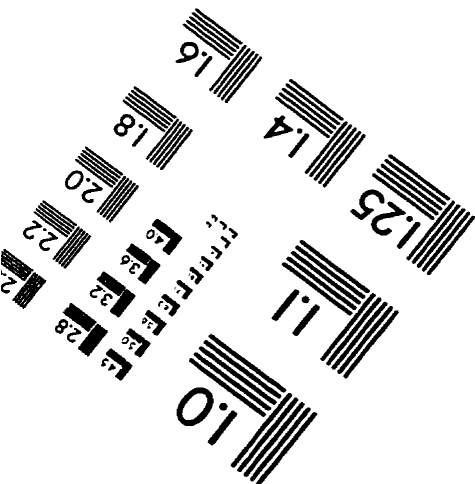
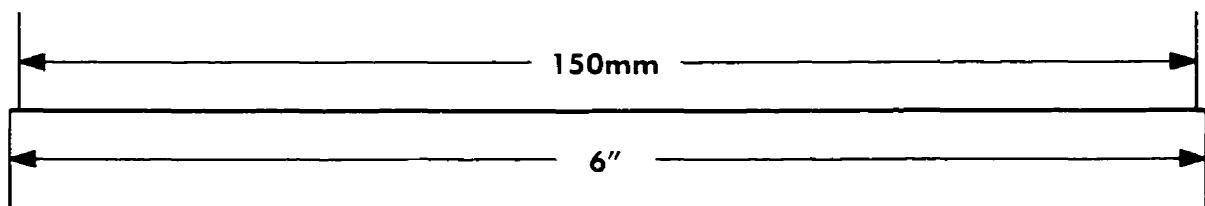
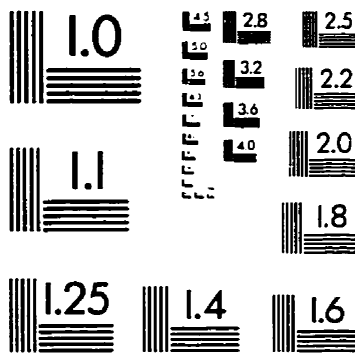
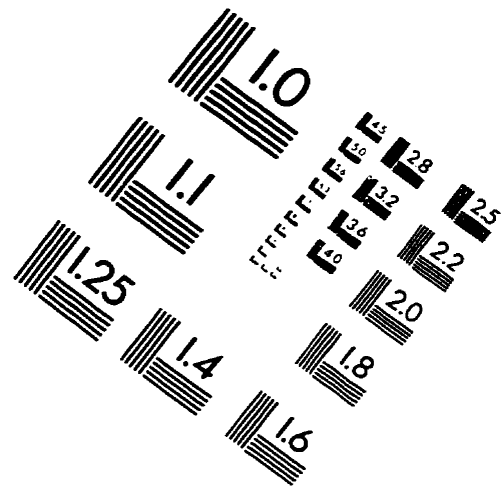
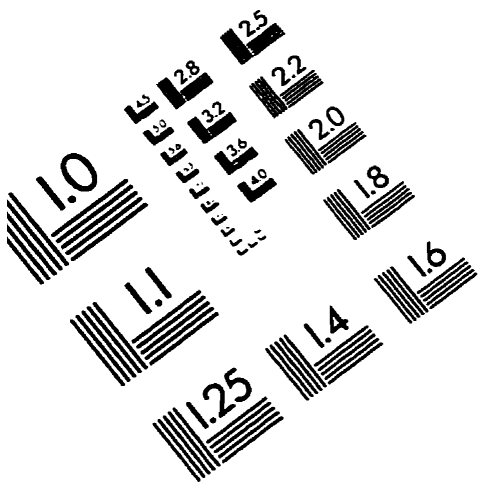


Figure 4-23. A fragment of an ^1H - ^1H NOESY spectrum in THF- d_8 at $+25^\circ\text{C}$, which exhibits the connectivity of $\mu\text{-H-Zr}$ to Cp, and $\text{C}_\alpha\text{H}_2$ groups in **45**. An asterisk denotes traces of relaxation noise arising from butane.

IMAGE EVALUATION TEST TARGET (QA-3)



APPLIED IMAGE, Inc
1653 East Main Street
Rochester, NY 14609 USA
Phone: 716/482-0300
Fax: 716/288-5989

© 1993, Applied Image, Inc., All Rights Reserved

